frontiers | Research Topics

Insights in pediatric cardiology: 2021

Edited by
Ruth Heying and Antonio Francesco Corno

Published in
Frontiers in Pediatrics
Frontiers in Cardiovascular Medicine

ISSN 1664-8714
ISBN 978-2-83251-090-2
DOI 10.3389/978-2-83251-090-2

About Frontiers

Frontiers is more than just an open access publisher of scholarly articles: it is a pioneering approach to the world of academia, radically improving the way scholarly research is managed. The grand vision of Frontiers is a world where all people have an equal opportunity to seek, share and generate knowledge. Frontiers provides immediate and permanent online open access to all its publications, but this alone is not enough to realize our grand goals.

Frontiers journal series

The Frontiers journal series is a multi-tier and interdisciplinary set of open-access, online journals, promising a paradigm shift from the current review, selection and dissemination processes in academic publishing. All Frontiers journals are driven by researchers for researchers; therefore, they constitute a service to the scholarly community. At the same time, the *Frontiers journal series* operates on a revolutionary invention, the tiered publishing system, initially addressing specific communities of scholars, and gradually climbing up to broader public understanding, thus serving the interests of the lay society, too.

Dedication to quality

Each Frontiers article is a landmark of the highest quality, thanks to genuinely collaborative interactions between authors and review editors, who include some of the world's best academicians. Research must be certified by peers before entering a stream of knowledge that may eventually reach the public - and shape society; therefore, Frontiers only applies the most rigorous and unbiased reviews. Frontiers revolutionizes research publishing by freely delivering the most outstanding research, evaluated with no bias from both the academic and social point of view. By applying the most advanced information technologies, Frontiers is catapulting scholarly publishing into a new generation.

What are Frontiers Research Topics?

Frontiers Research Topics are very popular trademarks of the *Frontiers journals series*: they are collections of at least ten articles, all centered on a particular subject. With their unique mix of varied contributions from Original Research to Review Articles, Frontiers Research Topics unify the most influential researchers, the latest key findings and historical advances in a hot research area.

Find out more on how to host your own Frontiers Research Topic or contribute to one as an author by contacting the Frontiers editorial office: frontiersin.org/about/contact

Insights in pediatric cardiology: 2021

Topic editors

Ruth Heying — University Hospital Leuven, Belgium

Antonio Francesco Corno — Children's Memorial Hermann Hospital, United States

Citation

Heying, R., Corno, A. F., eds. (2023). *Insights in pediatric cardiology: 2021*. Lausanne: Frontiers Media SA. doi: 10.3389/978-2-83251-090-2

Table of contents

frontiers | Frontiers in Pediatrics

TYPE Editorial
PUBLISHED 05 December 2022
DOI 10.3389/fped.2022.1059894

OPEN ACCESS

EDITED BY
Arjan Te Pas,
Leiden University, Netherlands

REVIEWED BY
Gaetano Thiene,
University of Padua, Italy

*CORRESPONDENCE
Ruth Heying
ruth.heying@uzleuven.be

SPECIALTY SECTION
This article was submitted to Pediatric Cardiology, a section of the journal Frontiers in Pediatrics

RECEIVED 02 October 2022
ACCEPTED 10 November 2022
PUBLISHED 05 December 2022

CITATION
Heying R and Corno AF (2022) Editorial: Insights in pediatric cardiology: 2021.
Front. Pediatr. 10:1059894.
doi: 10.3389/fped.2022.1059894

Editorial: Insights in pediatric cardiology: 2021

Ruth Heying[1]* and Antonio F. Corno[2]

[1]Department of Pediatric Cardiology, University Hospitals Leuven, Leuven, Belgium, [2]Children Heart Institute, Children's Memorial Hermann Hospital, UT Health Science Center, McGovern Medical School, Houston, TX, United States

KEYWORDS

pediatric cardiology, insights, imaging, kawasaki disease, fontan, future perspectives

Editorial on the Research Topic
Insights in pediatric cardiology: 2021

The rapid introduction of innovations in the clinical practice of pediatric cardiology, covering the entire field from the basic sciences to bedside application, has prompted us to promote this Research Topic on "Insights in Pediatric Cardiology: 2021".

This editorial initiative focuses on new insights, novel developments, current challenges, and future perspectives in the field of pediatric cardiology. Associated members of accomplished editorial boards have contributed with various topics, shedding light on current challenges, inspiring and providing direction to researchers in the field. Major progress has been made, especially in genetics, and various imaging techniques have been developed, allowing improvement in diagnoses and therapeutic options. Inflammatory diseases and associated general health care factors have gained increasing interest in the last decade.

We have collected 16 articles over the past 18 months in this Research Topic, and are pleased to introduce them to readers of *Frontiers in Pediatrics*.

Imaging modalities

One sector of pediatric cardiology where the most striking progress has been made is imaging. The advent of three-dimensional (3D) and four-dimensional (4D) reconstructions of the heart, as well as systemic and pulmonary circulations, has completely changed the knowledge on all details required for decision-making processes. Conventional images were the only images available a few years ago and are nowadays not sufficient in patient presentation. In this regard, Bui et al. (2021) presented the advantages of diagnostic modalities involving 3D visualization, such as 3D printed anatomical models as well as virtual and augmented reality; not only advantageous for clinical practice, but also for teaching and training. The review article analyzed the use of these new technologies in medical education, and included a thorough and honest report of their benefits and limitations.

An interesting study was reported by Ardakani et al. (2022) who studied, in aortic coarctation, the relationship between aortic shape and hemodynamic parameters by

means of computational simulations, purposely isolating morphological variables. Using aortic geometries derived from magnetic resonance imaging, computational simulations using a statistical shape modeling methodology were run in three aortic models: the absence of, surgically repaired, and unrepaired aortic coarctation. Even small alterations in the aortic morphology had an impact on key hemodynamic indices. The effective management of aortic coarctation affects long-term cardiovascular outcome phenomena, such as persistent hypertension in the absence of any clinically significant narrowing; this may be explained by differences observed in the aortic morphology.

In another retrospective study on aortic coarctation, Tuo et al. (2022) investigated the fetal echocardiographic parameters in the second and/or third trimester of pregnancy for all suspected cases aortic coarctation, in order to improve prenatal prediction after birth. Neonates were divided into two groups depending on the presence or absence of aortic coarctation after birth, and the criteria used for fetal diagnosis of aortic coarctation allowed accurate diagnosis of the most severe cases; however, the rate of false positives was relatively high for milder cases.

Closure of patent ductus arteriosus using interventional catheter techniques is still performed under fluoroscopy visualization. Many years after the first successful interventional closure under transesophageal echocardiographic guidance, Siagian et al. (2022) investigated the feasibility and safety of patent ductus arteriosus closure under echocardiography-only guidance over 1 year, comparing fluoroscopy and echocardiography-guided procedures in two groups of 30 children each. Primary endpoint procedural success was recorded, as well as secondary endpoints procedural time and the rate of adverse events. All patients presented successful closure of the patent ductus arteriosus, with residual shunts disappearing during follow-up in both groups. The procedural time was not significantly different between the fluoroscopy and echocardiography group.

Kawasaki disease

Because of migration in the last few decades, typical diseases like Kawasaki disease are now observed more frequently worldwide. Since the factors predicting high-risk Kawasaki disease remain unclear, Liu et al. (2022) studied the risk factors for resistance to intravenous immunoglobulin treatment and coronary artery aneurysm development in a high-risk Chinese pediatric population, comparing the performances of 11 scoring systems in a population of 346 children between 2013 and 2021. From the Kobayashi score and five Chinese system scores (Tang, Yang, Lan, Liping, and Wu), results of curve analyses were observed to be highest in the Liping scoring system for intravenous immunoglobulin resistance. The researchers concluded that the Liping scoring system is the most appropriate method to identify high-risk patients with Kawasaki disease for intravenous immunoglobulin resistance in the Chinese pediatric population.

Resistance to intravenous immunoglobulin therapy was also addressed by Li et al. (2022) The authors investigated the best available scoring models for the early identification of intravenous immunoglobulin-resistant diseases. In a very large patient population of >1,000 children across two separate hospitals, 15 variables in the training set were statistically different between intravenous immunoglobulin-sensitive and -resistant, including rash, duration of fever, peripheral blood neutrophil-to-lymphocyte ratio, prognostic nutritional index, percentage of monocytes and eosinophils, as well as high-sensitivity C-reactive protein. Based on the results of this study, a scoring model with elevated sensitivity, specificity, and accuracy of prediction was constructed to predict intravenous immunoglobulin resistance, which can greatly assist pediatricians in developing a suitable therapeutic strategy for these children.

In another interesting study on Kawasaki disease, Van Stijn et al. (2022) conducted an extensive literature review to identify patients with Kawasaki disease and their potential to develop coronary artery pathology, particularly coronary artery aneurysms, using an integrated cardiovascular program tailored to the severity of the existing coronary artery pathology. Their practical workflow included expert opinions from pediatric cardiologists, infectious disease specialists, and radiology experts, who should be able to anticipate the risk of coronary artery aneurysms in patients with Kawasaki disease.

Fontan circulation

Although the Fontan procedure has dramatically improved survival rates in patients with a single ventricle, long-term outcomes are still complicated by significant morbidity, with complications mainly due to elevated systemic venous pressure, which is characteristic of Fontan circulation. Consequently, these patients need close clinical and imaging monitoring, since early recognition of failing hemodynamics can be essential for long-term survival. Although echocardiography remains the first-in-line monitoring modality method, nowadays, cross-sectional imaging has become an essential tool in the evaluation of these patients. Ciliberti et al. (2022) analyzed the role of other diagnostic techniques, underlining the importance of cardiac magnetic resonance, particularly in simultaneously providing anatomic and functional information as well as essential information about extra-cardiac complications such as liver dysfunction and/or abnormal lymphatic drainage. Cardiac computerized tomography scanning may be useful when magnetic resonance is contraindicated, or for anatomical assessment in

uncooperative patients. Cardiac catheterization is currently reserved to measure specific hemodynamic parameters and for interventional procedures.

While the early advantages of fenestration in the Fontan procedure are well known, little evidence exists regarding the long-term consequences of Fontan fenestration and the effects of interventional closure of the fenestration when induced by the clinical situation. Because of this, Greenleaf et al. (2022) performed a systematic literature review and a meta-analysis of the latest outcomes of Fontan fenestration, analyzing 922 publications for parameters such as changes in oxygen saturation, cavo-pulmonary pressure, maximum heart rate during exercise, exercise duration, and oxygen saturation after fenestration closure. In 877 patients that received interventional catheter closure of the fenestration, at a mean interval of 27.4 months after fenestration closure, a significant increase in arterial oxygen saturation and exercise duration was determined; however, an associated increase in the mean cavo-pulmonary pressure also occurred. This study concluded that late closure of a Fontan fenestration improves resting oxygen saturation, exercise oxygen saturation, and exercise duration. Concrete conclusions remain guarded in relation to the management, creation, or enlargement of Fontan fenestrations. The lack of comparative data suggests the need for improved prospective trials to examine the role of fenestration in the management of late Fontan failure.

Associated health care issues

One of the most frequent health issues affecting current society is obesity, with significant consequences on the mortality and morbidity of adult populations, requiring a large number of resources and efforts by caregivers and society at large. Lee et al. (2021) screened a population of overweight adolescents with metabolic syndrome, and obtained a risk stratification for future cardiovascular disease in this population. Undoubtedly, this study will stimulate further investigations on the early development of obesity and the associated co-morbidities.

Children with congenital heart defects have a well-established risk of neuropsychiatric co-morbidities, including attention deficit/hyperactivity disorder (ADHD) symptoms; it is unknown whether the higher burden of ADHD symptoms is mainly driven by hyperactivity, inattention, or both. Lau-Jensen et al. (2021) compared a group of patients with simple congenital heart defects with age-matched controls and found a higher symptom burden across all ADHD scores and all symptom sub-scores, which was driven by both inattention and hyperactivity symptoms; inattention symptoms were more prominent. The authors suggested routine screening for ADHD symptoms in all children with congenital heart defects to facilitate adequate help and guidance since these symptoms are easily overlooked.

One of the leading causes of sudden, unexplained death of infants is sudden infant death syndrome (SIDS). While this dramatic health issue has been progressively recognized over the last few years, we are still far from an adequate policy for its prevention. Yamada et al. (2021) reported a research project to identify associations between SIDS and race/ethnicity, birth weight/gestational age, and socioeconomic/environmental factors in the referral area of North Carolina, USA. Based on the results of the study, since maternal, socioeconomic, and environmental risk factors are all associated with a higher incidence of SIDS in the population investigated, a thorough risk assessment should be performed in all infants at risk.

Returning to the field of connective tissue disease affecting systemic circulation, neurofibromatosis, also known as von Recklinghausen disease, a common autosomal dominant disorder caused by mutations in the *NF1* gene, is associated with early-onset systemic hypertension. Lu et al. (2021), in addition to a systematic literature review, performed a study on *NF1* mutations in two unrelated Chinese families with NF-1, who presented with early-onset hypertension. Using whole-exome sequencing, the authors identified one recurrent and one novel frame-shift mutation. Because hypertension is not a rare complication of *NF-1*, considering the phenotypic heterogeneity of *NF-1*, and based on the observational results, the authors suggested genetic testing as a tool for early and accurate diagnosis, especially in children and adolescents, to potentially prevent serious cardiovascular events.

Connective tissue disease

Connective diseases affecting the aorta, such as Marfan and Loeys-Dietz syndrome, have attracted particular interest due to the progress achieved in the accurate diagnosis of cardiovascular malformation using 3D imaging and the subsequent improvement in surgical outcomes. This approach has also allowed the treatment of an increasing number of adolescents and children. Camarda et al. (2022) investigated pediatric patients with Marfan and Loeys-Dietz syndrome and other undifferentiated connective tissue diseases, using magnetic resonance imaging to determine patient-specific fluid structure interaction models. The time-averaged wall shear stress and oscillatory shear index were measured and compared with age- and gender-matched control participants. The authors reported that differences in these two parameters were apparently driven by local morphological differences, particularly the dimensions of the ascending aorta and the cardiac output. This is another example of a potential foundation for larger future studies on connective tissue disorders in the pediatric population.

Right ventricular hypoplasia

Hirono et al. (2022) performed a systematic literature review of isolated right ventricular hypoplasia as a rare congenital myocardial disease, not associated with severe pulmonary or tricuspid valve malformation, and focused on evaluating clinical statuses and outcomes. The result of the study was that an early diagnosis of isolated right ventricular hypoplasia in children with cyanosis is associated with a high mortality.

Postural tachycardia

Postural tachycardia syndrome in children is quite a rare disease, but with serious potential consequences. Wang et al. (2022) investigated the predictive values of heart rate and blood pressure on the prognosis of postural tachycardia syndrome in a large group of children. The predictive value of the four combined indicators for prognosis was superior to that of the single factor, conventionally used. Based on these observations, the authors divided the patients into two groups: good and poor prognosis, and treated them accordingly, with encouraging outcomes.

Conclusion

The various interesting contributions collected in this Research Topic highlight key matters on the pathophysiology of congenital heart disease and its diagnostic management, herewith indicating future directions to improve the treatment of patients.

Author contributions

AFC conceptualized and wrote the original draft. AFC and RH reviewed and edited the submitted version. All authors contributed to the article and approved the submitted version.

Acknowledgments

As the Editors of this Research Topic, we would like to thank all authors who submitted their articles and shared their expert opinions and research results. We are also grateful to all reviewers for their valuable comments and insightful suggestions.

Conflict of interest

The authors declare that the research was conducted in the absence of any commercial or financial relationships that could be construed as a potential conflict of interest.

Publisher's note

frontiers in Pediatrics

ORIGINAL RESEARCH
published: 22 October 2021
doi: 10.3389/fped.2021.745805

Identification of Cardiovascular Risk Factors in Obese Adolescents With Metabolic Syndrome

*Jung Won Lee, Young Mi Hong and Hae Soon Kim**

Department of Pediatrics, Ewha Womans University School of Medicine, Seoul, South Korea

Objective: There are studies that show different associations between metabolic syndrome (MS) and cardiovascular disease in adolescent. This study is aimed to identify probable cardio-vascular risk factors in obese adolescents with MS.

Methods: Sixty-five obese adolescents with a body mass index (BMI) > 95 percentile were enrolled and divided into two groups with MS or without MS. Left ventricular mass (LVM), left ventricular mass index, ejection fraction, epicardial fat thickness, visceral fat thickness (VFT) and carotid intima-media thickness were measured. Anthropometric and blood chemistry parameters were estimated. Above parameters were compared based on presence or absence of MS.

Results: The prevalence of MS was 23.1% in obese adolescents. LVM showed significant correlation with body mass index (BMI), hip circumference (HC), fat mass, total cholesterol (TC), LDL-cholesterol (LDL-C) and waist circumference (WC). VFT significantly correlated with WC, BMI, hip circumflex (HC), obesity index (OI), fat %, fat mass, insulin, TC, LDL-C, insulin, triglyceride (TG), glucose, homeostatic model assessment for insulin resistance (HOMA-IR) and leptin.

Conclusions: Screening for the MS in overweight adolescents may help to predict risk of future cardiovascular disease. These data suggest that LVMI and VFT are significant parameters for predicting cardiovascular disease risk in obese adolescents.

Keywords: metabolic syndrome, visceral obesity, left ventricular mass index, visceral fat thickness, cardiovascular disease

OPEN ACCESS

Edited by:
Ruth Heying,
University Hospital Leuven, Belgium

Reviewed by:
Hala El-Bassyouni,
National Research Centre, Egypt
Emanuele Monda,
University of Campania Luigi Vanvitelli, Italy

****Correspondence:***
Hae Soon Kim
hyesk@ewha.ac.kr

Specialty section:
This article was submitted to Pediatric Cardiology, a section of the journal Frontiers in Pediatrics

Received: *22 July 2021*
Accepted: *22 September 2021*
Published: *22 October 2021*

Citation:
Lee JW, Hong YM and Kim HS (2021) Identification of Cardiovascular Risk Factors in Obese Adolescents With Metabolic Syndrome. Front. Pediatr. 9:745805. doi: 10.3389/fped.2021.745805

INTRODUCTION

The prevalence of adolescent metabolic syndrome (MS) has increased substantially due to lack of physical activity, unhealthy diet and lifestyle, and incomplete sleep due to presence of electrical devices.

However, there was no definition of adolescent MS until now, and most definitions have been adapted from the Adult Treatment Panel III (ATP III) definition, published by Cook et al. (1). The International Diabetes Federation (IDF) released its unique definition of MS in children and adolescents in 2007 (i.e., IDF 2007 definition), at the age of 10 yr and more, MS requires the presence of abdominal obesity (≥90th percentile) plus, the presence of two or more of elevated triglycerides (TG) (≥150 mg/dL), low high-density lipo-protein-cholesterol (HDL-C) (<40 mg/dL), high blood pressure (Systolic blood pressure ≥130 or diastolic blood pressure ≥ 85 mm Hg), and elevated plasma glucose (Fasting glucose ≥100 mg/dL or known type2 DM) (2).

Visceral fat and insulin resistance are key factors of MS development (3). The visceral fat accumulation is associated with vascular atherosclerosis and cardiovascular outcome after all (4). These consequences are from pro-inflammatory cytokines originated from visceral fat tissue (5). For example, epicardial fat around heart interacts with myocardium and coronary arteries through cytokines (6). Thus, definition of MS has expanded to include many inflammatory cytokines (7). It has been postulated that obesity dysregulates blood adipokine levels, may induce insulin resistance, and finally influence the development of MS and vascular complications (8).

Although increased number of metabolic risk factors and their complex interactions contribute to the occurrence of MS, this has not been well-studied in adolescent populations (9).

The aim of this study was to identify specific risk factors from visceral obesity closely related to future cardiovascular consequence in obese adolescent populations.

METHODS

Study Participants

Sixty five obese adolescents (31 males, 34 females) aged between 15 and 17 in a high school participated in this study. They were divided into two groups: the MS group (total = 15, male = 9, female = 6) and the group without MS (total = 50, male = 22, female = 28). We measured MS in adolescents using a modified cook's definition. Adolescent obesity was defined as body mass index (BMI) above the 95th percentile for age and sex by the survey of Korean Centers of Disease Control and Prevention in 2007 (10). Adolescents with other endocrine disease, psychiatric problem or other severe and chronic disease were excluded. Informed consents were obtained from the parents or guardians. The study was conducted according to the guidelines of the Declaration of Helsinki, and approved by Ethical Committee of Ewha Womans University, College of Medicine, Seoul, Korea (approval No: 0319/12.06.2020).

Anthropometric Measurement

Anthropometric data of weight, height, waist circumference (WC), BMI, obesity index (OI), hip circumflex (HC), fat mass, fat percentage and blood pressure (BP) from both groups were obtained. Both the height and weight were taken with light dressed and shoes were off on the height measuring instrument (JENIX, Samhwa Co., Ltd., Seoul, Korea), and the eyes were straightened. The vertical distance from the soles of the feet to the top of the head was measured and recorded up to 0.1 cm. The weight was recorded up to 0.1 kg. WC was measured at the mid-point between 12th rib and the mid portion of the superior iliac crest. BMI was calculated by dividing the body weight (kilogram) by height (meter) in meter square. OI was obtained by the equation using the standard weight value corresponding to the 50th percentile of the weight data chart for Korean children. HC was measured from the most protruding part of the hip. Fat mass and fat percentage were measured by bioelectric impedance analysis (BIA) (InBody 720, Biospace Co., Ltd., Seoul, Korea). BIA can be used as an alternative to gold standard dual-energy X-ray absorptiometry (DXA) admitting BIA underestimate body fat percentage values compared to DXA (11). BP was measured after 10 min of bed rest using an automatic oscillometric BP device in a supine position (Omron HEM-7320-LA, Omron Healthcare Co. Ltd, Kyoto, Japan).

Laboratory Measurement

Blood was taken from all 65 subjects after 14 h fasting. Blood glucose, total cholesterol, TG, low density lipoprotein-cholesterol (LDL-C), HDL-C, aspartate aminotransferase (AST), alanine aminotransferase (ALT), Serum TNF-α and IL-6 levels were measured by sandwich enzyme immunoassay-based Quantikine Human interleukine and TNF-α kit (R&D system Inc., Minneapolis, MN, USA). Serum leptin, adiponectin and insulin levels were measured using the Human Leptin 125 tubes radioimmunoassay kit (Linco Resarch Inc., St. Charles, MO, USA), radioimmunoassay human adiponectin 125 tubes radioimmunoas-say kit (Linco Research, Inc. St. Charles, MO, USA) and human insulin chemiluminescence immunoassay kit (insulin, Siemens Centaur, Holliston, MA, USA), respectively.

Insulin resistance was measured by the homeostasis model assessment of insulin resistance (HOMA-IR), by dividing the multiple of insulin (μU/mL) and serum glucose (mmol/L).

Carotid Artery Ultrasound Measurement

Carotid intima-media thickness (CIMT) was measured with neck ultrasound iU22 (Intelligent Ultrasound System, Philips Medical System, Amsterdam, The Netherlands). After the subjects lied down and rest for at least 30 min, probe was placed on common carotid artery 1 cm proximal from the carotid bifurcation. Three points of thickest intima-media lengths were measured and average was recorded.

Abdominal Ultrasonography Measurement

Abdominal fat thickness including subcutaneous fat thickness, visceral fat thickness and pre-peritoneal fat thickness were measured with abdominal ultrasound Acuson XP128 (Acuson, Mountain View, CA, USA) by placing a 3.5 MHz linear-array probe 1 cm above the navel at end-expiratory phase. Subcutaneous fat thickness was measured from skin to anterior abdominal muscle, visceral fat thickness from posterior abdominal muscle to anterior wall of aorta, and pre-peritoneal fat thickness from the subcutaneous layer to the peritoneum, respectively. Same experienced radiologist performed the measurement.

Echocardiographic Parameters Measurement

Echocardiographic parameters such as epicardial fat thickness (EFT), LV dimension, and systolic/diastolic parameters were estimated by echocardiography (Acuson Sequoia-C 512, Siemens, CA, USA). The subjects lied down in left lateral decubitus with using phased-array echocardiograms in M-mode, 2D, and pulsed and color-flow Doppler settings. EFT on the free wall of right ventricle was measured in parasternal long axis and short axis views. LV dimension was measured by perpendicular to the long axis of the left ventricle. Systolic and diastolic parameters such as stroke volume (SV) was determined by

the aortic annular cross-sectional area multiplied by the aortic time-velocity integral. Cardiac output (CO) was calculated by multiplying SV and the heart rate (HR). Ejection fraction (EF) was calculated from biplane Simpson formula and fractional shortening (FS) was calculated using left ventricular internal dimensions. Early diastolic (E), late atrial (A) peak velocities, E/A ratios, and E-wave deceleration time (ms) were measured from pulsed doppler mode in apical window. Left ventricular mass (LVM) was calculated calculated from American Society of Echocardiography guideline, and left ventricular mass index (LVMI) was calculated from LMV devided by body surface area (Monstella method).

LVM (g) = 0.8 [1.04 (STd + LVIDd + PWTd)3 – LVIDd3] + 0.6 g

- STd = interventricular septal thickness at end-diastole (mm)
- LVIDd = LV end-diastolic dimension (mm)
- PWTd = posterior wall thickness at end-diastole (mm)

Body surface area: $\{[Ht\ (cm) \times Bwt\ (kg)]/3{,}600\}^{1/2}$

- Ht: Height Bwt; body weight.

Brachial-Ankle Pulse Wave Velocity and Ankle Brachial Index Measurement

Brachial-ankle pulse wave velocity (baPWV) were measured using a volume-plethysmographic apparatus (Colin Co. Ltd., Komaki, Japan). The subject was examined in supine position for at least 5 min with taking their usual medication. The device gathered oscillometric waveforms and simultaneously calculates the time intervals between brachium and ankle waveforms. Two sets of baPWV values were measured and left and right data were showed. Ankle Brachial index (ABI) was calculated as the ratio of systolic BP in ipsilateral ankle and brachium.

Statistical Analysis

We performed statistical analyses using Statistical Package for the Social Sciences (SPSS) (version 20, SPSS Inc. Chicago, IL, USA). Data were presented as means and standard deviations. The comparison of continuous variables was done using the Student *t*-test or two-way ANOVA. Univariate and multivariate logistic regression models were implemented to examine the independent relationship between the dependent variable MS and other variables of metabolic parameters. *P*-value < 0.05 was considered as statistically significant.

RESULTS

The Prevalence of Metabolic Syndrome and Clustering of Metabolic Components

Of the total of sixty-five subjects (31 males, 34 females), 23.1% (15/65) showed an incidence of MS that satisfied more than three of the criteria of MS.

The percentage of the subjects meeting MS criteria were WC ≥ 90 percentile (52.3%), systolic BP or diastolic BP ≥ 90 percentile (mmHg) (52.3%), and HDL- C ≤ 40 (mg/dL) (46.2%), followed by TG ≥ 110(mg/dL) (26.2%) and fasting glucose ≥ 100 (mg/dL) (3.1%) in **Table 1**.

TABLE 1 | Prevalence of components of MS in obese adolescents.

Criteria	*N* (M/F)	%
WC ≥ 90 percentile	34(17/17)	52.3
SBP or DBP ≥ 90 percentile(mmHg)	34(13/21)	52.3
HDL-C < 40 (mg/dL)	30(17/13)	46.2
Triglyceride ≥ 110 (mg/dL)	17(11/6)	26.2
Fasting glucose ≥ 100 (mg/dL)	2(1/1)	3.1

MS, metabolic syndrome; WC, waist circumference; SBP, systolic blood pressure; DBP, diastolic blood pressure; HDL-C, high density lipotrotein-cholesterol; N, number; %, percent from total subjects.

Comparison of Anthropometric Data

There was no difference in anthropometric data between MS and non-MS groups of both females and males in **Table 2**.

Comparison of Biochemistry Parameters

LDL-C was significantly increased in MS females (131.1 ± 19.5 vs. 96.7 ± 27.5 mg/dL, $p = 0.007$), TG was significantly increased and HDL-C was significantly decreased in both MS males and MS females than control group. adolescents without MS. Adiponectin and insulin like growth factor binding protein 3 (IGFBP-3) were significantly decreased in MS females compared to non-MS females in **Table 3**.

Comparison of the Geometrical Analysis of the Carotid Artery

The geometrical analysis of the carotid artery had no differential data including intimal media thickness between two groups of both females and males in **Table 4**.

Comparison of Abdominal Sonographic Data

In the abdominal sonographic data, VFT was significantly higher in MS females compared to non-MS females (42.0 ± 7.5 vs. 31.1 ± 6.9 mm, $p = 0.004$) in **Table 5**.

Comparison of Echocardiographic Data

In the echocardiography data including epicardial fat thickness, there was significant increase in left ventricular mass (LVM) (205.9 ± 44.5 vs. 258.7 ± 59.0 g, $p = 0.008$) and left ventricular mass index (LVMI) (1.9 ± 0.4 vs. 2.4 ± 0.5 g/m^2, $p = 0.047$) in MS (+) males in **Table 6**.

Comparison of Pulse Wave Velocity and Ankle Brachial Index

There was significant increase of left ABI in the MS (+) females (106 ± 6.8 vs. 100.4 ± 7.9, $p = 0.021$). However, no significant difference was observed in heart rate, RbaPWV, LbaPWV and right ABI between the MS (–) and MS (+) groups in **Table 7**.

Correlation Between the LV Mass and Other Metabolic Parameters

LV mass is significantly associated with BMI, HC, fat mass, insulin, TC, LDL-C, and WC ($P < 0.05$) in **Table 8**.

TABLE 2 | Comparison of anthropometric data in obese adolescents.

	Male ($n = 31$)			Female ($n = 34$)		
	MS(–) ($n = 22$)	**MS(+) ($n = 9$)**	***P***	**MS(–) ($n = 28$)**	**MS(+) ($n = 6$)**	***P***
Age (year)	16.4 ± 0.9	16.3 ± 0.9	0.812	16.6 ± 0.8	16.5 ± 0.8	0.649
Height (cm)	171.1 ± 5.3	174.6 ± 3.9	0.089	159.2 ± 4.7	160.0 ± 5.2	0.74
Weight (kg)	84.3 ± 16.8	94.0 ± 13.8	0.139	70.0 ± 6.4	76.8 ± 14.2	0.297
BMI (kg/m^2)	28.6 ± 4.63	30.7 ± 3.8	0.248	27.5 ± 1.8	29.9 ± 4.2	0.234
HC (cm)	90.5 ± 11.3	97.5 ± 7.8	0.102	78.6 ± 4.2	84.9 ± 7.1	0.082
WC (cm)	103.8 ± 7.9	109.0 ± 9.2	0.124	99.3 ± 4.6	104.4 ± 9.1	0.048
WH-R	0.86 ± 0.07	0.89 ± 0.03	0.11	0.79 ± 0.04	0.82 ± 0.04	0.152
OI (%)	131.0 ± 20.5	139.3 ± 17.1	0.29	132.3 ± 9.4	143.1 ± 18.6	0.221
Fat (%)	31.7 ± 6.3	33.0 ± 5.3	0.586	41.6 ± 3.7	42.1 ± 4.5	0.778
Fat mass (kg)	27.6 ± 12.0	31.6 ± 9.0	0.376	29.6 ± 3.9	32.6 ± 7.9	0.195
SBP(mm Hg)	124.2 ± 13.3	129.3 ± 18.2	0.39	114.8 ± 8.4	118.8 ± 12.6	0.35
DBP(mm Hg)	76.1 ± 7.6	82.6 ± 16.2	0.277	71.0 ± 6.0	76.3 ± 8.3	0.078

MS, metabolic syndrome; BMI, body mass index; HC, hip circumference; WC, waist circumference; WH-R, waist hip ratio; OI, obesity index; SBP, systolic blood pressure; DBP, diastolic blood pressure.

TABLE 3 | Comparison of biochemistry parameters in obese adolescents.

	Male ($n = 31$)			Female ($n = 34$)		
	MS(–) ($n = 22$)	**MS(+) ($n = 9$)**	***P***	**MS(–) ($n = 28$)**	**MS(+) ($n = 6$)**	***P***
Glucose(mg/dL)	91.3 ± 7.3	86.2 ± 7.1	0.089	85.7 ± 4.4	89.3 ± 10.2	0.433
Insulin (mU/L)	17.1 ± 9.1	18.9 ± 10.4	0.667	13.0 ± 5.7	24.1 ± 21.5	0.265
HOMA-IR	3.8 ± 1.8	4.0 ± 2.3	0.742	2.7 ± 1.2	5.6 ± 5.8	0.277
TC (mg/dL)	161.7 ± 33.8	152.7 ± 36.5	0.517	165.8 ± 31.1	196.6 ± 24.3	0.031
LDL-C (mg/dL)	99.9 ± 26.2	91.3 ± 30.1	0.433	96.7 ± 27.5	131.1 ± 19.5	0.007
TG (mg/dL)	81.4 ± 36.4	145.3 ± 60.9	0.001	61.6 ± 26.8	151.8 ± 36.1	0.001
HDL-C (mg/dL)	51.0 ± 6.8	45.5 ± 2.6	0.003	59.4 ± 9.8	44.6 ± 2.6	0.000
AST (IU/L)	22.2 ± 6.8	39.1 ± 22.5	0.056	22.0 ± 6.4	30.3 ± 30.2	0.533
ALT (IU/L)	29.9 ± 16.0	52.7 ± 34.2	0.086	17.5 ± 10.1	47.5 ± 65.1	0.313
hs-CRP (mg/L)	1.4 ± 2.1	1.2 ± 2.0	0.828	1.6 ± 2.0	1.5 ± 1.3	0.888
IL-6 (pg/mL)	6.5 ± 3.3	4.9 ± 1.7	0.21	7.1 ± 7.1	6.2 ± 1.4	0.782
TNF-a (pg/mL)	3.4 ± 2.5	3.0 ± 2.2	0.804	31.4 ± 77.5	1.7 ± 2.2	0.537
Leptin (ug/L)	8.3 ± 4.7	9.7 ± 4.6	0.486	17.4 ± 6.5	18.9 ± 3.5	0.626
Adiponectin(ng/mL)	7379.5 ± 4789.6	6788.3 ± 2960.4	0.751	8514.3 ± 2938.4	5469.4 ± 1054.2	0.001
FFA (uEq/L)	561.6 ± 294.5	660.8 ± 358.4	0.434	655.3 ± 429.4	777.1 ± 174.3	0.504
IGFBP-3 (ng/mL)	3782.7 ± 508.7	3577.3 ± 413.4	0.295	3598.7 ± 491.3	4108.3 ± 258.4	0.02

MS, metabolic syndrome; HOMA-IR, homeostasis model assessment of insulin resistance; AST, aspartate aminotransferase; ALT, alanine aminotransferase; TC, total cholesterol; LDL-C, low density lipotrotein cholesterol; TG, triglyceride; HDL-C, high density lipotrotein cholesterol; hs-CRP, high sensitive C reactive protein; IL-6, interleukin-6; TNF, tumor necrosis factor; FFA, free fatty acid; IGFBP, insulin growth factor binding protein.

Correlation Between Visceral Fat Tissue and Other Metabolic Parameters

Visceral fat tissue is significantly associated with WC, DBP, TG, LDL-C, TC, glucose, BMI, HC, waist-hip ratio (WHR), OI, Fat mass, insulin, HOMA-IR, and leptin in **Table 9**.

DISCUSSION

Given that there is no well-established uniform definition of childhood MS (1), most frequently used definitions have been adopted from the Adult Treatment Panel III (ATP III) definition, modified and adapted by Cook et al. (12). And the IDF made the definition of MS in children $\geq$ 10 years of age in 2007 to find the global prevalence of MS. These two measurement definitions had different cut off levels for hyperglyceridemia and elevated blood pressure. In this study of MS in obese adolescents, we applied modified Cook's definitions of the ATP III definitions.

Prevalence of MS in adolescent in representative studies was 28.7% in the study of cook et al. (12). In this study, we found the

TABLE 4 | Comparison of geometrical parameters of carotid artery in the obese adolescents.

	Male ($n = 31$)			Female ($n = 34$)		
	MS(–) ($n = 22$)	**MS(+) ($n = 9$)**	***P***	**MS(–) ($n = 28$)**	**MS(+) ($n = 6$)**	***P***
IMT (mm)	0.6 ± 0.2	0.6 ± 0.1	0.67	0.5 ± 0.1	0.6 ± 0.2	0.506
S diameter (mm)	6.4 ± 0.1	6.4 ± 0.7	0.827	5.3 ± 0.5	5.3 ± 0.5	0.997
D diameter (mm)	6.5 ± 0.7	13.8 ± 21.5	0.367	6.0 ± 0.5	17.2 ± 24.5	0.366
LCSA (m^2)	28.7 ± 7.0	28.8 ± 4.2	0.986	22.3 ± 4.0	22.5 ± 4.1	0.895
WCSA (m^2)	12.4 ± 6.2	11.5 ± 3.3	0.689	9.3 ± 2.5	10.9 ± 4.8	0.284
CSC	0.2 ± 0.1	0.1 ± 0.1	0.207	0.1 ± 0.1	0.2 ± 0.1	0.179
CSD	0.01 ± 0.00	0.00 ± 0.00	0.183	0.01 ± 0.00	0.01 ± 0.00	0.208

MS, metabolic syndrome; IMT, intimal medial thickness; S diameter, carotid artery systolic diameter; D diameter, carotid artery diastolic diameter; LCSA, Lumen cross-sectional area; WCSA, wall cross-sectional area; CSC, cross-sectional compliance; CSD, cross-sectional distensibility.

TABLE 5 | Comparison of abdominal sonographic data in the obese adolescents.

	Total ($n = 65$)			Male ($n = 31$)		Female ($n = 34$)		
	MS (–) ($n = 50$)	**MS(+) ($n = 15$)**	***p***	**MS(–) ($n = 22$)**	**MS(+) ($n = 9$)**	**MS(–) ($n = 28$)**	**MS(+) ($n = 6$)**	***P***
VFT (mm)	34.6 ± 13.1	38.3 ± 12.7	0.038	37.9 ± 17.9	37.4 ± 20.2	31.1 ± 6.9	42.0 ± 7.5	0.034
SFT (mm)	20.5 ± 6.9	21.2 ± 4.8	0.595	21.4 ± 7.8	19.9 ± 5.7	19.4 ± 5.5	23.2 ± 2.3	0.455
PFT (mm)	12.8 ± 3.9	12.9 ± 3.4	0.996	10.9 ± 4.5	13.7 ± 4.8	14.9 ± 3.8	12.4 ± 2.3	0.957

VFT, visceral fat tissue; SFT, subcutaneous fat tissue; PFT, properitoneal fat tissue.

TABLE 6 | Comparison of echocardiographic data in the obese adolescents.

	Total ($n = 65$)			Male ($n = 31$)		Female ($n = 34$)		
	MS(–) ($n = 50$)	**MS(+) ($n = 15$)**	***P***	**MS(–) ($n = 22$)**	**MS(+) ($n = 9$)**	**MS(–) ($n = 28$)**	**MS(+) ($n = 6$)**	***P***
SV (mL)	63.5 ± 9.8	59.5 ± 14.4	0.065	66.7 ± 10.2	62.4 ± 9.4	61.8 ± 19.8	56.3 ± 11.5	0.767
CO (L)	4.7 ± 1.1	4.2 ± 0.9	0.065	4.7 ± 0.7	4.3 ± 1.0	4.7 ± 1.6	4.2 ± 0.8	0.631
IVS (mm)	1.0 ± 0.7	0.8 ± 0.6	0.167	0.9 ± 0.1	0.9 ± 0.1	1.0 ± 1.3	0.8 ± 0.1	0.265
PWT (mm)	0.9 ± 0.1	0.9 ± 0.1	0.725	1.0 ± 0.1	1.0 ± 0.1	0.8 ± 0.1	0.8 ± 0.1	0.999
EF (%)	61.3 ± 6.0	60.5 ± 3.8	0.465	59.5 ± 7.0	61.0 ± 3.7	62.8 ± 5.5	59.4 ± 3.7	0.595
FS (%)	32.8 ± 4.5	32.3 ± 2.8	0.74	32.3 ± 3.5	32.9 ± 2.7	33.9 ± 4.8	31.4 ± 2.9	0.104
LVM (g)	176 ± 36.7	211.6 ± 45.9	0.012	205.9 ± 44.5	258.7 ± 59.0	141.3 ± 21.0	158.0 ± 36.7	0.001
LVMI (g/m^2)	1.8 ± 0.7	2.2 ± 0.33	0.065	1.9 ± 0.4	2.4 ± 0.5	1.6 ± 0.2	1.9 ± 0.34	0.053
MVE (m/sec)	0.99 ± 0.2	0.93 ± 0.3	0.678	1.0 ± 0.2	0.9 ± 0.2	0.99 ± 0.2	0.95 ± 0.2	0.567
MVA(m/sec)	0.5 ± 0.1	0.5 ± 0.1	0.225	0.5 ± 0.1	0.5 ± 0.1	0.5 ± 0.1	0.5 ± 0.1	0.997
MVE/A	1.9 ± 0.6	2.0 ± 0.6	0.559	1.8 ± 0.4	2.1 ± 0.6	2.0 ± 0.5	2.0 ± 0.6	0.273
MVE-DT (ms)	152.6 ± 25.7	145.3 ± 36.8	0.381	159.7 ± 28.8	147.3 ± 36.7	148.3 ± 21.8	141.8 ± 36.8	0.886
EFT (PSAX) (mm)	0.2 ± 0.2	0.2 ± 0.04	0.68	0.2 ± 0.1	0.2 ± 0.03	0.2 ± 0.02	0.2 ± 0.04	0.978

MS, metabolic syndrome; SV, stroke volume; CO, cardiac output; IVS, interventricular septal thickness; PWT, posterior wall thickness; EF, ejection fraction; FS, fraction shortening; LVM, left ventricle Mass; LVMI, left ventricle mass index; E, early diastolic velocity; A, late atrial peak velocity; DT, deceleration time; EFT (PSAX), epicardial fat thickness at parasternal short axis view.

prevalence of MS in obese children was 23.1% (15/65) similar to previous studies.

It seems appropriate to apply the same factors from adults in establishing a definition of MS in adolescent, such as the dyslipidemia, hypertension, and obesity which tend to track into adulthood (12). But some components need further correction in adolescents. For instance, impaired fasting glucose is very low but impaired glucose tolerance is fairly common in childhood (13, 14). So fasting glucose threshold need to be lowered and impaired glucose tolerance should be proposed as components of the MS (15). The cut off level for fasting glucose it our study is 110 mg/dL, which is lower than that of ATPIII. Aside from this,

TABLE 7 | Comparison of pulse wave velocity and ankle brachial index in obese adolescents.

	Male ($n = 31$)			Female ($n = 34$)		
	Ms(–) ($n = 22$)	**MS(+) ($n = 9$)**	***P***	**MS(–) ($n = 28$)**	**MS(+) ($n = 6$)**	***P***
HR (/min)	73.4 ± 8.4	70.6 ± 9.2	0.323	70.6 ± 9.1	75.2 ± 10.1	0.134
RbaPWV (cm/s)	1102.8 ± 120.1	1117.8 ± 138.2	0.639	931.5 ± 92.8	946.5 ± 100.4	0.401
LbaPWV (cm/s)	1130.2 ± 115.1	1112.0 ± 143.2	0.843	913.3 ± 101.2	952.1 ± 103.2	0.221
RABI	102.8 ± 7.9	105.1 ± 6.5	0.321	105.8 ± 7.2	101.7 ± 6.8	0.088
LABI	104.1 ± 6.7	106.7 ± 5.4	0.601	106.5 ± 6.8	100.4 ± 7.9	0.021

MS, metabolic syndrome; HR, Heart rate; RbaPWV, right brachial ankle pulse wave velocity; LbaPWV, left brachial ankle pulse wave velocity; RBAI, right brachial ankle index; LBAI, left brachial ankle index.

TABLE 8 | Correlation between LV mass and other metabolic parameters.

	Estimate	**SE**	**Lower CL**	**Upper CL**	***P***
BMI (kg/m^2)	4.385	1.244	1.883	6.886	0.009
HC (cm)	2.121	0.639	0.835	3.406	0.017
Fat mass (kg)	1.767	0.543	0.673	2.861	0.022
OI (%)	0.922	0.287	0.343	1.5	0.052
Insulin (mU/L)	1.261	0.442	0.371	2.15	0.046
HOMA-IR	5.06	1.841	1.359	8.762	0.084
TC (mg/dL)	0.386	0.146	0.092	0.68	0.022
LDL-C (mg/dL)	0.397	0.168	0.059	0.734	0.012
WC (cm)	1.298	0.576	0.141	2.455	0.028

BMI, body mass index; HC, hip circumference; OI, obesity index; HOMA-IR, homeostasis model assessment of insulin resistance; TC, total cholesterol; WC, waist circumference; LDL –C, low density lipoprotein-cholesterol.

TABLE 9 | Correlations between visceral fat tissue and other metabolic parameters.

Variable	**Estimate**	**StdErr**	**LowerCL**	**UpperCL**	***P***
WC (cm)	1.074	0.19	0.692	1.455	<0.001
DBP (mm Hg)	0.476	0.205	0.065	0.887	0.024
TG (mg/dL)	0.118	0.041	0.036	0.199	0.006
LDL-C (mg/dL)	0.203	0.065	0.072	0.335	0.003
TC (mg/dL)	0.199	0.056	0.086	0.313	0.001
Glucose (mg/dL)	−0.59	0.285	−1.163	−0.018	0.044
BMI (kg/m^2)	2.537	0.43	1.673	3.401	<0.0001
HC (cm)	1.208	0.228	0.75	1.666	<0.0001
WHR	98.053	45.313	6.945	189.161	0.036
OI	0.553	0.101	0.35	0.756	<0.0001
Fat %	1.743	0.388	0.962	2.524	<0.0001
Fat mass (kg)	1.138	0.179	0.777	1.498	<0.0001
Insulin (mU/L)	0.548	0.177	0.193	0.903	0.003
HOMA-IR	1.958	0.75	0.451	3.466	0.012
Leptin (ug/L)	0.792	0.381	0.024	1.56	0.043

WC, waist circumference; DBP, diastolic blood pressure; TG, triglyceride; LDL-C, low density lipotrotein-cholesterol; TC, total cholesterol; BMI, body mass index; HC, hip circumference; WHR, waist hip ratio; OI, obesity index; HOMA-IR, homeostasis model assessment of insulin resistance.

the pubertal status, age range, ethnicity need to be considered in defining MS of adolescents (1, 7).

Visceral fat is usually measured by WC or other imaging methods. Among the parameters of MS, WC is easy and practical for screening children at risk of MS (2). Although WC is a better marker and widely used parameter of abdominal adipose tissue accumulation than the BMI, the increased WC is not sufficient to define visceral obesity alone, because of increased subcutaneous

fat (16). In this study, we used abdominal sonographic method to estimate the visceral fat and found that VFT had significant correlation with WC.

The accumulation of visceral fat contrary to abdominal subcutaneous fat plays a significant role in the pathophysiology of the MS with insulin resistance in adolescent (17, 18). Visceral fat accumulation affects the adipose tissue to over secret leptin and hyposecretion of adiponectin (14).

Leptins correlate with BMI in children. High plasma leptin level is related to the development of essential hypertension, hyperinsulinemia and dyslipidemia (19). Adiponectin originates mainly from adipocytes and is an adipocytokine that is acting against atherogenic, diabetic and pro-inflammatory effect (8). Decreased adiponectin levels are associated with dysmetabolic state and cause MS. Furthermore, visceral obesity may lead to ectopic fat deposition in skeletal muscle, liver, heart, etc. (16). In this study, there was increased VFT in both MS male and MS female compared to control.

EFT at right ventricle, left ventricular apex and atrium seems to correlate with visceral fat and act as cardiometabolic risk factor (20). Measuring echocardiographic epicardial fat tissue can be used as a method for quantification of visceral fat. The epicardial adipose tissue contact and interact with the myocardial tissue and coronary arteries by secreting pro-inflammatory cytokines and vasoactive peptides (6). These molecules can develop glucose intolerance and atherosclerosis and increase cardiovascular risk (6, 21). In our study, we found an increased EFT both in MS males and MS females.

Obesity and MS demand increased metabolic and blood supply due to greater adipose tissue, which increase blood volume and cardiac preload. And vascular alterations such as arterial stiffness and peripheral resistance increase afterload to the heart. Finally, they incur LV hypertrophy and LV diastolic dysfunction (22, 23). In our study, there was significant increase in LVM and LVMI in MS male. MS female also showed some trend of increased LVM without significance. In short, this study found VFT and LVM is significantly correlated with metabolic and cardiac parameters. So, screening for the MS in overweight adolescents may help to predict future cardiovascular disease.

As CVD is mainly result of atherosclerosis, the predictors of atherosclerosis are important. And CIMT is a highly predictive marker of progression of atherosclerosis in patients with MS (24). However, we could not find abnormal CIMT from both MS and non-MS groups in this study. This might be due to young age groups whose peripheral artery is very resistant to local vascular inflammation and atherosclerosis progression. Also, baPWV data from our study was not efficient either. In our study, female LABI only showed statistically significant difference. The reason why there was no statistical difference between the remaining data is believed to be due to the low accuracy of the test. Because baPWV method include peripheral vessels, it is less accurate and does not reflect the degree of arteriosclerosis in the central blood vessels, but rather changes in peripheral arteries can be reflected. Carotid-femoral PWV (cfPWV) is better alternative since it predicted cardiovascular mortality (25). However, femoral artery waveforms in cfPWV measure are difficult to accurately record in metabolic syndrome, obesity, diabetes, peripheral artery patients. So, we suggest other non-invasive and high accuracy central blood pressure measurements such as radial tonometry or brachial cuff pulse volume plethysmography for future research (26).

Previous studies of MS in adolescents showed abundant evidence of risk factors for CVD (18). For example, autopsy studies in childhood showed that obesity, high BP, high TG, and low HDL-C are related to coronary atherosclerosis (27, 28). So, early identification of these risk factors is important in chronic disease prevention (29, 30). In the present study, we found significant differences in VFT and LVM in obese adolescents with MS.

Hyperinsulinemia and insulin resistance are well-known risk factors for CVD. Hyperinsulinemia directly contributes to deteriorated renal function and increased risk of CVD (31). The foremost mechanism is an up-regulation of the renin-angiotensin system, which contribute to begin hypertension, heart failure and atherosclerosis (32). These hyperinsuliemia, insulin resistance and finally upregulated renin-angiotensin system, are thought to contribute to endothelial dysfunction, atherosclerosis and CVD (32). Another story of insulin dysregulation is insulin resistance syndrome (IRS). IRS comprise of hyperinsulinemia, dyslipidemia, hypertension, and obesity. A child whose parents have IRS have greater insulin resistance and CVD risks compared with those who do not (33). So, IRS in adolescent is of potential importance, because of the high prevalence of impaired glucose tolerance and obesity, and the increasing incidence of type 2 diabetes in adolescent (34).

Adolescent obesity-induced other metabolic complication is hyperuricemia. In our study, we did not collect uric acid levels. But uric acid is associated with cardiovascular, renal and metabolic diseases. It is because serum uric acid (SUA) is known as an antioxidant factor in the extracellular space, but as a pro-oxidant factor inside the cell (35).

Among these diseases, the link between SUA levels and hypertension seem to be the strongest. When children with high SUA were followed for 10 years, high incidence of MS in male subjects are observed (36). Also increased SUA is associated with new-onset primary hypertension in children (37). It is noted that hypertensive children with elevated SUA have a higher prevalence of obesity-related CVD (38). And one observational cohort study shows uric acid elevation is commonly found in hypertriglyceridemia, obesity, insulin resistance and hypertension. But they failed to show low uric acid level in well-controlled hypertension patients. Until now, whether elevated uric acid level actually causes CVD or increase MS remains to be confirmed (39).

There are several limitations to this study. First, the study included small cohort not enough to analyze all the data for each gender. Further research with large adolescent population is inevitable. Second, there is absence of follow up data. Third, there is lack of comprehensive assessment according to diverse adolescent age group, because the age range is confined to 15–18. Finally, even though measurements were conducted by same sonographer, there could be some intraobserver variability of reproducibility of measuring the parameters such as IMT, VFT, and EFT due to the sonographer's subjectivity. This could have been avoided by performing three measurements and averaging them.

Since the time between adolescent obesity and occurrence of clinical disease is relatively short, longitudinal prospective design dealing from adolescence to adulthood is needed to explore the complexity of interrelation of MS risk factors. The prospective study of longer time course may offer a better opportunity in adolescent obesity and CVD risk research.

Overall, We defined adolescent MS as to meet more than 3 categories (WC $\geq$ 90th percentile, BP $\geq$ 90th percentile, TG $\geq$ 110 mg/dL, HDL $\leq$ 40 mg/dL, fasting glucose $\geq$ 110 mg/dL). The study subjects are obese male and female adolescents defined as BMI above the 95th percentile for age and sex by the survey of Korean Centers of Disease Control and Prevention in 2007. In this setting, we found both VFT in inn total and female MS group and LVM in total and male adolescents were increased. Although there were statistical differences between male and female adolescents, it is meaningful that there were differences in VFT and LVM between the entire MS and non-MS groups.

In conclusion, one can assume that VFT and LVM are appropriate and possible markers for predicting increased future cardiovascular risk in obese adolescents.

DATA AVAILABILITY STATEMENT

The raw data supporting the conclusions of this article will be made available by the authors, without undue reservation.

ETHICS STATEMENT

The studies involving human participants were reviewed and approved by IRB at Ewha Womans University (Approval No: 0319/12/06.2020). Written informed consent to participate in this study was provided by the participants' legal guardian/next of kin.

AUTHOR CONTRIBUTIONS

JL, YH, and HK: conceptualization. JL: methodology, formal analysis, data curation, writing—original draft, and supervision. HK: investigation. YH and HK: writing—review and editing. All authors contributed to the article and approved the submitted version.

REFERENCES

1. Ford ES, Li C. Defining the metabolic syndrome in children and adolescents: will the real definition please stand up? *J Pediatr.* (2008) 152:160–4. doi: 10.1016/j.jpeds.2007.07.056
2. Zimmet P, Alberti KG, Kaufman F, Tajima N, Silink M, Arslanian S, et al. The metabolic syndrome in children and adolescents - an IDF consensus report. *Pediatr Diabetes.* (2007) 8:299–306. doi: 10.1111/j.1399-5448.2007.00271.x
3. McCracken E, Monaghan M, Sreenivasan S. Pathophysiology of the metabolic syndrome. *Clin Dermatol.* (2018) 36:14–20. doi: 10.1016/j.clindermatol.2017.09.004
4. Neeland IJ, Ross R, Després JP, Matsuzawa Y, Yamashita S, Shai I, et al. International atherosclerosis society; international chair on cardiometabolic risk working group on visceral obesity. Visceral and ectopic fat, atherosclerosis, and cardiometabolic disease: a position statement. *Lancet Diabetes Endocrinol.* (2019) 7:715–25. doi: 10.1016/S2213-8587(19)30084-1
5. Spoto B, Betta ED, Mattace-Raso F, Sijbrands E, Vilardi A, Parlongo RM, et al. Pro- and anti-inflammatory cytokine gene expression in subcutaneous and visceral fat in severe obesity. *Nutr Metab Cardiovasc Dis.* (2014) 24:1137–43. doi: 10.1016/j.numecd.2014.04.017
6. Iacobellis G, Barbaro G. The double role of epicardial adipose tissue as pro- and anti-inflammatory organ. *Horm Metab Res.* (2008) 40:442–5. doi: 10.1055/s-2008-1062724
7. Korner A, Kratzsch J, Gausche R, Schaab M, Erbs S, Kiess W. New predictors of the metabolic syndrome in children—role of adipocytokines. *Pediatr Res.* (2007) 6:640–5. doi: 10.1203/01.pdr.0000262638.48304.ef
8. Gnacińska M, Małgorzewicz S, Stojek M, Łysiak-Szydłowska W, Sworczak K. Role of adipokines in complications related to obesity: a review. *Adv Med Sci.* (2009) 54:150–7. doi: 10.2478/v10039-009-0035-2
9. Chen W, Srinivasan SR, Elkasabany A, Berenson GS. Cardiovascular risk factors clustering features of insulin resistance syndrome (Syndrome X) in a biracial (Black-White) population of children, adolescents, and young adults: the Bogalusa Heart Study. *Am J Epidemiol.* (1999) 150:667–74. doi: 10.1093/oxfordjournals.aje.a010069
10. Oh KW, Jang MJ, Lee NY, Moon JS, Lee CG, Yoo MH, et al. Prevalence and trends in obesity among Korean children and adolescents in 1997 and 2005. *Korean J Pediatr.* (2008) 51:950–5. doi: 10.3345/kjp.2008.51.9.950
11. Syed-Abdul MM, Soni DS, Barnes JT, Wagganer JD. Comparative analysis of BIA, IBC and DXA for determining body fat in American Football players. *J Sports Med Phys Fitness.* (2021) 61:687–92. doi: 10.23736/S0022-4707.21.11278-2
12. Cook S, Weitzman M, Auinger P, Nguyen M, Dietz WH. Prevalence of a metabolic syndrome phenotype in adolescents: find-ings from the third National Health and Nutrition Examination Survey, 1988–1994. *Arch Pediatr Adolesc Med.* (2003) 157:821–7. doi: 10.1001/archpedi.157.8.821
13. Sinha R, Fisch G, Teague B, Tamborlane WV, Banyas B, Allen K, et al. Prevalence of impaired glucose tolerance among children and adolescents with marked obesity. *N Engl J Med.* (2002) 346:802–10. doi: 10.1056/NEJMoa012578
14. Goran MI, Bergman RN, Avila Q, Watkins M, Ball GD, Shaibi GQ, et al. Impaired glucose tolerance and reduced beta-cell function in overweight Latino children with a positive family history for type 2 diabetes. *J Clin Endocrinol Metab.* (2004) 89:207–12. doi: 10.1210/jc.2003-031402
15. The Expert Committee on the Diagnosis and Classification of Diabetes Mellitus. Follow-up report on the diagnosis of diabetes mellitus. *Diabetes Care.* (2003) 26:3160–7. doi: 10.2337/diacare.26.11.3160
16. Després JP, Lemieux I, Bergeron J, Pibarot P, Mathieu P, Larose E, et al. Abdominal obesity and the metabolic syndrome: contribution to global cardiometabolic risk. *Arterioscler Thromb Vasc Biol.* (2008) 28:1039–49. doi: 10.1161/ATVBAHA.107.159228
17. Steinberger J, Daniels SR, Eckel RH, Hayman L, Lustig RH, McCrindle B, et al. American Heart Association atherosclerosis, hypertension, and obesity in the Young Committee of the Council on Cardiovascular Disease in the Young; Council on Cardiovascular Nursing; and Council on Nutrition, Physical Activity, and Metabolism. Progress and challenges in metabolic syndrome in children and adolescents: a scientific statement from the American Heart Association Atherosclerosis, Hypertension, and Obesity in the Young Committee of the Council on Cardiovascular Disease in the Young; Council on Cardiovascular Nursing; and Council on Nutrition, Physical Activity, and Metabolism. *Circulation.* (2009) 119:628–47. doi: 10.1161/CIRCULATIONAHA.108.191394
18. Cruz ML, Goran MI. The metabolic syndrome in children and adolescents. *Curr Diabetes Rep.* (2004) 4:53–62. doi: 10.1007/s11892-004-0012-x
19. Lago F, Gómez R, Gómez-Reino JJ, Dieguez C, Gualillo O. Adipokines as novel modulators of lipid metabolism. *Trends Biochem Sci.* (2009) 34:500–10. doi: 10.1016/j.tibs.2009.06.008
20. Gastaldeli A, Basta G. Ectopic fat and cardiovascular disease: what is the link? *Nutr Metab Cardiovasc Dis.* (2010) 20:481–90. doi: 10.1016/j.numecd.2010.05.005
21. Iacobellis G, Gao YJ, Sharma AM. Do cardiac and perivascular adipose tissue play a role in atherosclerosis? *Curr Diab Rep.* (2008) 8:20–4.

22. Bokor S, Frelut ML, Vania A, Hadjiathanasiou CG, Anastasakou M, Malecka-Tendera E, et al. Prevalence of metabolic syndrome in European children. *Int J Pediatr Obes.* (2008) 2:3–8. doi: 10.1080/17477160802404509
23. Cote AT, Harris KC, Panagiotopoulos C, Sandor GG, Devlin AM. Childhood obesity and cardiovascular dysfunction. *J Am Coll Cardiol.* (2013) 62:1309–19. doi: 10.1016/j.jacc.2013.07.042
24. Mazurek T, Zhang L, Zalewski A, Mannion JD, Diehl JT, Arafat H, et al. Human epicardial adipose tissue is a source of inflammatory mediators. *Circulation.* (2003) 108:2460–6. doi: 10.1161/01.CIR.0000099542.57313.C5
25. Pannier B, Guérin AP, Marchais SJ, Safar ME, London GM. Stiffness of capacitive and conduit arteries. Prognostic significance for end-stage renal disease patients. *Hypertension.* (2005) 45:592–6. doi: 10.1161/01.HYP.0000159190.71253.c3
26. McEniery CM, Cockcroft JR, Roman MJ, Franklin SS, Wilkinson IB. Central blood pressure: current evidence and clinical importance. *Eur Heart J.* (2014) 35:1719–25. doi: 10.1093/eurheartj/eht565
27. Berenson GS, Srinivasan SR, Bao W, Newman WP, Tracy RE, Wattigney WA. Association between multiple cardiovascular risk factors and atherosclerosis in children and young adults. The Bogalusa Heart Study. *N Engl J Med.* (1998) 338:1650–56. doi: 10.1056/NEJM199806043382302
28. McGill HC, McMahan CA, Herderick EE, Zieske AW, Malcom GT, Tracy RE, et al. Pathobiological determinants of atherosclerosis in youth (PDAY) research group. Obesity accelerates the progression of coronary atherosclerosis in young men. *Circulation.* (2002) 105:2712–8. doi: 10.1161/01.CIR.0000018121.67607.CE
29. Sardinha LB, Santos DA, Silva AM, Grøntved A, Andersen LB, Ekelund U. A comparison between BMI, waist circumference, and waist-to-height ratio for identifying cardio-metabolic risk in children and adolescents. *PLoS ONE.* (2016) 11:e0149351. doi: 10.1371/journal.pone.0149351
30. Wicklow BA, Becker A, Chateau D, Palmer K, Kzyrskij A, Sellers EA. Comparison of anthropometric measurements in children to predict metabolic syndrome in adolescence: analysis of prospective cohort data. *Int J Obes.* (2015) 39:1070–8. doi: 10.1038/ijo.2015.55
31. Chen J, Muntner P, Hamm LL, Fonseca V, Bautman V, Whelton PK, et al. Insulin resistance and risk of chronic kidney disease in nondiabetic US adults. *J Am Soc Nephrol.* (2003) 14:469–77. doi: 10.1097/01.ASN.0000046029.5333.09
32. Liu Z. The renin-angiotensin system and insulin resistance. *Curr Diab Rep.* (2007) 7:34–42. doi: 10.1007/s11892-007-0007-5
33. James SP, David RJ, Julia S, Antoinette M, Alan RS. Insulin resistance and cardiovascular disease risk factors in children of parents with the insulin resistance (metabolic) syndrome. *Diabetes Care.* (2004) 27:775–80. doi: 10.2337/diacare.27.3.775
34. Rosenbloom AL, Joe JR, Young RS, Winter WE. Emerging epidemic of type 2diabetes in youth. *Diabetes Care.* (1999) 22:345–54. doi: 10.2337/diacare.22.2.345
35. Johnson RJ, Sánchez-Lozada LG, Mazzali M, Feig DI, Kanbay M, Sautin YY. What are the key arguments against uric acid as a true risk factor for hypertension? *Hypertension.* (2013) 61:948–51. doi: 10.1161/HYPERTENSIONAHA.111.00650
36. Sun HL, Pei D, Lue KH, Chen YL. Uric acid levels can predict metabolic syndrome and hypertension in adolescents: a 10-year longitudinal study. *PLoS ONE.* (2015) 10:e0143786. doi: 10.1371/journal.pone.0143786
37. Feig DI, Johnson RJ. Hyperuricemia in childhood primary hypertension. *Hypertension.* (2003) 42:247–52. doi: 10.1161/01.HYP.0000085858.66548.59
38. Lauren DR, Edgar RM, Jeffrey JF, Lauren FL, Kathryn WH, Lawrence JA, et al. Elevated uric acid and obesity-related cardiovascular disease risk factors among hypertensive youth. *Pediatric Nephrology.* (2015) 30:2169–76. doi: 10.1007/s00467-015-3154-y
39. Michael HA, Hillel C, Shantha M, Salah K. Serum Uric Acid and Cardiovascular Events in Successfully Treated Hypertensive Patients. *Hypertension.* (1999) 34:144–50. doi: 10.1161/01.HYP.34.1.144

Conflict of Interest: The authors declare that the research was conducted in the absence of any commercial or financial relationships that could be construed as a potential conflict of interest.

Publisher's Note: All claims expressed in this article are solely those of the authors and do not necessarily represent those of their affiliated organizations, or those of the publisher, the editors and the reviewers. Any product that may be evaluated in this article, or claim that may be made by its manufacturer, is not guaranteed or endorsed by the publisher.

frontiers in Pediatrics

ORIGINAL RESEARCH
published: 06 December 2021
doi: 10.3389/fped.2021.786638

Hyperactivity and Inattention in Young Patients Born With an Atrial Septal or Ventricular Septal Defect

Sara Hirani Lau-Jensen[1*], *Benjamin Asschenfeldt*[2,3], *Lars Evald*[4] *and Vibeke E. Hjortdal*[1,2]

[1] *Department of Cardiothoracic Surgery, Rigshospitalet, University of Copenhagen, Copenhagen, Denmark,* [2] *Department of Clinical Medicine, Aarhus University, Aalborg, Denmark,* [3] *Department of Cardiothoracic and Vascular Surgery, Aarhus University Hospital, Aarhus, Denmark,* [4] *Hammel Neurodelvelopmental Center and University Research Clinic, Hammel, Denmark*

Background: Patients with congenital heart defects have a well-established risk of neuropsychiatric comorbidities. Inattention and hyperactivity are three to four times more frequent in children with complex congenital heart defects. We have previously shown a higher burden of overall attention deficit/hyperactivity disorder (ADHD) symptoms in adults with simple congenital heart defects as well. However, it is unknown whether the higher burden of ADHD symptoms is mainly driven by hyperactivity, inattention, or both.

Methods: The participants [simple congenital heart defect = 80 (26.6 years old), controls = 36 (25.3 years old)] and a close relative for each ($n = 107$) responded to the long version of the Conners' Adults ADHD Rating Scales questionnaire. Our primary and secondary outcomes are mean T-scores in the ADHD scores and symptom sub-scores.

Results: Patients with simple congenital heart defects reported a higher mean T-score at all three DSM-IV ADHD scores (ADHD—combined: 52.8 vs. 44.9, $p = 0.007$, ADHD—inattention: 55.5 vs. 46.4, $p = 0.002$, and ADHD—hyperactivity: 49.4 vs. 44.0, $p = 0.03$) and in all four ADHD symptom sub-scores (inattention/memory problems: 50.3 vs. 44.2, $p = 0.001$, hyperactivity/restlessness: 49.7 vs. 45.9, $p = 0.03$, impulsivity/emotional lability: 50.0 vs. 41.3, $p = 0.001$, and self-esteem problems: 53.8 vs. 46.3, $p = 0.003$). The results were maintained after the removal of outliers (incongruent responses), albeit the hyperactivity/restlessness ADHD symptom sub-score lost significance. Self- and informant ratings differed significantly on the ADHD—inattention score for the congenital heart defect group, where informants rated the ADHD—inattention scores better than the congenital heart defect patients rated themselves.

Conclusions: Patients with a simple congenital heart defect have a higher symptom burden across all ADHD scores and all symptom sub-scores. The higher burden of ADHD is driven by both inattention and hyperactivity symptoms, though the inattention symptoms seem more prominent. Close relatives were less aware of the inattention symptoms than the congenital heart defect patients themselves. Routine screening for

OPEN ACCESS

Edited by:
Ruth Heying,
University Hospital Leuven, Belgium

Reviewed by:
Daniel J. Licht,
Children's Hospital of Philadelphia, United States
Katya Els De Groote,
Ghent University Hospital, Belgium

****Correspondence:***
Sara Hirani Lau-Jensen
sara.hirani.lau-jensen@regionh.dk

Specialty section:
This article was submitted to Pediatric Cardiology, a section of the journal Frontiers in Pediatrics

Received: *30 September 2021*
Accepted: *01 November 2021*
Published: *06 December 2021*

Citation:
Lau-Jensen SH, Asschenfeldt B, Evald L and Hjortdal VE (2021) Hyperactivity and Inattention in Young Patients Born With an Atrial Septal or Ventricular Septal Defect. Front. Pediatr. 9:786638. doi: 10.3389/fped.2021.786638

ADHD symptoms may be warranted to facilitate adequate help and guidance as these symptoms are easily overlooked.

Clinical Trial Registration: www.ClinicalTrials.gov, identifier: NCT03871881.

Keywords: neuro-psychiatric disease, young adult, case - control, inattention, inattention deficit hyperactivity disorder, congenital hear defects, morbidity

INTRODUCTION

Congenital heart defects (CHDs) are the most common birth defect found in neonates (5.5–8/1,000 all births) (1, 2). With advancements in diagnostics and treatment, including pre-, peri-, and postoperative care and operation techniques, neonates with CHDs survive until childhood and adulthood (3–6). This alters the research focus from mortality to morbidity. A growing body of literature is found on morbidity in patients with complex CHDs. Less is found on patients with simple CHDs, even though the simple CHD is twice as common as the complex ones (2). Patients with CHDs (both complex and simple) have an increased risk of psychiatric and neurocognitive disabilities throughout life and twice the risk for being unemployed than the background population (7–15).

Attention deficit/hyperactivity disorder (ADHD) symptoms, such as inattention and hyperactivity, are found three to four times more frequent in children with complex CHDs (10). The severity of symptoms is found to be related to a disrupted brain network (16). The Diagnostic and Statistical Manual of Psychiatric Disorders, Edition IV (DSM-IV), published by the American Psychiatric Association, defines three different presentations of ADHD: ADHD—combined, ADHD—inattention, and ADHD—hyperactivity. ADHD—combined is diagnosed when clinically significant symptoms of both inattention and hyperactivity are present. In ADHD—inattention, symptoms of inattention are present without clinically significant symptoms of hyperactivity and *vice versa* in regard to ADHD—hyperactivity. In adults, ADHD has a negative impact on everyday life: ADHD increases the risk of unemployment and thereby lowers the overall income for the affected patient (17–19). Moreover, it decreases the quality of life not only for adults but also for children, adolescents, and their families. The negative effect is not entirely uniform but depends on the character and especially the severity of the ADHD symptoms (20).

We have previously found increased ADHD symptoms in patients with simple CHDs, looking at the overall ADHD score (15). It is unclear if the higher ADHD burden in these patients are driven mostly by hyperactivity or inattention symptoms. As these ADHD presentations differ in how they are perceived by others and differ in problem characteristics (21), it is important to make this distinction to best help the affected patients.

In this study, we aimed to evaluate the self- and informant-reported burden of ADHD symptoms in young adults with simple CHDs and investigate whether the symptoms are driven by sub-scores of inattention, hyperactivity, or both.

MATERIALS AND METHODS

The study complies with the Declaration of Helsinki (the World Medical Association, 2013). It is approved by the Danish Central Regional's Committee on Biomedical Research Ethics (chart: 1-10-72-233-17) and the Danish Data Protection Agency (chart: 2012-58-006). It is registered in clinicaltrials.gov (identifier: NCT03871881). All participants provided written informed consent prior to enrollment. The data that support the findings of this study are available from the corresponding author upon reasonable request.

Study Population

We included patients age >18 years with either an isolated atrial septal defect (ASD) or an isolated ventricular septal defect (VSD). We excluded patients with known syndromes (e.g., Trisomy 21), who had a previous stroke, with recent head trauma, who are pregnant, or who lack sufficient Danish language skills.

All patients had been diagnosed and treated for their CHD by a homogeneous group of anesthetists, cardiologists, and cardiac surgeons at Aarhus University Hospital, a tertiary referral hospital, in the years 1990 to 2000.

The study group was composed of 32 surgically closed VSDs, 34 surgically closed ASDs, 10 percutaneously closed ASDs, and four still open ASDs. The control group is composed of 39 healthy peers matched on age, gender, and educational level (International Standard Classification of Education 2011, ISCED).

Each participant provided a close relative (informant) to participate in the study as well.

Both the participants and their close relatives (informant) were asked to respond to the long version of the Conners' Adult ADHD Rating Scales (CAARS) questionnaire (total number of participants = 218).

Most of the participants in this study (except the participants with percutaneously closed ASDs and with open ASDs) have participated in a previous study by Asschenfeldt et al. (15). Please refer to this study for further detailed information on enrollment/recruitment procedures.

CAARS Questionnaire

The CAARS questionnaire consists of 66 questions, and it is designed to screen for ADHD symptoms. As an overall parameter, it provides an ADHD index score which is composed of the questions most likely to differentiate a person with ADHD from a person without ADHD. It is further composed of ADHD scores that differentiate between the DSM-IV diagnosis of the three presentations of ADHD:

(1) ADHD—combined, (2) ADHD—inattention, and (3) ADHD—hyperactivity.
It also includes four ADHD symptom sub-scores related to the ADHD diagnosis:

(1) inattention/memory problems, (2) hyperactivity/restlessness, (3) impulsivity/emotional lability, and (4) self-esteem problems.
The CAARS questionnaire is validated, and all ADHD scores and ADHD symptom sub-scores can be standardized to an age- and gender-corrected T-score (mean, 50; SD, 10) based on American normative data. Higher scores indicate a higher presence of symptoms.

An incongruent score for each participant can be calculated. A high incongruent score (>8) is most likely due to an unwilling participant, random answering, or a participant answering to make a specific impression. Exclusion of responses with an incongruent score >8 increases the validity of the answers.

Though the CAARS questionnaire is based on DSM-IV, the definition of ADHD has remained the same from DSM-IV and DSM-V.

Like most other psychiatric questionnaires, CAARS does not, by itself, provide a diagnosis. In this study, we will use the results to provide an estimate of a given burden of symptoms.

Statistics

The percentage of T-scores above 65 (corresponding to the 93rd percentile), representing a great likelihood for a clinical problem, was calculated for each group.

Data are presented as mean (±SD) or as *n* (%) where appropriate. Comparisons between all three groups were done with ANOVA, and when appropriate, *post-hoc* comparisons between two groups were made with either Welch *T*-test or Student's *T*-test.

Chi-square test was used to analyze a dichotomous outcome.

Our primary outcome was between group difference in the mean T-score of the four DSM-IV ADHD scores: ADHD—index, ADHD—combined presentation, ADHD—inattention presentation, and ADHD—hyperactivity presentation.

Post-hoc sub-analyses were done to compare the T-scores of the ADHD symptom sub-scores and to compare the primary outcome between subgroups of the surgically closed ASDs and the percutaneously closed ASDs.

Statistical analysis was performed on a with/without-outlier basis. Analysis of all participants was initially performed regardless of their incongruence score; however, in order to control for potential bias of outliers, patients with an incongruent score above 8 were excluded, and all of the above-mentioned analyses were rerun to test the robustness of the results.

The Benjamini–Hochberg method was used to correct false discovery rates caused by multiple testing.

A *p*-value of 0.05 is considered statistically significant.

Sample Size Justification

The sample size was calculated as in the study by Asschenfeldt et al. (15) and estimated on the basis of previously published full-scale IQ data (12). The sample size was determined to be 35 CHD patients to find a difference in IQ (the primary outcome of the previous study) with a power of 80% and a significance level of 0.05.

RESULTS

Baseline Characteristics/Demographics

The groups (CHD vs. controls) were comparable on sex/gender, age, body mass index, and ISCED education level (**Table 1**).

The participants gave a self-reported status of prior psychiatric diagnosis (**Table 1**). More of the participants in the CHD group had a prior psychiatric diagnosis than the participants in the control group.

As there were no differences in the mean T-scores between the VSD and the ASD group in any of the ADHD scores or symptom sub-scores, we analyzed these two groups combined as a CHD group (**Table 2**).

T-Score >65

In the CHD group, 15% of all T-scores were above 65 compared to 4% of the T-scores in the control group [RR = 4.61 (2.52, 8.5), $p < 0.001$] (**Figure 1**). If a participant has one or more T-scores above 65, the likelihood of a diagnosis of ADHD is higher. We found that a total of 31 participants (38.8%) in the CHD group had more than one T-score above 65 (**Table 3**).

DSM-IV ADHD Scores

We performed a *post-hoc* analysis of the different ADHD scores between the CHD and the control groups to characterize this difference in continuous T-scores.

The CHD group reported significantly higher means across all ADHD scores than the control group (**Table 2**).

We found no difference in the ADHD scores between the subgroup of ASD patients treated with percutaneous ASD closure ($N = 10$) compared to ASD patients treated with open surgery ($N = 34$) (ADHD index score: 50.7 vs. 55.8, $p = 0.3$, ADHD—combined: 48.8 vs. 53.4, $p = 0.3$, ADHD—inattention: 52.1 vs. 55.5, $p = 0.5$, and ADHD—hyperactivity: 47.0 vs. 50.3, $p = 0.5$) (**Figure 2**).

ADHD Symptoms Sub-scores

The CHD group reported a higher mean T-score in all of the four ADHD symptom sub-scores than the control group (**Table 2**).

Hedges' *g* effect size was calculated, and a medium effect size between groups on all ADHD scores and three out of four ADHD symptom sub-scores (inattention/memory problems, impulsivity/emotional lability, and self-esteem problems) were found. Only a small effect size was found on hyperactivity/restlessness symptoms (**Table 2**).

Self-Report vs. Informant Report

Compared to the informant report, the CHD group reported themselves as having more problems at the ADHD—inattention score, but not at the ADHD—hyperactivity score and ADHD—combined score (**Table 4**). No differences were found between self- and informant-reported ADHD symptom sub-scores. There

TABLE 1 | Demographics.

	ASD	VSD	CHD	Control
	(*n* = 48)	(*n* = 32)	(*n* = 80)	(*n* = 39)
Gender (*n*, %)				
Male	9 (18.8%)	14 (43.8%)	23 (28.8%)	14 (35.9%)
Female	39 (81.3%)	18 (56.3%)	57 (71.3%)	25 (64.1%)
Age				
Mean (SD)	28.7 (6.44)	23.4 (3.34)	26.6 (6.00)	25.3 (4.53)
Body mass index				
Mean (SD)	25.7 (5.68)	23.1 (2.96)	24.6 (4.93)	22.9 (3.20)
Education (*n*, %)				
ISCED primary education	2 (4.2%)	1 (3.1%)	3 (3.8%)	0 (0%)
ISCED secondary education	31 (64.6%)	26 (81.3%)	57 (71.3%)	25 (64.1%)
ISCED tertiary education	15 (31.3%)	5 (15.6%)	20 (25.0%)	14 (35.9%)
Any psychiatric disorder[a] (*n*, %)				
Yes	-	-	27 (33.8)	4 (10.3%)
ADHD, ADD				
Yes	-	-	7 (8.8%)	0 (0%)
Informant relationship (*n*, %)				
CHD—informant: (*n* = 75), information on *n* = 71				
Control—informant: (*n* = 32), information on all				
Parent	-	-	43 (57.3%)	12 (37.5%)
Spouse, partner	-	-	21 (29.6)	10 (31.3%)
Sibling	-	-	6 (8.5%)	8 (25.0%)
Friend	-	-	0 (0%)	2 (6.3%)
Unanswered	-	-	1 (1.4%)	0 (0%)
Duration of relation (years)				
Mean (SD)	-	-	18.9 (9.48)	17.4 (10.5)

ASD, atrial septum defects; VSD, ventricular septum defect; ISCED, International Standard Classification of Education.
[a]Psychosis, depression, OCD, anxiety, eating disorder, personality disorder, autism spectrum disorders and ADHD/ADD.

TABLE 2 | Mean and SD T-scores.

DMS-IV	ASD	VSD	CHD	Control	ASD vs. VSD[a]	CHD vs. control[a]	Hedges' g
ADHD index score							
Mean (SD)	54.0 (12.3)	53.6 (12.6)	53.8 (12.4)	45.1 (9.2)	0.9	0.001*	0.76
ADHD—combined							
Mean (SD)	51.6 (13.0)	54.5 (14.4)	52.8 (13.6)	44.9 (10.5)	0.3	0.007*	0.62
ADHD—inattention							
Mean (SD)	54.1 (12.7)	57.7 (13.8)	55.5 (13.2)	46.4 (11.4)	0.2	0.002*	0.72
ADHD—Hyperactivity							
Mean (SD)	48.8 (12.7)	50.3 (13.8)	49.4 (13.1)	44.0 (8.1)	0.6	0.03*	0.46
Symptoms							
Inattention/memory problems							
Mean (SD)	50.5 (9.0)	50.3 (11.7)	50.3 (10.1)	44.2 (7.2)	0.8	0.001*	0.66
Hyperactivity/restlessness							
Mean (SD)	49.0 (9.2)	50.7 (10.0)	49.7 (9.5)	45.9 (7.3)	0.4	0.03*	0.43
Impulsivity/emotional lability							
Mean (SD)	50.3 (12.2)	49.6 (14.5)	50.0 (13.1)	41.3 (9.0)	0.8	0.001*	0.73
Self-esteem problems							
Mean (SD)	55.2 (12.7)	51.7 (11.1)	53.8 (12.1)	46.3 (10.5)	0.2	0.003*	0.65

ASD, atrial septum defect; VSD, ventricular septum defect; CHD, congenital heart defect.
[a]T-test.
**p < 0.05 (after multiple analysis correction; Benjamini–Hochberg correction).*

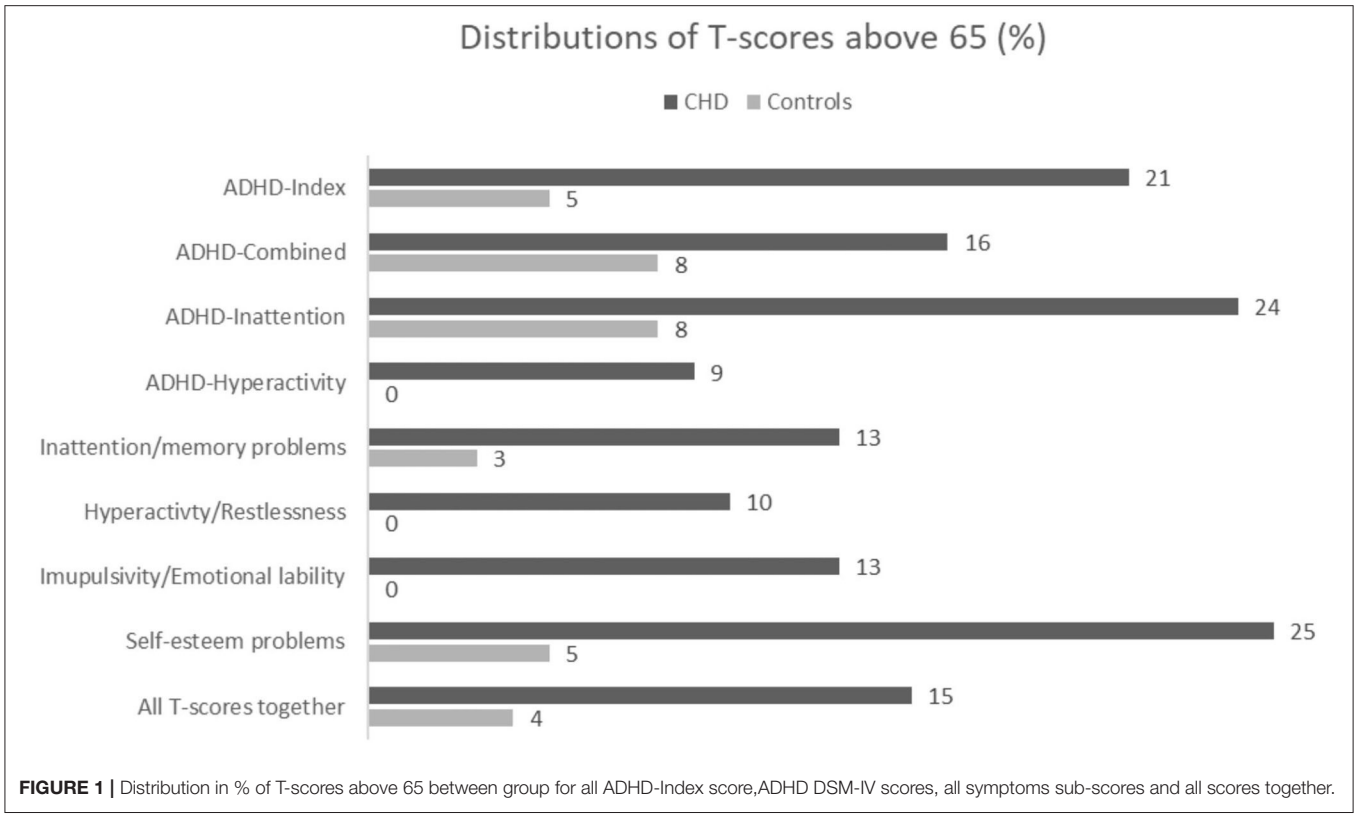

FIGURE 1 | Distribution in % of T-scores above 65 between group for all ADHD-Index score,ADHD DSM-IV scores, all symptoms sub-scores and all scores together.

TABLE 3 | Participants at risk for an ADHD diagnosis between the CHD group and the control group.

	CHD (*N* = 80)	Control (*N* = 39)
Count of T-scores above 65		
0	49 (61.3%)	35 (89.7%)
1–8	31 (38.8%)	4 (10.3%)

were no differences between self- and informant-reported scores in the control group (**Table 4**).

Excluding Incongruent Responses

Based on the CAARS incongruent subscore, a total of 14 participants were excluded (two percutaneously closed ASDs, five surgically closed ASDs, four surgically closed VSDs, and three controls), leaving a total number of 36 controls, 28 VSDs, and 41 ASDs (29 surgically closed ASDs, eight percutaneously closed ASDs, and four non-operated ASDs).

We again found no difference in the DSM-IV ADHD scores between the subgroup of ASD patients treated with open surgery compared to ASD patients treated with percutaneous ASD closure (ADHD Index score: 53.9 vs. 50.5, $p = 0.50$, ADHD—combined: 51.4 vs. 48.4, $p = 0.7$, ADHD—inattention: 53.1 vs. 53.3, $p = 1.0$, and ADHD—hyperactivity: 49.5 vs. 45.1, $p = 0.5$).

The CHD group reported a significantly higher means across all DSM-IV ADHD scores than the control group (**Table 5**). The CHD group likewise reported a higher mean T-score in three of the four ADHD symptom sub-scores than the control group, though we found no difference in mean T-scores in the hyperactivity sub-score (**Table 5**).

The 14 participants excluded in the above-mentioned analysis had a higher mean T-score on all scores and sub-scores both for the CHD group and for the control group [ADHD index score: 64.2 (SD 10.7) and 46.7 (SD 6.1), ADHD-combined score: 62.5 (SD 11.8) and 53.3 (SD 7.0), ADHD—inattention: 65.3 (SD 13.8) and 54.7 (SD 5.5), and ADHD—hyperactivity: 57.0 (SD 8.1) and 50.3 (8.1), inattention/memory problems: 60.6 (SD 8.1) and 47.3 (SD 3.1), impulsivity/emotional lability: 56.7 (SD 10.1) and 44.7 (SD 7.8), self-esteem problems: 62.9 (SD 9.5), and 47.7 (SD 8.4), hyperactivity/restlessness: 57.6 (SD 8.6) and 52.0 (SD 8.0)]. Moreover, 34% of T-scores in the excluded CHD group were above 65 vs. 0% in the excluded control group.

Self-Report vs. Informant Report Without Participants With Incongruent Answers

The CHD group reported themselves as having more problems at the ADHD—combined score and at the ADHD—inattention score, but not at the ADHD—hyperactivity score, compared to the informant report. There were no differences between self- and informant-reported scores in the control group (**Table 6**).

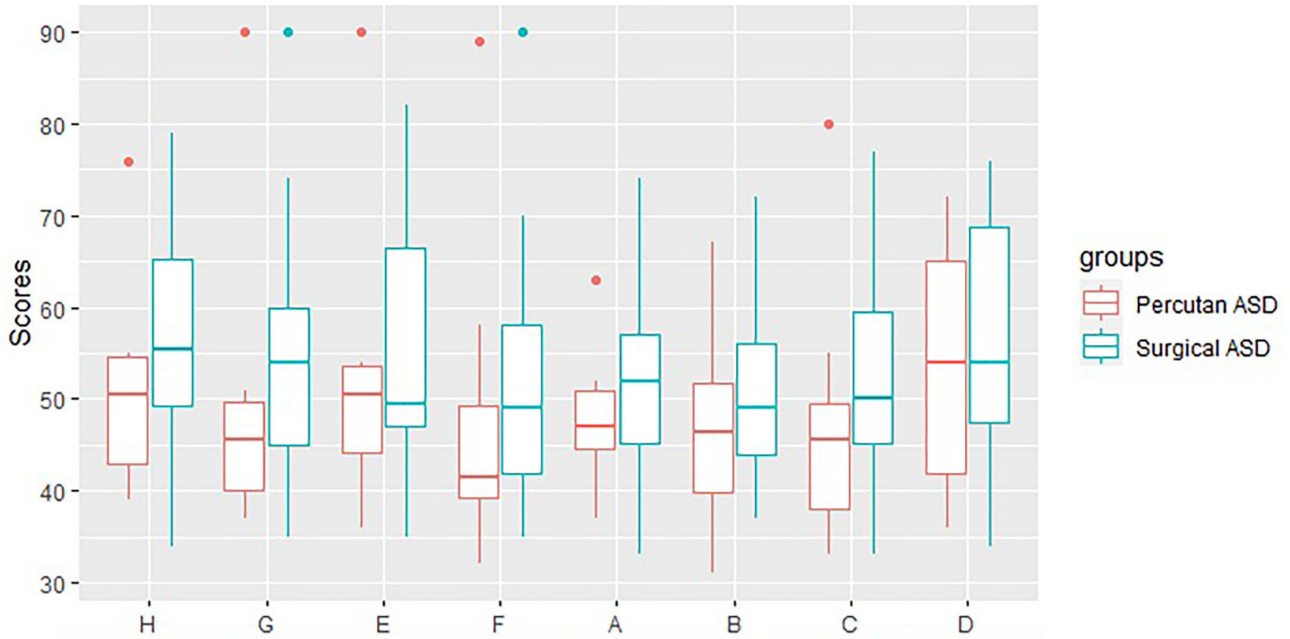

FIGURE 2 | CAARS scores for Perctuaneus ASD and Surgical ASD. H: ADHD-Index, G: ADHD-Combined, E: ADHD-Inattention, F: ADHD-Hyperactivity, A: Innatention/Memory problems, B: Hyperactivity/Restlessness, C: Impulsivity/Emotional lability, D: Self-esteem problems.

TABLE 4 | Congenital heart defect informant vs. congenital heart defect self-evaluation (mean and SD of T-scores).

	CHD			Control		
DMS-IV	**Self**	**Informant**	**Self vs. informant[a]**	**Self**	**Informant**	**Self vs. Informant[a]**
ADHD index score						
Mean (SD)	53.8 (12.3)	49.7 (11.4)	0.16	45.1 (9.2)	45.2 (8.1)	0.94
ADHD—combined score						
Mean (SD)	52.8 (13.6)	46.0 (9.1)	0.08	44.9 (20.5)	43.1 (7)	0.37
ADHD—inattention score						
Mean (SD)	55.5 (13.2)	46.9 (8.5)	0.003*	46.6 (11.4)	44.3 (7.3)	0.3
ADHD—hyperactivity score						
Mean (SD)	49.4 (13.1)	45.1 (9.9)	0.08	44.0 (8.1)	42.7 (6)	0.45
Symptoms						
Inattention/memory problems						
Mean (SD)	50.3 (10.1)	48.6 (11.0)	0.35	44.0 (7.5)	45.3 (7.6)	0.48
Hyperactivity/restlessness						
Mean (SD)	49.7 (9.5)	47.1 (9.4)	0.35	45.9 (7.3)	45.2 (7.4)	0.69
Impulsivity/emotional lability						
Mean (SD)	50.0 (13.1)	48.0 (9.6)	0.35	41.3 (9.0)	43.2 (5.8)	0.31
Self-esteem problems						
Mean (SD)	52.3 (12.0)	50.9 (10.9)	0.35	46.3 (10.5)	48.4 (9.6)	0.4

[a] *T-test.*

**p < 0.05 after multiple analysis correction (Benjamini–Hochberg correction).*

TABLE 5 | Mean and SD between groups of T-scores (when participants with incongruent answers are excluded).

Without incongruent answers DSM-IV ADHD scores	ASD	VSD	CHD	Control	ASD vs. VSD[a]	CHD vs. control[a]	Hedges' g
ADHD index score							
Mean (SD)	52.5 (11.9)	51.6 (12.0)	52.2 (11.9)	44.9 (9.4)	0.74	0.01*	0.66
ADHD—combined score							
Mean (SD)	50.0 (13.0)	52.9 (13.6)	51.2 (13.2)	44.3 (10.5)	0.38	0.02*	0.56
ADHD—inattention score							
Mean (SD)	52.5 (12.3)	56.1 (12.8)	54.0 (12.5)	45.9 (11.6)	0.25	0.01*	0.66
ADHD—hyperactivity score							
Mean (SD)	47.7 (13.2)	48.8 (12.5)	48.1 (12.9)	43.5 (8.0)	0.74	0.05*	0.4
Symptoms sub-scores							
Inattention/memory problems							
Mean (SD)	49.2 (8.4)	48.0 (10.9)	48.7 (9.4)	43.8 (7.7)	0.6	0.02*	0.55
Hyperactivity/restlessness							
Mean (SD)	47.8 (8.9)	49.2 (9.4)	48.4 (9.1)	45.4 (7.1)	0.53	0.12	0.35
Impulsivity/emotional lability							
Mean (SD)	49.7 (12.5)	47.8 (14.4)	49.0 (13.3)	41.1 (9.2)	0.56	0.01*	0.65
Self-esteem problems							
Mean (SD)	53.7 (12.5)	50.4 (11.0)	52.3 (12.0)	46.2 (10.8)	0.26	0.03*	0.53

Number of participants with incongruent answers: ASD = 7, VSD = 4, and controls = 3.
ASD, atrial septum defect; VSD ventricular septum defect; CHD, congenital heart defect.
[a] *T-test.*
$p < 0.05$ after multiple analysis correction.

TABLE 6 | Congenital heart defect informant vs. congenital heart defect self-evaluation.

	Without incongruent answers			Controls		
CHD						
DMS-IV ADHD scores	**Self**	**Informant**	**Self vs. informant[a]**	**Self**	**Informant**	**Self vs. Informant[a]**
ADHD index score						
Mean (SD)	52.2 (11.9)	48.1 (10.4)	0.3	44.9 (9.4)	45.7 (8.1)	0.73
ADHD—combined score						
Mean (SD)	51.2 (13.2)	42.2 (7.5)	0.03*	44.3 (10.5)	43.4 (7.1)	0.66
ADHD—inattention score						
Mean (SD)	54.0 (12.5)	45.6 (7.7)	0.002*	45.9 (11.6)	44.4 (7.5)	0.52
ADHD—hyperactivity score						
Mean (SD)	48.1 (12.9)	43.1 (8.4)	0.06	43.5 (8.0)	43 (6.1)	0.79
Symptom sub-scores						
Inattention/memory problems						
Mean (SD)	48.7 (9.4)	46.8 (9.3)	0.46	43.8 (7.7)	45.7 (7.7)	0.36
Hyperactivity/restlessness						
Mean (SD)	48.4 (9.1)	45.2 (7.7)	0.06	45.4 (7.1)	45.5 (7.6)	0.95
Impulsivity/emotional lability						
Mean (SD)	49.0 (13.3)	46.5 (8.6)	0.3	41.1 (9.2)	43.5 (5.7)	0.2
Self-esteem problems						
Mean (SD)	52.3 (12.0)	50.9 (10.9)	0.46	46.2 (10.8)	48.8 (9.7)	0.31

Mean and SD of T-scores (when participants with incongruent answers are excluded).
[a] *T-test.*
$p < 0.05$ after multiple analysis correction.

DISCUSSION

The aim of this study was to investigate the distribution in ADHD symptoms in young adults with simple CHD and investigate whether such a burden is mostly driven by inattention, hyperactivity, or both.

We found that the CHD group had a higher burden of ADHD symptoms in general (all of ADHD—combined, ADHD—inattention, and ADHD—hyperactivity) and all related symptoms (inattention/memory problems, impulsivity/emotional lability, hyperactivity/restlessness, and self-esteem problems) compared to healthy controls.

Nevertheless, this burden seems somewhat more dominated by inattention and less by hyperactivity symptoms, as the hyperactivity sub-scores reveal smaller effect sizes and did not reach significance after removing the incongruent responses. Typically, inattention symptoms continue into adulthood, whereas hyperactivity seems to burn out with age. This could be why we only find a small effect size in this group of young adults. In accordance to our findings, a higher burden of inattention symptoms, but not hyperactivity, has previously been documented in a combined group of complex (TGA) and simple (VSD) CHD children (age 10–17) when compared to a matched control group (22). We found both a higher burden of inattention and hyperactivity while not excluding the incongruent responses. These findings indicate that some participants in our CHD group have more hyperactivity symptoms that linger into adulthood despite the general adult ADHD presentation. When analyzing the participants with incongruent responses, we see that these participants have higher mean T-scores—especially in the CHD group. Two (11%) of the participants in the CHD group who had incongruent answers had a prior diagnosis of ADHD/ADD. We found that 34% of all T-scores in this group were above the 93rd percentile (corresponding to a great likelihood for clinical problems) compared to 15% for the CHD group as a whole. This suggests that the incongruent responses may be part of their symptomatology (or a desire to make a specific impression) and not due to unwillingness to answer the questions. More of the participants in the CHD group had a prior psychiatric diagnosis of any kind (33.8 vs. 10.3%) and more of them had a prior specific diagnosis of ADHD/ADD (8.8 vs. 0%) than the participants in the control group. The higher frequency of preexisting psychiatric diagnoses and our findings of previously undiscovered symptoms confirm that the psychiatric well-being of young adults with CHD is challenged.

The informants reported the CHD patients better (i.e., lower scores) than the CHD patients reported themselves at the scores for ADHD—inattention. There are different possibilities as to why we find this discrepancy between participants and informants. It could be that the participants over-report their problems because of symptoms of depression or general low self-worth. The discrepancy could also be due to informants being defensive in their responses ("things are better than I expected"), or it could be that the informants are not aware of the struggling at school or work because inattention problems are more "silent" than hyperactivity. Since the discrepancy is only seen with regards to ADHD—inattention, we think the latter to be most likely in this study. This corresponded well with another study that found that parents are less aware of the social difficulties experienced by children with ADHD—inattention (21). ADHD—inattention is associated with difficulties in academic achievements compared to ADHD—hyperactivity which is more associated with behavioral impairments that may be more evident at home (23). This correlated well with our findings. The problems of this patient group with inattention may not be apparent for other people—even people close to the patient. Awareness of potential inattention is the first step in managing these difficulties in a child or an adolescent. In this aspect, the treating physician has a special and important role in making the parent or other close relatives aware of these difficulties and their effect on academic achievements.

ADHD—combined and ADHD—inattention are associated with problems in social performance. ADHD—inattention is associated with social performance problems linked to more passive behaviors. ADHD—combined is associated with more aggressive behavior problems, which, in turn, are more visible to the outside world (21). Inattention symptoms are associated with negative performance on stimuli inhibition, vigilance, and processing speed (more than hyperactivity symptoms) (24, 25). These problems could explain the issues with social cognition found in patients with simple CHD (15). Most studies trying to describe the difference in cognitive and social functions between subtypes have focused on ADHD—inattention and ADHD—combined. Less have been made on ADHD—hyperactivity, and the results are conflicting. One study found that children with ADHD—hyperactivity have been found to have the same level of executive functioning and response inhibition as those with ADHD—inattention (26). Another study found that ADHD—hyperactivity had the best cognitive functioning and the best self-rated self-esteem of the subtypes (27).

Both patients with complex and simple CHDs have neurocognitive and psychiatric comorbidities compared to the general population (7–15). Our findings are in line with these previous studies. Different pathophysiological pathways have been suggested to explain these comorbidities, including brain development, brain hypoxia, brain vulnerabilities, surgical complications, and genetics.

Different pre-, peri-, and post-surgical complications are known risk factors for early and late neuropsychiatric comorbidities in patients with complex CHD (28, 29). Research has progressed to also include patients with simple CHD that only requires minor operations, and even some without any operations (7) and surgical complications cannot explain the neuropsychiatric complications detected in this patient group. In our study, we found no difference in ADHD scores between patients with surgically corrected ASDs and percutaneously corrected ASDs. However, our subgroups are small (ASD surgically corrected: $N = 34$ and ASD percutaneously corrected: $N = 10$). These findings are in line with the above-mentioned notion that other factors than surgical complications may play a bigger role in the development of neurocognitive and psychiatric morbidities in simple CHDs.

In the third trimester of pregnancy, the development of the brain is accentuated, and MRI scans *in utero* have shown

delayed brain maturation, decreased white and gray volumes, immature cortical gyrification, and affected brain metabolism (30–32). Related findings have also been found in newborns pre-operatively (33–35). Moreover, in a recently published study from our group, we found abnormal sulcal folding patterns in adults with simple CHDs (36). This supports a notion of a disruption in early brain development in these patients. The general perception is that some of the CHDs result in desaturated blood being delivered to the brain despite cerebral compensatory mechanisms (37). *De novo* damage to specific genes that are involved in both cardiac and neuro-development and function has been found in patients with complex CHD (38). These findings add to the pathophysiological pathways explaining the brain vulnerabilities and neuropsychological difficulties found in the patient group. Genetics could also very well be a contributor to the explanation of the poorer neuropsychological outcomes found in simple CHDs (39). Further research to investigate the possible pathophysiology behind the poorer neuropsychological long-term outcomes in simple CHDs is still needed.

A proper diagnosis of the three different ADHD presentations requires a psychiatric evaluation, and prevalence based on symptom criterions (such as CAARS) must be interpreted with caution since symptom criterions tend to overestimate (23). If a participant has one or more T-scores above 65, the likelihood of a diagnosis of ADHD is higher. We found that a total of 31 participants (38.8%) in the CHD group had more than one T-score above 65 despite only 7 (8.8%) were diagnosed with a ADHD/ADD diagnosis already. An explanation could be that the diagnosis of ADHD/ADD requires a psychiatric evaluation, and especially inattention problems are more difficult to detect. Therefore, some of the participants may not have been correctly recognized and referred to a psychiatrist.

We did not include information on socioeconomic status. We deal with young adults who have not yet established their own socioeconomic status, but they are most likely not adequately defined by the status of their parents. Therefore, we chose to match the control group to the CHD group by the educational level of the patients in the belief that the educational level would be the most accurate reflection of a lifetime socioeconomic status. Moreover, in a large meta-analysis, no correlation was found between socioeconomic status and the prevalence of ADHD (23), but the research is not consistent (40–43).

The observations made by the participant informants are surrogates for a proper psychiatric evaluation that would lead to a definitive ADHD diagnosis. In this light, we avoid extrapolating the results beyond statements about the difference in burden of ADHD and of related symptoms. As the participants in the CHD group are relatively well functioning, the burden of ADHD and symptoms and the quality of this burden were, in fact, what we wanted to explore.

A notable strength of this study is the control group of healthy peers matched on gender, age, and educational level instead of only the normative data provided in the CAARS manual. The CHD group is exclusively simple CHD (ASD and VSD) and not a mixture as most previous studies are. Another strength is that we had evaluations from both the participants themselves and a close relative, adding an extra layer to the understanding. Despite this being a relatively small study, a clinically significant difference was demonstrated.

Our control group had fewer high T-scores (above the 93rd percentile) than expected (4 vs. 7%). In general, the mean T-score for our control group was lower than the normative data provided by the CAARS manual (mean, 50; SD, 10). This is an expected finding as this is the case in many European and especially Scandinavian normative datasets (44–47). This emphasizes the importance of using a comparable control group. The Danish normative data for the CAARS questionnaire has not yet been established. To compensate for this somewhat expected difference in means between our Danish patient group, we used an age- and gender-matched control group as a comparison.

CONCLUSION

Young adults with simple CHD have a higher burden of ADHD compared with healthy peers. The difference is driven both by introvert symptoms, like inattention, and also extrovert symptoms (atypically for the age group), like hyperactivity, though the inattention symptoms seem more prominent, and these are more likely to be overlooked by close relatives. Awareness of potential inattention is the first step to managing these difficulties in a child or an adolescent. In this aspect, the treating physician has a special and important role in making the parent or other close relatives aware of these difficulties and their effect on academic achievements.

This study emphasizes the long-term neurodevelopmental struggles of patients with simple CHDs and underlines the importance of raising awareness of these hitherto unrecognized life-changing burdens—struggles that we, as healthcare providers (be it nurses or doctors), need to discuss with our patients and their families.

DATA AVAILABILITY STATEMENT

The raw data supporting the conclusions of this article will be made available by the authors, without undue reservation.

ETHICS STATEMENT

The studies involving human participants were reviewed and approved by Danish Central Regional's Committee on Biomedical Research Ethics (chart: 1-10-72-233-17). The patients/participants provided their written informed consent to participate in this study.

AUTHOR CONTRIBUTIONS

SL-J has contributed with data management, data analyzes and all manuscript writing. BA has conceptualised and designed the study and contributed with funding applications, data collection, input regarding data analyzes, supervision regarding interpretation of results and supervision with manuscript writing. LE and VH have conceptualised and

designed the study, they have contributed with general and detailed supervision in all aspects of the data management and manuscript writing.

FUNDING

SL-J was funded by The Danish Heart Foundation. The funding payed the salary for the SL-J, but the funder was not included in any aspect of data management, analysis, interpretation or manuscript writing.

ACKNOWLEDGMENTS

The authors warmly acknowledge our neuropsychology team (KA, AMB, EEP, KWJ, and RHP) for the assistance with data collection.

REFERENCES

1. Khoshnood B, Loane M, Garne E, Addor M-C, Arriola L, Bakker M, et al. Recent decrease in the prevalence of congenital heart defects in Europe. *J Pediatr*. (2013) 162:108–13.e2. doi: 10.1016/j.jpeds.2012.06.035
2. Dolk H, Loane M, Garne E. Congenital heart defects in Europe: Prevalence and perinatal mortality, 2000 to 2005. *Circulation.* (2011) 123:841–9. doi: 10.1161/CIRCULATIONAHA.110.958405
3. Botto LD, Correa A, Erickson JD. Racial and temporal variations in the prevalence of heart defects. *Pediatrics.* (2001) 107:E32. doi: 10.1542/peds.107.3.e32
4. Warnes CA, Liberthson R, Danielson GK, Dore A, Harris L, Hoffman JI, et al. Task force 1: the changing profile of congenital heart disease in adult life. *J Am Coll Cardiol.* (2001) 37:1170–5. doi: 10.1016/S0735-1097(01)01272-4
5. Marelli AJ, Mackie AS, Ionescu-Ittu R, Rahme E, Pilote L. Congenital heart disease in the general population: changing prevalence and age distribution. *Circulation.* (2007) 115:163–72. doi: 10.1161/CIRCULATIONAHA.106.627224
6. Marelli AJ, Ionescu-Ittu R, Mackie AS, Guo L, Dendukuri N, Kaouache M. Lifetime prevalence of congenital heart disease in the general population from 2000 to 2010. *Circulation.* (2014) 130:749–56. doi: 10.1161/CIRCULATIONAHA.113.008396
7. Olsen M, Sørensen HT, Hjortdal VE, Christensen TD, Pedersen L. Congenital heart defects and developmental and other psychiatric disorders: A Danish nationwide cohort study. *Circulation.* (2011) 124:1706–12. doi: 10.1161/CIRCULATIONAHA.110.002832
8. Nyboe C, Udholm S, Larsen SH, Rask C, Redington A, Hjortdal V. Risk of lifetime psychiatric morbidity in adults with atrial septal defect (from a nation-wide cohort). *Am J Cardiol.* (2020) 128:1–6. doi: 10.1016/j.amjcard.2020.04.047
9. Wernovsky G. Current insights regarding neurological and developmental abnormalities in children and young adults with complex congenital cardiac disease. *Cardiol Young.* (2006) 16 Suppl 1:92–104. doi: 10.1017/S1047951105002398
10. Shillingford AJ, Glanzman MM, Ittenbach RF, Clancy RR, Gaynor JW, Wernovsky G. Inattention, hyperactivity, and school performance in a population of school-age children with complex congenital heart disease. *Pediatrics.* (2008) 121:e759–767. doi: 10.1542/peds.2007-1066
11. Sarrechia I, Miatton M, François K, Gewillig M, Meyns B, Vingerhoets G, et al. Neurodevelopmental outcome after surgery for acyanotic congenital heart disease. *Res Dev Disabil.* (2015) 45–6:58–68. doi: 10.1016/j.ridd.2015.07.004
12. Schaefer C, von Rhein M, Knirsch W, Huber R, Natalucci G, Caflisch J, et al. Neurodevelopmental outcome, psychological adjustment, and quality of life in adolescents with congenital heart disease. *Dev Med Child Neurol.* (2013) 55:1143–9. doi: 10.1111/dmcn.12242
13. DeMaso DR, Calderon J, Taylor GA, Holland JE, Stopp C, White MT, et al. Psychiatric disorders in adolescents with single ventricle congenital heart disease. *Pediatrics.* (2017) 139:e20162241. doi: 10.1542/peds.2016-2241
14. Nyboe C, Fonager K, Larsen ML, Andreasen JJ, Lundbye-Christensen S, Hjortdal V. Effect of atrial septal defect in adults on work participation (from a nation wide register-based follow-up study regarding work participation and use of permanent social security benefits). *Am J Cardiol.* (2019) 124:1775–9. doi: 10.1016/j.amjcard.2019.08.041
15. Asschenfeldt B, Evald L, Heiberg J, Salvig C, Østergaard L, Dalby RB, et al. Neuropsychological status and structural brain imaging in adults with simple congenital heart defects closed in childhood. *J Am Heart Assoc.* (2020) 9:e015843. doi: 10.1161/JAHA.120.015843
16. Schmithorst VJ, Panigrahy A, Gaynor JW, Watson CG, Lee V, Bellinger DC, et al. Organizational topology of brain and its relationship to ADHD in adolescents with d-transposition of the great arteries. *Brain Behav.* (2016) 6:e00504. doi: 10.1002/brb3.504
17. Biederman J, Faraone S V. The effects of attention-deficit/hyperactivity disorder on employment and household income. *MedGenMed Medscape Gen Med.* (2006) 8:12.
18. Fletcher JM. The effects of childhood ADHD on adult labor market outcomes. *Health Econ.* (2014) 23:159–81. doi: 10.1002/hec.2907
19. Daley D, Jacobsen RH, Lange AM, Sørensen A, Walldorf J. The economic burden of adult 35 attention deficit hyperactivity disorder: a sibling comparison cost analysis. *Eur Psychiatry.* (2019) 61:41–8. doi: 10.1016/j.eurpsy.2019.06.011
20. Klassen AF, Miller A, Fine S. Health-related quality of life in children and adolescents who have a diagnosis of attention-deficit/hyperactivity disorder. *Pediatrics.* (2004) 114:e541–7. doi: 10.1542/peds.2004-0844
21. Maedgen JW, Carlson CL. Social functioning and emotional regulation in the attention deficit hyperactivity disorder subtypes. *J Clin Child Adolesc Psychol.* (2000) 29:30–42. doi: 10.1207/S15374424jccp2901_4
22. Holst LM, Kronborg JB, Jepsen JRM, Christensen JO, Vejlstrup NG, Juul K, et al. Attention-deficit/hyperactivity disorder symptoms in children with surgically corrected ventricular septal defect, transposition of the great arteries, and tetralogy of fallot. *Cardiol Young.* (2020) 30:180–7. doi: 10.1017/S1047951119003184
23. Willcutt EG. The prevalence of DSM-IV attention-deficit/hyperactivity disorder: a meta-analytic review. *Vol 9, Neurotherapeutics Neurotherapeutics.* (2012) 29:529–40. doi: 10.1007/s13311-012-0135-8
24. Chhabildas N, Pennington BF, Willcutt EG. A comparison of the neuropsychological profiles of the DSM-IV subtypes of ADHD. *J Abnorm Child Psychol.* (2001) 29:529–40. doi: 10.1023/a:1012281226028
25. Solanto MV, Gilbert SN, Raj A, Zhu J, Pope-Boyd S, Stepak B, et al. Neurocognitive functioning in AD/HD, predominantly inattentive and combined subtypes. *J Abnorm Child Psychol.* (2007) 35:729–44. doi: 10.1007/s10802-007-9123-6
26. Ahmadi N, Mohammadi MR, Araghi SM, Zarafshan H. Neurocognitive Profile of children with attention deficit hyperactivity disorders (ADHD): a comparison between subtypes. *Iran J Psychiatry.* (2014) 9:197–202.
27. Molavi P, Nadermohammadi M, Ghojehbeiglou HS, Vicario CM, Nitsche MA, Salehinejad MA, et al. Subtype-specific cognitive correlates and association with self-esteem: a quantitative difference. *BMC Psychiatry.* (2020) 20:502. doi: 10.1186/s12888-020-02887-4
28. Sananes R, Manlhiot C, Kelly E, Hornberger LK, Williams WG, Macgregor D, et al. Neurodevelopmental outcomes after open heart operations before 3 months of age. *ATS.* (2012) 93:1577–83. doi: 10.1016/j.athoracsur.2012.02.011
29. Sugimoto A, Ota N, Ibuki K, Miyakoshi C, Murata M, Tosaka Y, et al. Risk factors for adverse neurocognitive outcomes in school-aged patients after the fontan operation. *Eur J Cardiothorac Surg.* (2013) 44:454–61. doi: 10.1093/ejcts/ezt062
30. Donofrio MT, Bremer YA, Schieken RM, Gennings C, Morton LD, Eidem BW, et al. Autoregulation of cerebral blood flow in fetuses with congenital

heart disease: the brain sparing effect. *Pediatr Cardiol.* (2003) 24:436–43. doi: 10.1007/s00246-002-0404-0
31. Limperopoulos C, Tworetzky W, McElhinney DB, Newburger JW, Brown DW, Robertson RL, et al. Brain volume and metabolism in fetuses with congenital heart disease: evaluation with quantitative magnetic resonance imaging and spectroscopy. *Circulation.* (2010) 121:26–33. doi: 10.1161/CIRCULATIONAHA.109.865568
32. Clouchoux C, du Plessis AJ, Bouyssi-Kobar M, Tworetzky W, McElhinney DB, Brown DW, et al. Delayed cortical development in fetuses with complex congenital heart disease. *Cereb Cortex.* (2013) 23:2932–43. doi: 10.1093/cercor/bhs281
33. Miller SP, McQuillen PS, Hamrick S, Xu D, Glidden DV, Charlton N, et al. Abnormal brain development in newborns with congenital heart disease. *N Engl J Med.* (2007) 357:1928–38. doi: 10.1056/NEJMoa067393
34. Licht DJ, Shera DM, Clancy RR, Wernovsky G, Montenegro LM, Nicolson SC, et al. Brain maturation is delayed in infants with complex congenital heart defects. *J Thorac Cardiovasc Surg.* (2009) 137:529–37. doi: 10.1016/j.jtcvs.2008.10.025
35. Dimitropoulos A, McQuillen PS, Sethi V, Moosa A, Chau V, Xu D, et al. Brain injury and development in newborns with critical congenital heart disease. *Neurology.* (2013) 81:241–8. doi: 10.1212/WNL.0b013e31829bfdcf
36. Asschenfeldt B, Evald L, Yun HJ, Heiberg J, Østergaard L, Grant PE, et al. Abnormal left-hemispheric sulcal patterns in adults with simple congenital heart defects repaired in childhood. *J Am Heart Assoc.* (2021) 10:e018580. doi: 10.1161/JAHA.120.018580
37. Sun L, Macgowan CK, Sled JG, Yoo S-J, Manlhiot C, Porayette P, et al. Reduced fetal cerebral oxygen consumption is associated with smaller brain size in fetuses with congenital heart disease. *Circulation.* (2015) 131:1313–23. doi: 10.1161/CIRCULATIONAHA.114.013051
38. Ji W, Ferdman D, Copel J, Scheinost D, Shabanova V, Brueckner M, et al. *De novo* damaging variants associated with congenital heart diseases contribute to the connectome. *Sci Rep.* (2020) 10:7046. doi: 10.1038/s41598-020-63928-2
39. Møller Nielsen AK, Nyboe C, Lund Ovesen AS, Udholm S, Larsen MM, Hjortdal VE, et al. Mutation burden in patients with small unrepaired atrial septal defects. *Int J Cardiol Congenit Hear Dis.* (2021) 4:100164. doi: 10.1016/j.ijcchd.2021.100164
40. Nolan EE, Gadow KD, Sprafkin J. Teacher reports of DSM-IV ADHD, ODD, and CD symptoms in schoolchildren. *J Am Acad Child Adolesc Psychiatry.* (2001) 40:241–9. doi: 10.1097/00004583-200102000-00020
41. Canino G, Shrout PE, Rubio-Stipec M, Bird HR, Bravo M, Ramírez R, et al. The DSM-IV rates of child and adolescent disorders in Puerto Rico: prevalence, correlates, service use, and the effects of impairment. *Arch Gen Psychiatry.* (2004) 61:85–93. doi: 10.1001/archpsyc.61.1.85
42. Döpfner M, Breuer D, Wille N, Erhart M, Ravens-Sieberer U. How often do children meet ICD-10/DSM-IV criteria of attention deficit-/hyperactivity disorder and hyperkinetic disorder? Parent-based prevalence rates in a national sample–results of the BELLA study. *Eur Child Adolesc Psychiatry.* (2008) (Suppl. 1):59–70. doi: 10.1007/s00787-008-1007-y
43. Pineda D, Ardila A, Rosselli M, Arias BE, Henao GC, Gomez LF, et al. Prevalence of attention-deficit/hyperactivity disorder symptoms in 4- to 17-year-old children in the general population. *J Abnorm Child Psychol.* (1999) 27:455–62. doi: 10.1023/A:1021932009936
44. Szomlaiski N, Dyrborg J, Rasmussen H, Schumann T, Koch SV, Bilenberg N. Validity and clinical feasibility of the ADHD rating scale (ADHD-RS) a danish nationwide multicenter study. *Acta Paediatr.* (2009) 98:397–402. doi: 10.1111/j.1651-2227.2008.01025.x
45. Bilenberg N. The Child Behavior Checklist (CBCL) and related material: standardization and validation in Danish population based and clinically based samples. *Acta Psychiatr Scand Suppl.* (1999) 398:2–52. doi: 10.1111/j.1600-0447.1999.tb10703.x
46. Rescorla L, Achenbach T, Ivanova MY, Dumenci L, Almqvist F, Bilenberg N, et al. Behavioral and emotional problems reported by parents of children ages 6 to 16 in 31 societies. *J Emot Behav Disord.* (2007) 15:130–42. doi: 10.1177/10634266070150030101
47. Christiansen H, Kis B, Hirsch O, Philipsen A, Henneck M, Panczuk A, et al. German validation of the Conners Adult ADHD Rating Scales-self-report (CAARS-S) I: factor structure and normative data. *Eur Psychiatry.* (2011) 26:100–7. doi: 10.1016/j.eurpsy.2009.12.024

Conflict of Interest: The authors declare that the research was conducted in the absence of any commercial or financial relationships that could be construed as a potential conflict of interest.

Publisher's Note: All claims expressed in this article are solely those of the authors and do not necessarily represent those of their affiliated organizations, or those of the publisher, the editors and the reviewers. Any product that may be evaluated in this article, or claim that may be made by its manufacturer, is not guaranteed or endorsed by the publisher.

frontiers in Pediatrics

REVIEW
published: 07 December 2021
doi: 10.3389/fped.2021.760363

Role of Three-Dimensional Visualization Modalities in Medical Education

Ivy Bui[1,2], *Arunabh Bhattacharya*[1], *Si Hui Wong*[2], *Harinder R. Singh*[2,3] *and Arpit Agarwal*[2,3]*

[1] Department of Clinical and Applied Sciences Education, School of Osteopathic Medicine, University of the Incarnate Word, San Antonio, TX, United States, [2] Children's Hospital of San Antonio, San Antonio, TX, United States, [3] Baylor College of Medicine, Houston, TX, United States

For the past two decades, slide-based presentation has been the method of content delivery in medical education. In recent years, other teaching modalities involving three-dimensional (3D) visualization such as 3D printed anatomical models, virtual reality (VR), and augmented reality (AR) have been explored to augment the education experience. This review article will analyze the use of slide-based presentation, 3D printed anatomical models, AR, and VR technologies in medical education, including their benefits and limitations.

Keywords: three-dimensional printing, augmented reality, virtual reality, medical education, slide-based presentation

OPEN ACCESS

Edited by:
Hannes Sallmon,
Deutsches Herzzentrum Berlin, Germany

Reviewed by:
Andrew I. U. Shearn,
University of Bristol, United Kingdom
Tushar Jagzape,
All India Institute of Medical Sciences Raipur, India

***Correspondence:**
Arpit Agarwal
arpit.agarwal@bcm.edu

Specialty section:
This article was submitted to Pediatric Cardiology, a section of the journal Frontiers in Pediatrics

Received: *18 August 2021*
Accepted: *25 October 2021*
Published: *07 December 2021*

Citation:
Bui I, Bhattacharya A, Wong SH, Singh HR and Agarwal A (2021) Role of Three-Dimensional Visualization Modalities in Medical Education. Front. Pediatr. 9:760363. doi: 10.3389/fped.2021.760363

INTRODUCTION

The delivery of medical education has transformed with technological advancement—from the chalk and board to slide-based presentation, which has become the popular option among educators around the world for decades. In medical education, slide-based presentations have been implemented widely in the teaching of anatomy, pathology, embryology, etc. However, medical students often struggle to understand spatial relationship when using two-dimensional images to study anatomy. Hence, cadaveric learning and dissection was introduced as a three-dimensional (3D) option to help students identify organs and understand spatial relationship more realistically. However, cadavers are costly in terms of acquiring fees, delivery, maintainance, and they also face ethical issues (1). Therefore, other cost-effective options for 3D learning, like 3D printed models, augmented reality (AR), and virtual reality (VR) were explored to improve teaching approaches and students' learning experiences.

3D printing has recently gained popularity in many different industries such as aerospace, architecture, automotive, and education. This technology allows the conversion of an image from a digital file such as computed tomography (CT) or magnetic resonance imaging (MRI) into a solid and graspable object (2). In medical education, 3D printed models offer a multidirectional view that can enhance students' understanding of anatomical structures compared to 2D images from the textbook (3). Projects involving printed models have also encouraged development of critical thinking and team building skills for students, and provided opportunities for instructors to explore their creativity (4). For example, both students and instructors can explore a concept object by designing their own 3D model. This activity encourages active learning because the action of building offers hands-on learning experience and a more detailed look into the model (4). In addition, 3D printed model gives a better spatial visualization because users can pick up and rotate a model to view anatomical structures or pathologies (5).

Besides 3D printing, AR and VR also offer a wide range of benefits in education. Both modalities produce interactive 3D images with the main difference being the type of images. Images from AR are superimposed in the real world and allow users to remain in and interact with the real world, whereas VR produces simulated images in a synthetic world that removes the user from reality (6–8). Despite their differences, both education modalities can be used as options for distant interactive learning (9, 10). The use of these modalities results in higher satisfaction among students, as well as improvement in active learning and attention span (11, 12). Therefore, better learning outcomes with increased long-term knowledge retention, and also improved communication between teachers and students can be achieved (9, 13).

In education, there are two main types of learning approaches: passive learning and active learning. Passive learning is a teacher-centered approach where teachers deliver information to students, and students acquire knowledge without making conscious effort. On the other hand, active learning is a student-centered approach that requires students to make conscious efforts in the assigned activities. It also encourages students to ask questions and facilitates discussions through the interaction with learning models. Therefore, active learning is more than reading notes or listening to a lecture—it consists of active thinking and strengthens problem-solving skills. Hence, using 3D printing, AR and VR technology can increase students' attentional span, facilitate higher learning, and enrich the active learning experience.

This review paper aims to compare and contrast the four modalities: slide-based lecture, 3D printed models, AR, and VR technology, in medical education.

SLIDE-BASED LECTURE

Slide-based lectures have been implemented to teach students across the world for nearly two decades. This teaching modality gained its popularity due to its small learning curve and ability to put instructors in a lecturing mode (8). Slide-based lecturing allows easy organization of lecture material into slides for one presentation with the added benefit of including different effects such as sounds, animated pictures, colors, and graphs to keep students interested. Additionally, it allows instructors to compact intensive learning material into simple thirty to fifty slides for one lecture sitting. This gives them an opportunity to cover more material during a fixed semester schedule. These presentations can also be conveniently saved as a file on computers, USB drives or online storage so that it can be quickly shared with others with a click of a button. This functionality also saves instructors preparation time if the same lecture needs to be given every semester (8).

Research has demonstrated that slide-based lectures benefit students' cognitive learning in a number of different ways. Baker et al. showed that students expressed their preference to use slide-based presentation in class because it helped sustain their attention and kept information organized (10). Students can also directly make additional notes on the slides while their professors are going over the lecture. Furthermore, Nouri et al. reported that slide-based presentation improved students' attitudes toward the instructors and the class overall (6). The downside of slide-based presentation includes the lack of interactive learning as it encourages passive learning among students. Klemn et al. demonstrated that slide-based presentation decreased memory performance as students are not engaged in their learning. Instead of actively engaging in lessons and asking questions, students avoid taking notes and they tend to believe that they are able to follow, remember, or understand information more easily (7, 8). This method of teaching also fails to reflect on the meaning of the lessons (8).

Slide-based lectures are especially common in medical campuses today. Medical professors have been using the same teaching method when they go over hundred of slides to teach medical students in one sitting. This method of teaching lacks an interactive approach because students are often overwhelmed with the large number of slides (8). In medical training, slide-based presentation can have a negative effect on students' performance. Labrecque et al. proved a distinct difference between passive training through slide-based presentation and interactive training. In a central venous catheter needle access and dressing change course, nurses who were trained with slide-based presentation made more errors than those who were trained by direct observation and feedback (14). Therefore, interactive learning has been shown to be an important element in teaching students as it increases their attention span and helps them improve from previous mistakes. Nurses who were trained with observation and feedback reported that their learning sessions were more interesting to follow (14). Therefore, interactive teaching modalities using 3D printed models, AR and VR technology were explored to address the limitations of slide-based lecture.

3D PRINTING IN EDUCATION

For many years, traditional teaching methods such as didactic lectures, anatomical models, and cadaveric learning have been used to teach students. Students who learn anatomy through cadaveric dissection are limited with short-term knowledge acquisition, and they could not recall what they learned after a 2-week follow up (5). In addition, there are many ethical, financial, and logistical issues which resulted in a declining use of cadaveric dissection (5). Animal models are also a great resource for cadaver lab teaching. However, although they have lifelike soft tissue texture and can accurately reflect pathology, they still have anatomical variations and face ethical, cultural, and financial concerns.

Therefore, to improve anatomy learning experience and memory retention, different approaches have been applied in addition to cadaveric models. These include plastic idealistic models, plastinated specimens, body painting, atlas books, and 3D printed models. Hoyek et al. showed that students who studied anatomy using 3D models outperformed those who used 2D drawings from slide-based presentation in terms of spatial arrangement (15). Li et al. reported that those who used 3D

modalities scored higher on post-exposure test and had greater memory retention (5). 3D printed model is more advantageous because the subjects can grasp, rotate, and actually feel the texture of the objects, while 3D virtual modality still lacks the physical experience of a cadaver (5).

The addition of 3D printing into anatomy classrooms shows a promising future. 3D printer has the capability to produce models that are flexible and have a soft texture comparable to real organs at the expense of cost and production time (16). These models serve as great resources for both students and teachers (5). Li et al. showed an increase in students' satisfaction while learning anatomy as students preferred 3D printed models over 2D images (5). In a study published by the National Association of Biology Teachers, students reported that they often felt less creative and designed less impressive visual aid products with traditional learning methods. However, when using 3D printing, students become more engaged and creative in their projects because they invested more time to create their final products (17).

In clinical training, 3D printed models have helped in demonstrating complex anatomical structures (3, 18–20). White et al. reported that pediatric and pediatric/emergency medicine residents greatly benefited from studying cardiac anatomy of tetralogy of fallot (TOF) using 3D printed models. In their study, the residents studied two different heart defects: ventricular septal defect (VSD) and TOF using either a lecture with 2D images or 3D printed model. Their research showed that residents scored significantly higher on identification of anatomical structures on TOF 3D printed model (18). There was no difference found between 2D lecture and 3D printed model on VSD because the heart pathology can be easily understood without using 2D images or 3D models. This further proves that 3D printed models can be crucial in demonstrating complex spatial relationship in congenital heart defects (CHD) (18). White et al. also emphasized the advantages of 3D printed model in the training of various educational levels such as undergraduate, medical students, residents, nurses, and surgeons.

Besides its use in the teaching of anatomy, 3D printed model also greatly facilitates students' understanding of pathology. Students have been relying on 2D pictures from the textbook or slide-based presentation to study pathology. With 3D printing, students are able to feel pathological changes like a tumor or tissue texture changes. However, materials used in 3D printing are limited and currently unable to replicate the exact tissue texture that is present in real-life organs (5).

LIMITATION OF 3D PRINTING IN EDUCATION

Although 3D printed models do not require chemical maintance as in cadaver resources and students can use them outside of the lab, Wilk et al. reported that cadaveric learning is preferred because students can actually feel life tissue texture on cadavers and observe the impact of organ damage such as lung cancer, peptic ulcers, etc. (21).

3D printing poses as a new challenge for teachers because they would have to go through training courses in order to be able to print their own models. Trust et al. demonstrated that teachers should have basic technology skills to design a model and also know how to troubleshoot errors. Since 3D printing is relatively new in the market, printing errors from hardware issue may arise (4). Another challenge that was mentioned related to the long production time involved in printing a 3D model. Trust et al. reported that creating a four-inch model would take ∼4 h. The long production time in addition to troubleshooting would definitely take away valuable time that teachers can use to create content and teach students. Therefore, teachers should weigh the pros and cons of using 3D printing in their classroom.

Besides limitations in production time, the cost of 3D printing is high and can be another limiting factor. The cost of printing a model can be broken down into different components such as printer, software, CT scanning charge etc. For example, a printer can cost up to $65,000, with an additional cost of up to $15,000 for the software, and another $400/h for obtaining CT scans from a medical source (1, 2). Some institutions have another option to print the models through an external party. However, these parties may charge up to $600,000 for a model (1). Given this limitation, low cost options are currently being explored to make 3D models more affordable to increase its widespread use. However, every printer is limited to the material that it can use for printing. More afforable printers usually produce models with materials which are not ideal for learning due to its inflexible properties (3). Furthermore, the cost of these models increases as the size increases. Therefore, in order to ensure that students get the best learning experience with life-size models that closely replicate pathologies and tissue texture, the overall cost of a single model can be high which explains why 3D printed models are not widely distributed.

Despite its limitations, 3D printed models are still more cost-efficient compared to cadavers. A cadaver alone is about $8,500 without dissection and maintenance fees (1). Additionally, after a certain period of time, institutions might want to purchase a new cadaver due to wear and tear leading to changes in anatomical accuracy. In contrast, 3D models can be reused as they are durable and easy to maintain.

AR IN EDUCATION

In recent years, various reports have demonstrated the potential and efficacy of AR in education. For example, a chemistry classroom reported positive outcomes when their students used AR to study microstructures of different substances (22). AR technology has allowed students to control and combine different models and also work on inquiry-based experiements. In a post-interview session where students were picked randomly to rate their experiences with AR, students commented that they had positive learning attitude toward AR technology. The overall results showed that AR was much more interesting than traditional learning tools where teachers rely on teaching slides, and that AR enhanced long-term knowledge retention (22).

AR was also used in undergraduate science, technology, engineering, and mathematics (STEM) classrooms to assist with students' learning and cut down the workload of faculty. In

a study performed in first-year college students during their physics laboratory, students were divided into two groups: AR technology group, and traditional laboratory manual group (23). The 5-week experiment revealed that students who used AR technology followed their experiments more closely and made fewer errors. In an interview with the physics teacher, he indicated that his workload in the classroom was greatly reduced because students who used AR technology sought less help and understood complex physics problems more easily (23).

In medical education, AR technology has been implemeted to a limited extent to teach students anatomy, surgery, or pathology. In Thailand, health sciences students studied anatomy of the hand using either the Leap Motion AR or traditional cadaveric dissection (24). Leap Motion is a device that can overlay computer-generated 3D images of the skin, muscles, and bone that moves with real-time movement onto a real hand (24). Students that used Leap Motion demonstrated a better understanding of the hand anatomy at every anatomical level—from bones to muscles to skin, than those who did cadaveric dissection. Post-test questionaires showed that students had a positive attitude in learning about the hand anatomy using AR technology and that this new technology would be a useful substitute for textbooks (24).

Another AR technology, the Microsoft HoloLens, has been explored in the training of pathology residents. Through the use of the HoloLens, residents were able to communicate with their instructor located at a remote distance while viewing multiple gross pathology specimens (9). This allowed telepathology instruction where the attending was able to give guidance on what tissue areas were to be dissected. More importantly, Microsoft HoloLens allowed the residents to identify the tissue areas corresponding with the imaging result. For example, a breast specimen radiograph with a clip was displayed in the HoloLens. Resident who performed the autopsy was able to precisely locate the area of breast tissue with the clip as the radiograph from the HoloLens was coregistered with the corresponding specimen (9). Interactive gestures displayed by the HoloLens and voice commands allowed residents to successfully record organ weight, take notes and capture images of the pathology specimens.

LIMITATION OF AR IN EDUCATION

Since AR is a new technology, research has shown that students usually become more intrigued in learning as they would prefer to study with images and audio instead of reading text from lab manuals (23). As a result, students would spend less time reading and studying outside of class because they would only memorize the content related to AR technology (23). Despite this concern, the report showed that students using AR become more sensitive about laboratory safety compared to students who only read lab manuals (23).

Another limitation of AR technology is that it can induce simulator sickness in users if they use it for a prolonged period of time. Simulator sickness is characterized by eye strain, nausea, disorientation, and headaches (9). Hanna et al. discussed that the study participants reported no such adverse effects because their time of use ranged from a few minutes to an hour (9).

Lastly, it often takes time for the users to get familiar with the control options in AR since this technology is relatively new and its widespread use is limited. In a study performed which involved heart anatomy using AR, students were able to identify all of the features of the heart after a short delay at the beginning because students were unfamiliar with the application (25). In spite of unfamiliarity with the technology, user satisfaction was still reported, especially if they had higher computer knowledge—regardless of their age, gender, and educational level (26). Overall, AR is a reliable tool for educational purpose as it helps students to learn interactively and enables remote supervision.

VR IN EDUCATION

AR and VR can produce interactive 3D images, however, there are several differences between the two modalities. AR does not require a headset because its image can be easily generated with smart glasses, smart phones, or a headset. AR allows virtual experiences to be blended with the real world because the machine produces a superimposed 3D image (27). Unlike AR, VR usually comes with a headset, a digital device, and its 3D image completely replaces the real world (28, 29).

Like the other 3D modalities, VR can also be used to teach students about anatomy. Maresky et al. conducted a study to compare the use of VR and traditional learning modalities such as slides-based lecture and anatomy atlas textbook in the learning of cardiac anatomy. Cardiac anatomy has been a difficult subject to teach due to its complex 3D spatial orientation. It was reported that VR was able to display accurate anatomy and spatial arrangement, and that students interacted well with the heart structures. Undergraduate students who used VR for cardiac anatomy learning scored 21.4% higher than control group who used traditional modalities (30).

Coyne et al. discussed that VR has been useful in pharmacy education since it reinforced both didactic and laboratory learning. Before the advancement of VR technology, simulation mannequins, 3D modeling, and patients' case reports offered many benefits in pharmacy schools. Although mannequins can provide realistic assessment of students' performance related to patient safety, ethical behaviors, and patient care, the cost of mannequins have skyrocketed in the past few years making it increasingly unaffordable (12). VR, on the other hand, serves as an important element in promoting students' active engagment and allowing students to learn from mistakes. For example, in pharmacy school, lecture-based curriculum has been a major resource. However, VR has the ability to change the landscape of students' learning from passive to active. It changed the role of instructors from lecturing and reading off slides to serving as a guide while assisting their students (12). Students have more chances to ask questions, approach problems on their own, and spend less time relying on their instructors. In addition, active engagement is reinforced when students' memory retention on tedious subjects is increased. For example, better performance

is observed on drug pharmacokinetics, memorizing generic, and brand names when these difficult topics are incorporated into fun games in VR (12). Coyne et al. concluded that active learning is very important in healthcare education because it enhances critical thinking, teamwork, and creativity. In healthcare education, students cannot make mistakes on a real patient because that will violate the basic principles of medicine such as non-maleficence and beneficence. VR technology offers opportunities for students to learn from their mistakes and allow room for improvement by providing instructor's feedbacks (12). Therefore, VR technology not only promotes active engagement in the classroom, but also ensuring patient safety, and minimizing medical errors.

In terms of finances, VR comprises of two components: software and hardware, overall amounting to a lower cost. The price of a software, in fact, depends on the producers and its quality. A high-end VR hardware which includes a laptop and a headset would cost around £3,000 (31). VR technology helps reduce the fees and time needed for advanced training sessions for faculty because the software is usually comercially available which makes the set up very simple and allows easy access to faculty and learners (31).

LIMITATION OF VR IN EDUCATION

Although VR enhances learning experience of both students and teachers, it still cannot replace expert education and the natural human emotional expressions since the user is placed in a synthetic world. Pottle et al. demonstrated that 3D images generated by VR is just another method of delivering a message and its benefit does not cover every aspect. For example, VR is not a great tool to teach abdominal palpation because it only generates a physical representation of the abdomen (31). In addition, VR is not recommended in situations like delivering a bad news because VR is unable to replicate the complexity of human facial expressions and language which are still best illustrated by humans (31). Therefore, VR should not completely replace clinical training where clinical skills and empathy are best taught by experts.

There are also many adverse effects reported by users when they were immersed in the virtual 3D environment. 25% of VR users reported that they experienced headaches, 40% reported blurred vision, and 35% reported dizziness (32). A study was carried out to investigate the change in static balance after using VR application. Static balance and other adverse effects such as headache, dizziness, motion sickness, and eye fatigue were noted. Park et al. demonstrated that there were differences between VR display with a fixed and a changing background. In this study, healthy adult volunteers were separated into a control group, a VR game with a fixed display group, and a VR game with a changing motion backgroup group. The study showed that the VR display itself caused a negative change in balance as well as dizziness and eye strain (33). In addition, those who used VR game with changing motion background had higher sway velocity and sway length (33). Therefore, Park et al. recommended using only fixed background VR application to reduce adverse effects that can arise in rehabilitation program.

FUTURE CONSIDERATION

As compared to slide-based lecture, the cost for 3D printing, AR, and VR are still expensive, making it difficult to provide educational advantage to every student. Because of this reason, 3D printing, AR, and VR are not as popular as slide-based presentation. There are not many reports that give a comparison between the utility of 3D printing, AR, and VR. For example, Botden et al. discussed that most VR technologies lack tactile feedback features that are important in surgical training. In contrast, AR retains many of the virtual features of VR in addition to having a better haptic feedback (34). Both VR and AR can come with an additional handpiece device that provides sensory feedback. A pair of hand controllers allows VR users to feel the weight, movement, pressure, and resistance of an object as they try to grab an object with VR (34, 35). For

TABLE 1 | Comparison between slide-based presentation, 3D printed model, augmented reality, and virtual reality.

	Slide-based presentation	3D printed model	Augmented reality	Virtual reality
Initial set-up costs[a]	Low	Very high	High	High
Recurring cost	Minimal	USD $100–2 k[b]	Minimal	Minimal
Preparation time[c]	Few hours[d]	Hours to days[d]	Few hours[d]	Few hours[d]
User experience	Real world (2D)	Real world (3D)	Mixed reality	Virtual world
Students' learning	Passive	Active	Active	Active
Learning curve	Shortest	Short	Long	Long
Tactile feedback	None	Yes	Possible[e]	Possible[e]
Team discussion	Yes	Yes	Possible[f]	Possible[f]

[a] *The initial set-up cost refers to the cost of either slide-based presentation, 3D printer, VR, or AR device.*
[b] *The material cost of a 3D printed model ranges from USD $100–2 k, depending on the complexity.*
[c] *Preparation time refers to the time needed for educators to prepare a single project.*
[d] *The preparation time for slide-based presentation, 3D model, AR, and VR use depends on the technological skills of the educators.*
[e] *Both AR and VR can be coupled with hardware for a tactile experience.*
[f] *Team discussion on AR and VR can be possible with the correct hardware and software.*

AR, a wearable tactile display also known as Wearable Fabric Yielding Display (W-FYD) was recently introduced to augment interactions with an physical object. W-FYD allows users to feel the softness of an object as well as the sliding perception (36). In a study where stiffness of AR and VR was compared, 60% of the study participants rated VR as a stiffer device than AR (37). However, Gaffary et al. concluded that the stiffness in VR may be due to psychological effects. Currently, there are not many published literature that compares haptic feedbacks between AR and VR. Future research should look into this factor as haptic feedback is crucial in medical training, especially in telemedicine where students can learn about or palpate different tissue textures from a remote distance. **Table 1** summarizes the important features of slide-based presentation, 3D printing, AR, and VR.

CONCLUSION

Slide-based presentation, 3D printing, AR, and VR each have their benefits and limitations in medical education. Traditional slide-based presentation is inexpensive and takes less time to produce, however, it does not stimulate students' thinking nor help them with active learning. 3D printing, AR, and VR technology, on the other hand, are able to create an interactive environment. However, they are not as accessible as slide-based presentation due to their cost and extensive training. It should be noted that these learning technologies are best suited for their own learning objectives. 3D printed models allow students to physically interact with the anatomical model, enabling multidirectional views which improves the learning of spatial relationships in anatomy. AR and VR technology, on the other hand, offer a virtual experience. While VR completely switches the users to the virtual environment, the AR allows users to sense the real environment while experiencing the virtual world. The virtual experience that AR and VR offer improves memory retention, encourages student's participation in the lesson, boosts creativity, and enables easier access to telecommunication. Overall, these three modalities not only reduce the workload of instructors, but they also improve communication between the students and their instructors. For many years, students have been lectured by their instructors and applying passive learning to pass their classes. With these interactive technologies, students become more engaged and intrigued in their study material, resulting in more constructive questions being asked in class. 3D printing, AR, and VR have shown a promising future in education and educators should look into these modalities to improve teaching approach and students' engagement in the classrooms.

AUTHOR CONTRIBUTIONS

IB: extensive literature review, working on the first draft, and subsequent reiterations. SW: helping IB in literature review and subsequent reiterations. AB and HS: helping with editing and revising the manuscript. AA: conceptualizing the idea, guiding IB in literature review and helping with editing, and revising the manuscript. HS: helping with the final submission. All authors contributed to the article and approved the submitted version.

REFERENCES

1. McMenamin PG, Quayle MR, McHenry CR, Adams JW. The production of anatomical teaching resources using three-dimensional (3D) printing technology. *Anatom Sci Educ.* (2014) 7:479–86. doi: 10.1002/ase.1475
2. Farooqi KM, Cooper C, Chellian A, Saeed O, Chai PJ, Jambawalikar SR, et al. 3D printing and heart failure: the present and the future. *JACC Heart Fail.* (2019) 7:132–42. doi: 10.1016/j.jchf.2018.09.011
3. Hermsen JL, Roldan-Alzate, Anagnostopoulos APV. Three-dimensional printing in congenital heart disease. *J Thorac Dis.* (2020) 12:1194–203. doi: 10.21037/jtd.2019.10.38
4. Trust T, Maloy RW. Why 3D Print? the 21st-century skills students develop while engaging in 3D printing projects. *Comput Schools.* (2017) 34:253–66. doi: 10.1080/07380569.2017.1384684
5. Li KHC, Kui C, Lee EKM, Ho CS, Sunny Hei SH, Wu W, et al. The role of 3D printing in anatomy education and surgical training: a narrative review. *Med Ed Publish.* (2017) 6:1–12. doi: 10.15694/mep.2017.000092
6. Nouri A, Shahid A. The effect of PowerPoint presentations on student learning and attitudes. *Glob Perspect Account Educ.* (2005) 2:53.
7. Wecker C. Slide presentations as speech suppressors: when and why learners miss oral information. *Comput Educ.* (2012) 59:260–73. doi: 10.1016/j.compedu.2012.01.013
8. Klemm WR. Computer slide shows: a trap for bad teaching. *College Teach.* (2007) 55:121–4. doi: 10.3200/CTCH.55.3.121-124
9. Hanna MG, Ahmed I, Nine J, Prajapati S, Pantanowitz L. Augmented reality technology using Microsoft HoloLens in anatomic pathology. *Arch Pathol Lab Med.* (2018) 142:638–44. doi: 10.5858/arpa.2017-0189-OA
10. Baker JP, Goodboy AK, Bowman ND, Wright AA. Does teaching with PowerPoint increase students' learning? A meta-analysis. *Comput Educ.* (2018) 126:376–87. doi: 10.1016/j.compedu.2018.08.003
11. Di Serio Á, Ibáñez MB, Kloos CD. Impact of an augmented reality system on students' motivation for a visual art course. *Comput Educ.* (2013) 68:586–96. doi: 10.1016/j.compedu.2012.03.002
12. Coyne L, Merritt TA, Parmentier BL, Sharpton RA, Takemoto JK. The past present, and future of virtual reality in pharmacy education. *Am J Pharm Educ.* (2019) 83:7456. doi: 10.5688/ajpe7456
13. Cascales A, Laguna I, Pérez-López D, Perona P, Contero, M. An experience on natural sciences augmented reality contents for preschoolers. In: Shumaker R, editor. *Virtual, Augmented and Mixed Reality. Systems and Applications. VAMR.* Vol. 8022. Berlin, Heidelberg: Springer (2013). p. 2–4; 7–10. doi: 10.1007/978-3-642-39420-1_12
14. Labrecque S, Sauerland C, Donovan R, Haas JP, Montecalvo M. Didactic power point teaching method is not enough to assure compliance: Direct Observation (DO) and feedback are key elements. *Am J Infect Control.* (2013) 41:S64. doi: 10.1016/j.ajic.2013.03.132
15. Hoyek N, Collet C, Rienzo FD, Almeida MD, Guillot A. Effectiveness of three-dimensional digital animation in teaching human anatomy in an authentic classroom context. *Anatomic Sci Educ.* (2014) 7:430–7. doi: 10.1002/ase.1446
16. Lau I, Wong YH, Yeong CH, Abdul Aziz YF, Md Sari NA, Hashim SA, et al. Quantitative and qualitative comparison of low- and high-cost 3D-printed heart models. *Quant Imaging Med Surg.* (2019) 9:107–14. doi: 10.21037/qims.2019.01.02
17. McGahern P, Bosch F, Poli D. Enhancing learning using 3D printing: an alternative to traditional student project methods. *Am Biol Teach.* (2015) 77:376–7. doi: 10.1525/abt.2015.77.5.9
18. White SC, Sedler J, Jones TW, Seckeler M. Utility of three-dimensional models in resident education on simple and complex intracardiac congenital heart defects. *Congenit Heart Dis.* (2018) 13:1045–9. doi: 10.1111/chd.12673

19. Biglino G, Milano EG. Applications of 3D printing in paediatric cardiology: its potential and the need for gathering evidence. *Trans Pediatrics.* (2018) 7:219. doi: 10.21037/tp.2018.07.02
20. Illmann CF, Ghadiry-Tavi R, Hosking M, Harris KC. Utility of 3D printed cardiac models in congenital heart disease: a scoping review. *Heart.* (2020) 106:1631–7. doi: 10.1136/heartjnl-2020-316943
21. Wilk R, Likus W, Hudecki A, Sygula M, Rózycka-Nechoritis A, Nechoritis, et al. What would you like to print? Students' opinions on the use of 3D printing technology in medicine. *PLoS One.* (2020) 15:e0230851. doi: 10.1371/journal.pone.0230851
22. Cai S, Wang X, Chiang FK. A case study of Augmented Reality simulation system application in a chemistry course. *Comput Human Behav.* (2014) 37:31–40. doi: 10.1016/j.chb.2014.04.018
23. Akçayir M, Akçayir G, Pektaş HM, Ocakb MA. Augmented reality in science laboratories: the effects of augmented reality on university students' laboratory skills and attitudes toward science laboratories. *Comput Hum Behav.* (2016) 57:334–42. doi: 10.1016/j.chb.2015.12.054
24. Boonbrahm P, Kaewrat C, Pengkaew P, Boonbrahm S, Meni V. Study of the hand anatomy using real hand and augmented reality. *Int J Interact Mobile Technol.* (2018) 12:181–90. doi: 10.3991/ijim.v12i7.9645
25. Kiourexidou M, Natsis K, Bamidis P, Antonopoulos N, Papathanasiou E, Sgantzos M, et al. Augmented reality for the study of human heart anatomy. *Int J Electron Commun Comput Eng.* (2015) 6:658.
26. Xue H, Sharma P, Wild F. User satisfaction in augmented reality-based training using microsoft HoloLens. *Computers.* (2019) 8:9. doi: 10.3390/computers8010009
27. Low D, Lee CK, Lee LTD, Ng WH, Ang BT, Ng I, et al. Augmented reality neurosurgical planning and navigation for surgical excision of parasagittal, falcine and convexity meningiomas. *Br J Neurosurg.* (2010) 24:69–74. doi: 10.3109/02688690903506093
28. Chen FQ, Leng YF, Ge JF, Wang DW, Li C, Chen B, et al. Effectiveness of virtual reality in nursing education: meta-analysis. *J Med Internet Res.* (2020) 22:e18290. doi: 10.2196/18290
29. Porter ME, Heppelmann JE. Why every organization needs an augmented reality strategy. *HBR'S 10 MUST.* (2017) 95:46–57.
30. Maresky HS, Oikonomou A, Ali I, Ditkofsky N, Pakkal M, Ballyk B. Virtual reality and cardiac anatomy: exploring immersive three-dimensional cardiac imaging, a pilot study in undergraduate medical anatomy education. *Clin Anat.* (2019) 32:238–43. doi: 10.1002/ca.23292
31. Pottle J. Virtual reality the transformation of medical education. *Future Healthc J.* (2019) 6:181–5. doi: 10.7861/fhj.2019-0036
32. Moro C, Štromberga Z, Raikos A, Stirling A. The effectiveness of virtual and augmented reality in health sciences and medical anatomy. *Anat Sci Educ.* (2017) 10:549–59. doi: 10.1002/ase.1696
33. Park S, Lee G. Full-immersion virtual reality: Adverse effects related to static balance. *Neurosci Lett.* (2020) 733:134974. doi: 10.1016/j.neulet.2020.134974
34. Botden SMBI, Buzink SN, Schijven MP, Jakimowicz JJ. Augmented versus virtual reality laparoscopic simulation: What is the difference? *World J Surg.* (2007) 31:764–72. doi: 10.1007/s00268-006-0724-y
35. Alvarez-Lopez F, Maina MF, Saigí-Rubió F. Use of a low-cost portable 3D virtual reality gesture-mediated simulator for training and learning basic psychomotor skills in minimally invasive surgery: development and content validity study. *J Med Internet Res.* (2020) 22:e17491. doi: 10.2196/17491
36. Fani S, Ciotti S, Battaglia E, Moscatelli A, Bianchi M. W-FYD: a wearable fabric-based display for haptic multi-cue delivery and tactile augmented reality. *IEEE Trans Haptics.* (2018) 11:304–16. doi: 10.1109/TOH.2017.2708717
37. Gaffary Y, Le Gouis B, Marchal M, Argelaguet F, Arnaldi B, Lecuyer, et al. AR feels "Softer" than VR: haptic perception of stiffness in augmented versus virtual reality. *IEEE Trans Vis Comput Graph.* (2017) 23:2372–7. doi: 10.1109/TVCG.2017.2735078

Conflict of Interest: The authors declare that the research was conducted in the absence of any commercial or financial relationships that could be construed as a potential conflict of interest.

frontiers in Pediatrics

ORIGINAL RESEARCH
published: 10 December 2021
doi: 10.3389/fped.2021.770803

Risk Factors for Sudden Infant Death in North Carolina

Merick M. Yamada[1†], Michael B. Rosamilia[2†], Karen E. Chiswell[2], Alfred D'Ottavio[2], Tracy Spears[2], Claire Osgood[2], Marie Lynn Miranda[3], Nina Forestieri[4], Jennifer S. Li[1,2] and Andrew P. Landstrom[1,5]*

[1] Department of Pediatrics, Division of Pediatric Cardiology, Duke University School of Medicine, Durham, NC, United States, [2] Duke Clinical Research Institute, Duke University School of Medicine, Durham, NC, United States, [3] Department of Applied and Computational Mathematics and Statistics, University of Notre Dame, Notre Dame, IL, United States, [4] North Carolina Department of Health and Human Services, Raleigh, NC, United States, [5] Department of Cell Biology, Duke University School of Medicine, Durham, NC, United States

Background: Sudden infant death syndrome (SIDS) is the sudden, unexplained death of infants <1 year old. SIDS remains a leading cause of death in US infants. We aim to identify associations between SIDS and race/ethnicity, birth weight/gestational age, and socioeconomic/environmental factors in North Carolina (NC) to help identify infants at risk for SIDS.

Methods and Results: In this IRB-approved study, infant mortality 2007–2016 and death certificate-linked natality 2007–2014 were obtained from the NC Department of Health and Human Services. General, NC natality statistics 2007–2016 were obtained from CDC Wonder. Association between SIDS/total infant death and covariates (below) were calculated. Total infant mortality decreased 2007–2016 by an average of 14 deaths/100,000 live births per year, while SIDS incidence remained constant. Risk ratios of SIDS/total infant deaths, standardized to Non-Hispanic White, were 1.76/2.41 for Non-Hispanic Black and 0.49/0.97 for Hispanic infants. Increased SIDS risk was significantly and independently associated with male infant sex, Non-Hispanic Black maternal race/ethnicity, young maternal age, low prenatal care, gestational age <39 weeks, birthweight <2500 g, low maternal education, and maternal tobacco use ($p < 0.01$). Maternal previous children now deceased also trended toward association with increased SIDS risk.

Conclusions: A thorough SIDS risk assessment should include maternal, socioeconomic, and environmental risk factors as these are associated with SIDS in our population.

Keywords: SIDS, SIDS (sudden infant death syndrome), race, ethnicity, infant mortality, birthweight, gestational age

Edited by:
Ruth Heying,
University Hospital Leuven, Belgium

Reviewed by:
Alvise Guariento,
Hospital for Sick Children, Canada
Emanuele Monda,
University of Campania Luigi Vanvitelli, Italy
Estelle Naumburg,
Umeå University, Sweden
Karel Allegaert,
University Hospitals Leuven, Belgium

***Correspondence:**
Andrew P. Landstrom
andrew.landstrom@duke.edu

[†] These authors have contributed equally to this work and share first authorship

Specialty section:
This article was submitted to Pediatric Cardiology, a section of the journal Frontiers in Pediatrics

Received: *04 September 2021*
Accepted: *16 November 2021*
Published: *10 December 2021*

Citation:
Yamada MM, Rosamilia MB, Chiswell KE, D'Ottavio A, Spears T, Osgood C, Miranda ML, Forestieri N, Li JS and Landstrom AP (2021) Risk Factors for Sudden Infant Death in North Carolina. Front. Pediatr. 9:770803. doi: 10.3389/fped.2021.770803

HIGHLIGHTS

- Key Message: Sudden infant death syndrome remains a common cause of death in infants in North Carolina and has identifiable risk factors.
- What does it add to the existing literature: This study includes all SIDS cases in NC from 2007-2016, making it a larger and more contemporary population study.
- What is the impact: Low maternal education, low birth weight, less than 39 weeks gestational age, smoking, and non-Hispanic Black race are associated with SIDS. Hispanic ethnicity is a protective factor.

INTRODUCTION

Sudden infant death syndrome, or SIDS, is the sudden unexplained death of an apparently healthy infant <1 year old with no clear cause of death after evaluation, traditional autopsy, and review of clinical history (1), and is a diagnosis of exclusion (2). SIDS remains one of the leading causes of death in infants in the United States (3, 4) with about 3,500 deaths annually (2). The pathophysiology of SIDS is thought to be multifactorial and governed by the "triple risk hypothesis": an at-risk infant with underlying vulnerability that remains undefined, a critical development period in infancy, and exogenous risk factors (5). While recent evidence has suggested that only 10% of SIDS cases host likely pathogenic variants in channelopathy associated genes, this association represents an underlying susceptibility to cardiac arrhythmias in some SIDS infants (6–10). Further, there are known racial, socioeconomic, and environmental disparities in the incidence of SIDS (11), including Black race (2, 12), bed sharing, soft bedding, sleep surface, prematurity, smoking, birth weight, sleeping position, income, occupation, education, and housing (2, 13).

While total infant death has decreased across the United States, SIDS incidence has plateaued (4). This is true despite the national- and state-level interventions aimed at decreasing SIDS risk, including the passage of "The NC SIDS Law" in 2003 and the NC Back to Sleep Campaign. Given the persistence of SIDS deaths in the US, identification of additional risk factors associated with SIDS is needed to identify the at-risk infant. Previous studies have evaluated smaller groups of infants and have not studied multiple elements of the triple-risk hypothesis within the same cohort. In order to accurately evaluate SIDS risk in infants and direct preventative efforts accordingly, a recent, large sample, analyzing multiple elements of the triple risk hypothesis is necessary.

In this study, we evaluate a population-based cohort of deaths in North Carolina to identify associations between SIDS death and race/ethnicity, gestational age, birth weight, maternal level of education, tobacco use, and history of previous maternal child death (from any cause).

Abbreviations: SIDS, sudden infant death syndrome; NC, North Carolina; CDC, Centers for Disease Control.

METHODS

SIDS and Total Infant Mortality Data

This study was approved by the Duke University Health System Institutional Review Board. Infant mortality data were obtained from the North Carolina Department of Health and Human Services (NCDHHS). Data were abstracted from NC vital records from January 2007–July 2016. Data from 2016 were annualized in year-over-year analyses. The cohort of SIDS deaths had the following inclusion criteria: (1) NC death certificates from January 2007–July 2016, (2) age at death <1 year and not missing, and (3) underlying cause of death ICD10 code of R95 ("Sudden infant death syndrome") or R99 ("Other ill-defined and unspecified causes of mortality"). Exclusion criteria included patients missing birth or death certificates. Death certificates from the latter part of 2016 were not received from NCDHHS and thus were not included in analyses. Demographic data from death records were identified using maternal, self-identified race and ethnicity. Birth certificate data from all NC births 2007–2014 were also obtained from NCDHHS. Birth certificates 2015–2016 were not included in analyses due to lack of availability of this data to investigators. Though the temporal range of death certificates included exceeded that of the birth certificates, only incidence by race/ethnicity over time was analyzed on death certificates. SIDS death records were linked with corresponding birth certificates by sex, date of birth, and full name. Partial matches, defined as any birth and death certificate with matching sex, date of birth, and a full name off by a single letter, were all included in the data set. Death records missing a matched birth certificate were excluded from analyses of covariates of SIDS risk.

Natality Data

NC natality statistics were obtained from the CDC Wonder database 2007–2016 (14). Births were filtered by maternal bridged-race and maternal ethnicity with inclusion of Non-Hispanic White, Non-Hispanic Black, and Hispanic. CDC Wonder-derived birth data was used for analysis of demographic data to include the full cohort of SIDS death certificates 2007–2016.

Analysis of Demographic Data

SIDS and total infant death incidences per 100,000 live births were calculated for race/ethnicity by year. As all data are from a complete population, inference testing was not performed. Change in incidence per year over the study period for SIDS and total infant death were calculated using a linear model. Mean differences between races/ethnicities by year over the study period for SIDS and total infant deaths, as well as related risk ratios were calculated. Risk ratios were standardized to Non-Hispanic White Incidence. Hispanic White and Hispanic Black are combined in the Hispanic group as >95% of all Hispanic births in the state of NC during the study period were Hispanic White.

Analysis of Covariates of SIDS Risk

We selected potential covariates associated with SIDS risk from birth certificate data for analysis. This included sex of the baby, maternal race/ethnicity, maternal age at the time of birth

(binned into 5-year intervals), Kotelchuck prenatal care index (categorized by sufficiency), obstetrician estimate of gestational age <39 weeks (compared with ≥39 weeks), birthweight <2500 g (compared with ≥2500 g), maternal education of 0–8 years or 9–12 years (compared with any college), any tobacco use during or in the year prior to pregnancy (compared with no tobacco use), and mother with at least one previous birth now dead (compared with mothers with no previous births now dead). Our cutoffs of gestational age, birthweight, and prenatal care are based on the typical designation of a full-term vs. preterm, low- vs. normal-birthweight infants, and sufficient prenatal care respectively (15–17). Divisions of tobacco smoking and maternal education variables were created based on logical cutoffs in our data set (ex. smoking vs. non-smoking).

The odds ratios of these covariates in SIDS infants vs. non-SIDS infants were calculated via univariate analysis and adjusted using a multivariable logistic regression model, including all mentioned covariates. All ORs were calculated for births 2007-−2014. All analyses were performed using RStudio V1.3 and SAS V9.4.

RESULTS

Incidence of Sudden Infant Death Syndrome and Total Infant Death in North Carolina

To determine the relationship between race/ethnicity and the incidence of SIDS, we analyzed NC death records and natality data 2007–2016. A total of 1,170,505 babies were born to mothers residing in the state of NC over the study period. There were 8,691 total infant deaths and 1,209 SIDS deaths, comprising 14% of total infant deaths (**Table 1**). A detailed flow diagram depicting the included and excluded cases is provided in **Supplementary Figure 1**. SIDS incidence over the study period was 105/100,000 live births with a non-significant change in incidence year-over-year (average decrease of 0.15 deaths/100,000 live births per year 95% CI [−4.3, 4.6]) (**Figure 1**). By race, SIDS incidence per 100,000 live births was 95 in Non-Hispanic White infants, 167 in Non-Hispanic Black infants, and 46 in Hispanic infants (**Table 2**). Non-Hispanic Black infants had a 1.76 risk ratio of SIDS compared to Non-Hispanic White infants. Interestingly, the Hispanic infants risk ratio of SIDS compared to Non-Hispanic White infants was 0.49 (**Table 2**). Overall, these findings show that the incidence of SIDS in NC has remained constant over the years 2007-2016 with persistent disparities between races/ethnicities disproportionately impacting Non-Hispanic Black infants. Further, Hispanic infants have a lower relative risk of SIDS compared to Non-Hispanic White infants.

To determine the influence of race, ethnicity, and total infant death in SIDS, we first stratified population data by race and ethnicity. The overall incidence of total infant death was 763/100,000 live births with an average decrease of 14 deaths/100,000 live births per year (95% CI [−22, −6.0], **Figure 1**). Total infant death incidence per 100,000 live births was 565 in Non-Hispanic White infants, 1,363 in Non-Hispanic Black infants, and 551 in Hispanic infants. Non-Hispanic Black infants had a 2.41 risk ratio and Hispanic infants had a 0.97 risk ratio of infant mortality compared to Non-Hispanic Caucasian infants (**Table 2**). Together, these findings show that there was a decrease in the incidence of total infant death in NC from 2007-2016, but a persistent, disproportionate impact on Non-Hispanic Blacks in both SIDS and total infant death.

TABLE 1 | Demographics of the 2007–2016 cohort of SIDS, total infant deaths, and births.

	Total*	NH**White	NH Black	Hispanic
SIDS	1,155	607	462	86
Total Infant Death	8,546	3,713	3,831	1,002
Births	1,113,611	652,978	279,254	181,379

**Total analyzed in the 2007–2016 cohort. Excludes other races (<5%) and missing data (<1%).*
***Non-Hispanic.*

TABLE 2 | Relative risk of mortality incidence per 100,000 live births from SIDS and total infant death by race and ethnicity normalized to Non-Hispanic White.

	Ethnicity	Risk Ratio
SIDS	NH* White	1
	NH Black	1.76
	Hispanic	0.49
Total	NH White	1
	NH Black	2.41
	Hispanic	0.97

**Non-Hispanic.*

Associations With Sudden Infant Death Syndrome

To determine the relationship between SIDS incidence and covariates of sex of the baby, maternal race/ethnicity, maternal age at the time of birth, Kotelchuck prenatal care index, gestational age, birthweight, maternal education, tobacco use, and mother with at least one previous birth now dead, we performed a multivariable logistic regression comparing births resulting in a SIDS death vs. all other births, yielding adjusted odds ratios (ORs). A table of SIDS and non-SIDS infant proportions by covariate is included in **Supplemental Table 1**. The odds of developing SIDS was significantly ($p < 0.01$) decreased with female sex (OR 0.80), non-Hispanic White or Hispanic race/ethnicity compared with non-Hispanic Black (OR 0.78 and 0.35, respectively), maternal age of 25–29, 30–34, and ≥35 compared with ≤19 (ORs 0.67, 0.45, and 0.27, respectively), Kotelchuck prenatal care index of intermediate, adequate, and adequate plus sufficiency (ORs 0.60, 0.54, and 0.56, respectively), and increased with gestational age <39 weeks (OR 1.33), birthweight <2500 g (OR 1.72), maternal education of 0–8 years or 9–12 years (ORs 1.85 and 1.62, respectively), and any tobacco use during or in the three months prior to pregnancy relative to non-SIDS infants (OR 3.13). The odds of developing SIDS trended toward a decrease with maternal age 20–24 years compared with ≤19 years (OR 0.88, $p =$

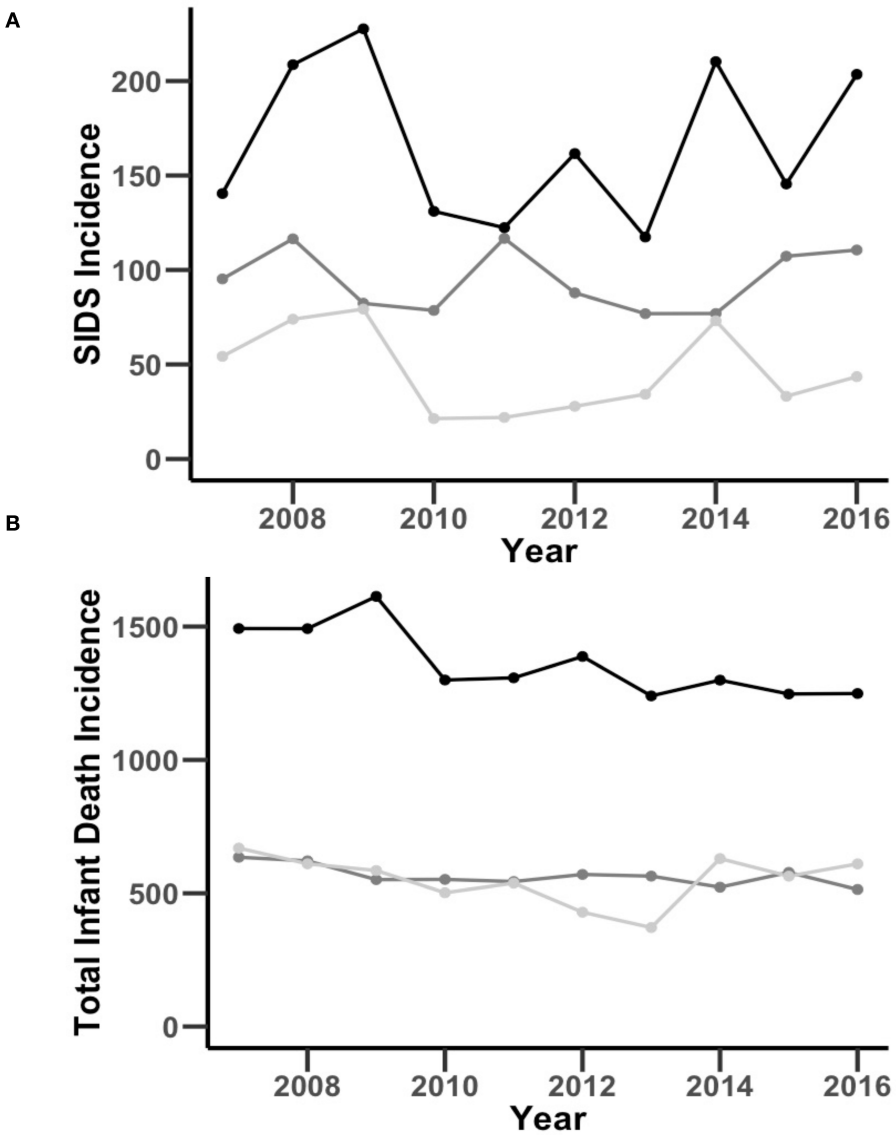

FIGURE 1 | Comparison of NC SIDS **(A)** and total infant death **(B)** incidence per 100,000 live births by race and ethnicity over time through the years of 2007–2016. The black, dark gray, and light gray lines represent Non-Hispanic Black, Non-Hispanic White, and Hispanic incidence per 100,000 live births, respectively.

0.23), or other race/ethnicity compared with Non-Hispanic Black (OR 0.69, $p = 0.056$), and an increase when infant's mother had at least one previous birth now dead (OR 1.10, $p = 0.76$). All adjusted ORs are summarized in **Figure 2**. We also calculated univariate associations with SIDS incidence (**Supplementary Table 2**). Taken together, these findings suggest that numerous host and environmental factors are significantly associated with SIDS incidence.

DISCUSSION

In 1992, the American Academy of Pediatrics debuted the Back to Sleep Campaign recommending that babies be put to sleep in the non-prone position, which led to a decrease in total SIDS deaths by 40%. Unfortunately, in the past two decades, there has been a stable number of SIDS deaths in the United States (2). Concordant with national statistics, we observed that the total incidence of infant death in NC has decreased, but SIDS incidence has remained constant. Our results also agree with other studies that have shown that Non-Hispanic Black infants are at a disproportionately high SIDS risk (12, 18). We also find that lower maternal education level (19), lower maternal age, male sex of the baby, and prior sibling death are associated with increased SIDS risk (20). Many of these associations have been previously shown in other studies; however, this study utilizes a more robust statistical approach, with a multivariable model, in a larger and more recent population to demonstrate

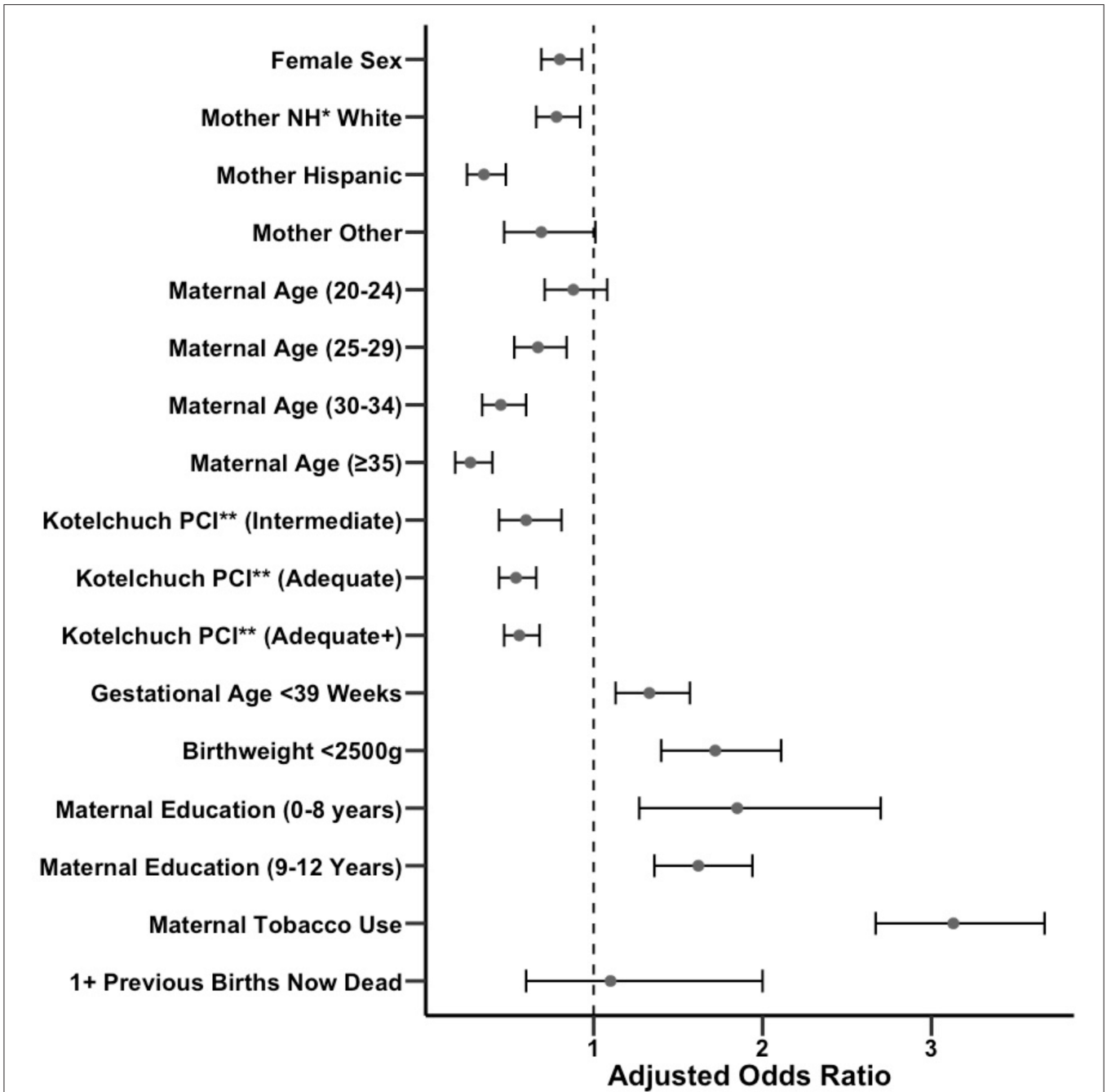

FIGURE 2 | Forest plot of adjusted odds ratios for exposure to various covariates in SIDS vs. non-SIDS infants with confidence intervals. Unadjusted odds ratios are also provided in **Supplementary Table 2**. *NH, Non-Hispanic. **PCI, Prenatal Care Index.

independent risk factors for SIDS. Of note, incidence of SIDS and total infant death was higher in NC compared with all US births (105/100,000 vs. 73/100,000 live births for SIDS and 763/100,000 vs. 560/100,000 live births for total infant death respectively). Furthermore, NC rates of SIDS risk factors exceeded statistics for the entire US population including a higher smoking rate before/during pregnancy (12.2 vs. 9.4%) and a lower average birthweight (3,258 grams vs. ∼3,500 grams) (21, 22). Overall, our data are in agreement with prior studies about SIDS risk factors, with novel elements including a state-wide population analysis with a larger sample size, a more recent cohort, and a larger number of studied covariates.

Other studies have attempted to explain the racial disparity in SIDS. For example, it has been described that racial discrimination affecting Black women is a risk factor for poor pregnancy outcomes, which seems to be related to chronic

stress leading to enhanced inflammatory response, compromised fetal development and adverse pregnancy outcomes (12, 23). Examples of adverse pregnancy outcomes include low birthweight and prematurity which, as we have described, are both correlated to SIDS risk. Therefore, there is a highly plausible connection between racial disparities and SIDS, mediated, in part, by pregnancy outcomes. Additionally, there are cultural factors that may play a role in infant care practices (24). As has been shown in previous studies (25, 26), we found that Hispanic ethnicity was associated with a reduction in SIDS incidence. Previous literature has suggested protective factors that are more prevalent in Hispanic families that may lead to a lower SIDS risk, including multigenerational home and greater family support. In summary, the racial and ethnic disparities we observed are potentially explained by outcomes related to systemic racism and cultural differences.

While we did not directly examine the pathways underlying biological or environmental associations with SIDS, we can generate hypotheses for explanatory mechanisms for directly analyzed covariates based on previous literature. Explanations for the association between prematurity and/or low birthweight and SIDS relate to problems of underdevelopment of respiratory control. For example, a 1998 study proposed a link between lung underdevelopment, known as apnea of prematurity, and SIDS (27). Furthermore, underdeveloped respiratory centers in premature and low birthweight babies may play a role in elevating SIDS risk (28). There are also several likely contributors in the causal pathway between maternal smoking and SIDS, including elevated respiratory infection risk and worse pregnancy outcomes, such as prematurity and low birthweight (29–31). Regarding the observed association between maternal education and SIDS, there are clear links between adequacy of prenatal care, education level and health literacy (32). Given that most SIDS prevention efforts to date have focused on parental education and behavior modification for infant care, a link between health literacy and SIDS is quite likely. Of note, regarding prenatal care specifically, we found that the majority of SIDS risk reduction from increasing prenatal care came from moving from the inadequate prenatal care group to the intermediate prenatal care group (17). This finding reinforces the goal of maximizing prenatal care, even when "adequate" levels cannot be reached. Finally, while not statistically significant, we observed an association between SIDS and at least one of the mother's previous births now deceased. This association can be explained both by the growing literature on evidence of the role of genetic predisposition in SIDS, as well as the fact that siblings may experience similar parental child-care practices (20, 33, 34). To gain more insight into the heritability of SIDS on a population level, sibling and twin studies must be performed. Overall, there is at least one plausible explanation linking each of our observed risk factors to SIDS.

One potential factor influencing SIDS risk that we did not directly measure due to data constraint is insurance status, as this influences access to healthcare and health education resources and has been associated with many health outcomes. Mothers in NC, along with newborn infants, have a mix of insurance types, private and public. In NC, all infants born to mothers with Medicaid are automatically guaranteed enrollment in Medicaid until they turn 1 year of age. Medicaid is also available to qualifying mothers while pregnant and for 60 days post-partum (35). Of note, in SIDS, insurance status has not been shown to be an independent risk factor in models incorporating income (36).

As we have observed, SIDS is multifactorial and complex. Improved understanding of risk factors and health disparities can improve our care for these populations and, hopefully, lead to a decrease in SIDS.

Limitations

This study is retrospective and observational in nature. Additionally, not all birth certificates were available for the entire SIDS death population, and birth certificates were not available to us after 2014, meaning that the cohort for racial/ethnic associations was somewhat different from that involved in calculation of other variable associations.

CONCLUSIONS

In our study of NC deaths 2007–2016, we find that the incidence of total infant death has decreased over time while SIDS incidence has remained constant, with a higher SIDS risk in Non-Hispanic Black infants, and a lower SIDS risk in Hispanic infants compared to Non-Hispanic White infants. Additional observed variables associated with SIDS include male sex, low prenatal care, prematurity, low birthweight, low maternal education, maternal smoking, and having a previous child die. The considerable differences in SIDS incidence related to biological and environmental conditions highlight the need for SIDS risk assessment, along with a concentration of effort into reducing health disparities in pregnancy and early life.

DATA AVAILABILITY STATEMENT

The raw data supporting the conclusions of this article will be made available by the authors, without undue reservation.

ETHICS STATEMENT

The studies involving human participants were reviewed and approved by Duke University Health System Institutional Review Board. Written informed consent for participation was not required for this study in accordance with the national legislation and the institutional requirements. Written informed consent was not obtained from the individual(s) for the publication of any potentially identifiable images or data included in this article.

DISCLOSURE

This manuscript was previously presented as a poster at the Duke University School of Medicine Department of Pediatrics Retreat and the American Academy of Pediatrics Conference 2021.

AUTHOR CONTRIBUTIONS

MY, MR, CO, MM, JL, and AL: planned the study, interpreted the findings, drafted the manuscript and/or revised the manuscript. NF: provided data. KC, AD'O, and TS: provided data support, analysis, and statistical analysis. JL and AL: provided study oversight. All authors contributed to the article and approved the submitted version.

FUNDING

This study received funding from Pfizer Foundation grant (MR training fellowship) and the Duke Clinical Translational Science Institute (MR training fellowship). These funders were not involved in the study design, collection, analysis, interpretation of data, and the writing of the article or the decision to submit for publications. This study also received funding from the Centers for Disease Control and Prevention (NU50DD004933-03-00). JL is supported by grants from NCATS, CDC, and AHA. AL is supported by grants from the NIH, CDC, American Sudden Infant Death Syndrome Institute, and the Duke Children's Health and Discovery Initiative.

ACKNOWLEDGMENTS

This article was previously presented as a poster at the Duke University School of Medicine Department of Pediatrics Retreat and the American Academy of Pediatrics Conference 2021.

SUPPLEMENTARY MATERIAL

The Supplementary Material for this article can be found online at: https://www.frontiersin.org/articles/10.3389/fped.2021.770803/full#supplementary-material

REFERENCES

1. Willinger M, James LS, Catz C. Defining the sudden infant death syndrome (SIDS): deliberations of an expert panel convened by the national institute of child health and human development. *Pediatr Pathol.* (1991) 11:677–84. doi: 10.3109/15513819109065465
2. Carlin RF, Moon RY. Risk Factors, Protective Factors, and Current Recommendations to reduce sudden infant death syndrome: a review. *JAMA Pediatr.* (2017) 171:175–80. doi: 10.1001/jamapediatrics.2016.3345
3. Shapiro-Mendoza CK, Camperlengo L, Ludvigsen R, et al. Classification system for the sudden unexpected infant death case registry and its application. *Pediatrics.* (2014) 134:e210–9. doi: 10.1542/peds.2014-0180
4. Singh GK Yu SM. Infant mortality in the united states, 1915-2017: large social inequalities have persisted for over a century. *Int J MCH AIDS.* (2019) 8:19–31. doi: 10.21106/ijma.271
5. Guntheroth WG, Spiers PS. The triple risk hypotheses in sudden infant death syndrome. *Pediatrics.* (2002) 110:e64. doi: 10.1542/peds.110.5.e64
6. Monda E, Sarubbi B, Russo MG, et al. Unexplained sudden cardiac arrest in children: clinical and genetic characteristics of survivors. *Eur J Prev Cardiol.* (2020). doi: 10.1177/2047487320940863
7. Border WL, Benson DW. Sudden infant death syndrome and long QT syndrome: the zealots versus the naysayers. *Heart Rhythm.* (2007) 4:167–9. doi: 10.1016/j.hrthm.2006.12.019
8. Andreasen C, Refsgaard L, Nielsen JB, et al. Mutations in genes encoding cardiac ion channels previously associated with sudden infant death syndrome (SIDS) are present with high frequency in new exome data. *Can J Cardiol.* (2013) 29:1104–9. doi: 10.1016/j.cjca.2012.12.002
9. Tester DJ, Dura M, Carturan E, et al. A mechanism for sudden infant death syndrome (SIDS): stress-induced leak via ryanodine receptors. *Heart Rhythm.* (2007) 4:733–9. doi: 10.1016/j.hrthm.2007.02.026
10. Tester DJ, Ackerman MJ. Sudden infant death syndrome: how significant are the cardiac channelopathies? *Cardiovasc Res.* (2005) 67:388–96. doi: 10.1016/j.cardiores.2005.02.013
11. Gibson E, Dembofsky CA, Rubin S, Greenspan JS. Infant sleep position practices 2 years into the "back to sleep" campaign. *Clin Pediatr (Phila).* (2000) 39:285–9. doi: 10.1177/000992280003900505
12. Matoba N, Collins JW. Jr. Racial disparity in infant mortality. *Semin Perinatol.* (2017) 41:354–9. doi: 10.1053/j.semperi.2017.07.003
13. Spencer N, Logan S. Sudden unexpected death in infancy and socioeconomic status: a systematic review. *J Epidemiol Community Health.* (2004) 58:366–73. doi: 10.1136/jech.2003.011551
14. CDC WONDER Online Database. In: *United States Department of Health and Human Services (US DHHS) CfDCaPC, National Center for Health Statistics (NCHS)*. Division of Vital Statistics. Atlanta, GA: Centers for Disease Control and Prevention (2007–2019).
15. Spong CY. Defining "term" pregnancy: recommendations from the defining "term" pregnancy workgroup. *JAMA.* (2013) 309:2445–6. doi: 10.1001/jama.2013.6235
16. Koch LA, Weymuller CA, James E. Reduction of mortality from premature birth; some practical measures. *J Am Med Assoc.* (1948) 136:217–21. doi: 10.1001/jama.1948.02890210001001
17. Kotelchuck M. The adequacy of prenatal care utilization index: its US distribution and association with low birthweight. *Am J Public Health.* (1994) 84:1486–9. doi: 10.2105/AJPH.84.9.1486
18. Goldberg N, Rodriguez-Prado Y, Tillery R, Chua C. Sudden infant death syndrome: a review. *Pediatr Ann.* (2018) 47:e118–e23. doi: 10.3928/19382359-20180221-03
19. Kahn A, Bauche P, Groswasser J, Dramaix M, Scaillet S. Working Group GBdPF. Maternal education and risk factors for sudden death in infants working group of the groupe belge de pediatres francophones. *Eur J Pediatr.* (2001) 160:505–8. doi: 10.1007/s004310100783
20. Garstang JJ, Campbell MJ, Cohen MC, et al. Recurrent sudden unexpected death in infancy: a case series of sibling deaths. *Arch Dis Child.* (2020) 105:945–50. doi: 10.1136/archdischild-2019-318379
21. Centers for Disease Control and Prevention. *Sudden Unexpected Infant Death and Sudden Infant Death Syndrome*. Georgia, GA: Centers for Disease Control and Prevention (2019).
22. Kondracki AJ. Prevalence and patterns of cigarette smoking before and during early and late pregnancy according to maternal characteristics: the first national data based on the 2003 birth certificate revision, United States, 2016. *Reprod Health.* (2019) 16:142. doi: 10.1186/s12978-019-0807-5
23. Mendez DD, Hogan VK, Culhane JF. Institutional racism, neighborhood factors, stress, and preterm birth. *Ethn Health.* (2014) 19:479–99. doi: 10.1080/13557858.2013.846300
24. Stiffler D, Ayres B, Fauvergue C, Cullen D. Sudden infant death and sleep practices in the Black community. *J Spec Pediatr Nurs.* (2018) 23:e12213. doi: 10.1111/jspn.12213
25. Womack LS, Rossen LM, Hirai AH. Urban-rural infant mortality disparities by race and ethnicity and cause of death. *Am J Prev Med.* (2020) 58:254–60. doi: 10.1016/j.amepre.2019.09.010
26. Pollack HA, Frohna JG. A competing risk model of sudden infant death syndrome incidence in two US birth cohorts. *J Pediatr.* (2001) 138:661–7. doi: 10.1067/mpd.2001.112248
27. Hodgman JE. Apnea of prematurity and risk for SIDS. *Pediatrics.* (1998) 102:969–71. doi: 10.1542/peds.102.4.969a

28. Takashima S, Mito T, Becker LE. Neuronal development in the medullary reticular formation in sudden infant death syndrome and premature infants. *Neuropediatrics.* (1985) 16:76–9. doi: 10.1055/s-2008-1052547
29. Dybing E, Sanner T. Passive smoking, sudden infant death syndrome (SIDS) and childhood infections. *Hum Exp Toxicol.* (1999) 18:202–5. doi: 10.1191/096032799678839914
30. Martin TR, Bracken MB. Association of low birth weight with passive smoke exposure in pregnancy. *Am J Epidemiol.* (1986) 124:633–42. doi: 10.1093/oxfordjournals.aje.a114436
31. Fleming KA. Viral respiratory infection and SIDS. *J Clin Pathol.* (1992) 45:29–32.
32. Kickbusch IS. Health literacy: addressing the health and education divide. *Health Promot Int.* (2001) 16:289–97. doi: 10.1093/heapro/16.3.289
33. Arnestad M, Crotti L, Rognum TO, et al. Prevalence of long-QT syndrome gene variants in sudden infant death syndrome. *Circulation.* (2007) 115:361–7. doi: 10.1161/CIRCULATIONAHA.106.658021
34. Brownstein CA, Poduri A, Goldstein RD, Holm IA. The Genetics of Sudden Infant Death Syndrome. In: Duncan JR, Byard RW, editors. *SIDS Sudden Infant and Early Childhood Death: The Past, the Present and the Future Adelaide (AU).* Adelaide: University of Adelaide Press (2018). p. 846. doi: 10.20851/sids-31
35. Maternal Support (Baby Love Program). *North Carolina Department of Health and Human Services*. NC Medicaid Division of Health Benefits (2021).
36. Lahr MB, Rosenberg KD, Lapidus JA. Maternal-infant bedsharing: risk factors for bedsharing in a population-based survey of new mothers and implications for SIDS risk reduction. *Matern Child Health J.* (2007) 11:277–86. doi: 10.1007/s10995-006-0166-z

Conflict of Interest: MR received a consulting fee from Nabla Bio for an unrelated project.

The remaining authors declare that the research was conducted in the absence of any commercial or financial relationships that could be construed as a potential conflict of interest.

frontiers in Pediatrics

ORIGINAL RESEARCH
published: 20 December 2021
doi: 10.3389/fped.2021.785982

Identification of *NF1* Frameshift Variants in Two Chinese Families With Neurofibromatosis Type 1 and Early-Onset Hypertension

Yi-Ting Lu, Di Zhang, Xin-Chang Liu, Qiong-Yu Zhang, Xue-Qi Dong, Peng Fan, Yan Xiao and Xian-Liang Zhou**

Department of Cardiology, National Center for Cardiovascular Diseases, Fuwai Hospital, Chinese Academy of Medical Sciences and Peking Union Medical College, Beijing, China

Background: Neurofibromatosis type 1 (NF-1) is a common autosomal dominant disorder caused by mutations in the *NF1* gene. It is characterized by multiple café-au-lait macules, cutaneous neurofibromas, optic glioma, Lisch nodules, and axillary and inguinal freckling. The aim of this study was to investigate *NF1* mutations in two Chinese families with NF-1 who presented with early-onset hypertension, and to determine the prevalence of hypertension associated with NF-1 to better understand this complication.

Methods: Whole-exome sequencing was performed for the probands with NF-1 from two unrelated families. Possible pathogenic mutation was predicted by bioinformatic tools. Sanger sequencing was used to confirm candidate variants in all available individuals for familial co-segregation analysis. We also performed a systematic literature review of studies that reported the prevalence of hypertension in patients with NF-1.

Results: In family 1, a recurrent mutation c.6789_6792delTTAC in *NF1* was identified in the proband but in no other family members, indicating that this is a *de novo* mutation. In family 2, a novel mutation c.6934_6936delGCAinsTGCT in *NF1* was detected in the proband and two other family members, which co-segregated with the disease phenotype within the family. Both mutations were predicted to be pathogenic by bioinformatic analysis. We found hypertension was a relatively common complication of NF-1, with a prevalence range of 6.1–23.4%. Ambulatory blood pressure monitoring is a stable method for detecting initial alterations of the blood pressure pattern, particularly for pre-hypertension.

Conclusions: We identified one recurrent (c.6789_6792delTTAC) and one novel frame-shift mutation (c.6934_6936delGCAinsTGCT) in two unrelated families with NF-1 using whole-exome sequencing. In consideration of phenotypic heterogeneity in NF-1, genetic testing is a robust tool which helps early and accurate diagnosis. Because hypertension is not a rare complication of NF-1, routine screening for hypertension in patients with NF-1, especially children and adolescents, is important to avoid serious cardiovascular events.

Keywords: neurofibromatosis type 1, *NF1*, early-onset hypertension, frame-shift mutation, genetic analysis

OPEN ACCESS

Edited by:
Ruth Heying,
University Hospital Leuven, Belgium

Reviewed by:
Simone Martinelli,
National Institute of Health (NIH), Italy
Gianluca Piccolo,
Giannina Gaslini Institute (IRCCS), Italy

****Correspondence:***
Yan Xiao
xiaoyan@fuwaihospital.org
Xian-Liang Zhou
zhouxianliang0326@hotmail.com

Specialty section:
This article was submitted to Pediatric Cardiology, a section of the journal Frontiers in Pediatrics

Received: *29 September 2021*
Accepted: *30 November 2021*
Published: *20 December 2021*

Citation:
Lu Y-T, Zhang D, Liu X-C, Zhang Q-Y, Dong X-Q, Fan P, Xiao Y and Zhou X-L (2021) Identification of NF1 Frameshift Variants in Two Chinese Families With Neurofibromatosis Type 1 and Early-Onset Hypertension. Front. Pediatr. 9:785982. doi: 10.3389/fped.2021.785982

INTRODUCTION

Neurofibromatosis type 1 (NF-1, MIM 162200), also known as von Recklinghausen disease, is a progressive autosomal dominant disorder. NF-1 is one of the most common hereditary diseases with an estimated prevalence of 1 in 2,500 to 1 in 3,000 persons worldwide (1, 2). The disease is caused by mutations in the neurofibromin gene (*NF1*), a tumor suppressor gene mapping to 17q11.2, and spans 60 exons with an approximate size of 350 kb. *NF1* encodes neurofibromin, which belongs to the Ras-guanosine triphosphatase (RAS-GTPase) activating protein family. Loss-of-function mutations in *NF1* lead to intracellular neurofibromin protein deficiency, followed by over-activation of RAS signaling to the downstream pathways, which consequently leads to the development of phenotypes characterized by pigmentary lesions and predispositions to neoplastic disorders (3).

Despite having an early complete penetrant age by 5 years, the clinical expression of NF-1 is highly variable from one individual to another (4). NF-1 affects a wide range of organs, characterized by multiple café-au-lait macules (CALM), cutaneous neurofibromas, optic glioma, Lisch nodules, and axillary and inguinal freckling. Cognitive difficulties, skeletal abnormalities, and mental disorders are also common and the severity of symptoms is closely related to long-term impaired quality of life (5). Because of the phenotypic heterogeneity, timely diagnosis of NF-1 is challenging and genetic analysis is considered a robust tool that can assist with molecular diagnosis and intrafamilial genetic counseling.

Hypertension is not rare in patients with NF-1 (with a prevalence of 16–19% in children), no matter whether it is the essential form or secondary to renal or aortic vasculopathy, or pheochromocytoma (6, 7). Hypertension complications or NF-1 itself are both associated with increased cardio-cerebrovascular risk (8, 9). Routine blood pressure screening is indispensable to effectively detect elevated blood pressure and avoid severe negative effects on targeted organs. The proportion of patients with renovascular hypertension or hypertension caused by pheochromocytoma who also develop NF-1 has been analyzed previously (10, 11). We focused on the prevalence of hypertension and various screen methodology for hypertension in the general NF-1 population.

Here, we investigated two unrelated Chinese families with NF-1 characterized by early-onset hypertension by whole-exome sequencing and Sanger sequencing and identified one recurrent *NF1* variant c.6789_6792delTTAC and one novel heterozygous mutation c.6934_6936delGCAinsTGCT in families 1 and 2, respectively. We also summarize the data from previous clinical studies into the hypertension associated with NF-1 to better understand this complication.

MATERIALS AND METHODS

Subjects

Two unrelated families, comprising four patients with NF-1 and three unaffected individuals, were recruited for this study. The pedigree chart was shown in **Figure 1**. Both families had no consanguineous marriages. Patient 1 (proband II-1 in family 1), a 26-year-old man with symptoms of multiple CALM, cutaneous neurofibromas on his chest and back, axillary and inguinal freckling, early-onset hypertension, hypokalemia, and a history of stroke, was referred to the Department of Hypertension in Fuwai Hospital (Beijing, China). Patient 2 (proband III-1 in family 2) was a 14-year-old adolescent boy with CALM and axillary and inguinal freckling who was initially admitted to hospital because of early-onset hypertension and headache. The diagnosis of NF-1 critically depends on the revised diagnosis criteria for NF-1 updated in 2021 (12). The diagnosis of hypertension in adults and adolescents is based on the European Society of Cardiology and the European Society of Hypertension guidelines for the management of arterial hypertension (13). During hospitalization, detailed clinical data, including medical history, physical examination, and laboratory and imaging evaluation, were collected.

This study complied with the principles of the Declaration of Helsinki and was approved by the Ethics Committee of Fuwai Hospital. Informed consent forms were obtained in advance from all the recruited participants.

Whole-Exome Sequencing and Bioinformatic Analysis

To identify candidate genes and causal variants, whole-exome sequencing was performed on the two probands (II-1 in family 1 and III-1 in family 2). Genomic DNA was extracted from peripheral blood leukocytes from all the participants using a QIA Amp DNA Blood Mini kit (QIAGEN, Hilden, Germany) in accordance with the manufacturer's protocol. The concentration and quality of each DNA samples were evaluated by Thermal Nanodrop 2000 and agarose gel electrophoresis, respectively. To generate the DNA libraries, genomic DNA fragmentation, end repair, adapter ligation, and PCR enrichment were performed according to Illumina protocols. A GenCap exome capture kit (MyGenostics GenCap Enrichment technologies) was used for exome capture. DNA sequencing was performed on the Illumina HiSeq X Ten system. After removing Low-quality reads and adaptor sequences, the Burrows-Wheeler Aligner tool was used to align the clean reads to the human reference genome (UCSC, GRCh37/hg19). Duplicate reads were removed using the Picard software (http://broadinstitute.github.io/picard/). Subsequently, insertions/deletions and single nucleotide polymorphisms were identified using GATK (http://www.broadinstitute.org/gsa/wiki/index.php/Home_Page) and SOAPsnp (http://soap.genomics.org.cn/soapsnp.html). Variants were filtered in multiple databases, including the 1,000 Genomes Project database (http://browser.1000genomes.org/), dbSNP (https://www.ncbi.nlm.nih.gov/snp/), the Human Gene Mutation Database (HGMD, http://www.hgmd.cf.ac.uk/), and Exome Aggregation Consortium (http://exac.broadinstitute.org/). Additional *in silico* analyses were performed using PolyPhen-2 (http://genetics.bwh.harvard.edu/pph2/), SIFT (http://sift.jcvi.org/), and MutationTaster (http://www.mutationtaster.org/) (14). The neurofibromin amino acid sequences from eight different species were aligned using ClustalW (https://www.genome.jp/tools-bin/clustalw). The pathogenicity of potential

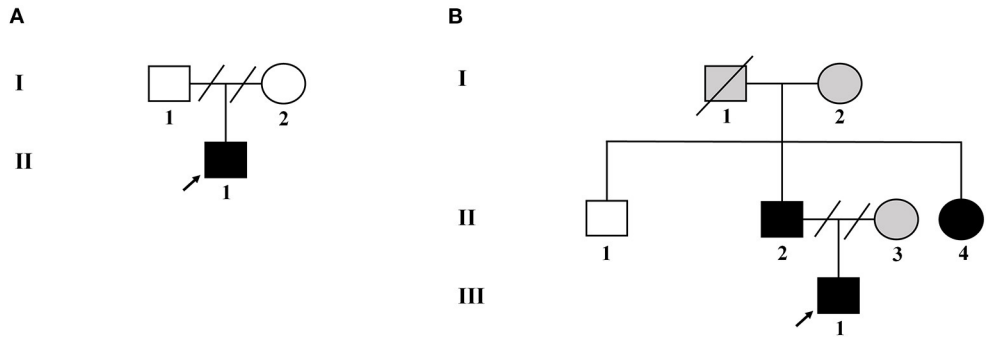

FIGURE 1 | Pedigree of the two unrelated Chinese families with NF-1. **(A)** Pedigree of family 1. **(B)** Pedigree of family 2. Black filled symbols represent affected subjects. Arrowhead indicates the probands. Empty symbols depict unaffected members. Gray filled symbols indicate the subjects without genetic testing. Connecting lines combined with slashes indicate the state of divorce. Diagonal line means decreased subjects.

mutations was evaluated according to the American College of Medical Genetics and Genomics guidelines for the interpretation of sequence variants that were published in 2015 (15).

Sanger Sequencing Validation

Sanger sequencing was used to confirm the candidate variants detected by the whole-exome sequencing within the two families. Co-segregation analyses were performed in relevant available individuals. The designed primer sequences are listed in **Supplementary Table 1** and the sequencing results were read using Chromas software (version 2.22; Technelysium Pty, Ltd.).

Systematic Review

We performed literature research using "neurofibromatosis type 1," "von Recklinghausen disease," "neurofibromatosis-1," "hypertension," "elevated blood pressure," and "blood pressure" in the PubMed and Embase databases with no year limit. Publications that met the following predetermined criteria were excluded: (1) articles were not in English; (2) article types were book section, or review; (3) articles were related to pulmonary, gestational, intracranial, or intraocular hypertension; (4) animal models or fundamental experiments were involved. Only articles with subjects who were general patients with NF-1 were included in the review. Variables including author, years of publication, number of patients with NF-1, method of blood pressure measurement, blood pressure results, secondary causes of hypertension, and complications of NF-1 were extracted from the selected articles by two authors independently.

RESULTS

Clinical Manifestations

Patient 1 was a 26-year-old man (proband II-1 in family 1) who was admitted to the Fuwai Hospital with suspected NF-1 and early-onset hypertension. When he was 6 years old, a mass with a diameter of 7 mm was found on his left palm, which was later confirmed as neurofibroma by pathological biopsy after resection (clinical data not available). Gradually, multiple CALM and cutaneous neurofibromas appeared, distributing mainly on his abdomen and anterior and posterior thorax (**Figures 2A,B**). When he was 25.5 years old, he presented with syncope and was diagnosed with cerebral hemorrhage. Later, he was found to have hypertension and hypokalemia with no symptoms during his rehabilitation for cerebral hemorrhage in the local hospital and then admitted to the Fuwai Hospital. An echocardiogram and renal artery and aortic computed tomography (CT) did not reveal any abnormalities, whereas adrenal CT showed a space-occupying lesion of the right adrenal gland, which was presumed to be an adrenal neurofibroma. Laboratory examinations including urine free normetanephrine (NMN) and metanephrine (MN) were all normal (NMN 185μg/24h, normal range 28-615μg/24h; MN 149μg/24h, normal range 14-282 μg/24h) except for hypokalemia (3.12 mmol/L, normal range 3.5–5.3 mmol/L) and a slightly elevated plasma renin concentration (66.1 μIU/mL, normal range 4.4–46.1 μIU/mL), ruling out the possibility of pheochromocytoma. Ophthalmologic examination found Lisch nodules in this patient; his parents showed no abnormal clinical symptoms.

Four individuals in family 2 participated in the study. The proband was a 14-year-old adolescent boy (III-1 in family 2) referred to hospital for early-onset hypertension with severe headache. Physical examination found mental retardation (low IQ, attention deficit and hyperactivity disorder), multiple CALM on his neck and trunk, and axillary freckling (**Figures 2C,D**). Head CT showed no abnormalities and the adrenal CT screen showed that the medial branch of the left adrenal gland was slightly thickened. Laboratory examination including serum electrolytes and blood biochemistry test was normal. Because of economic constraints, the proband's father had refused further examinations. The proband' father (II-2), and aunt (II-4) presented with multiple cutaneous neurofibromas (**Figure 2E**), and no abnormalities were found in his uncle (II-1). Because the proband's parents were divorced, no related information about the proband's mother (II-3) was obtained.

Genetic Analysis

The whole-exome sequencing of the samples from the two probands yielded approximate 17 GB and 11 GB raw data with more than 99% coverage of the target region. The average

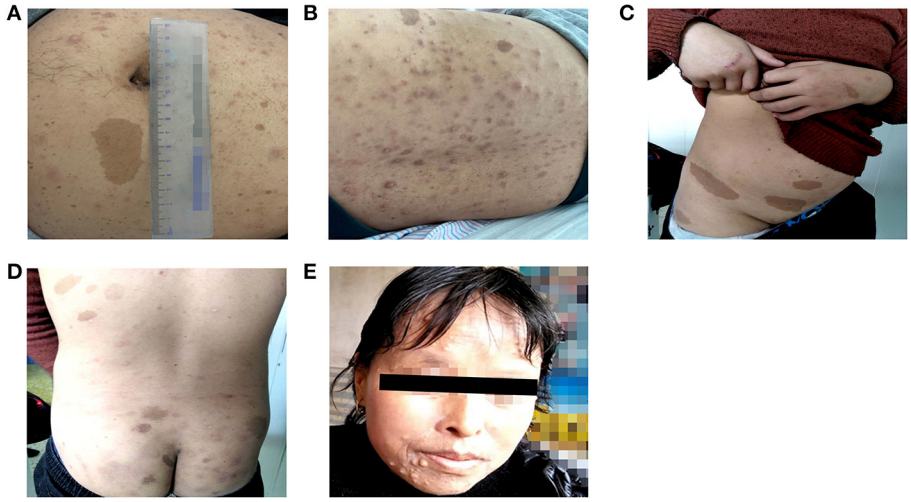

FIGURE 2 | Cutaneous lesions of patients in two unrelated families. **(A,B)** Multiple Café-au-lait macules and cutaneous neurofibromas of patient 1. **(C,D)** Multiple Café-au-lait macules scattered in patient 2. **(E)** Cutaneous neurofibromas of patient 2′ aunt.

TABLE 1 | Annotations of two candidate variants detected in two NF-1 families.

Subjects	Variation	Exon	Mutation type	*De novo*	Het/Hom	Novel mutation	Mutation-Taster	PhastCons	Pathogenicity analysis of ACMG standard	Allele frequency of the identified variants in the general population
1	c.6789_6792delTTAC	45	Deletion	Yes	Het	No	Disease-causing	1	Pathogenic (PVS1 + PM2 + PP4 + PS2)	None
2	c.6934_6936delGCAinsTGCT	46	Deletion-insertion	No	Het	Yes	Disease-causing	1	Pathogenic (PVS1 + PM2 + PP4)	None

NF-1, neurofibromatosis type 1; het, heterozygote; hom, homozygote; ACMG, American College of Medical Genetics and Genomics; the allele frequency of the identified variants in the general population are queried in the gnomAD database.

sequencing depths were 213 and 123 in proband II-1 (family 1) and III-1 (family 2), respectively, with more than 98% of the bases read at 10 × coverage and 97% bases read at 20 × coverage. Two heterozygous frame-shift mutations, c.6789_6792delTTAC and c.6934_6936delGCAinsTGCT in *NF1* (NM_000267) were supposed as candidate causative variants associated with the phenotypes of probands II-1 (family 1) and III-1 (family 2), respectively. Both variants were predicted to be pathogenic by MutationTaster and have not been reported in the 1,000 Genome Project, ExAC_ALL, or ExAC_EAS databases (**Table 1**). The results were confirmed by Sanger sequencing (**Figures 3A–D**). Moreover, the region in which variant c.6934_6936delGCAinsTGCT is located was found to be highly conserved in the CLUSTALW multiple alignment of neurofibromin amino acid sequences from eight different species (**Figure 3E**). Four NF-1 patients were identified in the two families. In family 1, one recurrent mutation, c.6789_6792delTTAC, was detected in proband II-1. The mutation was not detected in his parents and was considered as a *de novo* variant. In family 2, a novel potential mutation, c.6934_6936delGCAinsTGCT, was detected in the proband (III-1) and another two family members (II-2, and II-4), which co-segregated with the disease presentation in this family.

Systematic Literature Review

Through the literature search, we retrieved a total of 363 articles after excluding duplications; the selection flowchart is shown in **Figure 4A**. After reading the title, abstract, or full text, a total of 75 eligible articles were identified, comprising six cohorts from seven articles. It should be noted that the enrolled patients of the two articles published by Tedesco et al. (16, 17) were identical, but they used different blood pressure measurement methods. The variables we analyzed are extracted from the selected articles by two authors independently and the results are listed in **Table 2**.

DISCUSSION

In this study, we identified two frame-shift mutations in *NF1* among four affected individuals from two unrelated Chinese families using whole-exome sequencing. One mutation (c.6789_6792delTTAC) is a *de novo* mutation

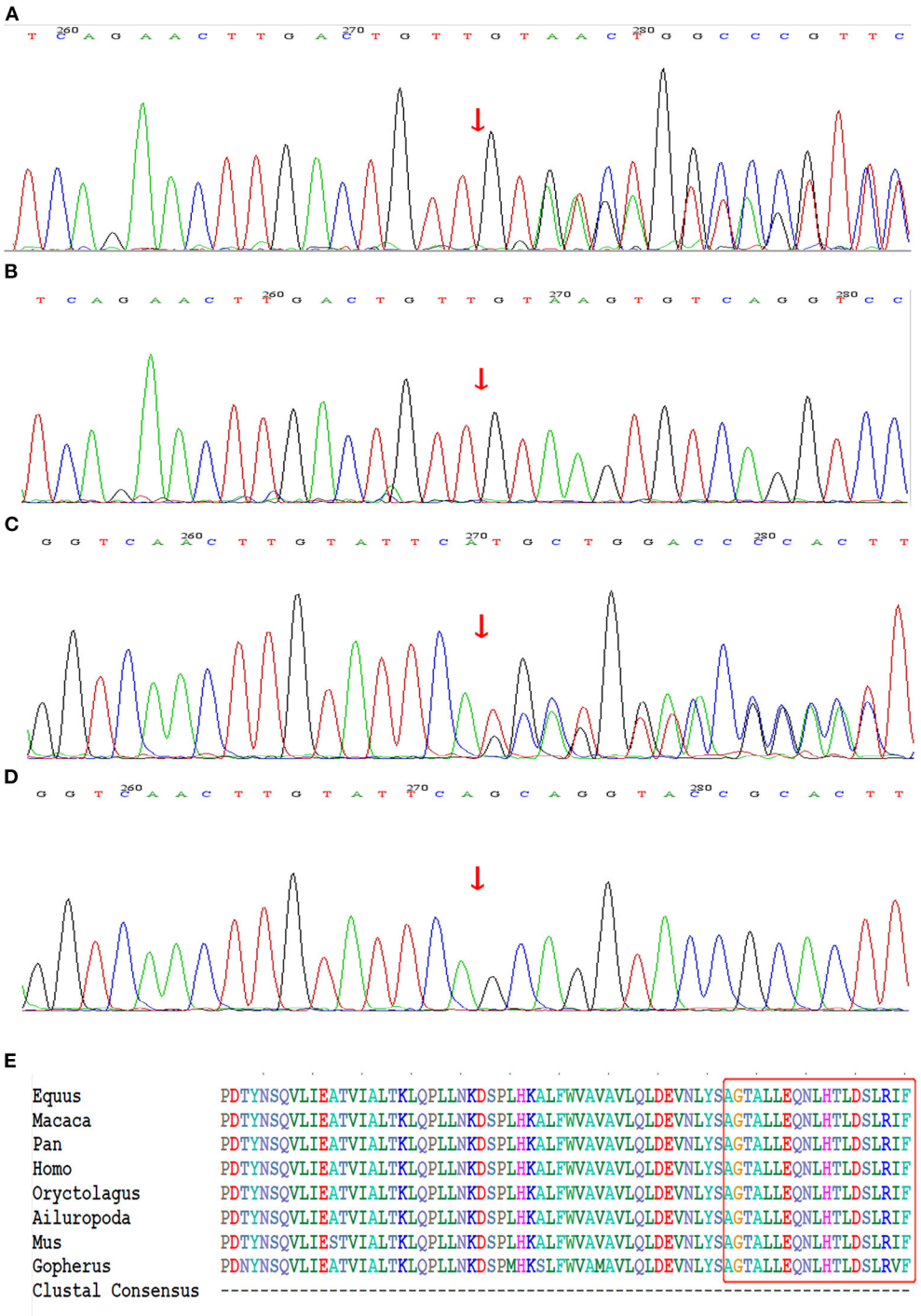

FIGURE 3 | Genetic sequencing results of *NF1* gene. **(A)** The recurrent frame-shift mutation c.6789_6792delTTAC (arrow) found in the index patient of family 1. **(B)** Wild-type found in unaffected subjects of family 1. **(C)** The novel frame-shift mutation c.6934_6936delGCAinsTGCT (arrow) found in affected subjects of family 2. **(D)** Wild-type found in unaffected subject of family 2. **(E)** The mutation region of neurofibromin protein identified in family 2 is highly conserved by analyzing orthologs from 8 various species on CLUSTALW tool.

that has been reported previously; the other mutation (c.6934_6936delGCAinsTGCT) is reported here for the first time, to our knowledge, with evident pathogenicity predicted by the bioinformatic analysis and family co-segregation. Furthermore, by conducting a systematic literature review on patients with NF-1 associated with hypertension, we found that hypertension

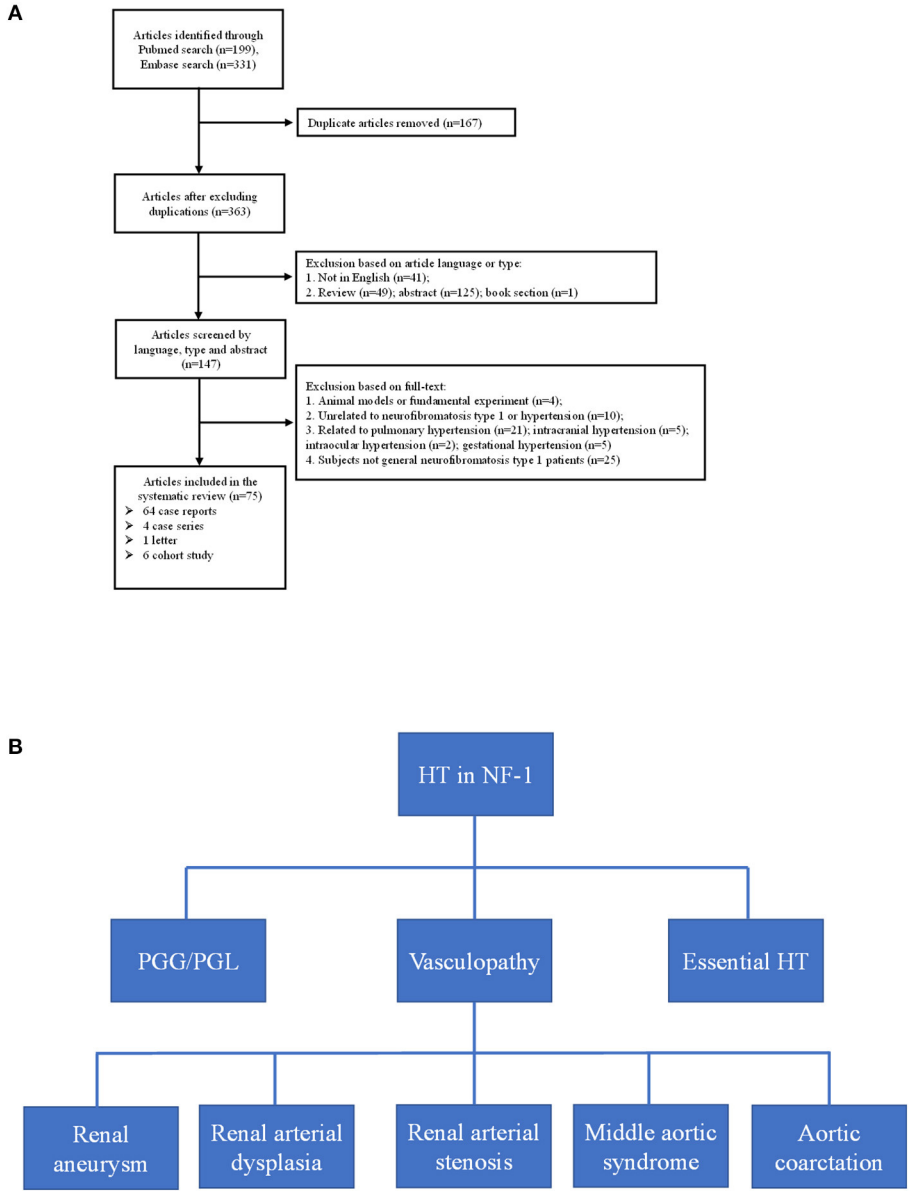

FIGURE 4 | (A) Flow-chart of the eligible articles extraction. **(B)** Etiologies of neurofibromatosis type 1 with hypertension. HT, hypertension; PGG/PGL, pheochromocytoma/paraganglioma.

was a relatively common complication of NF-1, with a prevalence of 6.1–23.4%.

NF-1 is one of the most common genetic disease caused by mutations in *NF1*, which encodes neurofibromin protein. Neurofibromin functions as a RAS-GTPase activating protein that accelerates the conversion of the active form RAS-GTP to the inactive form RAS-GDP (23). Neurofibromin deficiency results in unchecked RAS signaling followed by improper activation of multiple downstream pathways, such as the RAS/mitogen-activated protein kinase (RAS/MAPK), and PI3K-mTOR pathways, leading to unregulated cell survival and proliferation (24).

Because of the large size and complex structure of *NF1*, to date, more than 3710 *NF1* mutations have been collected in the HGMD database but exact mutation hot spots have not been identified. Nearly half of affected individuals reported till now had *de novo* mutations in *NF1* and an absence of a familial NF-1 history, which is what we found for the proband (II-1) of family 1 (25). The mutation c.6789_6792delTTAC detected in family 1 has been reported previously. In 1995, Robinson et al. (26) were the first to identify this small deletion mutation by PCR amplification of specific exon of *NF1* among 92 unrelated patients with NF-1. The c.6789_6792delTTAC mutation caused a frame shift that led to the formation of a premature stop

TABLE 2 | Summary of clinical characteristics of eligible studies included in the literature review.

References	NF-1 patients enrolled	% Male	Age, years mean ± SD (range)	Diagnostic criteria	BP measurements	BP condition (number, %)			Secondary cause of HT	Complications of NF-1 associated with HT (patient number)
						Normal	Pre-HT	HT		
Virdis (18)	57	-	- (range 1.5–23)	NA	OBPM	48/57 (84.2)		9/57 (15.8)*	RAS	RAS (2), brain glioma (3)
Dubov (19)	224	53.1	9.1±4.1 (range 2–17)	NIH	OBPM	107/114 (93.9)* 141/164 (86.0)#		7/114 (6.1)* 23/164 (14.0)#	Not screened	NA
Lama (20)	69	52.2	11±4 (range 5–25)	NIH	OBPM	48/68 (70.6)*	15/68 (22.0)*	5/68 (7.4)*	Screened, but not found	Plexiform cervical neurofibroma (1), pulmonary valve stenosis (1), secundum atrial septal defect (1), left pulmonary artery stenosis (1), mild mitral regurgitation (1), mild aortic regurgitation (1), atrial septal aneurysm (1), hypertrophic cardiomyopathy (1)
					ABPM	57/68 (84.0)		11/68 (16.0)		
Zinnamosca (21)	48	47.9	40.5 ± 14 (range NA)	NIH	OBPM	37/48 (77.1)#		11/48 (22.9)#	Pheochromocytoma	Bilateral adrenal pheochromocytoma (1), unilateral adrenal pheochromocytoma (5), autoimmune thyroiditis (1), multiple endocrine neoplasia type 2A (1), Multinodular goiter (1)
Fossali (22)	27	40.7	12.8 ± NA (range 4.2–24)	NA	OBPM	22/27 (81.5)#	2/27 (7.4)#	3/27 (11.1)#	RAS, MAS	Renal artery stenosis in MAS (2), proximal renal artery stenosis (1)
Tedesco (16, 17)	64	53.1	12 ± 4 (range 5–25)	NIH	OBPM	49/64 (76.5)*		15/64 (23.4)*	RAS	Nephrotic syndrome (1), plexiform cervical neurofibroma (1), RAS (4)
					ABPM	54/64 (84.0)		10/64 (16.0)		

*BP, blood pressure; NF-1, neurofibromatosis type 1; HT, hypertension; OBPM, office blood pressure monitor; ABPM, ambulatory blood pressure monitor; NIH, diagnostic criteria established by National Institutes of Health; RAS, renal artery stenosis; MAS, middle aortic stenosis; NA, not mentioned; *blood pressure measurement elevated at least three different sessions; #blood pressure elevated at once or twice sessions.*

signal five codons downstream, resulting in a truncated protein. Subsequently, several patients carrying the same mutation have been identified, suggesting this 4-bp region of the exon may be prone to mutation (27–29). This might be because the symmetrical sequence tends to form a loop-like structure, leaving an unpaired loop-region, which includes the 4-bp region, more accessible for the generation of deletion variants (26, 30). The novel variant c.6934_6936delGCAinsTGCT identified in family 2 caused the replacement of alanine with cysteine at codon 2,312 and created a frame-shift that led to the formation of a premature stop codon at position 2,318. The CLUSTALW multiple alignment of neurofibromin amino acid sequences from eight different species showed the region in which variant c.6934_6936delGCAinsTGCT is located was highly conserved. Moreover, the MutationTaster prediction together with the evaluation of American College of Medical Genetics and Genomics standards indicted that c.6934_6936delGCAinsTGCT was a disease-causing mutation.

Hypertension is not rare in patients with NF-1 for essential or secondary causes. In our study, both probands had early-onset hypertension. Our literature review found six cohorts from seven articles that considered the prevalence of pre-hypertension and hypertension in patients with NF-1; 7.4–22% and 6.1–23.4% for pre-hypertension and hypertension, respectively (16–22). In five of the studies (16–20, 22), the patients were children and young adults (1.5–25 years) with a high prevalence of early-onset hypertension, suggesting the necessity of regular blood pressure monitor in young patients with NF-1, and the patients in the study conducted by Zinnamosca et al. (21) were middle-aged adults. Dubov et al. (19) found the lowest prevalence of hypertension (6.1%) by measuring office blood pressure of 114 patients with NF-1, whereas Tedesco et al. (17) found the highest prevalence (23.4%) using the same method and criteria in a different cohort of 64 patients with NF-1. The prevalence identified by Virdis et al. (18) using office blood pressure measurement was 15.7%, which was in the middle of the above two study. The hypertension prevalence reported by Tedesco et al. (16) using ambulatory blood pressure (ABPM) is consistent with that of the Lama et al. (20) study (approximately 16.0%) in which ABPM also was used. The differences of hypertension prevalence in these studies may be due not only to the different NF-1 populations but also to the different methodologies used to monitor blood pressure. Generally, ABPM is considered to be a reliable and stable diagnostic procedure to detect hypertension (31). Early diagnosis and understanding the etiologies of hypertension in patients with NF-1 is a prerequisite for blood pressure control, in avoid of poor outcome including hemorrhagic stroke, retinal arterial microaneurysms, end stage renal disease and so on (32, 33). After summarizing the literature of eligible cohorts, case reports, case series and so on, the secondary causes of hypertension basically include renal aneurysm, renal arterial dysplasia, renal artery stenosis, aortic coarctation, pheochromocytoma, and middle aortic syndrome (**Figure 4B**). In our study, the possibility of secondary hypertension in the two probands was mostly ruled out by the imaging and laboratory examination, and the early-onset hypertension was considered to be possibly associated with low-grade vasculopathy (20).

NF-1 disease demonstrates with complete penetrance but high phenotypic variability is present even in families that carry the same mutation (34), as was reflected in our study. In family 2, the types and degrees of clinical manifestations of the affected members varied. Mental retardation was found only in the proband, and the other members with NF-1 showed normal behavior. Moreover, the proband's aunt and father had cutaneous neurofibroma, but the proband did not. NF-1 is an age-dependent progressive disorder, and therefore the phenotypic variability may be partly explained by age differences among patients (35). Several large familial NF-1 studies revealed that unlinked modifier genes may influence the expression of the disease (36, 37). Recently, using a systems biology strategy, Kowalski et al. (38) identified 10 candidate modifier genes related to the NF-1 phenotype, namely *AKT1*, *BRAF*, *EGFR*, *LIMK1*, *PAK1*, *PTEN*, *RAF1*, *SDC2*, *SMARCA4*, and *VCP*. What's more, D'Amico et al. (39) identified that gain-of-function and hypomorphic variants in *PTPN11*, a positive regulator of RAS, have been shown to worsen and mitigate, respectively, the severity of the NF1 phenotype. Besides, the allelic heterogeneity of constitutional *NF1* mutations, environmental factors may also be associated with phenotypic variability (40, 41). Overall, the exact mechanism of clinical variability in NF-1 remains unclear and may involve a combination of multiple factors.

Because of the wide mutation spectrum and variable phenotypes expressed, only a few reliable genotype–phenotype correlations have been reported in NF-1 so far. Patients with *NF1* microdeletions tended to develop more severe phenotypes that manifest as learning disabilities, facial dysmorphism, cardiovascular anomalies, increased numbers of neurofibromas, and malignant peripheral nerve sheath tumors (42, 43). Among the intragenic *NF1* mutations, the deletion mutation p.Met922del in exon 17 has been correlated with a mild phenotype of typical pigment lesions (CALM or freckling), learning difficulties, and lacking forms of neurofibromas (44, 45). Other intragenic missense mutations that influenced p.Arg1809 have also been correlated with mild presentation characterized by a pigmentary phenotype, Noonan-like features, pulmonic stenosis, stature dysplasia, and absence of visible neurofibromas (46, 47). Kang et al. (48) studied patients with different mutation types and found that patients with truncating/splicing mutations and large deletions tended to present with a more severe phenotype and earlier onset age than those with missense types. Recently, Scala et al. (49) identified that frameshift variants and whole gene deletion were correlated with skeletal abnormalities, whereas neurofibromas were negatively associated with missense variants. Moreover, they found that the presence of structural brain alterations was associated with c.3721C>T variant, whereas Lisch nodules and endocrinological disorders were more common observed in NF-1 patients with c.6855C>A variant. However, apart from the phenotypic diversity in family 2, because the recurrent mutation detected in proband II-1 in family 1 was *de novo* and the clinical information of previously reported patients with the same mutation was limited, we failed to construct genotype–phenotype correlations in this study.

Because patients with NF-1 are at increased multiple risk of developing cerebrovascular diseases and benign or malignant tumors, early identification can help targeted examination, multidisciplinary management, and long-term clinical monitoring (8, 50). Genetic testing can provide valuable clues to NF-1 based on molecular diagnosis, especially for young patients with no positive family history or typical symptoms who do not meet the criteria for a clinical diagnosis (50). It is also necessary to conduct genetic counseling for first-degree or second-degree relatives of affected patients. Next-generation sequencing technologies have helped make the molecular analysis of mutations in the large wide-spectrum *NF1* gene more cost/time-effective and highly precise. Furthermore, regular multi-systematic follow-ups should be offered to affected patients to prevent the occurrence of fatal complications.

CONCLUSION

In summary, we identified one recurrent frame-shift mutation c.6789_6792delTTAC and one novel frame-shift mutation c.6934_6936delGCAinsTGCT in two unrelated families with NF-1 from China. Genetic testing is a useful and precise method for diagnosing the disease at the molecular level in spite of phenotypic variability. Hypertension is not a rare complication of NF-1, and it was seen in both probands in this study. Routine screening for hypertension in patients with NF-1, especially children and adolescents, is important to avoid serious cardiovascular events. Given the phenotypic variability, more research is needed to unravel the mechanisms that influence how genetic and other factors determine the NF-1 phenotypes.

DATA AVAILABILITY STATEMENT

The datasets for this article are not publicly available due to concerns regarding participant/patient anonymity. Requests to access the datasets should be directed to the corresponding author.

ETHICS STATEMENT

The studies involving human participants were reviewed and approved by the Ethics Committee of Fuwai Hospital. Written informed consent to participate in this study was provided by the participant's legal guardian/next of kin.

AUTHOR CONTRIBUTIONS

Y-TL, YX, and X-LZ designed, supervised the study, and modified the manuscript. Y-TL, DZ, and X-CL collected samples and clinical information. Y-TL, X-QD, and Q-YZ performed the experiments. Y-TL and PF performed the data analysis. Y-TL and DZ wrote the manuscript. All authors reviewed this work.

FUNDING

This work was supported by the Non-profit Central Research Institute Fund of Chinese Academy of Medical Sciences (2019XK320057), the National Key Research and Development Program of China (2016YFC1300100).

ACKNOWLEDGMENTS

We thank all the subjects for participating in this study.

SUPPLEMENTARY MATERIAL

The Supplementary Material for this article can be found online at: https://www.frontiersin.org/articles/10.3389/fped.2021.785982/full#supplementary-material

REFERENCES

1. Hirbe AC, Gutmann DH. Neurofibromatosis type 1: a multidisciplinary approach to care. *Lancet Neurol.* (2014) 13:834–43. doi: 10.1016/S1474-4422(14)70063-8
2. Williams VC, Lucas J, Babcock MA, Gutmann DH, Korf B, Maria BL. Neurofibromatosis type 1 revisited. *Pediatrics.* (2009) 123:124–33. doi: 10.1542/peds.2007-3204
3. Gottfried ON, Viskochil DH, Couldwell WT. Neurofibromatosis Type 1 and tumorigenesis: molecular mechanisms and therapeutic implications. *Neurosurg Focus.* (2010) 28:E8. doi: 10.3171/2009.11.FOCUS09221
4. Delis KT, Gloviczki P. Neurofibromatosis type 1: from presentation and diagnosis to vascular and endovascular therapy. *Perspect Vasc Surg Endovasc Ther.* (2006) 18:226–37. doi: 10.1177/1531003506296488
5. Armand ML, Taieb C, Bourgeois A, Bourlier M, Bennani M, Bodemer C, et al. Burden of adult neurofibromatosis 1: development and validation of a burden assessment tool. *Orphanet J Rare Dis.* (2019) 14:94. doi: 10.1186/s13023-019-1067-8
6. Bergqvist C, Servy A, Valeyrie-Allanore L, Ferkal S, Combemale P, Wolkenstein P, et al. Neurofibromatosis 1 French national guidelines based on an extensive literature review since 1966. *Orphanet J Rare Dis.* (2020) 15:37. doi: 10.1186/s13023-020-1310-3
7. Sivasubramanian R, Meyers KE. Hypertension in children and adolescents with turner syndrome (TS), neurofibromatosis 1 (NF1), and williams syndrome (WS). *Curr Hypertens Rep.* (2021) 23:18. doi: 10.1007/s11906-021-01136-7
8. Terry AR, Jordan JT, Schwamm L, Plotkin SR. Increased risk of cerebrovascular disease among patients with neurofibromatosis type 1: population-based approach. *Stroke.* (2016) 47:60–5. doi: 10.1161/STROKEAHA.115.011406
9. Friedman JM, Arbiser J, Epstein JA, Gutmann DH, Huot SJ, Lin AE, et al. Cardiovascular disease in neurofibromatosis 1: report of the NF1 Cardiovascular Task Force. *Genet Med.* (2002) 4:105–11. doi: 10.1097/00125817-200205000-00002
10. Kim SS, Stein DR, Ferguson MA, Porras D, Chaudry G, Singh MN, et al. Surgical management of pediatric renovascular hypertension and midaortic syndrome at a single-center multidisciplinary program. *J Vasc Surg.* (2020) 74:79-89. doi: 10.1016/j.jvs.2020.12.053
11. Moramarco J, El Ghorayeb N, Dumas N, Nolet S, Boulanger L, Burnichon N, et al. Pheochromocytomas are diagnosed incidentally and at older age in neurofibromatosis type 1. *Clin Endocrinol.* (2017) 86:332–9. doi: 10.1111/cen.13265
12. Legius E, Messiaen L, Wolkenstein P, Pancza P, Avery RA, Berman Y, et al. Revised diagnostic criteria for neurofibromatosis type 1 and Legius

syndrome: an international consensus recommendation. *Genet Med.* (2021) 23:1506–13. doi: 10.1038/s41436-021-01170-5
13. Williams B, Mancia G, Spiering W, Agabiti Rosei E, Azizi M, Burnier M, et al. 2018 ESC/ESH Guidelines for the management of arterial hypertension. *Eur Heart J.* (2018) 39:3021–104. doi: 10.1097/HJH.0000000000001940
14. Schwarz JM, Rodelsperger C, Schuelke M, Seelow D. MutationTaster evaluates disease-causing potential of sequence alterations. *Nat Methods.* (2010) 7:575–6. doi: 10.1038/nmeth0810-575
15. Richards S, Aziz N, Bale S, Bick D, Das S, Gastier-Foster J, et al. Standards and guidelines for the interpretation of sequence variants: a joint consensus recommendation of the American college of medical genetics and genomics and the association for molecular pathology. *Genet Med.* (2015) 17:405–24. doi: 10.1038/gim.2015.30
16. Tedesco MA, Di Salvo G, Ratti G, Natale F, Calabrese E, Grassia C, et al. Arterial distensibility and ambulatory blood pressure monitoring in young patients with neurofibromatosis type 1. *Am J Hypertens.* (2001) 14:559–66. doi: 10.1016/S0895-7061(00)01303-0
17. Tedesco MA, Ratti G, Di Salvo G, Martiniello AR, Limongelli G, Grieco M, et al. Noninvasive evaluation of arterial abnormalities in young patients with neurofibromatosis type 1. *Angiology.* (2000) 51:733–41. doi: 10.1177/000331970005100905
18. Virdis R, Balestrazzi P, Zampolli M, Donadio A, Street M, Lorenzetti E. Hypertension in children with neurofibromatosis. *J Hum Hypertens.* (1994) 8:395–7.
19. Dubov T, Toledano-Alhadef H, Chernin G, Constantini S, Cleper R, Ben-Shachar S. High prevalence of elevated blood pressure among children with neurofibromatosis type 1. *Pediatr Nephrol.* (2016) 31:131–6. doi: 10.1007/s00467-015-3191-6
20. Lama G, Graziano L, Calabrese E, Grassia C, Rambaldi PF, Cioce F, et al. Blood pressure and cardiovascular involvement in children with neurofibromatosis type1. *Pediatr Nephrol.* (2004) 19:413–8. doi: 10.1007/s00467-003-1397-5
21. Zinnamosca L, Petramala L, Cotesta D, Marinelli C, Schina M, Cianci R, et al. Neurofibromatosis type 1 (NF1) and pheochromocytoma: prevalence, clinical and cardiovascular aspects. *Arch Dermatol Res.* (2011) 303:317–25. doi: 10.1007/s00403-010-1090-z
22. Fossali E, Signorini E, Intermite RC, Casalini E, Lovaria A, Maninetti MM, et al. Renovascular disease and hypertension in children with neurofibromatosis. *Pediatr nephrol.* (2000) 14:806–10. doi: 10.1007/s004679900260
23. Bajaj A, Li QF, Zheng Q, Pumiglia K. Loss of NF1 expression in human endothelial cells promotes autonomous proliferation and altered vascular morphogenesis. *PLoS ONE.* (2012) 7:e49222. doi: 10.1371/journal.pone.0049222
24. Nix JS, Blakeley J, Rodriguez FJ. An update on the central nervous system manifestations of neurofibromatosis type 1. *Acta Neuropathol.* (2020) 139:625–41. doi: 10.1007/s00401-019-02002-2
25. Evans DG, Howard E, Giblin C, Clancy T, Spencer H, Huson SM, et al. Birth incidence and prevalence of tumor-prone syndromes: estimates from a UK family genetic register service. *Am J Med Genet.* (2010) 152A:327–32. doi: 10.1002/ajmg.a.33139
26. Robinson PN, Boddrich A, Peters H, Tinschert S, Buske A, Kaufmann D, et al. Two recurrent nonsense mutations and a 4 bp deletion in a quasi-symmetric element in exon 37 of the NF1 gene. *Hum Genet.* (1995) 96:95–8. doi: 10.1007/BF00214193
27. Boddrich A, Robinson PN, Schulke M, Buske A, Tinschert S, Nurnberg P. New evidence for a mutation hotspot in exon 37 of the NF1 gene. *Hum Mutat.* (1997) 9:374–7. doi: 10.1002/(SICI)1098-1004(1997)9:4<374::AID-HUMU15>3.0.CO;2-#
28. Fahsold R, Hoffmeyer S, Mischung C, Gille C, Ehlers C, Kucukceylan N, et al. Minor lesion mutational spectrum of the entire NF1 gene does not explain its high mutability but points to a functional domain upstream of the GAP-related domain. *Am J Hum Genet.* (2000) 66:790–818. doi: 10.1086/302809
29. Origone P, De Luca A, Bellini C, Buccino A, Mingarelli R, Costabel S, et al. Ten novel mutations in the human neurofibromatosis type 1 (NF1) gene in Italian patients. *Hum Mutat.* (2002) 20:74–5. doi: 10.1002/humu.9039
30. Ekvall S, Sjors K, Jonzon A, Vihinen M, Anneren G, Bondeson ML. Novel association of neurofibromatosis type 1-causing mutations in families with neurofibromatosis-Noonan syndrome. *Am J Med Genet.* (2014) 164A:579–87. doi: 10.1002/ajmg.a.36313
31. Hermida RC, Mojon A, Fernandez JR, Otero A, Crespo JJ, Dominguez-Sardina M, et al. Ambulatory blood pressure monitoring-based definition of true arterial hypertension. *Minerva Med.* (2020) 111:573–88. doi: 10.23736/S0026-4806.20.06834-2
32. Faris M, Baliss M, Coni R, Nambudiri V. Severe hypertension leading to hemorrhagic stroke in neurofibromatosis type 1. *Cureus.* (2021) 13:e14658. doi: 10.7759/cureus.14658
33. Lu J, Liu H, Zhang L, Ma L, Zhou H. Corkscrew retinal vessels and retinal arterial macroaneurysm in a patient with neurofibromatosis type 1: a case report. *Medicine.* (2018) 97:e11497. doi: 10.1097/MD.0000000000011497
34. Shofty B, Constantini S, Ben-Shachar S. Advances in molecular diagnosis of neurofibromatosis type 1. *Semin Pediatr Neurol.* (2015) 22:234–9. doi: 10.1016/j.spen.2015.10.007
35. Pasmant E, Vidaud M, Vidaud D, Wolkenstein P. Neurofibromatosis type 1: from genotype to phenotype. *J Med Genet.* (2012) 49:483–9. doi: 10.1136/jmedgenet-2012-100978
36. Sabbagh A, Pasmant E, Laurendeau I, Parfait B, Barbarot S, Guillot B, et al. Unravelling the genetic basis of variable clinical expression in neurofibromatosis 1. *Hum Mol Genet.* (2009) 18:2768–78. doi: 10.1093/hmg/ddp212
37. Szudek J, Joe H, Friedman JM. Analysis of intrafamilial phenotypic variation in neurofibromatosis 1 (NF1). *Genet Epidemiol.* (2002) 23:150–64. doi: 10.1002/gepi.1129
38. Kowalski TW, Reis LB, Finger Andreis T, Ashton-Prolla P, Rosset C. Systems biology approaches reveal potential phenotype-modifier genes in neurofibromatosis Type 1. *Cancers.* (2020) 12:2416. doi: 10.3390/cancers12092416
39. D'Amico A, Rosano C, Pannone L, Pinna V, Assunto A, Motta M, et al. Clinical variability of neurofibromatosis 1: a modifying role of cooccurring PTPN11 variants and atypical brain MRI findings. *Clin Genet.* (2021) 100:563–72. doi: 10.1111/cge.14040
40. Rasmussen SA, Friedman JM. NF1 gene and neurofibromatosis 1. *Am J Epidemiol.* (2000) 151:33–40. doi: 10.1093/oxfordjournals.aje.a010118
41. Sabbagh A, Pasmant E, Imbard A, Luscan A, Soares M, Blanche H, et al. NF1 molecular characterization and neurofibromatosis type I genotype-phenotype correlation: the French experience. *Hum Mutat.* (2013) 34:1510–8. doi: 10.1002/humu.22392
42. Pasmant E, Sabbagh A, Spurlock G, Laurendeau I, Grillo E, Hamel MJ, et al. NF1 microdeletions in neurofibromatosis type 1: from genotype to phenotype. *Hum Mutat.* (2010) 31:E1506–18. doi: 10.1002/humu.21271
43. Kehrer-Sawatzki H, Mautner VF, Cooper DN. Emerging genotype-phenotype relationships in patients with large NF1 deletions. *Hum Genet.* (2017) 136:349–76. doi: 10.1007/s00439-017-1766-y
44. Koczkowska M, Callens T, Gomes A, Sharp A, Chen Y, Hicks AD, et al. Expanding the clinical phenotype of individuals with a 3-bp in-frame deletion of the NF1 gene (c.2970_2972del): an update of genotype-phenotype correlation. *Genet Med.* (2019) 21:867–76.
45. Upadhyaya M, Huson SM, Davies M, Thomas N, Chuzhanova N, Giovannini S, et al. An absence of cutaneous neurofibromas associated with a 3-bp inframe deletion in exon 17 of the NF1 gene (c.2970-2972 delAAT): evidence of a clinically significant NF1 genotype-phenotype correlation. *Am J Hum Genet.* (2007) 80:140–51. doi: 10.1086/510781
46. Pinna V, Lanari V, Daniele P, Consoli F, Agolini E, Margiotti K, et al. p.Arg1809Cys substitution in neurofibromin is associated with a distinctive NF1 phenotype without neurofibromas. *Eur J Hum Genet.* (2015) 23:1068–71. doi: 10.1038/ejhg.2014.243
47. Rojnueangnit K, Xie J, Gomes A, Sharp A, Callens T, Chen Y, et al. High incidence of noonan syndrome features including short stature and pulmonic stenosis in patients carrying NF1 missense mutations affecting p.Arg1809: genotype-phenotype correlation. *Hum Mutat.* (2015) 36:1052–63. doi: 10.1002/humu.22832
48. Kang E, Kim YM, Seo GH, Oh A, Yoon HM, Ra YS, et al. Phenotype categorization of neurofibromatosis type I and correlation to NF1 mutation types. *J Hum Genet.* (2020) 65:79–89. doi: 10.1038/s10038-019-0695-0
49. Scala M, Schiavetti I, Madia F, Chelleri C, Piccolo G, Accogli A, et al. Genotype-phenotype correlations in neurofibromatosis type 1: a single-center cohort study. *Cancers.* (2021) 13:1879. doi: 10.3390/cancers13081879

50. Gutmann DH, Ferner RE, Listernick RH, Korf BR, Wolters PL, Johnson KJ. Neurofibromatosis type 1. *Nat Rev Dis Primers.* (2017) 3:17004. doi: 10.1038/nrdp.2017.4

Conflict of Interest: The authors declare that the research was conducted in the absence of any commercial or financial relationships that could be construed as a potential conflict of interest.

Publisher's Note: All claims expressed in this article are solely those of the authors and do not necessarily represent those of their affiliated organizations, or those of the publisher, the editors and the reviewers. Any product that may be evaluated in this article, or claim that may be made by its manufacturer, is not guaranteed or endorsed by the publisher.

frontiers in Pediatrics

ORIGINAL RESEARCH
published: 30 March 2022
doi: 10.3389/fped.2022.802469

Predictive Value of Heart Rate and Blood Pressure on the Prognosis of Postural Tachycardia Syndrome in Children

Shuo Wang[1,2], *Runmei Zou*[1], *Hong Cai*[1] *and Cheng Wang*[1]*

[1] *Department of Pediatric Cardiovasology, Children's Medical Center, The Second Xiangya Hospital, Central South University, Changsha, China,* [2] *Department of Neonatology, Xiangya Hospital, Central South University, Changsha, China*

OPEN ACCESS

Edited by:
Imran Saeed,
East Midlands Congenital Heart Centre, United Kingdom

Reviewed by:
Martin Poryo,
Saarland University Hospital, Germany
Emanuele Monda,
University of Campania Luigi Vanvitelli, Italy
Jannos Siaplaouras,
Independent Researcher, Fulda, Germany

****Correspondence:***
Cheng Wang
wangcheng2nd@csu.edu.cn
orcid.org/0000-0002-7120-0654

Specialty section:
This article was submitted to Pediatric Cardiology, a section of the journal Frontiers in Pediatrics

Received: *26 October 2021*
Accepted: *03 February 2022*
Published: *30 March 2022*

Citation:
Wang S, Zou R, Cai H and Wang C (2022) Predictive Value of Heart Rate and Blood Pressure on the Prognosis of Postural Tachycardia Syndrome in Children. Front. Pediatr. 10:802469. doi: 10.3389/fped.2022.802469

Background: To investigate the predictive value of heart rate (HR) and blood pressure (BP) on the prognosis of postural tachycardia syndrome (POTS) in children.

Materials and Methods: 53 cases of children aged 5 to 15 years who visited in the Pediatric Syncope Specialist Clinic of The Second Xiangya Hospital of Central South University for unexplained syncope or syncope precursor were diagnosed with POTS by head-up tilt test (HUTT) as the POTS group. 38 healthy children aged 5 to 16 years who underwent physical examination at the Child Health Care Clinic of the hospital in the same period were matched as controls (control group). The children with POTS were followed up after 3 months of treatment and were divided into good prognosis group (40 cases) and poor prognosis group (13 cases) according to the results of HUTT re-examination and whether the symptoms improved or not. HR and BP indicators were collected from each group at baseline and during HUTT.

Results: There were 91 research subjects, of which 45 are males, with a mean age of 11.52 ± 2.13 years. (1) HR at 5 and 10 min (HR 5 and HR 10, respectively), HR difference at 5 and 10 min (HRD 5 and HRD 10, respectively), and HR and BP product at 5 and 10 min (RPP 5 and RPP 10, respectively) were greater in the POTS group than in the control group ($P < 0.01$). (2) HR 5, HR 10, HRD 5, HRD 10, and RPP 10 in children with POTS were smaller in the good prognosis group than the poor prognosis group ($P < 0.01$). (3) The area under curve was 0.925 on the four combined indicators (HR 5, HR 10, HRD 5, and HRD 10), predicting a good prognosis of POTS, sensitivity of 99.99%, and specificity of 75.00%.

Conclusions: HR 5, HR 10, HRD 5, HRD 10, and RPP 10 and the four combined indicators (HR 5, HR 10, HRD 5, and HRD 10) had predictive value for the POTS prognosis in children. The predictive value of the four combined indicators for the POTS prognosis was better than that of the single HR 5, HRD 5, and RPP 10.

Keywords: postural tachycardia syndrome, heart rate, systolic blood pressure, rate-pressure product, children

INTRODUCTION

Postural tachycardia syndrome (POTS) is one of the common hemodynamic types of neurally mediated syncope (NMS) in children, characterized by an excessive increase in heart rate (HR) during sudden changes in body position, which may be combined with unexplained chest tightness, dizziness or even syncope, and other symptoms of orthostatic intolerance (OI), which improve or disappear after lying down (1).

The current diagnosis of POTS is based on the standing test (ST) or the head-up tilt test (HUTT), and prognostic assessment methods for POTS have been reported in the literature (2–15). Studies have suggested that certain biological markers have predictive value for the POTS prognosis in children, such as hydrogen sulfide production in red blood cells (2), flow-mediated dilation of brachial artery (3), decrease in systolic blood pressure (SBP) or change in diastolic blood pressure when switching from a supine position to an erect position (4), body mass index (BMI) (5), baroreflex sensitivity (6), 24-h urinary sodium level (7), plasma C-type natriuretic peptide (8), midregional fragment of pro-adrenomedullin (9), postural plasma norepinephrine levels (10), salivary cortisol levels (11), HR variability (HRV) in electrocardiographic indices (12), corrected QT interval dispersion (QTcd) (13, 14), and HR and HR difference (HRD) (15). However, there is still a necessity to explore new simple non-invasive and affordable indicators to predict the POTS prognosis in children.

HR and blood pressure (BP) are the basic physiological indicators for physical function. Swai et al. (16) found that the time domain analysis of HR and HRV is a valid indicator to discriminate healthy subjects from patients with POTS by meta-analysis, but research for sensitivity and specificity is lacking. Deng et al. (4) reported that hypovolemia, elevated plasma acetylcholine levels, and abnormal vascular tone can all take effect on BP and are considered to be the main causes of POTS. The rate-pressure product (RPP) is the result of multiplying HR and SBP, which could reflect the cardiac workload and myocardial oxygen consumption, and is a good indicator for clinical assessment of human health (17), reflecting the synergistic effect of HR and SBP on the changes presented on the body, and is more meaningful than using HR or BP alone to predict cardiovascular events (18, 19). Wang et al. (20) reported that combining HR and BP parameters at different time points of HUTT can significantly improve the diagnostic efficacy of POTS. From this, we supposed that HR and BP indicators at different time points of HUTT have predictive value for the POTS prognosis. In this research, we collected HR and BP indicators at different time points of HUTT at the first visit and the follow-up HUTT with the POTS after 3 months of treatment to investigate the possible association between above indicators and the POTS prognosis and to provide a reference for the construction of a prognostic estimation model for POTS in children.

METHODS

Participants

Clinical data were collected from April 2012 to May 2019 on 53 cases of children aged 5 to 15 years (POTS group), who attended the Pediatric Syncope Specialist Outpatient Clinic, The Second Xiangya Hospital, Central South University, for unexplained syncope or syncope precursor and were diagnosed with POTS. 38 children aged 5 to 16 years who underwent physical examination at the hospital's Specialized Pediatric Health Clinic during the same period were matched by age and gender as the control group. All research subjects completed HUTT with written informed consent signed by themselves or by their parents.

The POTS group was followed up after 3 months of treatment. According to the results of HUTT re-examination and whether the symptoms improved or not, they were divided into good prognosis group and poor prognosis group.

HUTT

The diagnosis of POTS in this research involved only the baseline head-up tilt test (BHUT) (1). Research subjects discontinued cardiovascular active drugs that may affect autonomic function for more than five half-lives and related foods such as coffee prior to the trial. Before the experiment, 4 h of fasting and drinking were prohibited. The examination time was arranged from 8:00 a.m. to 11:00 a.m., and the environment was quiet and room temperature was 20°C−24°C. For the HUTT, the tilting device was the SHUT-100 tilt test monitoring software system, Beijing Standley Technology Co., Ltd. (Beijing, China). The subjects were kept supine on the tilt bed over 10 min, and their HR, BP, and electrocardiogram (ECG) were monitored and recorded. After recording the baseline ECG and BP of the subject in the prone position, the subject was tilted 60° with the head high and feet low position within 15 s. The HR, BP, and ECG indicators were monitored dynamically during the tilt for 10 min or at the time point of a positive response.

Symptom Score

Symptom scores were used to assess the efficacy after treatment for POTS. The score was calculated on the basis of the frequency of clinical symptoms, the baseline score, and the follow-up score. The score includes the following clinical symptoms: dizziness, chest tightness, nausea, palpitations, headache, blurred vision, cold sweats, and syncope. The symptom scores were calculated on the basis of the following criteria: 0, no symptoms; 1, less than one time per month on average; 2, two to four times per month on average; 3, two to seven times per week on average; and 4, more than one time per day on average. The final score is the sum of each score (14, 15).

Inclusion and Exclusion Criteria

Inclusion criteria are as follow: (1) children under 18 years old; (2) OI symptoms such as dizziness, headache, weakness, blurred vision, chest tightness, palpitations, hand tremor, limited movement in an upright position, and even syncope; and (3) HUTT (1): Supine HR is normal, and, during the initial 10 min of HUTT or the ST, HR increases ≥40 bpm or is ≥130 bpm (in children 6∼12 years old) or ≥125 bpm (in adolescents 12∼18 years old), without orthostatic hypotension (BP decrease >20/10 mmHg).

Exclusion criteria are as follows: excluding patients with organic cardiopulmonary diseases, neurogenic diseases, immunological diseases, and metabolic and endocrine

TABLE 1 | Comparison of general information for control group and POTS group (Mean ± SD).

Characteristics	Male/Female	Age (years)	Height (cm)	Weight (kg)
Control ($n = 38$)	19/19	11.08 ± 2.28	143.57 ± 14.80	37.55 ± 11.92
POTS ($n = 53$)	26/27	11.83 ± 1.98	153.30 ± 13.08	41.64 ± 9.75
t/χ^2	0.008	−1.675	−3.314	−1.797
P-Value	0.929	0.097	0.001	0.076

POTS, postural tachycardia syndrome.

TABLE 2 | Comparison of general information for good prognosis group and poor prognosis group (Mean ± SD).

Characteristics	Male/Female	Age (years)	Height (cm)	Weight (kg)
Good prognosis ($n = 40$)	23/17	12.38 ± 1.94	157.62 ± 13.35	44.15 ± 8.76
Poor prognosis ($n = 13$)	3/10	11.65 ± 1.98	151.90 ± 12.85	40.83 ± 10.02
t/χ^2	3.377	−1.167	−1.381	−1.071
P-Value	0.066	0.249	0.173	0.289

POTS, postural tachycardia syndrome.

diseases causing syncope or syncope precursor symptoms, and non-pharmacological treatments for POTS were effective.

POTS Treatment Methods

In the condition that non-pharmacological treatment (health education, autonomic nervous function exercise, and increase the intake of water and salt) is ineffective (1), the combination of metoprolol 1 mg/(kg·d) was administered orally in two divided doses for a period of 3 months.

Prognosis of POTS

If the clinical symptom improved and the HUTT was not consistent with the criteria for POTS, then the good prognosis group was considered. If the clinical symptom did not improve and the HUTT still consistent with the criteria for POTS, then the poor prognosis group was considered.

Measurement Indicators

HR of HUTT at 0, 5, and 10 min (HR 0, HR 5, and HR 10, respectively); HRD between HR 0, HR 5, and HR 10 (HRD 0, HRD 5, and HRD 10, respectively); SBP of HUTT at 0, 5, and 10 min (SBP 0, SBP 5, and SBP 10, respectively); RPP of HUTT at 0, 5, and 10 min (RPP 0, RPP 5, and RPP 10, respectively).

RPP (bpm·mmHg) = HR (bpm) × SBP (mmHg).

Statistical Analysis

SPSS statistical software (version number: 25.0, IBM Corp, Armonk, New York, USA) and MedCalc statistical software (version number: 19.0.7) were used to statistically analyze the data. Data with normally distributed were expressed as mean ± SD and count data were expressed as frequency (rate). Statistical analysis was performed by *t*-test and χ^2 test. The sensitivity and specificity of the predictive value for the predictors were evaluated according to the receiver operating characteristic (ROC) curve, and the area under the curve (AUC) was used to indicate the predictive ability of the predictors: $0.5 \leq$ AUC<0.7 means low predictive ability; $0.7 \leq$ AUC<0.9 means moderate predictive ability; and AUC ≥ 0.9 means good predictive ability. When the Youden index was the largest, its sensitivity and specificity reached the best, and this cutoff point was selected as the boundary value of the predictive index. A difference was considered statistically significant at $P < 0.05$ (two-sided).

RESULTS

Demographic Characteristics

A total of 91 children were enrolled in this research, which consisted of 53 cases in the POTS group (26 males and 27 females, mean age 11.83 ± 1.98 years) and 38 cases in the control group (19 males and 19 females, mean age 11.08 ± 2.28 years). The POTS group was divided into 40 cases with good prognosis (23 males and 17 females, mean age 12.38 ± 1.94 years) and 13 cases with poor prognosis (3 males and 10 females, mean age 11.65 ± 1.98 years) according to the results of HUTT re-examination and whether the symptoms improved or not.

The height of the POTS group was higher than the control group ($P < 0.05$). No statistically significant differences were seen between the POTS and control groups in gender, age, and weight ($P > 0.05$). No statistically significant differences were seen between good prognosis group and poor prognosis group in gender, age, height, and weight ($P > 0.05$) (**Tables 1**, **2**).

Symptom Score

The baseline score was 2.68 ± 0.85 and the follow-up score (3 months later) was 1.02 ± 0.31, with the follow-up score significantly lower than the baseline score ($P < 0.01$). The score of the good prognosis group was 0.95 ± 0.22, the score of the poor prognosis group was 1.23 ± 0.44 ($P < 0.05$).

TABLE 3 | Comparison of HUTT parameters for control group and POTS group (Mean ± SD).

Characteristics	HR 0 (bpm)	HR 5 (bpm)	HR 10 (bpm)	HRD 5 (bpm)	HRD 10 (bpm)	SBP 0 (mmHg)	SBP 5 (mmHg)	SBP 10 (mmHg)	RPP 0 (bpm·mmHg)	RPP 5 (bpm·mmHg)	RPP 10 (bpm·mmHg)
Control (n = 38)	77.68 ± 10.37	95.79 ± 13.89	96.05 ± 12.43	18.11 ± 10.44	18.37 ± 10.53	106.79 ± 12.54	107.79 ± 10.46	108.97 ± 9.66	8335.47 ± 1758.30	10371.42 ± 1910.20	10523.18±1771.48
POTS (n = 53)	76.15 ± 12.66	102.42 ± 15.18	102.34 ± 16.77	26.26 ± 12.22	26.19 ± 14.97	110.30 ± 10.22	112.42 ± 11.69	111.98 ± 11.39	8409.96 ± 1715.90	11564.32 ± 2411.28	11446.49±2549.37
t	0.613	−2.127	−2.054	−3.335	−2.925	−1.470	−1.944	−1.321	−2.202	−2.253	−2.038
P-Value	0.541	0.036	0.043	0.001	0.004	0.145	0.055	0.190	0.840	0.013	0.045

HUTT, head-up tilt test; POTS, postural tachycardia syndrome; HR, heart rate; SBP, systolic blood pressure; RPP, rate-pressure product.

TABLE 4 | Comparison of HUTT parameters for good prognosis group and poor prognosis group (Mean ± SD).

Characteristics	HR 0 (bpm)	HR 5 (bpm)	HR 10 (bpm)	HRD 5 (bpm)	HRD 10 (bpm)	SBP 0 (mmHg)	SBP 5 (mmHg)	SBP 10 (mmHg)	RPP 0 (bpm·mmHg)	RPP 5 (bpm·mmHg)	RPP 10 (bpm·mmHg)
Good prognosis (n = 40)	75.73 ± 9.93	98.73 ± 12.43	96.90 ± 13.96	23.00 ± 9.99	21.18 ± 11.66	109.08 ± 9.84	112.40 ± 11.31	112.10 ± 10.73	8307.78 ± 1250.60	11125.45 ± 1952.35	10819.58 ± 2144.26
Poor prognosis (n = 13)	77.46 ± 19.29	113.77 ± 17.65	119.08 ± 13.52	37.00 ± 13.67	41.58 ± 14.29	111.85 ± 11.58	112.46 ± 13.29	111.62 ± 13.72	8724.38 ± 2744.77	12914.69 ± 3192.12	13375.46 ± 2807.01
t	−0.311	−3.406	−5.012	−3.836	−5.261	−0.624	−0.016	−0.132	−0.530	−1.908	−3.455
P-Value	0.760	0.001	0.000	0.000	0.000	0.536	0.987	0.896	0.605	0.076	0.001

HUTT, head-up tilt test; POTS, postural tachycardia syndrome; HR, heart rate; SBP, systolic blood pressure; RPP, rate-pressure product.

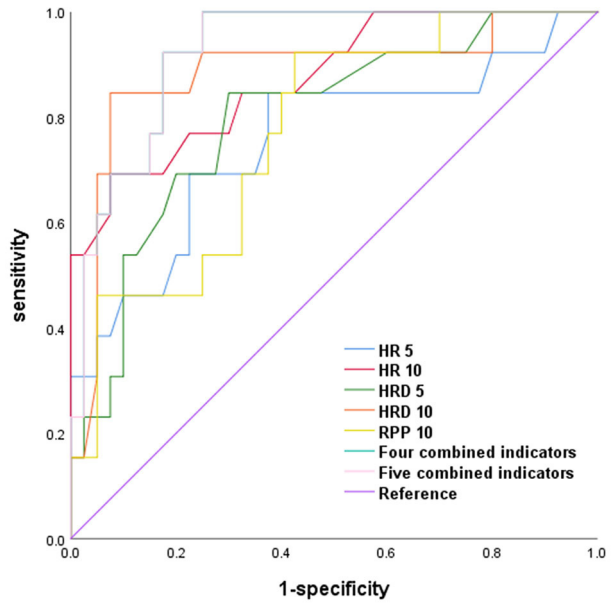

FIGURE 1 | ROC comparison of HR, HRD, RPP, and combined indicators to predict the POTS prognosis.

Comparison of HUTT Indicators for Different Groups

HR 5, HR 10, HRD 5, HRD 10, RPP 5, and RPP 10 were larger in the POTS group than in the control group ($P < 0.01$). HR 0, SBP 0, SBP 5, SBP 10, and RPP 0 did not show statistically significant differences between POTS and control groups ($P > 0.05$). HR 5, HR 10, HRD 5, HRD 10, and RPP 10 in the good prognosis group were lower than the poor prognosis group ($P < 0.01$). HR 0, SBP 0, SBP 5, SBP 10, RPP 0, and RPP 5 did not show statistical differences between the good prognosis group and the poor prognosis group ($P > 0.05$) (**Tables 3**, **4**).

Comparison of the Predictive Value of Each Indicator for the POTS Prognosis

HR 5, HR 10, HRD 5, HRD 10, and RPP 10, the four combined indicators (HR 5, HR 10, HRD 5, and HRD 10), and the five combined indicators (HR 5, HR 10, HRD 5, HRD 10, and RPP10) all had a good predictive value for the POTS prognosis ($P < 0.01$).

The AUC of the four combined indicators (HR 5, HR 10, HRD 5, and HRD 10) predicting the POTS prognosis was larger than that of HR 5, HRD 5, and RPP 10 ($Z = 2.026$, 2.045, and 2.696, respectively; $P = 0.043$, 0.041, and 0.007), which suggests that the predictive value of the four combined indicators was better than that of HR 5, HRD 5, and RPP 10, and the sensitivity and specificity were 99.99 and 75.00%, respectively. However, the predictive value of the five combined indicators (HR 5, HR 10, HRD 5, HRD 10, and RPP 10) was not better than that of the four combined indicators, suggesting that RPP 10 was inappropriate to be added in the combined indicators to predict the POTS prognosis (**Figure 1**; **Tables 5**, **6**).

DISCUSSIONS

POTS prognostic estimation is very important for clinically reducing physical accidental injuries caused by OI. Certain biological markers (2–11) and electrocardiographic markers (12–15) have been found to have predictive value for the POTS prognosis. HR is modulated by autonomic nerves system and humoral regulation. BP reflects the influence of stroke output, peripheral vascular resistance, HR, elasticity of aorta wall, circulating blood volume and vascular capacity, and other comprehensive factors on the body. HR and BP are commonly and easily available physiological indicators in clinical practice, which can reflect the vital signs of physical function and also the changes of internal environment, and have been gradually applied in the diagnosis and prognosis of many diseases.

A series of changes in hemodynamics will take place while a healthy child is held in an erect position for 30 s (21–23). As the body stands erect, gravity causes blood to pool from the chest to the lower abdomen and lower limbs. This transfer of fluid directly reduces the amount of venous return and effective circulating blood volume by ∼500 to 1,000 ml. As a result of reduced venous return, ventricular filling decreases, leading to a decrease in cardiac output and BP, even though mean arterial pressure remains constant (21–23), excitation of the aortic arch and carotid sinus pressure receptors causes a decrease in vagal excitability and an increase in sympathetic excitability, which, in turn, increases HR, cardiac contractility and peripheral vascular resistance to compensate for the deficit in cardiac output, maintaining BP in the normal range and avoiding syncope due to insufficient cerebral blood supply (24). The sympathetic and vagal excitability of children with POTS are in a state of imbalance, with a decrease in vagal excitability predominating, resulting in a higher HR than in healthy children. This research showed no difference in HR at baseline between children with POTS and controls, indicating that the HR of children with POTS at calm rest was essentially the same as that of healthy children. When POTS children were transferred to the erect position, the venous return decreased; the larger the HRD, the faster the HR rapidly and the shorter the ventricular diastole; and the increased peripheral resistance decreased stroke volume and cerebral perfusion, which easily induced syncope (23). Children with POTS have increased blood volume and electrolytes, increased venous filling, increased venous return and ventricular filling, and increased cardiac output and BP after increased water and salt intake (e.g., take oral rehydration salts) (25). Meanwhile, because of the increase of venous return, the sympathetic excitability decreased compared with that before treatment, the peripheral vascular resistance decreased, the positive inotropic effect of the heart was relatively weakened, and the mechanism of HR increase before treatment to compensate for the insufficient cardiac output was released, and the tachycardia symptoms were relieved in children with POTS after uprightness (26, 27). The treatment of the POTS children with metoprolol directly antagonizes catecholamines at the cellular level, inhibits adrenaline-dependent triggering activity, relatively prolongs ventricular diastole, increases cardiac output per beat, and improves blood volume and muscle

TABLE 5 | Comparison of ROC results for the predictive value of different indicators on the POTS' prognosis.

Characteristics	AUC	95%CI	*P* -Value	Cut-off	Sensitivity (%)	Specificity (%)
HR 5 (bpm)	0.753	0.584–0.922	0.007	99.50	84.60	62.50
HR 10 (bpm)	0.873	0.761–0.986	0.000	115.50	69.20	92.50
HRD 5 (bpm)	0.798	0.658–0.938	0.001	27.50	84.60	70.00
HRD 10 (bpm)	0.884	0.759–0.999	0.000	36.50	84.60	92.50
RPP 5 (bpm·mmHg)	0.669	0.489–0.849	0.069	11548.50	69.20	62.50
RPP 10 (bpm·mmHg)	0.769	0.629–0.909	0.004	10988.00	92.30	57.50
Four combined indicators	0.925	0.856–0.994	0.000	-	99.99	75.00
Five combined indicators	0.925	0.856–0.994	0.000	-	99.99	75.00

POTS, postural tachycardia syndrome; HR, heart rate; HRD, heart rate difference; RPP, rate-pressure product.
Four combined indicators: HR 5, HR 10, HRD 5, HRD 10.
Five combined indicators: HR 5, HR 10, HRD 5, HRD 10, RPP 10.

TABLE 6 | *Z*-test for comparing the predictive value of different ROCs.

Characteristics	Difference in AUC	*Z*-Value	95%CI	*P*-Value
HR 5 vs. Four combined indicators	0.172	2.026	0.006, 0.339	0.043
HR 10 vs. Four combined indicators	0.052	1.080	−0.042, 0.146	0.280
HRD 5 vs. Four combined indicators	0.127	2.045	0.005, 0.249	0.041
HRD 10 vs. Four combined indicators	0.041	0.812	−0.058, 0.141	0.417
RPP 10 vs. Four combined indicators	0.156	2.696	0.043, 0.269	0.007

POTS, postural tachycardia syndrome; HR, heart rate; HRD, heart rate difference; RPP, rate-pressure product.
Four combined indicators: HR 5, HR 10, HRD 5, HRD 10.

sympathetic activity, resulting in a relative improvement in the occurrence of transient ischemia in the brain and a certain degree of relief of POTS symptoms (14, 26, 28). In this research, HR 5, HR 10, HRD 5, and HRD 10 were associated with the POTS prognosis. HR 5, HR 10, HRD 5, and HRD 10 were higher in POTS than controls. HR 5, HR 10, HRD 5, and HRD 10 were lower in the good prognosis group than in the poor prognosis group, which may be related to the relatively mild imbalance of neurohumoral regulation in the POTS children in the good prognosis group, and, thus, the changes of HR and HRD were lower.

HR is associated with disease prognosis. Inaguma et al. (29) reported that, in a multicenter prospective cohort study of 1,102 dialysis patients, resting HR before the first dialysis was found to be associated with all-cause mortality after starting dialysis. Patients with HR $\geq$ 101 bpm had significantly higher all-cause mortality than those with HR between 80 and 100 bpm, suggesting that HR may have a predictive value for disease regression. Various indicators such as HR and BP have also been reported in the literature to predict the occurrence of syncopal-like disorders (30, 31), but the predictive value of using HR or BP alone is limited (32), so this research added HRD, RPP, and combined indicators to enhance the previously limited predictive value to justify the reasonability of HR and HRD at the time of HUTT to predict the POTS prognosis.

This research found an association between RPP 10 and the POTS prognosis. RPP is the product of resting HR and SBP, which was associated with hypertensive target organ damage. As a mixed index, small changes in any of its components (e.g., a 1 mmHg increase in BP or a 1 bpm increase in HR) will produce a greatly impact to final RPP value, amplifying the impact of the physiological index and facilitating clinical observation. RPP is more suitable than the results of a single indicator (HR or BP) and provides a more comprehensive judgment of cardiovascular events compared to changes in a single indicator of HR or BP, so controlling BP and HR fluctuations can alleviate clinical symptoms in children with POTS. Verma et al. (33) found that RPP was significantly increased in patients with organic heart disease and that HR and SBP were prognostic markers of heart failure, with reduced ejection fraction in heart failure; from baseline to discharge, increased HR and SBP were associated with 30 days morbidity and mortality and increased heart failure hospitalization in patients with significantly reduced ejection fraction. Kiviniemi et al. (34) reported that post-exercise RPP values are a valid predictor of cardiac mortality in patients with coronary artery disease and type 2 diabetes, enabling risk stratification of patients with ischemic heart disease and diabetes. Gobel et al. (35) considered myocardial oxygen consumption in male patients with normal BP at rest and steady state and observed maximal exercise tolerance in angina pectoris and found that HR and RPP were good predictors reflecting myocardial oxygen consumption during exercise in patients with ischemic heart disease with normal BP. However, it has also been suggested that RPP predicts myocardial oxygen consumption in relation to species. Aksentijević et al. (36) observed that RPP values correlated with myocardial oxygen consumption in the dog or human heart, but similar results for RPP were not observed in the rat or mouse heart.

The significantly higher RPP 10 in children with POTS in this research compared to controls may be related to an increase in plasma epinephrine in erect posture, resulting in a positive correlation between RPP and plasma epinephrine (37). Children with POTS present with clinical symptoms at plasma norepinephrine levels ≥600 ng/L, and the duration of elevated plasma norepinephrine in the erect position is 30 min, much longer than the duration of elevated norepinephrine in healthy children (38). Moreover, the present research showed that RPP 10 was significantly lower in the good prognosis group compared to the poor prognosis group after POTS treatment in children, which may be due to factors such as relatively lower myocardial oxygen consumption in the good prognosis group with POTS, or relatively less stress caused by plasma epinephrine, or differences with the etiology of POTS (34, 35, 38), suggesting that RPP 10 can be used as a predictor for risk stratification of POTS.

It evidently shows that HR, HRD, and RPP and the four combined indicators (HR 5, HR 10, HRD 5, and HRD 10) have some clinical value as indicators with low clinical cost, easy access, and easy acceptance by children and their families, especially for prognostic assessment of POTS in children, and also provide new thoughts for the establishment of prognostic models of POTS in the clinic.

CONCLUSIONS

HR, HRD, and RPP at different time points during HUTT have a high value in assessing the POTS prognosis in children. Combining a number of valuable indicators can significantly improve the effectiveness of their assessment.

STRENGTHS AND LIMITATIONS

This research innovatively incorporated the RPP as an indicator to predict the POTS prognosis and combined valuable indicators to substantially improve the predictive value. These findings will facilitate the construction of new predictive models and deepen the understanding of the mechanisms of POTS.

The present research is a single-center, retrospective parallel case-control study with limitations such as data bias, relatively small research sample size, and a single center from one region. The applicability of the results of this research to children in other regions needs to be tested externally through a large sample, multicenter research.

DATA AVAILABILITY STATEMENT

The datasets generated for this study are available on request to the corresponding author. Requests to access these datasets should be directed to CW, wangcheng2nd@csu.edu.cn.

ETHICS STATEMENT

The studies involving human participants were reviewed and approved by the Medical Ethical Committee, The Second Xiangya Hospital, Central South University. Written informed consent to participate in this study was provided by the participants' legal guardian/next of kin.

AUTHOR CONTRIBUTIONS

SW and CW conceived the research. SW, RZ, and HC collected and reviewed subjects' data. SW performed statistical analysis and drafted the manuscript. All authors contributed to its revision.

FUNDING

This work was supported by 2020 Hunan Province Clinical Medical Technology Innovation Guidance Project (2020SK53405).

ACKNOWLEDGMENTS

The authors thank the research personnel and the research volunteers involved with the project.

REFERENCES

1. Wang C, Li Y, Liao Y, Tian H, Huang M, Dong X, et al. 2018 Chinese Pediatric Cardiology Society (CPCS) guideline for diagnosis and treatment of syncope in children and adolescents. *Sci Bull.* (2018) 63:1558–64. doi: 10.1016/j.scib.2018.09.019
2. Yang J, Zhao J, Du S, Liu D, Fu C, Li X, et al. Postural orthostatic tachycardia syndrome with increased erythrocytic hydrogen sulfide and response to midodrine hydrochloride. *J Pediatr.* (2013) 163:1169–73. doi: 10.1016/j.jpeds.2013.04.039
3. Liao Y, Yang J, Zhang F, Chen S, Liu X, Zhang Q, et al. Flow-mediated vasodilation as a predictor of therapeutic response to midodrine hydrochloride in children with postural orthostatic tachycardia syndrome. *Am J Cardiol.* (2013) 112:816–20. doi: 10.1016/j.amjcard.2013.05.008
4. Deng W, Liu Y, Liu AD, Holmberg L, Ochs T, Li X, et al. Difference between supine and upright blood pressure associates to the efficacy of midodrine on postural orthostatic tachycardia syndrome (POTS) in children. *Pediatr Cardiol.* (2014) 35:719–25. doi: 10.1007/s00246-013-0843-9
5. Li H, Wang Y, Liu P, Chen Y, Feng X, Tang C, et al. Body mass index (BMI) is associated with the therapeutic response to oral rehydration solution in children with postural tachycardia syndrome. *Pediatr Cardiol.* (2016) 37:1313–8. doi: 10.1007/s00246-016-1436-1
6. Li H, Liao Y, Wang Y, Liu P, Sun C, Chen Y, et al. Baroreflex sensitivity predicts short-term outcome of postural tachycardia syndrome in children. *PLoS ONE.* (2016) 11:e167525. doi: 10.1371/journal.pone.0167525
7. Zhang Q, Liao Y, Tang C, Du J, Jin H. Twenty-four-hour urinary sodium excretion and postural orthostatic tachycardia syndrome. *J Pediatr.* (2012) 161:281–4. doi: 10.1016/j.jpeds.2012.01.054
8. Lin J, Han Z, Li H, Chen SY Li X, Liu P, et al. Plasma C-type natriuretic peptide as a predictor for therapeutic response to metoprolol in children with postural tachycardia syndrome. *PLoS ONE.* (2015) 10:e121913. doi: 10.1371/journal.pone.0121913
9. Zhang F, Li X, Ochs T, Chen L, Liao Y, Tang C, et al. Midregional pro-adrenomedullin as a predictor for therapeutic response to midodrine hydrochloride in children with postural orthostatic tachycardia syndrome. *J Am Coll Cardiol.* (2012) 60:315–20. doi: 10.1016/j.jacc.2012.04.025

10. Zhang Q, Chen X, Li J, Du J. Orthostatic plasma norepinephrine level as a predictor for therapeutic response to metoprolol in children with postural tachycardia syndrome. *J Transl Med.* (2014) 12:249. doi: 10.1186/s12967-014-0249-3
11. Lin J, Zhao H, Shen J, Jiao F. Salivary cortisol levels predict therapeutic response to a sleep-promoting method in children with postural tachycardia syndrome. *J Pediatr.* (2017) 191:91–5. doi: 10.1016/j.jpeds.2017.08.039
12. Wang Y, Zhang C, Chen S, Liu P, Wang Y, Tang C, et al. Heart rate variability predicts therapeutic response to metoprolol in children with postural tachycardia syndrome. *Front Neurosci.* (2019) 13:1214. doi: 10.3389/fnins.2019.01214
13. Lu W, Yan H, Wu S, Chen S, Xu W, Jin H, et al. Electrocardiography-derived predictors for therapeutic response to treatment in children with postural tachycardia syndrome. *J Pediatr.* (2016) 176:128–33. doi: 10.1016/j.jpeds.2016.05.030
14. Wang Y, Sun Y, Zhang Q, Zhang C, Liu P, Wang Y, et al. Baseline corrected QT interval dispersion is useful to predict effectiveness of metoprolol on pediatric postural tachycardia syndrome. *Front Cardiovasc Med.* (2022) 8:808512. doi: 10.3389/fcvm.2021.808512
15. Wang S, Zou R, Cai H, Wang Y, Ding Y, Tan C, et al. Heart rate and heart rate difference predicted the efficacy of metoprolol on postural tachycardia syndrome in children and adolescents. *J Pediatr.* (2020) 224:110–4. doi: 10.1016/j.jpeds.2020.05.017
16. Swai J, Hu Z, Zhao X, Rugambwa T, Ming G. Heart rate and heart rate variability comparison between postural orthostatic tachycardia syndrome versus healthy participants; a systematic review and meta-analysis. *BMC Cardiovasc Disord.* (2019) 19:320. doi: 10.1186/s12872-019-01298-y
17. Villella M, Villella A, Barlera S, Franzosi MG, Maggioni AP. Prognostic significance of double product and inadequate double product response to maximal symptom-limited exercise stress testing after myocardial infarction in 6296 patients treated with thrombolytic agents. GISSI-2 Investigators Grupo Italiano per lo Studio della Sopravvivenza nell-Infarto Miocardico. *Am Heart J.* (1999) 137:443–52. doi: 10.1016/S0002-8703(99)70490-4
18. Cai H, Wang S, Zou R, Wang Y, Wang C. Circadian rhythms of blood pressure and rate pressure product in children with postural tachycardia syndrome. *Auton Neurosci.* (2020) 228:102715. doi: 10.1016/j.autneu.2020.102715
19. Whitman M, Jenkins C, Sabapathy S, Adams L. Comparison of heart rate blood pressure product versus age-predicted maximum heart rate as predictors of cardiovascular events during exercise stress echocardiography. *Am J Cardiol.* (2019) 124:528–33. doi: 10.1016/j.amjcard.2019.05.027
20. Wang S, Zor R, Cai H, Ding Y, Xiao H, Wang X, et al. Efficiency of heart rate and heart rate difference at different time points during head-up tilt test in the diagnosis of postural tachycardia syndrome in children and adolescents. *Chin J Contemp Pediatr.* (2020) 22:780–4. doi: 10.7499/j.issn.1008-8830.2003133
21. Cornwell WK, Tarumi T, Stickford A, Lawley J, Roberts M, Parker R, et al. Restoration of pulsatile flow reduces sympathetic nerve activity among individuals with continuous-flow left ventricular assist devices. *Circulation.* (2015) 132:2316–22. doi: 10.1161/CIRCULATIONAHA.115.017647
22. Markham DW, Fu Q, Palmer MD, Drazner MH, Meyer DM, Bethea BT, et al. Sympathetic neural and hemodynamic responses to upright tilt in patients with pulsatile and nonpulsatile left ventricular assist devices. *Circ Heart Fail.* (2013) 6:293–9. doi: 10.1161/CIRCHEARTFAILURE.112.969873
23. Bai W, Chen S, Jin H, Du J. Vascular dysfunction of postural tachycardia syndrome in children. *World J Pediatr.* (2018) 14:13–7. doi: 10.1007/s12519-017-0104-8
24. Stewart JM, Medow MS, Montgomery LD, McLeod K. Decreased skeletal muscle pump activity in patients with postural tachycardia syndrome and low peripheral blood flow. *Am J Physiol Heart Circ Physiol.* (2004) 286:H1216–22. doi: 10.1152/ajpheart.00738.2003
25. Zhang W, Zou R, Wu L, Luo X, Xu Y, Li F, et al. The changes of electrolytes in serum and urine in children with neurally mediated syncope cured by oral rehydration salts. *Int J Cardiol.* (2017) 233:125–9. doi: 10.1016/j.ijcard.2016.12.138
26. Mar PL, Raj SR. Postural orthostatic tachycardia syndrome: mechanisms and new therapies. *Annu Rev Med.* (2020) 71:235–48. doi: 10.1146/annurev-med-041818-011630
27. Chen G, Du J, Jin H, Huang Y. Postural tachycardia syndrome in children and adolescents: pathophysiology and clinical management. *Front Pediatr.* (2020) 8:474. doi: 10.3389/fped.2020.00474
28. Olshansky B, Cannom D, Fedorowski A, Stewart J, Gibbons C, Sutton R, et al. Postural orthostatic tachycardia syndrome (POTS): a critical assessment. *Prog Cardiovasc Dis.* (2020) 63:263–70. doi: 10.1016/j.pcad.2020.03.010
29. Inaguma D, Koide S, Takahashi K, Hayashi H, Hasegawa M, Yuzawa Y, et al. Association between resting heart rate just before starting the first dialysis session and mortality: a multicentre prospective cohort. *Nephrology.* (2018) 23:461–8. doi: 10.1111/nep.13048
30. Kochiadakis GE, Orfanakis A, Chryssostomakis SI, Manios EG, Kounali DK, Vardas PE. Autonomic nervous system activity during tilt testing in syncopal patients, estimated by power spectral analysis of heart rate variability. *Pacing Clin Electrophysiol.* (1997) 20:1332–41. doi: 10.1111/j.1540-8159.1997.tb06788.x
31. Furlan R, Piazza S. Dell'Orto S, Barbic F, Bianchi A, Mainardi L, et al. Cardiac autonomic patterns preceding occasional vasovagal reactions in healthy humans. *Circulation.* (1998) 98:1756–61. doi: 10.1161/01.CIR.98.17.1756
32. Pitzalis M, Massari F, Guida P, Iacoviello M, Mastropasqua F, Rizzon B, et al. Shortened head-up tilting test guided by systolic pressure reductions in neurocardiogenic syncope. *Circulation.* (2002) 105:146–8. doi: 10.1161/hc0202.102982
33. Verma AK, Sun J, Hernandez A, Teerlink JR, Schulte PJ, Ezekowitz J, et al. Rate pressure product and the components of heart rate and systolic blood pressure in hospitalized heart failure patients with preserved ejection fraction: Insights from ASCEND-HF. *Clin Cardiol.* (2018) 41:945–52. doi: 10.1002/clc.22981
34. Kiviniemi AM, Kenttä TV, Lepojärvi S, Perkiömäki JS, Piira O, Ukkola O, et al. Recovery of rate-pressure product and cardiac mortality in coronary artery disease patients with type 2 diabetes. *Diabetes Res Clin Pract.* (2019) 150:150–7. doi: 10.1016/j.diabres.2019.03.007
35. Gobel FL, Norstrom LA, Nelson RR, Jorgensen CR, Wang Y. The rate-pressure product as an index of myocardial oxygen consumption during exercise in patients with angina pectoris. *Circulation.* (1978) 57:549–56. doi: 10.1161/01.CIR.57.3.549
36. Aksentijević D, Lewis HR, Shattock MJ. Is rate-pressure product of any use in the isolated rat heart? Assessing cardiac 'effort' and oxygen consumption in the Langendorff-perfused heart. *Exp Physiol.* (2016) 101:282–94. doi: 10.1113/EP085380
37. Krakoff LR, Dziedzic S, Mann SJ, Felton K, Yeager K. Plasma epinephrine concentration in healthy men: correlation with systolic pressure and rate-pressure product. *J Am Coll Cardiol.* (1985) 5:352–6. doi: 10.1016/S0735-1097(85)80058-9
38. Kanjwal K, Saeed B, Karabin B, Kanjwal Y, Grubb BP. Clinical presentation and management of patients with hyperadrenergic postural orthostatic tachycardia syndrome. A single center experience. *Cardiol J.* (2011) 19:527–31. doi: 10.5603/CJ.2011.0008

Conflict of Interest: The authors declare that the research was conducted in the absence of any commercial or financial relationships that could be construed as a potential conflict of interest.

Publisher's Note: All claims expressed in this article are solely those of the authors and do not necessarily represent those of their affiliated organizations, or those of the publisher, the editors and the reviewers. Any product that may be evaluated in this article, or claim that may be made by its manufacturer, is not guaranteed or endorsed by the publisher.

frontiers | Frontiers in Pediatrics

ORIGINAL RESEARCH
published: 20 April 2022
doi: 10.3389/fped.2022.812644

Risk Factors for Resistance to Intravenous Immunoglobulin Treatment and Coronary Artery Abnormalities in a Chinese Pediatric Population With Kawasaki Disease: A Retrospective Cohort Study

*Jie Liu, Yanyun Huang, Cheng Chen, Danyan Su, Suyuan Qin and Yusheng Pang**

Department of Pediatrics, First Affiliated Hospital of Guangxi Medical University, Nanning, China

OPEN ACCESS

Edited by:
Ruth Heying,
University Hospital Leuven, Belgium

Reviewed by:
Gabriele Simonini,
University of Florence, Italy
Balahan Makay,
Dokuz Eylül University, Turkey

***Correspondence:**
Yusheng Pang
pangyush@163.com

Specialty section:
This article was submitted to Pediatric Cardiology, a section of the journal Frontiers in Pediatrics

Received: *10 November 2021*
Accepted: *14 March 2022*
Published: *20 April 2022*

Citation:
Liu J, Huang Y, Chen C, Su D, Qin S and Pang Y (2022) Risk Factors for Resistance to Intravenous Immunoglobulin Treatment and Coronary Artery Abnormalities in a Chinese Pediatric Population With Kawasaki Disease: A Retrospective Cohort Study. Front. Pediatr. 10:812644. doi: 10.3389/fped.2022.812644

Background: The factors predicting high-risk Kawasaki disease (KD) remain unclear. Therefore, we aimed to determine the risk factors for resistance to intravenous immunoglobulin (IVIG) treatment and coronary artery aneurysm (CAA) development in a Chinese pediatric population with high-risk KD.

Methods: We compared the performances of 11 scoring systems that have been reported to predict IVIG resistance among patients with KD hospitalized from January 2013 through August 2021. Patients were risk-stratified based on the optimal scoring system. The association of baseline characteristics with IVIG treatment resistance and CAA development was investigated within the high-risk group of KD.

Results: In total, 346 pediatric patients with KD were included, of whom 63 (18.2%) presented with IVIG resistance. The Kobayashi score and five Chinese scoring system scores (Tang et al., Yang et al., Lan et al., Liping et al., and Wu et al.) were significantly higher in the IVIG non-responsive KD group than in the IVIG responsive KD group, and the results of the receiver operating characteristic (ROC) curves analysis were observed to be highest in the Xie Liping scoring system for IVIG resistance (area under the curve, 0.650). Especially, 87 (25.1%) patients comprised the high-risk KD group based on this optimal scoring system (≥5 points). IVIG resistance was significantly associated with the total bilirubin-to-albumin ratio (B/A ratio) [odds ratio, 7.427; 95% confidence interval (CI): 1.022–53.951]. The area under the ROC was 0.703 (95% CI: 0.586–0.821), and the cutoff point was 0.383, which indicated a sensitivity and specificity for predicting treatment resistance of 58% and 80%, respectively. The serum albumin level (odds ratio, 1.401; 95% CI: 1.049–1.869) and Z score of the left main coronary artery (odds ratio, 9.023; 95% CI: 1.070–76.112) were independent predictors of CAA development.

Conclusions: In the Chinese pediatric population with KD, the Xie Liping scoring system is the most appropriate method for identifying high-risk patients, and IVIG resistance

could be predicted based on the B/A ratio. Serum albumin level and Z score of the left main coronary artery at baseline were warning indicators for CAA development. More intensified or adjunctive therapies and close follow-up should be considered for high-risk patients with these risk factors.

Keywords: Kawasaki disease, high-risk, intravenous immunoglobulin resistance, coronary artery aneurysm, risk factor

INTRODUCTION

Coronary artery aneurysm (CAA), the chief feature of Kawasaki disease (KD), has gradually become the most common cause of acquired cardiac disease in childhood, and the incidence of the disease has increased every year (1). Owing to the lack of specificity and dispersion of the typical symptoms, a diagnosis of KD in clinics is primarily based on an awareness of the comprehensive knowledge of the disease presentation, and KD is often missed or misdiagnosed, resulting in missing the best timing of intravenous immunoglobulin (IVIG) treatment.

Patients with no response to IVIG therapy are at a high risk of CAA development and other serious cardiovascular complications, despite receiving several rescue treatments (2–6). With an increased awareness of severe cardiovascular complications in KD, there has been considerable effort in trying to determine predictors for IVIG resistance at initial presentation in patients with KD, and multiple scoring systems based on clinical and laboratory data for predicting IVIG resistance have been developed, such as those reported by Kobayashi et al. (3), Egami et al. (7), and Sano et al. (8). Studies have discovered that patients with KD with a high Kobayashi risk score are at increased risk for IVIG resistance and may be at risk for developing a more severe coronary artery disease among the Japanese population (3). In a further investigation, adverse coronary artery outcomes have reduced from 23 to 3% by adding prednisolone to the primary IVIG treatment in high-risk KD patients with a Kobayashi risk score of ≥5 points (9). However, evidence supporting the use of the Kobayashi score for predicting IVIG resistance or CAA development in the United Kingdom and Thailand cohorts is poor (10, 11), suggesting that these scoring systems have a marked geographic diversity, which has been confirmed by studies in non-Japanese populations (12, 13).

Globally, China is among the countries with a high prevalence of KD, and many scoring systems have been developed according to the characteristics of the studied populations from various regions. Nevertheless, such scoring systems are of limited use in other regions. Likewise, data regarding the risk factors for high-risk KD are also scarce. Therefore, the present study aimed to determine the risk factors that may help clinicians identify children with high-risk KD at risk of IVIG resistance and CAA development before primary treatment among the Chinese population.

MATERIALS AND METHODS

Study Design and Population

We retrospectively reviewed the clinical records of consecutive children with KD treated between January 2013 and August 2021 at the Pediatrics Department of First Affiliated Hospital of Guangxi Medical University, China. The criteria for the diagnosis of KD were as follows: diagnosis of KD was compliant with the Diagnostic Guidelines for Kawasaki Disease (sixth revision, issued by the Japan Kawasaki Disease Research Committee in 2020) (14), and CAA was defined as a Z score for the coronary artery internal diameter of ≥2.5 after 1 month of the disease course according to the guideline on diagnosis and management of cardiovascular sequelae in Kawasaki disease (JCS/JSCS 2020) (15). Children were excluded, if treatment after the first 10 days of the onset of fever and the diagnosis of KD were not clear, if they received IVIG or corticosteroid (e.g., methylprednisolone or prednisone) therapy outside the hospital, or had incomplete data required for statistical analyses.

All patients received initial IVIG (2 g/kg per 24 h) and oral aspirin (30–50 mg/kg per day) until resolution of their fever for 72 h at least. Then, they received aspirin (3–5 mg/kg per day) for 2 months from disease onset. Patients with IVIG resistance, defined as having persistent or recrudescent fever (temperature, >38.0°C) for at least 36 h but not longer than 7 days after completion of the initial IVIG infusion (2 g/kg), received a second dose of gamma globulin therapy (2 g/kg). Corticosteroid (methylprednisolone was administered by intravenous injection at a dose of 2 mg/kg per day, twice a day. Afterwards, the administration was tapered and withdrawn until the normalization of the C-reactive protein (CRP) levels, and oral prednisolone administration was initiated from 2 mg/kg and reduced to 1 mg/kg and finally to 0.5 mg/kg per day and tapered for ≥2 weeks) was administered due to unremitting fever after completion of the second IVIG treatment. According to their responsiveness to the initial IVIG treatment, all children were divided into two groups as follows: the IVIG responsive ($n = 283$) and IVIG non-responsive KD groups ($n = 63$).

As is well known, the focus of clinical attention has been on how to screen patients with a high risk of IVIG resistance and administer intensive therapy. Currently, there is no universal risk scoring system that applies to all populations. Based on this, differences in 11 existing scoring systems (3, 7, 8, 12, 16–22) that have been previously reported to identify patients with KD at high risk of IVIG resistance were compared between the study groups. Patients were assigned scores according to the rules of

each scoring system (see **Supplementary File 1**). Eligible patients were diagnosed with high-risk KD using the optimal scoring system and the association of baseline characteristics with IVIG treatment resistance and CAA development was investigated within the high-risk group of KD. To further verify our results, we analyzed high-risk patients with KD based on the Kobayashi score, which is widely used in Japanese patients, using the same assay (see **Supplementary File 2**).

Data Collection

The following clinical and laboratory data collected from the medical charts of the patients enrolled in this study were reviewed using a standardized form: (i) general demographic data: age, sex, height, weight, and body mass index (BMI); (ii) clinical manifestations: duration of fever before admission, pediatric sequential organ failure assessment (pSOFA) score on the day of admission, illness day at treatment (illness day 1 = 1st day of fever), response to IVIG therapy, incidence of incomplete KD and CAA, and total score based on the optimal scoring system; and (iii) laboratory indicators: the highest value was selected for analysis in the case of the white blood cell count (WBC), neutrophil count, aspartate aminotransferase (AST) level, alanine aminotransferase (ALT) level, total bilirubin (TSB) level, and CRP level, whereas the lowest value was selected in the case of the lymphocyte count, hemoglobin concentration, platelet (PLT) count, serum albumin (ALB) concentration, and serum sodium concentration. All the laboratory indicators were collected for assessment at the time during the acute febrile period and before the initial IVIG treatment. We calculated the neutrophil-to-lymphocyte count ratio, platelet-to-lymphocyte count ratio, TSB-to-ALB ratio (B/A ratio), and capillary leakage index based on the aforementioned indicators. We also collected data on the coronary arterial internal diameters of the right coronary artery, left main coronary artery, left anterior descending artery, and left circumflex coronary artery from echocardiography that was performed once a week within 2 months after disease onset, and the Z score of the coronary artery corrected for the body surface area was determined and recorded (iv).

Statistical Analyses

Normality of distribution was verified using the Shapiro–Wilk and homogeneity tests. Measurement data with a normal distribution are expressed as means ± standard deviations, and the two-independent sample t-test was used to compare such data between the groups. Measurement data that did not have a normal distribution are expressed as medians (four-digit interval) [P_{50} (P_{25}, P_{75})], and these data were compared between the groups using the Mann–Whitney U test. Enumeration data are expressed as a percentage (%). The chi-square or Pearson's chi-square test was used to perform intergroup comparisons. Significant indices were analyzed using multivariate logistic regression analysis to determine the risk factors, and the best threshold for the significant parameter was constructed using receiver operating characteristic (ROC) curves. The *P*-values were two-tailed with $P < 0.05$ considered statistically significant. Statistical analyses were performed using SPSS, version 26.0 (IBM Corp., Armonk, NY, USA).

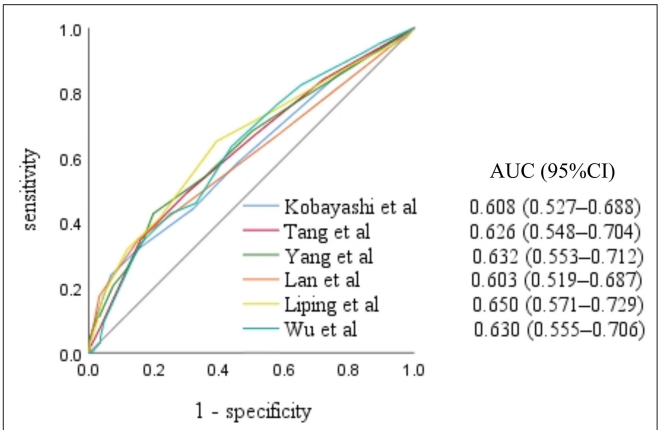

FIGURE 1 | Receiver operating characteristic curves for the scoring systems scores in the intravenous immunoglobulin non-responsive Kawasaki disease group. AUC, area under the curve; CI, confidence interval.

RESULTS

Baseline Characteristics

Over the period of observation, 452 children were admitted to the Pediatrics of First Affiliated Hospital of Guangxi Medical University with a diagnosis of KD. In total, 106 children were excluded from this study, including 53 children who were diagnosed after 10 days of illness, 17 children who received IVIG or corticosteroid therapy outside the hospital, and 36 with incomplete clinical or laboratory data. Ultimately, 346 children were included in this study. Of them, 63 (18.2%) children had initial IVIG resistance, and 16 (25.4%) of those children received corticosteroid therapy in addition to the second dose of gamma globulin therapy. Afterwards their symptoms alleviated and no other biologic agents, such as infliximab, cyclosporine, anakinra, cyclophosphamide, or plasma exchange, were administered during this period. The mean age of the IVIG non-responsive KD group was 30 months (range, 2–152 months) with a male-to-female ratio of 2.7:1 (46 boys and 17 girls); there were 27 cases (42.9%) of incomplete KD and 19 cases (30.2%) of CAA. The mean age of the IVIG responsive KD group was 28 months (range, 2–158 months) with a male-to-female ratio of 2.3:1 (198 boys and 85 girls); there were 117 cases (41.3%) of incomplete KD and 69 cases (24.4%) of CAA. There were no disease recurrences or deaths in either group.

Comparisons of the Scoring Systems

Results of the analysis of the 11 scoring systems by study group are presented in the **Supplementary File 1**. The Kobayashi score (3) and five Chinese scoring system scores (12, 18, 20–22) were higher in the IVIG non-responsive KD group than in the IVIG responsive KD group, and the differences were statistically significant (all, $P < 0.05$). The area under the ROC curve for the Xie Liping risk scoring system was the largest, with an area of 0.650 [95% confidence interval (CI): 0.571–0.729], while the Kobayashi score had an area of 0.608 (95% CI: 0.527–0.688) (**Figure 1**).

TABLE 1 | Comparison of the baseline characteristics between the intravenous immunoglobulin non-responsive and responsive sub-groups.

	Total ($n = 87$)	IVIG non-responsive sub-group ($n = 26$)	IVIG responsive sub-group ($n = 61$)	*P*-value
Age [month, P_{50} (P_{25}, P_{75})]	31.00 (20.00, 51.00)	28.50 (13.75, 63.25)	31.00 (20.00, 44.50)	0.721
<1 year [*n* (%)]	9 (10.3)	4 (15.4)	5 (8.2)	0.533
Male [*n* (%)]	66 (75.9)	20 (76.9)	46 (75.4)	0.880
Height [m, P_{50} (P_{25}, P_{75})]	0.92 (0.78, 1.05)	0.92 (0.77, 1.11)	0.92 (0.81, 1.03)	0.623
Weight [kg, P_{50} (P_{25}, P_{75})]	13.00 (10.00, 16.00)	13.50 (9.35, 17.55)	12.80 (10.00, 15.50)	0.478
BMI [kg/m^2, P_{50} (P_{25}, P_{75})]	15.33 (14.61, 16.60)	15.88 (14.51, 17.30)	15.24 (14.65, 16.39)	0.173
pSOFA score (point, mean ± SD)	0.70 ± 1.52	1.12 ± 2.16	0.52 ± 1.12	0.097
Fever duration before admission (day, mean ± SD)	6.29 ± 3.04	6.58 ± 3.60	6.16 ± 2.79	0.565
Days of illness at primary treatment (day, mean ± SD)	6.84 ± 3.48	5.96 ± 3.86	7.21 ± 3.26	0.125
≤4 days [*n* (%)]	19 (21.8)	10 (38.5)	9 (14.8)	0.014
≤5 days [*n* (%)]	42 (48.3)	17 (65.4)	25 (41.0)	0.037
Incomplete KD [*n* (%)]	50 (57.5)	16 (61.5)	34 (55.7)	0.616
CAA [*n* (%)]	18 (20.7)	7 (26.9)	11 (18.0)	0.349
Score (12) (point, mean ± SD)	6.06 ± 1.13	6.50 ± 1.24	5.87 ± 1.04	0.017
White blood cell count ($\times 10^9$/L, ref. 5–12$\times 10^9$/L, mean ± SD)	15.40 ± 7.03	12.96 ± 6.59	16.44 ± 7.01	0.034
Neutrophils count ($\times 10^9$/L, ref. 1.8–6.3$\times 10^9$/L, mean ± SD)	11.36 ± 6.39	10.00 ± 5.73	11.93 ± 6.62	0.197
NLR [P_{50} (P_{25}, P_{75})]	4.94 (2.38, 8.00)	5.52 (2.61, 11.35)	4.66 (2.32, 7.36)	0.209
Hemoglobin (g/L, ref. 120–160 g/L, mean ± SD)	101.69 ± 12.67	104.57 ± 14.80	100.47 ± 11.56	0.168
Platelet count ($\times 10^{12}$/L, ref. 125–350$\times 10^9$/L, mean ± SD)	340.13 ± 155.03	318.55 ± 187.88	349.33 ± 139.48	0.400
PLR [P_{50} (P_{25}, P_{75})]	125.00 (83.33,250.00)	225.00 (75.80, 333.33)	125.00 (83.33, 200.00)	0.080
CRP [mg/L, ref. 0–10 mg/L, P_{50} (P_{25}, P_{75})]	97.20 (40.74, 180.63)	98.40 (53.13, 145.28)	97.12 (39.49, 192.00)	0.989
Sodium [mmol/L, ref. 137–147 mmol/L, mean ± SD]	134.66 ± 3.79	132.98 ± 3.55	135.37 ± 3.70	0.007
≤133 mmol/L [n(%)]	32 (36.8)	14 (53.8)	18 (29.5)	0.031
ALT [U/L, ref. 7–45 U/L, mean ± SD]	67.95 ± 61.34	93.10 ± 60.28	57.23 ± 59.06	0.012
AST [U/L, ref. 13–40 U/L, P_{50} (P_{25}, P_{75})]	32.00 (24.00, 46.00)	46.60 (31.50, 95.50)	30.00 (22.00, 37.50)	<0.001
Total bilirubin [μmol/L, ref. 3.4–20.5 μmol/L, P_{50} (P_{25}, P_{75})]	7.40 (4.00, 15.70)	13.80 (5.80, 20.90)	6.60 (3.45, 11.65)	0.007
Albumin (g/L, ref. 40–55 g/L, mean ± SD)	31.79 ± 4.33	30.90 ± 4.75	32.16 ± 4.13	0.217
≤34 g/L [*n* (%)]	67 (77.0)	20 (76.9)	47 (77.0)	0.990
B/A ratio [P_{50} (P_{25}, P_{75})]	0.24 (0.12, 0.53)	0.39 (0.22, 0.73)	0.21 (0.11, 0.36)	0.003
CLI [P_{50} (P_{25}, P_{75})]	3.11 (1.28, 5.13)	3.22 (1.72, 4.57)	3.10 (1.22, 5.33)	0.897

IVIG, intravenous immunoglobulin; BMI, body mass index; pSOFA, pediatric sequential organ failure assessment; KD, Kawasaki disease; CAA, coronary artery aneurysm; NLR, neutrophil-to-lymphocyte count ratio; PLR, platelet-to-lymphocyte count ratio; CRP, C-reactive protein; ALT, alanine aminotransferase; AST, aspartate aminotransferase; B/A ratio, total bilirubin-to-albumin ratio; CLI, capillary leakage index.

Intragroup Comparisons Between the High-Risk KD Groups to Analyze the Risk Factors for High-Risk KD

Analysis of Risk Factors for IVIG Resistance in High-Risk KD

Comparisons of the Clinical Characteristics

Eighty-seven hospitalized children were diagnosed with high-risk KD according to the optimal scoring system (Xie Liping risk score of ≥ 5 points). Of these, 26 patients with IVIG resistance were enrolled in the IVIG non-responsive sub-group, and eight (30.8%) of them had used corticosteroid therapy in addition to the second dose of gamma globulin therapy. The remaining 61 patients were enrolled in the IVIG responsive sub-group. The sum of scores based on the Xie Liping risk scoring system, and the proportion of days of illness at primary treatment (<4 or 5 days), were higher in the IVIG non-responsive sub-group than in the IVIG responsive sub-group with statistically significant differences (both, $P < 0.05$). However, there were no statistically significant differences between the sub-groups with respect to age, sex, height, weight, BMI, pSOFA score, fever duration before admission, and the incidence of incomplete KD or CAA (all, $P >$

TABLE 2 | Results of logistic regression analyses of intravenous immunoglobulin resistance.

Characteristics	Univariable		Multivariable	
	Odds ratio (95% CI)	*P*-value	Odds ratio (95% CI)	*P*-value
White blood cell count	1.083 (1.004–1.168)	0.038	1.087 (0.972–1.215)	0.157
Sodium	1.199 (1.045–1.376)	0.010	1.099 (0.938–1.285)	0.243
ALT	1.009 (1.001–1.018)	0.020	1.001 (0.989–1.013)	0.887
AST	1.025 (1.009–1.040)	0.002	1.015 (0.992–1.038)	0.206
B/A ratio	3.069 (1.126–8.364)	0.028	7.427 (1.022–53.951)	0.047
Days of illness at primary treatment	1.136 (0.962–1.342)	0.133	1.245 (0.983–1.580)	0.069
CRP	0.999 (0.992–1.006)	0.786	0.995 (0.985–1.005)	0.313
Platelet count	1.001 (0.998–1.004)	0.396	1.004 (0.999–1.009)	0.135
<1 year	0.491 (0.121–2.000)	0.321	0.479 (0.093–2.452)	0.377

CI, confidence interval; ALT, alanine aminotransferase; AST, aspartate aminotransferase; B/A ratio, total bilirubin-to-albumin ratio; CRP, C-reactive protein.

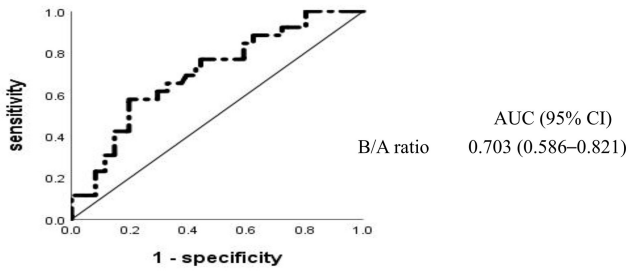

FIGURE 2 | Receiver operating characteristic curves for intravenous immunoglobulin resistance in high-risk Kawasaki disease. AUC, area under the curve; CI, confidence interval; B/A, total bilirubin-to-albumin ratio.

TABLE 3 | Baseline B/A ratios for predicting high-risk Kawasaki disease.

Baseline B/A ratio	Sensitivity, %	Specificity, %	PPV, %	NPV, %
≥0.383	58	80	55.6	81.7
≥0.373	58	79	53.6	81.4
≥0.361	58	77	51.7	81.0
≥0.387	54	80	53.8	80.3
≥0.357	58	75	50.0	80.7

B/A ratio, total bilirubin-to-albumin ratio; PPV, positive predictive value; NPV, negative predictive value.

0.05). In terms of laboratory indicators, the IVIG non-responsive sub-group showed higher values of the serum ALT, AST, TSB, and B/A ratio and lower values of the WBC and serum sodium than those of the IVIG responsive sub-group, and the differences were statistically significant (all, $P < 0.05$), as shown in **Table 1**.

Results of the Multi-Factor Logistic Analysis

To determine the relative effect of each risk factor for IVIG resistance in high-risk KD, we performed a logistic regression analysis, which revealed that high-risk KD with IVIG resistance was significantly associated with six baseline laboratory variables (WBC, serum levels of ALT, AST, TSB, and sodium, and B/A ratio) and two clinical characteristics (days of illness at primary treatment and the Xie Liping risk score). These variables plus the CRP level, PLT count, and age <1 year, all of which were previously reported as risk factors for IVIG resistance (3, 7, 16, 22, 23), but not the Xie Liping risk score or TSB level, were included in the logistic regression analysis (**Table 2**). The B/A ratio, calculated as the TSB level divided by the ALB level, was included in the multivariable analysis instead of the two separate indicators; the Xie Liping risk score was also excluded from the multivariable analysis because the variables included in this risk score, such as days of illness at primary treatment, the serum sodium level, age, the WBC count instead of the percentage of neutrophils, and B/A ratio instead of the ALB level, were included in the multivariable model. The B/A ratio was the only significant independent predictor of IVIG resistance in high-risk KD cases. The area under the ROC curve for the B/A ratio was 0.703 (95% CI: 0.586–0.821) (**Figure 2**), and the sensitivity and specificity for predicting IVIG resistance in high-risk KD patients were 58% and 80%, respectively, at a cutoff point of 0.383 (**Table 3**). Similarly, the B/A ratio was observed to be a significant predictor of IVIG resistance in high-risk patients with KD based on the Kobayashi score [OR: 10.336 (95% CI: 1.240–86.126), $P = 0.031$].

Analysis of Risk Factors for CAA in High-Risk KD

Comparisons of the Clinical Characteristics

Although there were 87 patients in the high-risk group, only 18 (20.7%) of these patients had CAA, and there were no statistically significant differences between the sub-groups with respect to the demographic and clinical manifestations (all, $P > 0.05$). The univariable analysis identified only one laboratory index, the serum ALB level, which, together with the Z score of the coronary artery internal diameter in the acute phase of high-risk KD, was significantly associated with CAA development (**Table 4**). Multivariable analysis revealed that the serum ALB level and the Z score of the left main coronary artery internal diameter were significant independent predictors of CAA development, and this difference remained significant when corrected for age and sex (**Table 5**). In high-risk patients with KD based on the Kobayashi score, the Z-score of the left main coronary artery internal diameter was also significantly

TABLE 4 | Comparisons of the baseline characteristics between the coronary artery aneurysm and non-coronary artery aneurysm sub-groups.

	Total ($n = 87$)	CAA sub-group ($n = 18$)	Non-CAA sub-group ($n = 69$)	*P*-value
Age (month, mean± SD)	36.49 ± 25.86	35.44 ± 36.71	36.77 ± 22.54	0.848
<1 year [*n* (%)]	9 (10.3)	4 (22.2)	5 (7.2)	0.155
Male [*n* (%)]	66 (75.9)	14 (77.8)	52 (75.4)	1.000
Height (m, mean ± SD)	0.93 ± 0.18	0.90 ± 0.25	0.94 ± 0.16	0.503
Weight (kg, mean ± SD)	13.92 ± 5.84	13.85 ± 8.26	13.94 ± 5.10	0.952
BMI (kg/m^2, mean ± SD)	15.70 ± 1.65	16.26 ± 1.67	15.55 ± 1.63	0.107
pSOFA score [point, P_{50} (P_{25}, P_{75})]	0.00 (0.00, 1.00)	0.50 (0.00, 2.00)	0.00 (0.00, 1.00)	0.102
Fever duration before admission (day, mean ± SD)	6.29 ± 3.04	6.72 ± 3.66	6.17 ± 2.88	0.499
Days of illness at primary treatment (day, mean ± SD)	6.84 ± 3.48	7.72 ± 4.56	6.61 ± 3.14	0.228
≤4 days [*n* (%)]	19 (21.8)	5 (27.8)	14 (20.3)	0.716
≤5 days [*n* (%)]	42 (48.3)	6 (33.3)	36 (52.2)	0.154
Incomplete KD [*n* (%)]	50 (57.5)	8 (44.4)	42 (60.9)	0.209
IVIG resistance [*n* (%)]	26 (29.9)	7 (38.9)	19 (27.5)	0.349
Score (12) [point, mean ± SD]	6.06±1.13	6.17±1.20	6.03±1.12	0.649
White blood cell count [×10^9/L, ref. 5–12×10^9/L, P_{50} (P_{25}, P_{75})]	14.47 (10.75, 20.05)	18.77 (8.80, 23.69)	13.95 (11.27, 18.71)	0.245
Neutrophils count (×10^9/L, ref.1.8–6.3×10^9/L, mean ± SD)	11.36 ± 6.39	13.90 ± 7.77	10.69 ± 5.87	0.058
NLR (mean ± SD)	5.70 ± 4.35	6.42 ± 3.67	5.52 ± 4.52	0.438
Hemoglobin (g/L, ref. 120–160 g/L, mean ± SD)	101.69 ± 12.67	97.40 ± 14.15	102.81 ± 12.11	0.107
Platelet count (×10^{12}/L, ref. 125–350×10^9/L, mean ± SD)	340.13 ± 155.03	310.91 ± 180.20	347.75 ± 148.31	0.372
PLR (mean ± SD)	168.44 ± 114.75	145.95 ± 104.35	174.31 ± 117.31	0.353
CRP (mg/L, ref. 0–10 mg/L, mean ± SD)	105.39 ± 65.04	118.62 ± 65.74	101.94 ± 64.89	0.335
Sodium (mmol/L, ref. 137–147 mmol/L, mean ± SD)	134.66 ± 3.79	134.21 ± 4.09	134.77 ± 3.73	0.579
≤133 mmol/L [*n* (%)]	32 (36.8)	7 (38.9)	25 (36.2)	0.835
ALT [U/L, ref. 7–45 U/L, P_{50} (P_{25}, P_{75})]	49.00 (21.00, 96.00)	62.00 (30.50, 93.00)	43.00 (18.50,108.00)	0.335
AST (U/L, ref. 13–40 U/L, mean ± SD)	44.44 ± 32.89	40.72 ± 26.22	45.41 ± 34.52	0.593
Total bilirubin (μmol/L, ref. 3.4–20.5 μmol/L, mean ± SD)	13.24 ± 16.27	16.74 ± 17.15	12.32 ± 16.03	0.307
Albumin (g/L, ref. 40–55 g/L, mean ± SD)	31.79 ± 4.33	29.13 ± 3.53	32.48 ± 4.27	0.003
≤34 g/L [*n* (%)]	67 (77.0)	16 (88.9)	51 (73.9)	0.303
B/A ratio (mean ± SD)	0.43 ± 0.57	0.60 ± 0.68	0.38 ± 0.53	0.157
CLI (mean ± SD)	3.34 ± 2.07	4.06 ± 2.22	3.16 ± 2.01	0.100
Z score of coronary artery internal diameter				
Left main coronary artery (mean ± SD)	2.34 ± 1.09	3.69 ± 0.92	1.99 ± 0.82	<0.001
Right coronary artery (mean ± SD)	2.03 ± 1.38	3.23 ± 1.32	1.72 ± 1.22	<0.001
Baseline maximum *Z* score (mean ± SD)	2.65 ± 1.13	4.01 ± 0.79	2.30 ± 0.93	<0.001

CAA, coronary artery aneurysm; BMI, body mass index; pSOFA, pediatric sequential organ failure assessment; KD, Kawasaki disease; IVIG, intravenous immunoglobulin; NLR, neutrophil-to-lymphocyte count ratio; PLR, platelet-to-lymphocyte count ratio; CRP, C-reactive protein; ALT, alanine aminotransferase; AST, aspartate aminotransferase; B/A ratio, total bilirubin-to-albumin ratio; CLI, capillary leakage index.

associated with CAA development [OR: 19.097 (95% CI: 1.871–194.902), $P = 0.013$].

ROC Analysis of the Risk Factors for CAA

Multivariate logistic regression analysis showed that a low level of serum ALB and a high Z score of the left main coronary artery internal diameter were significantly associated with CAA. The respective areas under the ROC curve for the serum ALB level and Z score of the left main coronary artery internal diameter were 0.713 and 0.927, at cutoff points of 30.7 g/L and 2.8 (**Figure 3**). **Figure 4** shows the incidence of CAA in high-risk patients by risk factor and demonstrates that the risk of CAA development increased with an increase in the number of risk factors.

DISCUSSION

This study identified risk factors for resistance to IVIG treatment and CAA development in a Chinese pediatric population with high-risk KD. In addition, we observed that in our patient group with KD, the Xie Liping risk score (12) had potential value in predicting IVIG resistance, and the B/A ratio alone was highly associated with IVIG resistance in high-risk patients with a score ≥ 5 points. Unexpectedly, the obtained results were revealed to be similar for the high-risk patients with KD as defined by a Kobayashi score ≥4 points (see **Supplementary File 2**). TSB, which is the numerator in the equation for the B/A ratio, is positively associated with IVIG resistance, whereas the serum ALB level, which is the denominator, is negatively associated with

TABLE 5 | Results of logistic regression analyses of coronary artery aneurysm.

Characteristic	Univariable		Multivariable		Adjust[#]	
	Odds ratio (95% CI)	*P*-value	Odds ratio (95% CI)	*P*-value	Odds ratio (95% CI)	*P*-value
Albumin	1.255(1.071–1.468)	0.005	1.361 (1.053–1.757)	0.019	1.401 (1.049–1.869)	0.022
Z score of left main coronary artery	9.505(3.266–27.669)	<0.001	8.025 (1.062–60.620)	0.044	9.023 (1.070–76.112)	0.043
Z score of right coronary artery	2.654 (1.576–4.469)	<0.001	1.232 (0.490–3.101)	0.657	1.206 (0.466–3.122)	0.699
Baseline maximum *Z* score	7.250 (2.882–18.239)	<0.001	1.632 (0.162–16.460)	0.678	1.734 (0.154–19.518)	0.656

[#]*Indicates a significant relationship after correction for age and sex; CI, confidence interval.*

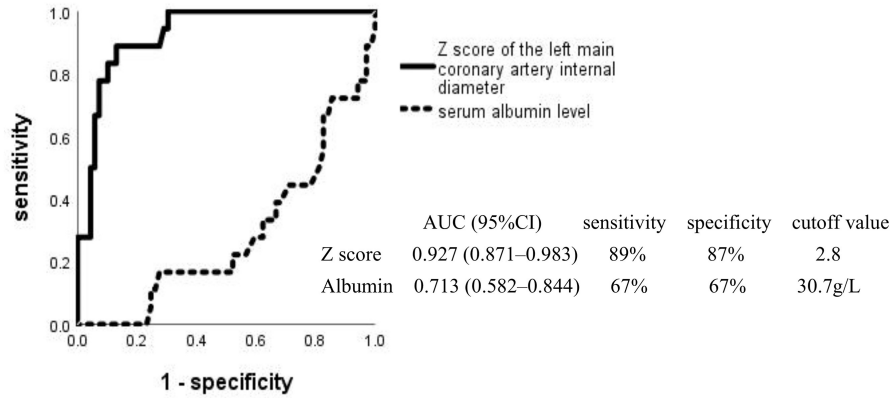

FIGURE 3 | Receiver operating characteristic curves for coronary artery aneurysm development in high-risk Kawasaki disease. AUC, area under the curve; CI, confidence interval.

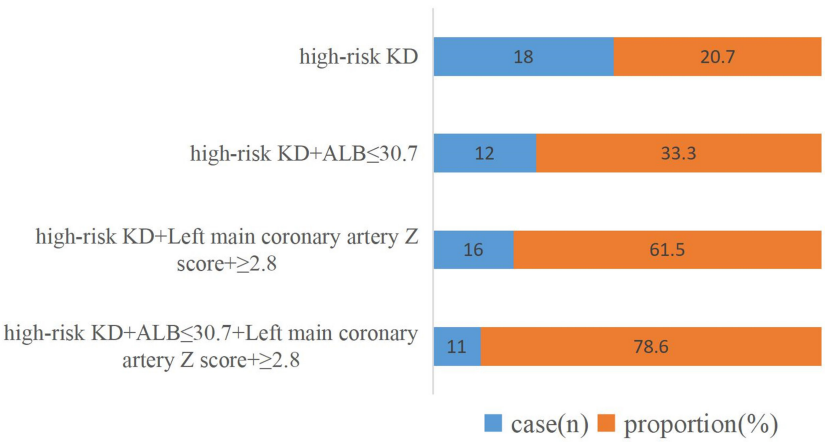

FIGURE 4 | Incidence of coronary artery abnormalities after disease onset per risk factor. KD, Kawasaki disease; ALB, serum albumin level.

IVIG resistance; both these variables are reported to predict IVIG resistance (8, 12, 14, 19, 20, 22). However, our findings were not entirely consistent with the findings of the aforementioned studies. We observed that the B/A ratio was the only risk factor associated with IVIG resistance. In conjunction with those reported in the literature, our results may indicate that an isolated indicator is of limited utility in predicting IVIG resistance for high-risk patients with KD; thus, a composite index that incorporates some laboratory indicators may be of greater value. To the best of our knowledge, the present study is the first to suggest that a high B/A ratio is a risk factor for predicting IVIG resistance in high-risk patients with KD, although future large-scale studies are needed to verify this finding.

The present study discovered that a low serum ALB level and a high Z score of the left main coronary artery internal diameter at baseline were independently associated with CAA development in high-risk patients with KD, which was consistent with the findings of a study regarding the risk factors for coronary

aneurysms and progressive coronary dilatation in Taiwanese patients (24). Hepatic dysfunction as a common complication during the acute KD episode has been evidenced in past studies (25), in which hypoalbuminemia was the most common type. The serum ALB level is also one of the variables included in the Harada score (26) in Japan, which has a cutoff < 35 g/L and was designed to predict CAA development. The possible mechanisms of hypoalbuminemia in CAA secondary to KD are related to the capillary permeability associated with systemic vasculitis (27), and the present study also observed a higher capillary leakage index in the CAA sub-group compared with that in the non-CAA sub-group. However, the difference failed to reach statistical significance, suggesting that high-risk KD patients with higher inflammatory reactions and stronger immune responses have a higher leakage of serum ALB, which may be a characteristic of high-risk patients with CAA, indicating that it is important to follow these patients carefully.

Coronary artery lesions have always been a popular research topic in KD, and the extent of coronary artery expansion during the acute phase of the disease has a negative correlation with the chance for them to return to normal; giant coronary artery aneurysms do not revert to a normal morphology (28–30). Several studies have reported that the likelihood of coronary artery regression within the normal range depends on the size of the baseline Z score of the coronary artery (31, 32). The results obtained in the current study are comparable to those of the previous one. Our study observed that the baseline Z score of the left main coronary artery before the primary treatment was a heightened risk factor for CAA development, and the same result was observed in the high-risk patients with KD as defined by a Kobayashi score ≥4 points (see **Supplementary File 2**). However, inconsistent with the results of a multicenter and prospective observational study that was conducted in Japan, our study showed no relationships between age <1 year or IVIG resistance and CAA development (23), which was probably because of the small sample size of high-risk patients with KD. Our study may have been underpowered to conduct a highly informative multivariate analysis. Nevertheless, the binary logistic regression analysis also revealed that a high Z score of the left main coronary artery was highly significantly related to a higher likelihood of CAA development at 1 month of illness in high-risk patients with KD. Even after correction for age and sex, our results remained significant, suggesting that close monitoring with frequent echocardiography is needed for high-risk patients with these risk factors.

Our study has some limitations. First, the sample size of this study limited the power of the analyses; hence, studies with larger sample sizes are warranted. Second, because of non-routine testing, some indicators that have been reported to be associated with IVIG resistance or CAA were not considered in the study design, e.g., the levels of serum procalcitonin, interleukin-6, and brain natriuretic peptide. Third, the collection of limited laboratory data precluded the testing of other scoring systems, and the Xie Liping risk score, which was developed in China to predict IVIG resistance, has not been adapted to other ethnicities, and high-risk patients with KD, as defined by this scoring system, may not be generalizable to other populations. However, the results obtained for high-risk patients with KD, as defined by the Kobayashi score, were mostly similar. Since all the participants in our study were Chinese, the Xie Liping risk score was appropriate. Hence, more prospective studies are needed to validate a more valuable risk scoring system for identifying children with high-risk KD.

CONCLUSIONS

In the Chinese pediatric population with KD, the Xie Liping scoring system is the most appropriate method for identifying high-risk patients, and IVIG resistance could be predicted based on the B/A ratio. Serum ALB level and Z score of the left main coronary artery at baseline were risk factors significantly associated with CAA development. To reduce CAA development in high-risk patients, more intensified or adjunctive therapies should be considered, and intensive monitoring with echocardiography should be required. Future studies are needed to verify the association of these risk factors in different ethnic populations.

DATA AVAILABILITY STATEMENT

The original contributions presented in the study are included in the article/**Supplementary Material**, further inquiries can be directed to the corresponding author.

ETHICS STATEMENT

The approval for this research was obtained from the Medical Ethics Committee of the First Affiliated Hospital of GuangXi Medical University [Code Number: 2021(KY-E-240)] and informed consent was obtained from the parents of each participant.

AUTHOR CONTRIBUTIONS

JL, YH, DS, and YP: conceptualization. JL, CC, and SQ: formal analysis. DS and SQ: methodology. JL and YH: writing—original draft. JL and YP: writing—review and editing. All authors approved the final manuscript to be submitted and agreed to be accountable for all aspects of the work.

ACKNOWLEDGMENTS

We thank Dr. Zhao WeiYing for the helpful advice and discussions. We also gratefully acknowledge Ye BingBing, Yue QiaoYu, Huang YuQin, and Wei ChangQing from the Pediatrics Department of First Affiliated Hospital of Guangxi Medical University who instructed and assisted us during the manuscript preparation.

SUPPLEMENTARY MATERIAL

The Supplementary Material for this article can be found online at: https://www.frontiersin.org/articles/10.3389/fped.2022.812644/full#supplementary-material

REFERENCES

1. Taubert KA, Rowley AH, Shulman ST. Nationwide survey of Kawasaki disease and acute rheumatic fever. *J Pediatr.* (1991) 119:279–82. doi: 10.1016/s0022-3476(05)80742-5
2. Beiser AS, Takahashi M, Baker AL, Sundel RP, Newburger JW, A. predictive instrument for coronary artery aneurysms in Kawasaki disease. US Multicenter Kawasaki disease Study Group. *Am J Cardiol.* (1998) 81:1116–20. doi: 10.1016/s0002-9149(98)00116-7
3. Kobayashi T, Inoue Y, Takeuchi K, Okada Y, Tamura K, Tomomasa T, et al. Prediction of intravenous immunoglobulin unresponsiveness in patients with Kawasaki disease. *Circulation.* (2006) 113:2606–12. doi: 10.1161/CIRCULATIONAHA.105.592865
4. Uehara R, Belay ED, Maddox RA, Holman RC, Nakamura Y, Yashiro M, et al. Analysis of potential risk factors associated with nonresponse to initial intravenous immunoglobulin treatment among Kawasaki disease patients in Japan. *Pediatr Infect Dis J.* (2008) 27:155–60. doi: 10.1097/INF.0b013e31815922b5
5. Burns JC, Capparelli EV, Brown JA, Newburger JW, Glode MP. Intravenous gamma-globulin treatment and retreatment in Kawasaki disease. US/Canadian Kawasaki syndrome Study Group. *Pediatr Infect Dis J.* (1998) 17:1144–8. doi: 10.1097/00006454-199812000-00009
6. Adachi S, Sakaguchi H, Kuwahara T, Uchida Y, Fukao T, Kondo N. High regression rate of coronary aneurysms developed in patients with immune globulin-resistant Kawasaki disease treated with steroid pulse therapy. *Tohoku J Exp Med.* (2010) 220:285–90. doi: 10.1620/tjem.220.285
7. Egami K, Muta H, Ishii M, Suda K, Sugahara Y, Iemura M, et al. Prediction of resistance to intravenous immunoglobulin treatment in patients with Kawasaki disease. *J Pediatr.* (2006) 149:237–40. doi: 10.1016/j.jpeds.2006.03.050
8. Sano T, Kurotobi S, Matsuzaki K, Yamamoto T, Maki I, Miki K, et al. Prediction of non-responsiveness to standard high-dose gamma-globulin therapy in patients with acute Kawasaki disease before starting initial treatment. *Eur J Pediatr.* (2007) 166:131–7. doi: 10.1007/s00431-006-0223-z
9. Miyata K, Kaneko T, Morikawa Y, Sakakibara H, Matsushima T, Misawa M, et al. Efficacy and safety of intravenous immunoglobulin plus prednisolone therapy in patients with Kawasaki disease (Post RAISE): a multicentre, prospective cohort study. *Lancet Child Adolesc Health.* (2018) 2:855–62. doi: 10.1016/S2352-4642(18)30293-1
10. Davies S, Sutton N, Blackstock S, Gormley S, Hoggart CJ, Levin M, et al. Predicting IVIG resistance in UK Kawasaki disease. *Arch Dis Child.* (2015) 100:366–8. doi: 10.1136/archdischild-2014-307397
11. Jarutach J, Roymanee S, Wongwaitaweewong K. Verification of "Japanese scoring systems" to predict IVIG resistance and identification of predictors for IVIG resistance in Thai children with Kawasaki disease. *Pediatr Cardiol.* (2021) 42:1799–804. doi: 10.1007/s00246-021-02668-0
12. LiPing X, Juan G, Yang F, Lan H, Chen C, WeiLi Y, et al. Questioning the establishment of clinical prediction model for intravenous immunoglobulin resistance in children with Kawasaki disease. *Chin J Evid Based Pediatr.* (2019) 14:169–75. doi: 10.3969/j.issn.1673-5501.2019.03.002
13. Rigante D, Andreozzi L, Fastiggi M, Bracci B, Natale MF, Esposito S. Critical overview of the risk scoring systems to predict non-responsiveness to intravenous immunoglobulin in Kawasaki syndrome. *Int J Mol Sci.* (2016) 17:278. doi: 10.3390/ijms17030278
14. Kobayashi T, Ayusawa M, Suzuki H, Abe J, Ito S, Kato T, et al. Revision of diagnostic guidelines for Kawasaki disease (6th revised edition). *Pediatr Int.* (2020) 62:1135–8. doi: 10.1111/ped.14326
15. Fukazawa R, Kobayashi J, Ayusawa M, Hamada H, Miura M, Mitani Y, et al. JCS/JSCS 2020 guideline on diagnosis and management of cardiovascular sequelae in Kawasaki disease. *Circ J.* (2020) 84:1348–407. doi: 10.1253/circj.CJ-19-1094
16. Fu PP, Du ZD, Pan YS. Novel predictors of intravenous immunoglobulin resistance in Chinese children with Kawasaki disease. *Pediatr Infect Dis J.* (2013) 32:e319–23. doi: 10.1097/INF.0b013e31828e887f
17. Kawamura Y, Takeshita S, Kanai T, Yoshida Y, Nonoyama S. The combined usefulness of the neutrophil-to-lymphocyte and platelet-to-lymphocyte ratios in predicting intravenous immunoglobulin resistance with Kawasaki disease. *J Pediatr.* (2016) 178:281–284.e1. doi: 10.1016/j.jpeds.2016.07.035
18. Lan X, Jing Z, Lunyu Y, Ling Q, Ying Y, Xiaochun Y. Predictive analysis of intravenous immunoglobulin unresponsive Kawasaki disease. *J Clin Pediatr.* (2018) 36:765–71. doi: 10.3969/j.issn.1000-3606.2018.10.010
19. Lin MT, Chang CH, Sun LC, Liu HM, Chang HW, Chen CA, et al. Risk factors and derived formosa score for intravenous immunoglobulin unresponsiveness in Taiwanese children with Kawasaki disease. *J Formos Med Assoc.* (2016) 115:350–5. doi: 10.1016/j.jfma.2015.03.012
20. Tang Y, Yan W, Sun L, Huang J, Qian W, Ding Y, et al. Prediction of intravenous immunoglobulin resistance in Kawasaki disease in an East China population. *Clin Rheumatol.* (2016) 35:2771–6. doi: 10.1007/s10067-016-3370-2
21. Wu S, Liao Y, Sun Y, Zhang CY, Zhang QY, Yan H, et al. Prediction of intravenous immunoglobulin resistance in Kawasaki disease in children. *World J Pediatr.* (2020) 16:607–13. doi: 10.1007/s12519-020-00348-2
22. Yang S, Song R, Zhang J, Li X, Li C. Predictive tool for intravenous immunoglobulin resistance of Kawasaki disease in Beijing. *Arch Dis Child.* (2019) 104:262–7. doi: 10.1136/archdischild-2017-314512
23. Miyata K, Miura M, Kaneko T, Morikawa Y, Sakakibara H, Matsushima T, et al. Risk factors of coronary artery abnormalities and resistance to intravenous immunoglobulin plus corticosteroid therapy in severe Kawasaki disease: an analysis of Post RAISE. *Circ Cardiovasc Qual Outcomes.* (2021) 14:e007191. doi: 10.1161/CIRCOUTCOMES.120.007191
24. Liu MY, Liu HM, Wu CH, Chang CH, Huang GJ, Chen CA, et al. Risk factors and implications of progressive coronary dilatation in children with Kawasaki disease. *BMC Pediatr.* (2017) 17:139. doi: 10.1186/s12887-017-0895-8
25. Burns JC, Glodé MP. Kawasaki syndrome. *Lancet.* (2004) 364:533–44. doi: 10.1016/S0140-6736(04)16814-1
26. Harada K. Intravenous gamma-globulin treatment in Kawasaki disease. *Acta Paediatr Jpn.* (1991) 33:805–10. doi: 10.1111/j.1442-200x.1991.tb02612.x
27. Ballmer PE. Causes and mechanisms of hypoalbuminaemia. *Clin Nutr.* (2001) 20:271–3. doi: 10.1054/clnu.2001.0439
28. Akagi T, Rose V, Benson LN, Newman A, Freedom RM. Outcome of coronary artery aneurysms after Kawasaki disease. *J Pediatr.* (1992) 121:689–94. doi: 10.1016/s0022-3476(05)81894-3
29. Beitzke A, Zobel G. Coronary aneurysm in Kawasaki syndrome: incidence and prognosis. *Klin Padiatr.* (1989) 201:33–9. doi: 10.1055/s-2007-1025272
30. Newburger JW, Takahashi M, Gerber MA, Gewitz MH, Tani LY, Burns JC, et al. Diagnosis, treatment, and long-term management of Kawasaki disease: a statement for health professionals from the Committee on Rheumatic Fever, Endocarditis and Kawasaki Disease, Council on Cardiovascular Disease in the Young, American Heart Association. *Circulation.* (2004) 110:2747–71. doi: 10.1161/01.CIR.0000145143.19711.78
31. Friedman KG, Gauvreau K, Hamaoka-Okamoto A, Tang A, Berry E, Tremoulet AH, et al. Coronary artery aneurysms in Kawasaki disease: risk factors for progressive disease and adverse cardiac events in the US population. *J Am Heart Assoc.* (2016) 5:3289. doi: 10.1161/JAHA.116.003289
32. Son MBF, Gauvreau K, Tremoulet AH, Lo M, Baker AL, de Ferranti S, et al. Risk model development and validation for prediction of coronary artery aneurysms in Kawasaki disease in a North American population. *J Am Heart Assoc.* (2019) 8:e011319. doi: 10.1161/JAHA.118.011319

Conflict of Interest: The authors declare that the research was conducted in the absence of any commercial or financial relationships that could be construed as a potential conflict of interest.

frontiers | Frontiers in Pediatrics

SYSTEMATIC REVIEW
published: 21 April 2022
doi: 10.3389/fped.2022.794053

Clinical Status and Outcome of Isolated Right Ventricular Hypoplasia: A Systematic Review and Pooled Analysis of Case Reports

Keiichi Hirono[1], Hideki Origasa[2], Kaori Tsuboi[1], Shinya Takarada[1], Masato Oguri[1], Mako Okabe[1], Nariaki Miyao[1], Hideyuki Nakaoka[1], Keijiro Ibuki[1], Sayaka Ozawa[1] and Fukiko Ichida[3]*

[1] Departments of Pediatrics, Graduate School of Medicine, University of Toyama, Toyama, Japan, [2] Biostatistics and Clinical Epidemiology, Graduate School of Medicine, University of Toyama, Toyama, Japan, [3] Department of Pediatrics, International University of Health and Welfare, Tokyo, Japan

OPEN ACCESS

Edited by:
Ruth Heying,
University Hospital Leuven, Belgium

Reviewed by:
Danny Eytan,
Technion Israel Institute of Technology, Israel
Zakhia Saliba,
Hôtel-Dieu de France, Lebanon

***Correspondence:**
Keiichi Hirono
khirono1973@gmail.com

Specialty section:
This article was submitted to Pediatric Cardiology, a section of the journal Frontiers in Pediatrics

Received: *13 October 2021*
Accepted: *14 March 2022*
Published: *21 April 2022*

Citation:
Hirono K, Origasa H, Tsuboi K, Takarada S, Oguri M, Okabe M, Miyao N, Nakaoka H, Ibuki K, Ozawa S and Ichida F (2022) Clinical Status and Outcome of Isolated Right Ventricular Hypoplasia: A Systematic Review and Pooled Analysis of Case Reports. Front. Pediatr. 10:794053. doi: 10.3389/fped.2022.794053

Background: Isolated right ventricular hypoplasia (IRVH), not associated with severe pulmonary or tricuspid valve malformation, is a rare congenital myocardial disease. This study aims to evaluate the clinical status and outcome of IRVH.

Methods: A systematic search of keywords on IRVH was conducted. Studies were searched from MEDLINE, EMBASE, Cochrane Central Register of Controlled Trials, and Igaku Chuo Zasshi (Ichushi) published between January 1950 and August 2021.

Results: Thirty studies met the inclusion criteria. All of these studies were case reports and included 54 patients (25 males and 29 females). The median age of the patients was 2.5 years old (0–15.3 years). Of the 54 patients, 13 (24.1%) reported a family history of cardiomyopathy. Moreover, 50 (92.6%), 19 (35.2%), and 17 (31.5%) patients were diagnosed with cyanosis, finger clubbing, and dyspnea, respectively. Furthermore, 53 (98.2%) patients had a patent foramen ovale or an atrial septal defect (ASD). Z-score of the tricuspid valve diameter on echocardiogram was -2.16 ± 1.53, concomitant with small right ventricular end-diastolic volume. In addition, 29 (53.7%), 21 (38.9%), 7 (13.0%), and 2 (3.7%) patients underwent surgery, ASD closure, Glenn operation, and one and a half ventricular repair, respectively. Among them, nine (20.4%) patients expired, and the multivariable logistic regression analysis showed that infancy, heart failure, and higher right ventricular end-diastolic pressure were risk factors for death.

Conclusions: IRVH was diagnosed early in children with cyanosis and was associated with high mortality. This systematic review and pooled analysis provided evidence to assess the of IRVH degree in order to evaluate the clinical status and outcome of IRVH.

Keywords: right ventricular hypoplasia, heart failure, cyanosis, patent foramen ovale, tricuspid valve

INTRODUCTION

Isolated right ventricular (RV) hypoplasia (IRVH), not associated with severe pulmonary or tricuspid valvar malformations, or ventricular septal defect (VSD), is a rare congenital myocardial disease. IRVH was first described in 1950 by Cooley et al. (1) and only limited case reports and case series have been published until recently (1–7). IRVH is also characterized by a small RV cavity, a patent foramen ovale (PFO) or an atrial septum defect (ASD), and a normal RV outflow tract concurrent with normally developed pulmonary valves (PV) (2). The clinical IRVH spectrum varies considerably from severe cyanosis, congestive heart failure, and early infant death to mild cyanosis (2, 8–14). This study aims to evaluate the clinical status and outcome of IRVH.

MATERIALS AND METHODS

Eligibility

This study was conducted following the Preferred Reporting Items for Systematic Reviews and Meta-analyses guidelines (**Supplementary Table 1**) (15). This study protocol conformed to the ethical guidelines of the Declaration of Helsinki 1964 and was approved by the Research Ethics Committee of the University of Toyama (approval no. R2021087), Toyama, Japan.

A systematic search was conducted utilizing IRVH-related keywords, regardless of the presence or absence of clinical outcomes. IRVH was defined as (1) not having pulmonary valve stenosis or pulmonary atresia, (2) not having tricuspid valve malformation, (3) not having congenital heart disease other than PFO or ASD, or (4) not having arrhythmogenic RV cardiomyopathy or Uhl's disease. The exclusion criteria were (1) studies that did not focus on IRVH, (2) articles that did not present original research (conference abstracts, editorials, or commentaries), (3) non-human studies (animal studies or *in vitro* experiments), (4) duplicated studies, and (5) any studies that the investigators deemed irrelevant to the objective.

Study Identification

MEDLINE, EMBASE, Cochrane Central Register of Controlled Trials on the Ovid platform, and the Japanese literature database Igaku Chuo Zasshi (Ichushi) were searched for studies published in any language between January 1950 and August 2021. The experienced librarians at the National Center for Child Health and Development, who were also affiliated with Cochrane Japan, Tokyo, Japan, performed searches using the terms described in **Supplementary Table 2**.

Study Selection

Two investigators performed independent reviews of the articles. The titles and abstracts of all articles were read through during the initial screening, and articles that met the exclusion criteria were excluded. All articles were reviewed and identified for eligibility for secondary screening. A third reviewer moderated a face-to-face meeting whenever the two reviewers disagreed on an article's eligibility to determine its suitability.

Abbreviations: IRVH, Isolated right ventricular hypoplasia; HF, Heart failure; RV, Right ventricular; PV, Pulmonary valves; PFO, Patent foramen ovale; ASD, Atrium septum defect; TV, Tricuspid valve; RVEDV, Right ventricular end-diastolic volume; RVEDP, Right ventricular end-diastolic pressure.

Assessment of Risk of Bias in Included Studies

The following key domains were assessed following the guidance in the Cochrane Handbook (version 5.1.0) (16): (1) random sequence generation (selection bias), (2) allocation sequence concealment (selection bias), (3) blinding of participants and personnel (performance bias), (4) blinding of outcome assessment (detection bias), (5) incomplete outcome data (attrition bias), (6) selective outcome reporting (reporting bias), and (7) other biases. Two review authors (KH and SO) independently assessed the risk of bias of included studies. Disagreements were resolved by consensus. Study authors of eligible studies were contacted to resolve uncertainties and provide further data to reduce exclusion bias and minimize missing data.

Statistical Analysis

Continuous variables were expressed as means ± standard deviation (SD) or median [interquartile range (IQR)] values. Categorical variables were expressed as numbers and percentages. Continuous variables were compared using the unpaired *t*-test, non-parametric Mann–Whitney *U*-test, or one-way analysis of variance. However, categorical variables were compared using χ^2 statistics or Fisher's exact test, as appropriate. Univariate regression tests were performed on all variables, and a multivariate logistic regression was performed on statistically significant variables ($P < 0.05$). The variables for inclusion were carefully selected, to ensure parsimony of the final models given the number of events. Statistical analyses were performed using the JMP software (version 13; SAS Institute, Cary, NC, USA). A *p*-value of <0.05 was considered statistically significant.

RESULTS

Literature Search and Characteristics of the Eligible Studies

Four databases were utilized to identify 273 articles. Of the articles, 211 were excluded based on ineligibility determined by having titles and abstracts suggesting apparent ineligibility (**Figure 1**). Two investigators independently evaluated the entire contents of the remaining 62 articles and ultimately identified 31 articles as eligible for the study (2–8, 11–13, 17–38). All of these studies were case reports.

Risk of Bias

The risk of bias was assessed for all included studies (**Supplementary Table 3**).

Case Demographics

Data from 54 patients (25 males and 29 females) who had IRVH (**Tables 1**, **2**) were obtained from the 31 included studies, all of which were case reports. The median age of the patients was 2.5 (0–15.3 years) years old. The follow-up period was

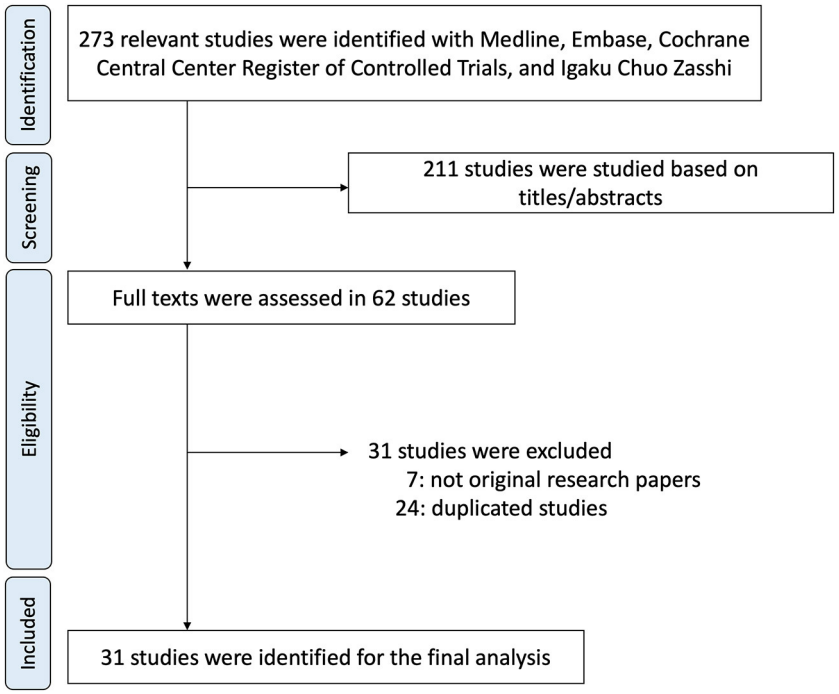

FIGURE 1 | Flow chart of the study.

1.3 (0.3–4.3) years. Moreover, 13 (24.1%) patients reported a family history of IRVH. Furthermore, 50 (92.6%), 19 (35.2%), and 17 (31.5%) patients were diagnosed with cyanosis, finger clubbing, and dyspnea, respectively. Only three (5.6%) patients had arrhythmia.

Cardiovascular Characteristics

Of the patients, 40 (74.0%), 28 (51.9%), and nine (16.7%) were diagnosed by angiogram, echocardiogram, and magnetic resonance imaging (MRI), respectively. In addition, 11 (20.4%) and 42 (77.8%) patients had PFO and ASD, respectively. The Z-score of the diameter of the tricuspid valve on echocardiogram was-2.16 ± 1.53, concomitant with small right ventricular end-diastolic volume (RVEDV; **Tables 2**, **3**). The right ventricular end-diastolic pressure (RVEDP) was lower in the survivors than that in the deceased ($p = 0.0361$).

Surgical Treatment

A total of 29 (53.7%) patients underwent surgery. Specifically, 21 (38.9%), 4 (7.4%), 7 (13.0%), 2 (3.7%), and 1 (5.9%) patient underwent ASD closure, systemic-to-pulmonary artery (SP) shunt placement, a Glenn operation, one and a half ventricular repair, and Fontan surgery (**Tables 2**, **3**). Moreover, four patients underwent multiple surgeries; two patients had SP shunt twice and the other two patients had ASD closure and then one and a half ventricular repair. Arterial oxygen saturation was higher in patients who underwent ASD closure than that in patients who underwent Glenn operation or one and a half ventricular repair or the patient without surgery (**Figure 2**).

Clinical Outcomes

Nine (16.7%) patients expired; seven and two patients were diagnosed at <1 year and in adulthood, respectively. The multivariable logistic regression analysis showed that <1 year at diagnosis, heart failure, and >12 mmHg of RVEDP were independent risk factors for death ($p < 0.05$, respectively; **Table 4**).

DISCUSSION

This study revealed that IRVH was diagnosed early in children with cyanosis and was associated with high mortality between 1959 and 2000. It is believed that this is the first systematic review to evaluate the association between IRVH and surgery.

IRVH is characterized by trabecular musculature underdevelopment and a small RV cavity (2). An ASD or a PFO serves as an escape route causing a right-to-left shunt, resulting in cyanosis. This clinical symptom has a wide outcome spectrum, from mortality in early infancy to mild cyanosis. Congestive heart failure and deep cyanosis can appear during infancy in seven cases, whereas symptoms (e.g., mild cyanosis, dyspnea, and clubbed finger) may be found later in cases with less malformation. This may depend on hypoplasia degree and interatrial communication size.

TABLE 1 | Characteristics of 54 IRVH cases from 31 studies.

#	Reference	Age (years)	Sex	PFO/ ASD	FX of IRVH	Cyanosis	Finger clubbing	Dyspnea	Fatigability	Heart failure	Murmur	Arrhythmia	Angio	Echo	Surgery	TV	PV	Outcome
1	Gasul et al. (17)	4	F	ASD	No	Yes	No	No	No	Yes	No	No	No	No	Yes	Normal	Normal	Alive
2	Sackner et al. (7)	0.2	M	PFO	No	Yes	No	Yes	No	Yes	No	No	No	No	No	Small	N/A	Died
3		30	M	ASD	Yes	No	No	Yes	Yes	Yes	Yes	No	Yes	No	No	Normal	N/A	Died
4		22	M	ASD	Yes	Yes	Yes	No	Yes	Yes	Yes	No	Yes	No	No	small	small	Died
5		13	F	ASD	Yes	No	No	Yes	Yes	No	Yes	No	Yes	No	No	N/A	N/A	Alive
6	Medd et al. (18)	0	M	PFO	Yes	Yes	No	No	Yes	No	No	No	Yes	No	No	Small	Normal	Died
7		0	F	PFO	Yes	Yes	No	No	No	No	No	No	Yes	No	No	Small	Normal	Died
8	Enthoven et al. (19)	23	F	PFO	No	Yes	No	No	No	No	No	No	Yes	No	Yes	N/A	N/A	Alive
9	Fay and Lynn (4)	6	F	ASD	No	Yes	Yes	No	No	No	Yes	No	Yes	No	Yes	N/A	N/A	Alive
10	Raghib et al. (20)	0	F	ASD	Yes	Yes	No	Yes	No	No	No	No	Yes	No	No	Small	Normal	Died
11	Davachi et al. (21)	0	F	ASD	Yes	Yes	No	Yes	No	No	Yes	No	Yes	No	No	Small	Normal	Died
12	Okin et al. (6)	0.3	F	ASD	No	Yes	No	No	No	No	No	No	Yes	No	No	N/A	N/A	Alive
13	Becker et al. (22)	0	M	PFO	No	Yes	No	No	No	No	Yes	No	Yes	No	Yes	N/A	Normal	Died
14	Van Der Hauwert and Michaelsson (2)	14	M	ASD	No	Yes	Yes	Yes	No	No	Yes	No	Yes	No	Yes	Normal	N/A	Alive
15		13	F	ASD	No	Yes	Yes	Yes	No	No	Yes	No	Yes	No	Yes	Normal	N/A	Alive
16	Okada et al. (32)	6	M	ASD	No	Yes	Yes	No	No	No	Yes	No	Yes	No	Yes	Normal	Normal	Alive
17	Haneda et al. (34)	6	M	ASD	No	Yes	Yes	No	No	No	Yes	No	Yes	No	Yes	Normal	Normal	Alive
18	Haneda et al. (33)	8	F	ASD	No	Yes	Yes	No	No	No	No	No	Yes	No	Yes	Normal	Small	Alive
19	Haworth et al. (23)	0.5	M	ASD	No	Yes	Yes	No	No	No	No	No	Yes	No	Yes	N/A	N/A	Alive
20		2	F	ASD	No	Yes	Yes	No	No	No	Yes	No	Yes	No	Yes	N/A	N/A	Alive
21		6	M	ASD	No	Yes	Yes	No	No	No	Yes	No	Yes	No	Yes	Small	N/A	Alive
22	Folger (25)	0	M	ASD	No	Yes	No	No	No	No	No	No	Yes	No	No	Small	Normal	Alive
23	Sugiki et al. (35)	2	F	ASD	No	Yes	Yes	No	No	No	Yes	No	No	No	Yes	Normal	Small	Alive
24	Kondo et al. (8)	0	M	ASD	No	Yes	No	No	No	No	No	No	Yes	No	No	Normal	Normal	Alive

(Continued)

TABLE 1 | Continued

#	Reference	Age (years)	Sex	PFO/ ASD	FX of IRVH	Cyanosis	Finger clubbing	Dyspnea	Fatigability	Heart failure	Murmur	Arrhythmia	Angio	Echo	Surgery	TV	PV	Outcome
25		0	M	ASD	No	Yes	No	No	No	No	No	No	Yes	Yes	No	Normal	Normal	Died
26	Satokawa et al. (26)	49	F	ASD	No	Yes	Yes	No	No	No	No	No	No	Yes	Yes	Normal	Normal	Alive
27	Hasegawa et al. (27)	0.06	F	ASD	No	Yes	No	No	No	No	Yes	No	Yes	No	Yes	Small	Normal	Alive
28	Wolf et al. (28)	0	F	PFO	No	Yes	No	No	No	No	Yes	Yes	Yes	Yes	Yes	Small	Normal	Alive
29	Thatai et al. (29)	1.5	M	ASD	No	Yes	Yes	No	No	No	Yes	No	Yes	Yes	Yes	Small	Small	Alive
30	Kobayashi and Arai (36)	0	M	ASD	Yes	Yes	Yes	Yes	No	No	No	No	No	Yes	No	Normal	Normal	Alive
31		0	M	PFO	Yes	Yes	No	No	No	No	No	No	No	Yes	No	Small	Normal	Alive
32	Goh et al. (5)	42	F	ASD	No	Yes	No	Yes	Yes	Yes	No	No	Yes	No	Yes	N/A	N/A	Alive
33	Ota et al. (37)	37	F	ASD	No	Yes	Yes	Yes	Yes	No	No	Yes	Yes	Yes	Yes	Normal	Normal	Alive
34	Joy et al. (30)	1	F	ASD	No	Yes	No	No	No	No	Yes	No	Yes	Yes	Yes	N/A	Normal	Alive
35		2	F	ASD	No	Yes	No	No	No	No	Yes	No	Yes	Yes	Yes	Small	Normal	Alive
36		9	M	ASD	No	Yes	No	No	No	No	Yes	No	Yes	Yes	Yes	Small	Normal	Alive
37		3	F	ASD	No	Yes	No	No	No	No	No	No	No	Yes	No	Small	Normal	Alive
38		0.1	M	ASD	No	Yes	No	No	No	No	No	No	No	Yes	No	Normal	Normal	Alive
39		1.5	F	ASD	No	Yes	No	No	No	No	Yes	No	Yes	Yes	Yes	Small	Normal	Alive
40	Chessa et al. (31)	34	M	ASD	Yes	Yes	No	No	No	No	No	No	Yes	Yes	No	Small	N/A	Alive
41		0	M	ASD	Yes	Yes	Yes	No	No	No	No	No	Yes	Yes	No	Small	Normal	Alive
42	Koriyama et al. (38)	0	M	PFO	No	Yes	No	No	No	No	No	No	No	Yes	No	Small	Small	Alive
43	Kim et al. (39)	6	F	ASD	No	Yes	No	Yes	No	No	No	No	No	Yes	Yes	Small	Normal	Alive
44	Lombardi et al. (40)	0	F	ASD	No	Yes	No	No	No	No	No	No	No	Yes	No	Normal	Normal	Alive
45		0	F	ASD	No	Yes	No	No	No	No	No	No	Yes	Yes	No	Small	Normal	Alive
46		0	M	ASD	No	Yes	No	No	No	No	No	No	No	Yes	No	Small	Normal	Alive
47	Qasim et al. (41)	9	M	No	Yes	No	No	No	No	No	No	No	No	Yes	No	Normal	Normal	Alive
48		9	F	PFO	Yes	No	No	No	No	No	No	Yes	No	Yes	No	Normal	Normal	Alive
49	Khajali et al. (42)	22	F	ASD	No	Yes	Yes	Yes	No	No	Yes	No	Yes	Yes	Yes	Normal	Normal	Alive
50		36	F	ASD	No	Yes	No	Yes	No	No	No	No	Yes	Yes	Yes	Normal	Normal	Alive
51		35	F	PFO	No	Yes	Yes	Yes	No	No	No	No	Yes	Yes	Yes	N/A	N/A	Alive
52		19	M	ASD	No	Yes	Yes	Yes	No	No	No	No	Yes	Yes	Yes	N/A	N/A	Alive
53		28	M	ASD	No	Yes	No	Yes	No	No	No	No	Yes	Yes	No	N/A	N/A	Alive
54		20	F	PFO	No	Yes	No	Yes	No	No	No	No	Yes	Yes	Yes	N/A	N/A	Alive

PFO, patent foramen ovale; ASD, atrial septal defect; FX, family history; IRVH, isolated right ventricular hypoplasia; HF, heart failure; Angio, angiogram; Echo, echocardiogram; TV, tricuspid valve; PV, pulmonary valve; F, female; M, male; and N/A, Not applicable.

TABLE 2 | Clinical characteristics of isolated right ventricular hypoplasia from previous studies.

	Total $n = 54$	**Alive** $n = 45$	**Deceased** $n = 9$	***p*-value**
Age (years)	2.5 (0–15.3)	6 (0.08–16.5)	0 (0–11.1)	0.0455
Sex (male)	25 (46.3%)	19 (42.2%)	6 (66.7%)	0.2748
Family history of IRVH	13 (24.1%)	7 (15.6%)	6 (66.7%)	0.0037
Symptom				
SpO2	80.3 ± 7.1	80.5 ± 7.1	77.5 ± 10.6	0.5579
CyaNosis	50 (92.6%)	42 (93.3%)	8 (88.9%)	0.5289
Finger clubbing	19 (35.2%)	18 (40.0%)	1 (11.1%)	0.1369
Dyspnea	17 (31.5%)	13 (28.9%)	4 (44.4%)	0.4394
Fatigability	6 (11.1%)	3 (6.7%)	3 (33.3%)	0.0512
Heart failure	5 (9.3%)	2 (4.4%)	3 (33.3%)	0.0281
Arrhythmia	3 (5.6%)	17 (37.8%)	4 (44.4%)	0.723
Modalities for diagnosis				
Angiogram	40 (74.0%)	32 (71.1%)	8 (88.9%)	0.4182
RVEDP (mmHg)	10.6 ± 4.8	10.0 ± 4.8	14.3 ± 3.2	0.0361
Echocardiogram	28 (51.9%)	27 (60.0%)	1 (11.1%)	0.0101
TVD Z-score	−2.16 ± 1.53	−2.16 ± 1.53	N/A	
MRI	9 (16.7%)	9 (20.0%)	0 (0%)	0.3280
RVEDVI (ml/m^2)	46.7 ± 14.4	46.7 ± 14.4	N/A	
RVEF (%)	41.9 ± 11.0	41.9 ± 11.0	N/A	
PFO/ASD	53 (98.2%)	44 (93.8%)	9 (100%)	0.1382
Surgery	29 (53.7%)	28 (62.2%)	1 (11.1%)	0.0082
ASD closure	21 (38.9%)	21 (46.7%)	0 (0%)	0.0086
SP shunt	4 (7.4%)	3 (6.7%)	1 (11.1%)	0.5289
Glenn	7 (13.0%)	7 (15.6%)	0 (0%)	0.5861
One and a half repair	2 (3.7%)	2 (4.4%)	0 (0%)	1.0000
Fontan	1 (1.9%)	1 (2.2%)	0 (0%)	1.0000
Death	9 (16.7%)	0 (0%)	9 (100%)	<0.0001

IRVH, isolated right ventricular hypoplasia; SpO2, arterial oxygen saturation; RVEDP, right ventricular end-diastolic pressure on angiogram; TVD Z-score, Z-score of the diameter of the tricuspid valve on echocardiogram; RVEDVI, index of right ventricular end-diastolic volume on cardiac magnetic resonance imaging; RVEF, right ventricular ejection fraction on angiogram; PFO, patent foramen ovale; ASD, atrial septal defect; SP, shunt systemic-to-pulmonary artery shunt; Glenn, Glenn operation; and Fontan, Fontan surgery.

From the systematic review and pooled analysis of the current study, IRVH was frequently observed in those patients diagnosed at <1 year. Thus, IRVH may be thought of as a primary developmental RV anomaly or that it may be due to a reduced tricuspid flow during the fetal stage (18). The resultant restrictive physiology reduces RV inflow *via* a detrimental feedback loop when the tricuspid size and RV compliance are decreased because of RV hypoplasia. In addition, the blood entering the RV is reduced further as the inflow of blood flowing from the right to the left atrium *via* a PFO or an ASD is increased.

Diagnostic tests are crucial to the differential diagnosis of IRVH from other diseases with cyanosis, and the diagnosis and evaluation of the syndrome severity were routinely performed by angiogram, echocardiography, and MRI. Cardiac catheterization can provide precise hemodynamics including RV filling and capacity quantification of the right-to-left shunts *via* ASD or PFO. MRI can provide comprehensive evaluations, and is widely used in the assessment of congenital heart defects. Moreover, MRI provides precise data on ventricular function and volume (43). Although the change of modalities may reflect the historical transition from angiography to echocardiography or MRI, combining multimodalities to assess IRVH hemodynamics and morphology is crucial to diagnose and make therapeutic management.

The surgical option may also vary according to the severity of RV hypoplasia from biventricular repair with ASD closure to univentricular repair with a Glenn operation and one and a half ventricular repair (2, 11, 23, 30, 33, 44). Although cyanosis was found in both the living and deceased patients, heart failure, reflecting on higher RVEDP, was observed more frequently in deceased patients, indicating that ASD closure could be undertaken in patients with mild IRVH. These data suggested that surgical options were limited for deceased patients in whom IRVH was more severe and symptomatic. Thus, right-to-left atrial communication is unnecessary for survival if RV hypoplasia is less severe, and such patients are expected to have a good prognosis. In contrast, the right-to-left atrial communication is necessary for survival if RV hypoplasia is

TABLE 3 | Summary of surgical and medical management of previous studies on patients with isolated right ventricular hypoplasia (from 2000 to 2021).

#	Reference	Age (years)	Sex	PFO/ASD	Symptoms	SpO2 (%)	TVD Z-score	RVEDVI (ml/m^2)	RVEF (%)	RVEDP (mmHg)	Type of surgery	Medical treatment	Outcome
40	Chessa et al. (31)	34	M	ASD	Cyanosis	N/A	N/A	N/A	N/A	N/A	None	None	Alive
41		0	M	ASD	Cyanosis, finger clubbing	N/A	N/A	N/A	N/A	N/A	None	None	Alive
42	Koriyama et al. (38)	0	M	PFO	Cyanosis	70	−4.21	N/A	64	N/A	None	O_2, NO, NTG	Alive
43	Kim et al. (39)	6	F	ASD	Cyanosis, dyspnea	76	−3.5	79	N/A	N/A	ASD closure, then one and half ventricle repair and tricuspid annuloplasty	Diuretics	Alive
44	Lombardi et al. (40)	0	F	ASD	Cyanosis	70	−1.29	N/A	N/A	N/A	None	O_2	Alive
45		0	F	ASD	Cyanosis	88	−2.9	N/A	N/A	N/A	None	Dobutamine, mechanical ventilation	Alive
46		0	M	ASD	Cyanosis	86	−1.1	N/A	N/A	N/A	None	O_2	Alive
47	Qasim et al. (41)	9	M	No	No	N/A	0.77	N/A	N/A	N/A	None	None	Alive
48		9	F	PFO	arrhythmia	N/A	0.04	N/A	N/A	N/A	None	None	Alive
49	Khajali et al. (42)	22	F	ASD	Cyanosis, finger clubbing, dyspnea, murmur	85	N/A	38	45	17	ASD closure	Diuretics	Alive
50		36	F	ASD	Cyanosis, dyspnea	86	N/A	45	35	18	ASD closure, then one and half ventricle repair	None	Alive
51		35	F	PFO	Cyanosis, finger clubbing, dyspnea	78	N/A	41	36	20	Glenn	None	Alive
52		19	M	ASD	Cyanosis, finger clubbing, dyspnea	82	N/A	39	30	12	Glenn and semiclosure of ASD	None	Alive
53		28	M	ASD	Cyanosis, dyspnea	79	N/A	40	42	11	One and half ventricle repair was refused	Diuretics	Alive
54		20	F	PFO	Cyanosis, dyspnea	88	N/A	45	41	10	ASD closure	Diuretics	Alive

PFO, patent foramen ovale; ASD, atrial septal defect; SpO2, arterial oxygen saturation; TVD Z-score, Z-score of the diameter of the tricuspid valve on echocardiogram; RVEDVI, index of the right ventricular end-diastolic volume on cardiac magnetic resonance imaging; RVEF, right ventricular ejection fraction on angiogram; RVEDP, right ventricular end-diastolic pressure on angiogram; Glen, Glenn operation; O_2, Oxygen; NO, nitric oxide; NTG, nitroglycerin; and N/A, Not applicable.

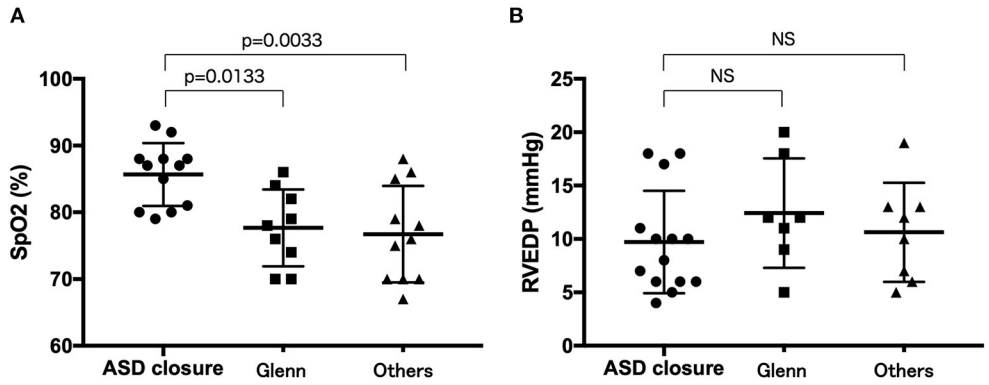

FIGURE 2 | Comparison of arterial oxygen saturation **(A)** and right ventricular end-diastolic pressure **(B)** between the patients who underwent ASD closure, Glenn operation, or one and a half ventricular repair and those who did not underwent surgery. *ASD closure* patients who underwent ASD closure, *Glenn* patients who underwent Glenn operation or one and a half ventricular repair, *others* patients who did not undergo surgery.

TABLE 4 | Univariable and multivariable logistic regression analyses for independent predictors of mortality.

	Univariate			Multivariate		
	Odds ratio	**95% CI**	***p*-value**	**Odds ratio**	**95% CI**	***p*-value**
Male	2.737	0.6373–14.287	0.1778			
Age < 1 y	7.750	1.633–56.660	0.0089	9.962×10^{7}	2.194 –	0.0168
Family history of IRVH	10.857	2.325–62.250	0.0024			
Heart failure	10.75	1.504–95.885	0.0191	6.395×10^{14}	9.273 –	0.0027
RVEDP > 12 mmHg	8.003×10^{7}	3.6275–	0.0029	8.596×10^{13}	5.771 –	0.0027

CI, confidence interval; IRVH, isolated right ventricular hypoplasia; RVEDP, right ventricular end-diastolic pressure on angiogram.

more severe, and such patients are expected to have cyanosis and a poor prognosis, indicating Glenn operation or one and a half ventricular surgery. Thus, arterial oxygen saturation may be a predictive maker for deciding on surgery to assess the cyanosis degree.

Extrapolating from certain congenital heart anomalies with diastolic dysfunction of the right ventricle, such as severe pulmonary stenosis or atresia, certain mild to moderate forms of Ebstein's disease, in which the question arises of the feasibility of closure of the interatrial communication, in this type of pathophysiology of right to left interatrial shunt, a balloon occlusion test would be necessary before closing this communication. Percutaneous closure will follow in favorable cases.

Interestingly, the results of the current study showed that 24.1% of the patients had a family history of IRVH. Several reports have suggested that the mode of IRVH inheritance is an autosomal-dominant pattern (7, 18, 20, 21, 31, 36). Although genetic variants have not been reported, higher IRVH inheritance and positive family history is a risk factor for survival which may indicate that IRVH may be caused by a genetic disorder.

Study Limitations

Quantitative analyses were not performed in this systematic review due to the heterogeneity between studies and the limited amount of data in addition to the IRVH ambiguous definition. Any randomized controlled trials were not included because all the included studies were cohort studies and case series with small sample sizes. Therefore, we conducted a pooled analysis of these case report data to analyze factors related to life expectancy. Numerical data including RV size, tricuspid valve diameter, pulmonary valve diameter, or ASD size, could not be obtained from all the included studies. Therefore, the classification of cardiac phenotypes was subjective. This study considered >70 years, Treatments were developed that improved disease outcomes during the study period, which may have altered the results of the study. Several of the studies were retrospective and thus did no not perform long-term patient follow-up.

CONCLUSION

This systematic review and pooled analysis provided evidence to assess IRVH degree, and evaluate the clinical status and outcome of IRVH. Combining multiple modalities (e.g., cardiac MRI, echocardiography, and angiography) may be important in the diagnosis and treatment of each patient because the IRVH severity varies. However, the IRVH etiology has not yet been elucidated. The registry study we are conducting is ongoing. Further studies are warranted to reveal the IRVH

etiology, including its genetic background and hemodynamic evaluation, which will lead to better IRVH management and treatment.

DATA AVAILABILITY STATEMENT

The original contributions presented in the study are included in the article/**Supplementary Material**, further inquiries can be directed to the corresponding author.

AUTHOR CONTRIBUTIONS

All authors listed have made a substantial, direct, and intellectual contribution to the work and approved it for publication.

FUNDING

KH was supported by grants from The Ministry of Education, Culture, Sports, Science and Technology in Japan (Grant-in-Aid for Scientific Research Nos. 18K07785 and 21K08124).

ACKNOWLEDGMENTS

The authors wish to acknowledge to Hitoshi Moriuchi, Haruna Hirai and Eriko Masuda for their expert technical assistance.

SUPPLEMENTARY MATERIAL

The Supplementary Material for this article can be found online at: https://www.frontiersin.org/articles/10.3389/fped.2022.794053/full#supplementary-material

REFERENCES

1. Cooley RN, Sloan RD, Hanlon CR, Bahnson HT. Angiocardiography in congenital heart disease of cyanotic type. II observations on tricuspid stenosis or atresia with hypoplasia of the right ventricle. *Radiology.* (1950) 54:848–68. doi: 10.1148/54.6.848
2. Van der Hauwaert LG, Michaelsson M. Isolated right ventricular hypoplasia. *Circulation.* (1971) 44:466–74. doi: 10.1161/01.CIR.44.3.466
3. Beitzke A. [Isolated right ventricular hypoplasia]. *Helv Paediatr Acta.* (1978) 33:567–76.
4. Fay JE, Lynn RB. Isolated right ventricular hypoplasia with atrial septal defect. *Can Med Assoc J.* (1963) 88:812–3.
5. Goh K, Sasajima T, Inaba M, Yamamoto H, Kawashima E, Kubo Y. Isolated right ventricular hypoplasia: intraoperative balloon occlusion test. *Ann Thorac Surg.* (1998) 65:551–3. doi: 10.1016/S0003-4975(97)01362-3
6. Okin JT, Vogel JH, Pryor R, Blount SG. Isolated right ventricular hypoplasia. *Am J Cardiol.* (1969) 24:135–40. doi: 10.1016/0002-9149(69)90060-5
7. Sackner MA, Robinson MJ, Jamison WL, Lewis DH. Isolated right ventricular hypoplasia with atrial septal defect or patent foramen ovale. *Circulation.* (1961) 24:1388–402. doi: 10.1161/01.CIR.24.6.1388
8. Kondo O, Ono Y, Arakaki Y, Takahashi O, Kamiya T. [Isolation right ventricular hypoplasia: report of two cases]. *J Cardiol.* (1989) 19:637–46.
9. Bondarev Iu I. Mal'sagov GU, Riumina EN. [Hypoplasia of the right ventricle with interatrial communication through the coronary sinus]. *Kardiologiia.* (1977) 17:76–9.
10. Buendia A, Munoz A, Attie F, Esquivel J, Kuri J, Munoz L, et al. [Isolated hypoplasia of the right ventricle]. *Arch Inst Cardiol Mex.* (1981) 51:471–9.
11. Cabrera A, Lekuona I, Galdeano JM, Lombardero JL, Pastor E, Vazquez C, et al. [Isolated hypoplasia of the right ventricle. study of 3 cases]. *An Esp Pediatr.* (1985) 23:281–6.
12. Branco LM, Goncalves JM, Velho HV, Ferreira MG, Oliveira JA, Agapito AF, et al. [Isolated hypoplasia of the right ventricle–apropos of a case]. *Rev Port Cardiol.* (1989) 8:791–4.
13. Amaral FT, Moreira-Neto FF, Sgarbieri RN, Carvalho SR, Haddad JL. [Congenital isolated hypoplasia of the right ventricle]. *Arq Bras Cardiol.* (1996) 66:277–9.
14. Hirono K, Miyao N, Yoshinaga M, Nishihara E, Yasuda K, Tateno S, et al. A significance of school screening electrocardiogram in the patients with ventricular noncompaction. *Heart Vessels.* (2020) 35:985–95. doi: 10.1007/s00380-020-01571-7
15. Moher D, Liberati A, Tetzlaff J, Altman DG, Group P. Preferred reporting items for systematic reviews and meta-analyses: the PRISMA Statement. *Open Med.* (2009) 6:e1000097. oi: 10.1371/journal.pmed.1000097
16. Cumpston M, Li T, Page MJ, Chandler J, Welch VA, Higgins JP, et al. Updated guidance for trusted systematic reviews: a new edition of the cochrane handbook for systematic reviews of interventions. *Cochrane Database Syst Rev.* (2019) 10:ED000142. doi: 10.1002/14651858.ED000142
17. Gasul BM, Weinberg M, Luan LL, Fell EH, Bicoff J, Steiger Z. Superior vena cava-right main pulmonary artery anastomosis: surgical correction for patients with Ebstein's anomaly and for congenital hypoplastic right ventricle. *J Am Med Assoc.* (1959) 171:1797–803. doi: 10.1001/jama.1959.03010310029008
18. Medd WE, Neufeld HN, Weidman WH, Edwards JE. Isolated hypoplasia of the right ventricle and tricuspid valve in siblings. *Br Heart J.* (1961) 23:25–30. doi: 10.1136/hrt.23.1.25
19. Enthoven R, Dunst R, Benjamin R. Congenital hypoplasia of the right ventricule and tricuspid valve with survival into adult life. *Am J Cardiol.* (1963) 11:5. doi: 10.1016/0002-9149(63)90016-X
20. Raghib G, Amplatz K, Moller JH, Jue KL, Edwards JE. Hypoplasia of right ventricle and of tricuspid valve. *Am Heart J.* (1965) 70:7. doi: 10.1016/0002-8703(65)90337-6
21. Davachi F, McLean RH, Moller JH, Edwards JE. Hypoplasia of the right ventricle and tricuspid valve in siblings. *J Pediatr.* (1967) 71:869–74. doi: 10.1016/S0022-3476(67)80014-3
22. Becker AE, Becker MJ, Moller JH, Edwards JE. Hypoplasia of right ventricle and tricuspid valve in three siblings. *Chest.* (1971) 60:273–7. doi: 10.1378/chest.60.3.273
23. Haworth SG, Shinebourne EA, Miller GA. Right-to-left interatrial shunting with normal right ventricular pressure. A puzzling haemodynamic picture associated with some rare congenital malformations of the right ventricle and tricuspid valve. *Br Heart J.* (1975) 37:386–91. doi: 10.1136/hrt.37.4.386
24. Guerin F, Hazan E, Herreman F, Toussaint M. [Hypoplasia of the right ventricle with inter-atrial communication and without any other abnormality. apropos of a case treated surgically by closure of the inter-atrial communication]. *Arch Mal Coeur Vaiss.* (1977) 70:653–61.
25. Folger GM. Solitary hypoplasia of the right ventricle: a case report. *Angiology.* (1985) 36:646–9. doi: 10.1177/000331978503600909
26. Satokawa H, Iwaya F, Igari T, Hoshino S, Yamaguchi N, Maruyama Y, et al. case of right atrial thrombosis associated with isolated right ventricular hypoplasia. *Fukushima J Med Sci.* (1990) 36:91–5.
27. Hasegawa N, Sekiguchi A, Nagata N, Ookawa Y, Ito K, Miyazawa Y. [A case report: successful direct closure of atrial septal defect in isolated right ventricular hypoplasia]. *Kyobu Geka.* (1992) 45:179–82.
28. De Wolf D, Naeff MS, Losekoot G. Right ventricular hypoplasia: outcome after conservative perinatal management. *Acta Cardiol.* (1994) 49:267–73.
29. Thatai D, Kothari SS, Wasir HS. Right to left shunting in atrial septal defect due to isolated right ventricular hypoplasia. *Indian Heart J.* (1994) 46:177–8.
30. Joy MV, Venugopalan P, Sapru A, Subramanyan R. Isolated hypoplasia of right ventricle with atrial septal defect: a rare form of cyanotic heart disease. *Indian Heart J.* (1999) 51:440–3.

31. Chessa M, Redaelli S, Masszi G, Iascone M, Carminati M. Familial occurrence of isolated right ventricular hypoplasia. *Am J Med Genet.* (2000) 90:356–7. doi: 10.1002/(SICI)1096-8628(20000228)90:5<356::AID-AJMG2>3.0.CO;2-C
32. Okada Y, Horiuchi T, Ishitoya T, Ishizawa H. [Case of isolated right ventricular hypoplasia]. *Kyobu Geka.* (1972) 25:291–3.
33. Haneda K, Akino Y, Sato N, Horiuchi T. [A case report of isolated right ventricular hypoplasia: hemodynamic evaluation of 11 years following ASD closure]. *Nihon Kyobu Geka Gakkai Zasshi.* (1988) 36:2678–81.
34. Haneda K, Yamaki S, Kagawa K, Shibota M, Horiuchi T. Isolated right ventricular hypoplasia. *Shinzo.* (1974) 6:8.
35. Sugiki K, Izumiyama O, Tsukamoto M, Abe T, Komatsu S. [A successful surgical correction of isolated right ventricular hypoplasia with a large atrial septal defect after 3 conservative shunt operations]. *Nihon Kyobu Geka Gakkai Zasshi.* (1985) 33:2128–32.
36. Kobayashi T, Arai K. A familial case of isolated right ventricular hypoplasia; fetal echo cardiographic diagnosis. *Nihon Syoni Junkanki Gakkai Zasshi.* (1994) 10:6.
37. Ota H, Saijo Y, Saitou S, Yoshida A, Ido A, Ishii Y, et al. An adult case of isolated right ventricular hypoplasia. *Shinzo.* (1998) 30:6.
38. Koriyama T, Ehara E, Sugimito H, Ito Y, Shisida N, Miyagi N, et al. Syonika. *Rinsho.* (2000) 53:6.
39. Kim H, Park EA, Lee W, Chung JW, Park JH, Kim GB, et al. Magnetic resonance imaging findings of isolated right ventricular hypoplasia. *Int J Cardiovasc Imaging.* (2012) 28:149–52. doi: 10.1007/s10554-012-0162-x
40. Lombardi M, Tagliente MR, Pirolo T, Massari E, Vairo U. Transient and anatomic isolated right-ventricular hypoplasia. *J Cardiovasc Med.* (2016) 17:e257–63. doi: 10.2459/JCM.0b013e328364dc3b
41. Qasim A, Dasgupta S, Aly AM. Asymptomatic right ventricular hypoplasia in twin siblings: a normal variant or cause of early mortality? *Case Rep Pediatr.* (2019) 2019:6871340. doi: 10.1155/2019/6871340
42. Khajali Z, Arabian M, Aliramezany M. Best management in isolated right ventricular hypoplasia with septal defects in adults. *J Cardiovasc Thorac Res.* (2020) 12:237–43. doi: 10.34172/jcvtr.2020.36
43. Abouzeid CM, Shah T, Johri A, Weinsaft JW, Kim J. Multimodality imaging of the right ventricle. *Curr Treat Options Cardiovasc Med.* (2017) 19:82. doi: 10.1007/s11936-017-0584-9
44. Scicchitano P, Gesualdo M, Cortese F, Acquaviva T, de Cillis E, Bortone AS, et al. Atrial septal defect and patent foramen ovale: early and long-term effects on endothelial function after percutaneous occlusion procedure. *Heart Vessels.* (2019) 34:1499–508. doi: 10.1007/s00380-019-01385-2

Conflict of Interest: The authors declare that the research was conducted in the absence of any commercial or financial relationships that could be construed as a potential conflict of interest.

Publisher's Note: All claims expressed in this article are solely those of the authors and do not necessarily represent those of their affiliated organizations, or those of the publisher, the editors and the reviewers. Any product that may be evaluated in this article, or claim that may be made by its manufacturer, is not guaranteed or endorsed by the publisher.

frontiers | Frontiers in Cardiovascular Medicine

ORIGINAL RESEARCH
published: 27 April 2022
doi: 10.3389/fcvm.2022.883067

Establishment and Validation of a Multivariate Predictive Scoring Model for Intravenous Immunoglobulin-Resistant Kawasaki Disease: A Study of Children From Two Centers in China

Changjian Li[1,2†], Shu Wu[1†], Yuanyuan Shi[3†], Ying Liao[1], Yan Sun[1], Hui Yan[1], Qingyou Zhang[1], Jia Fu[2], Dan Zhou[2], Yong Zhang[2], Hongfang Jin[1]* and Junbao Du[1,4]**

[1] Department of Pediatrics, Peking University First Hospital, Beijing, China, [2] Department of Cardiology, Wuhan Children's Hospital (Wuhan Maternal and Child Healthcare Hospital), Tongji Medical College, Huazhong University of Science and Technology, Wuhan, China, [3] Department of General Medicine, Wuhan Fourth Hospital, Puai Hospital, Tongji Medical College, Huazhong University of Science and Technology, Wuhan, China, [4] Key Laboratory of Molecular Cardiovascular Sciences, The Ministry of Education, Beijing, China

OPEN ACCESS

Edited by:
Ruth Heying,
University Hospital Leuven, Belgium

Reviewed by:
Hiroyuki Wakiguchi,
Yamaguchi University, Japan
Emanuele Monda,
University of Campania Luigi Vanvitelli, Italy
Ping Huang,
Guangzhou Medical University, China

***Correspondence:**
Yong Zhang
zhangyong1@zgwhfe.com
Hongfang Jin
jinhongfang51@126.com
Junbao Du
junbaodu1@126.com

[†] These authors have contributed equally to this work and share first authorship

Specialty section:
This article was submitted to Pediatric Cardiology, a section of the journal Frontiers in Cardiovascular Medicine

Received: 24 February 2022
Accepted: 05 April 2022
Published: 27 April 2022

Citation:
Li C, Wu S, Shi Y, Liao Y, Sun Y, Yan H, Zhang Q, Fu J, Zhou D, Zhang Y, Jin H and Du J (2022) Establishment and Validation of a Multivariate Predictive Scoring Model for Intravenous Immunoglobulin-Resistant Kawasaki Disease: A Study of Children From Two Centers in China. Front. Cardiovasc. Med. 9:883067. doi: 10.3389/fcvm.2022.883067

Background: Early identification of intravenous immunoglobulin (IVIG)-resistant Kawasaki disease (KD) is important for making a suitable therapeutic strategy for children with KD.

Methods: This study included a training set and an external validation set. The training set included 635 children (588 IVIG-sensitive and 47 IVIG-resistant KD) hospitalized in Wuhan Children's Hospital, Hubei, China. Univariate analyses and binary logistic regression equation was incorporated to find the associated variables of the IVIG-resistant KD. A scoring model for predicting IVIG-resistant KD was established according to odds ratio (OR) values and receiver operating characteristic curves. The external validation set consisted of 391 children (358 IVIG-sensitive and 33 IVIG-resistant KD) hospitalized in Peking University First Hospital, Beijing, China. The predictive ability of the model of IVIG-resistant KD were externally validated by the real clinically diagnosed KD cases.

Results: Fifteen variables in the training set were statistically different between IVIG-sensitive and IVIG-resistant KD children, including rash, duration of fever, peripheral blood neutrophil-to-lymphocyte ratio (NLR), prognostic nutritional index (PNI), percentage of monocytes and percentage of eosinophils, and serum alanine aminotransferase, aspartate aminotransferase, total bilirubin (TB), direct bilirubin, glutamyl transpeptidase, prealbumin, sodium ion, potassium ion and high-sensitivity C-reactive protein. According to logistic equation analysis, the final three independent correlates to IVIG-resistant KD were serum TB $\geq$ 12.8 μmol/L, peripheral blood NLR $\geq$ 5.0 and peripheral blood PNI $\leq$ 52.4. According to the OR values, three variables

were assigned the points of 2, 2 and 1, respectively. When the score was ≥ 3 points, the sensitivity to predict IVIG-resistant KD was 80.9% and the specificity was 77.6%. In the validation set, the sensitivity, specificity and accuracy of the predictive model of IVIG-resistant KD were 72.7%, 84.9%, and 83.9%, respectively.

Conclusion: A scoring model was constructed to predict IVIG-resistant KD, which would greatly assist pediatricians in the early prediction of IVIG-resistant KD.

Keywords: Kawasaki disease, intravenous immunoglobulin-resistant, predictive scoring model, binary logistic regression, prognostic nutritional index

INTRODUCTION

Kawasaki disease (KD) is an acute vasculitic disease, the pathogenesis of which has not yet been clear (1). In particular, coronary artery lesion (CAL) is a complication that severely affects the prognosis of KD and is a primary reason for acquired heart defects in some children (2). In severe cases, KD may even be complicated with cardiac tamponade and giant coronary artery aneurysms (3, 4). With the use of intravenous immunoglobulin (IVIG), however, the incidence of CAL has decreased significantly (3, 5). Nevertheless, 10 to 20% of children with KD did not have a satisfactory control of the fever after receiving the initial standard dose of IVIG, and this group of children was called IVIG non-responsive or IVIG-resistant KD (1, 6, 7). Importantly, the pathological process of vasculitis could not be interrupted and relieved in time due to the persistence of a high inflammatory response in IVIG-resistant children, which leads to a significantly higher incidence of CAL in these children on the one hand (8), and increases the cost of hospitalization on the other.

Several studies have shown that the initial IVIG combined with corticosteroids could decrease the occurrence of IVIG resistance and CAL (9, 10). However, some studies reported that corticosteroids could increase the occurrence of CAL (11), and the treatment of corticosteroids as a second-line treatment for KD was highly controversial (12–14). The Italian Society of Pediatrics recently stated that corticosteroids could be used in combination with the initial administration of IVIG in "high-risk" children (15). This provided the possibility of concomitant corticosteroids at the time of initial IVIG in IVIG-resistant children, and therefore, further studies are needed to predict this subset of children with KD who may be resistant to IVIG and thus to evaluate in advance whether to give corticosteroids, which may be essential to improve the prognosis of the children. In fact, there were many predictive measures associated with IVIG non-response, the Japanese Kobayashi score, Egami score and Sato score systems, for instance (16–18).

Currently, a Japanese team used the IVIG-resistance prediction model in clinical and some prospective multicenter clinical control studies (9, 19). However, there was a significant decrease in the sensitivity of the Japanese scoring model across countries and regions (20, 21). There were also some studies on IVIG-resistance prediction models in China (22–26), but some models suffered from low sensitivity and specificity, lack of validation, or relatively small sample size. Thus, it is extremely necessary to establish a scoring model with a strong predictive power based on a training and an external validation design in China.

Therefore, this study was undertaken to explore a useful predictive scoring model of IVIG-resistant KD to help pediatricians in implementing proper assessment and treatment strategy for children with KD.

MATERIALS AND METHODS

Subjects

We screened 1056 patients with KD, of whom 1026 (97.2%) were eligible (**Figure 1**). The study consisted a training set and an external validation set. In the training set, 635 children hospitalized in Wuhan Children's Hospital were included from January 2018 to October 2019. Of whom, 588 children (388 males and 200 females) suffered from IVIG-sensitive KD and another 47 children (30 males and 17 females) suffered from IVIG-resistant KD. Their median ages were 23.0 (12.0, 42.0) months for children with IVIG-sensitive KD and 22.0 (12.0, 39.0) months for those with IVIG-resistant KD, respectively. In addition, 391 patients hospitalized in the Department of Pediatrics, Peking University First Hospital between January 2008 and October 2019 were enrolled in the validation set. Among them, 358 children (226 males and 132 females) were IVIG-sensitive KD and 33 children (26 males and 7 females) were IVIG-resistant KD. Their median ages were 22.0 (12.0, 39.0) months for children with IVIG-sensitive KD, and 34.0 (14.5, 53.0) months for those with IVIG-resistant KD, respectively.

Criteria for the diagnosis of classic KD (CKD): CKD was classified as containing 5 or more of the 6 clinical characteristics; or the existence of 4 clinical characteristics, excluding fever caused by other diseases or rash diseases, presence of coronary artery dilatation. Six of these clinical characteristics were as below: (1) fever; (2) conjunctival congestion; (3) orofacial lesions: red lips, strawberry tongue; (4) rash; (5) peripheral limb changes: redness and swelling of palms and feet in the initial phase, and peeling of skin at the ends of limbs in the recovery phase; and (6) non-suppurative cervical lymphadenitis (27, 28).

Criteria for the diagnosis of incomplete KD (IKD): IKD was characterized by the existence of 3 of the 6 clinical characteristics and combined with CAL; or only 3 or 4 major clinical characteristics without CAL, but with one of the "other important clinical features". Other important clinical features

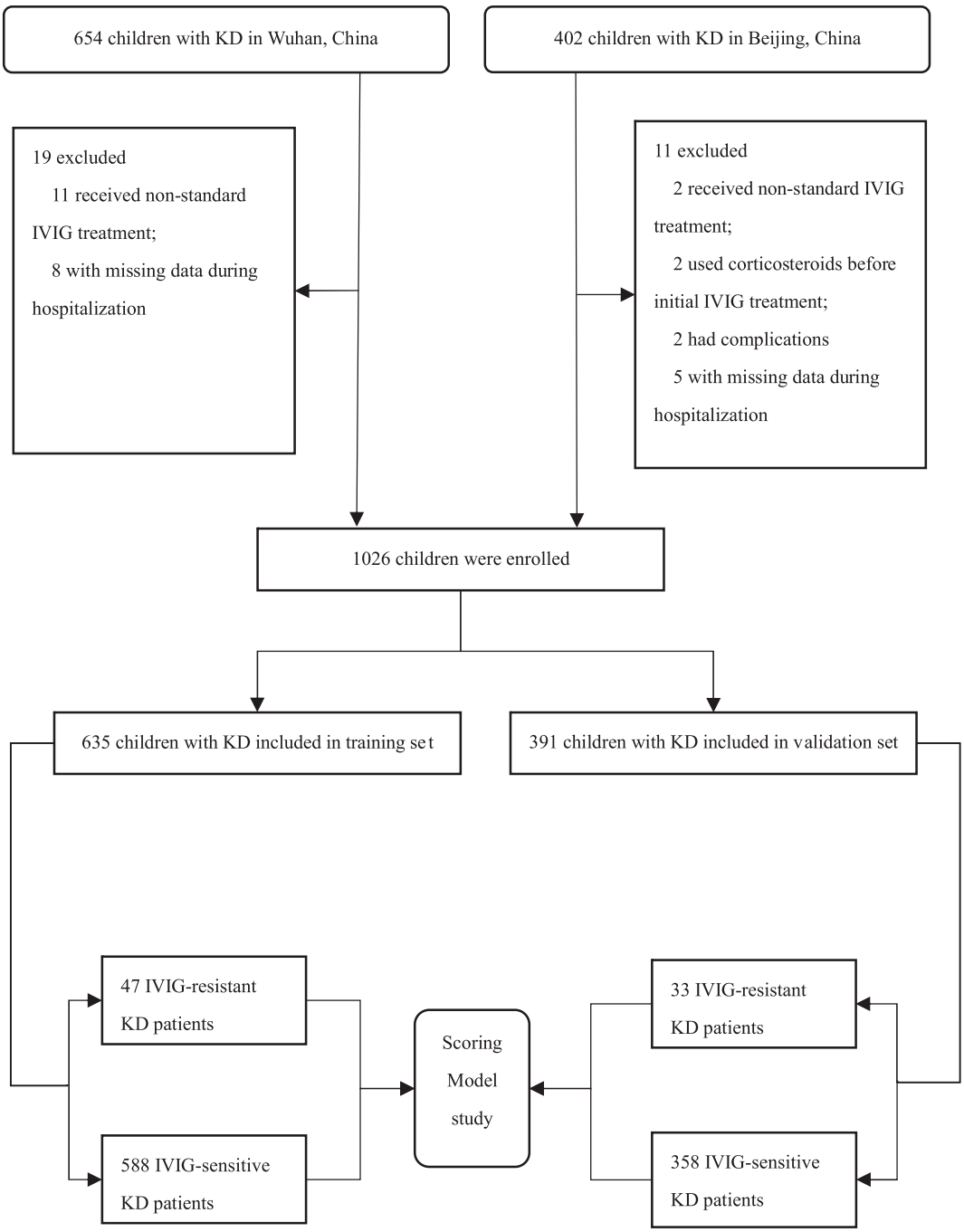

FIGURE 1 | Flow chart of study subject inclusion. IVIG, intravenous immunoglobulin; KD, Kawasaki disease.

were referred to the diagnostic guidelines in the United States and Japan (1, 27, 28).

Criteria for diagnosis of IVIG-resistant KD: IVIG-resistant KD was defined according to the KD diagnostic criteria and having fever or re-fever after 36 h of initial IVIG treatment (1, 27, 29).

Inclusion criteria: children hospitalized with CKD or IKD had their blood routine examination and biochemistry indicator tests completed within 2 days prior to treatment with IVIG; IVIG and aspirin were routinely administered in accordance with guideline criteria (1).

Exclusion criteria: children received non-standard IVIG treatment; use of corticosteroids or other immunosuppressive drugs before the initial IVIG treatment; use of corticosteroids or other immunosuppressive drugs at the same time as the initial IVIG treatment; presence of other serious complications such as

macrophage activation syndrome, shock, severe infection, septic lesions, multi-organ dysfunction, hemophagocytic syndrome, etc.; and some clinical data missing during hospitalization.

Data Collection

The medical records of the study subjects were obtained from the electronic case system (Donghua, Beijing, China and Kaihua, Beijing, China). The information included the demographic data, clinical characteristics and the laboratory results. The demographic data included hospitalization date, hospitalization number, sex, age and body mass index (BMI). Clinical features included CKD symptoms (duration of fever before initial IVIG, conjunctival congestion, red lips/strawberry tongue, enlarged lymph nodes, rash, stiff hands and feet), frequency and dose of IVIG, presence of complications (macrophage activation syndrome, shock, severe infections, combined septic lesions, multi-organ dysfunction, hemophagocytic syndrome) and other underlying diseases (malnutrition, flat blood, liver disease, other autoimmune diseases, etc.). Laboratory test results included routine blood test results, biochemical indicators (liver function, cardiac enzymes and electrolytes), infection indicators (high-sensitivity C-reactive protein, hsCRP), and cardiac ultrasound (marking coronary artery diameter and *Z*-value) at the acute stage of KD (usually no more than 10 days). The above medical records were recorded by a dedicated staff and carefully proofread by another professional.

The study was approved by the Ethics Committee of Wuhan Children's Hospital (2022R007–E01) and Peking University First Hospital (2020–108), and a waiver of the informed consent was granted.

Treatment Protocol

Immediately after the initial diagnosis of CKD or IKD was established, all patients were given standard treatment for KD, including IVIG (2 g/kg) and oral aspirin (30–50 mg/kg/day) in 3 divided doses (1, 30). A downward adjustment of the aspirin to a low dose of 3–5 mg/kg/day after 48 to 72 h of fever resolution in children was done and maintained for 6–8 weeks in the absence of CAL. For children who developed CAL, aspirin was discontinued until the CAL recovered (1).

Laboratory Tests

Blood routine examination, biochemical indicators and hsCRP were performed as follows. At the child's first admission to the hospital prior to the initial use of IVIG, 2.0 mL of venous blood was obtained with an EDTA–K2 anticoagulated vacuum collection tube and mixed upside down and sent to the laboratory for testing. A fully automated hematology analyzer XN–3000 (Sysmex, Kobe, Japan) and BC–6800 plus (Mindray, Shenzhen, China) was used to measure blood routine examination. At the same time, 2.0 mL of venous blood was collected and centrifuged using a BY–600A centrifuge (Baiyang, Beijing, China) at 3300 *g* for 5 min. The non-hemolyzed serum was obtained, generally using a Cobas–8000 automatic biochemical analyzer (Roche, Mannheim, Germany) for biochemical parameters and a BNII auto-analyzer system (Siemens, Erlangen, Germany) for hsCRP. All specimens were tested on the machine within 2 h in the laboratory department, and the results were verified by a dedicated staff in the laboratory. Then, the blood routine, liver function, electrolytes, cardiac enzymes and hsCRP were uploaded to the electronic medical record system. Our fully automated testers were regularly calibrated and accuracy tested with coefficients of variation within normal limits. In particular, prognostic nutritional index (PNI) = albumin (ALB, g/L) + 5 × absolute value of lymphocytes ($\times 10^9$/L) (31) and neutrophil-to-lymphocyte ratio (NLR) = neutrophils ($\times 10^9$/L)/lymphocytes ($\times 10^9$/L).

Statistical Method

We used SPSS 23.0 (IBM, New York, NY, United States) for the data analysis. If the data of continuous variables in both the IVIG-sensitive and IVIG-resistant groups obeyed a normal distribution (Shapiro–Wilk test), the difference was compared by *t*-test, otherwise by the Mann–Whitney *U* test. The chi-square test was performed to compare the difference in dichotomous variables. Variables with statistical differences between groups were added to the multifactorial analysis ($P < 0.05$). Covariance diagnosis was performed and covariates were excluded before entering the multifactorial analysis. And continuous variables were transformed into dichotomous variables for an easy use. Finally, the above statistically different dichotomous variables were included into a binary logistic regression equation, and independent associated factors were obtained by stepwise regression using the backward conditional method. $P > 0.05$ for the Hosmer-Lemeshow test suggested a good fit of the equation. And finally, a predictive scoring model was established by assigning the scores by the odds ratio (OR) values of each independent risk factor, and the total points of the assignment were summarized for each child. The receiver operating characteristic (ROC) curve was performed to calculate the maximum Youden index corresponding to the cutoff value, sensitivity and specificity of the total score. Finally, in external validation set, scores were computed separately for each child, and a four-grid table was constructed based on the true clinical diagnosis and the cutoff value of the predictive scoring model to validate the sensitivity, specificity and accuracy of the model. Statistical differences were set at $P < 0.05$.

RESULTS

Demographic Features and Clinical Manifestations Between Intravenous Immunoglobulin-Sensitive and Intravenous Immunoglobulin-Resistant Kawasaki Disease Children in Training Set

In the training set, no statistical differences were found in gender, age, height, weight, and BMI between IVIG-sensitive and IVIG-resistant KD children ($P > 0.05$). The clinical manifestations of KD in training set mainly included the duration of fever before initial IVIG, conjunctival congestion, red lips/strawberry tongue, enlarged lymph nodes, rash, and stiffness of hands and feet. The

TABLE 1 | Demographic features and clinical manifestations between IVIG-sensitive and IVIG-resistant KD children in the training set.

Items	IVIG-sensitive KD	IVIG-resistant KD	Z/x^2	*P*-value
Patients (n)	588	47		
Gender (M/F)	388/200	30/17	0.090	0.764
Age (month)	23 (12–42)	22 (12–39)	−0.340	0.734
Height (cm)	87.0 (75.0–100.0)	82.0 (78.0–97.0)	−0.476	0.634
Weight (kg)	12.0 (10.0–15.0)	11.5 (9.5–14.5)	−0.730	0.466
BMI (kg/m^2)	16.0 (14.8–17.5)	15.8 (14.8–18.0)	−0.362	0.717
Fever before IVIG (day)	6 (5–7)	5 (5–6)	−3.738	<0.001
Conjunctivitis (Yes/No)	501/87	39/8	0.169	0.681
Oral changes (Yes/No)	526/62	44/3	0.820	0.365
Cervical lymphadenopathy (Yes/No)	339/249	21/26	0.097	0.755
Palm edema (Yes/No)	335/253	32/15	2.203	0.138
Rash (Yes/No)	420/168	41/6	5.465	0.019
CAL (Yes/No)	543/45	44/3	0.100	0.751
CKD (Yes/No)	332/256	32/15	2.403	0.121

IVIG, intravenous immunoglobulin; KD, Kawasaki disease; M/F, male/female; BMI, body mass index; CAL, coronary artery lesions; CKD, classic Kawasaki disease.

median days of fever before the initial IVIG were shorter in the IVIG-resistant group than the IVIG-sensitive group (5 days vs. 6 days, $P < 0.001$), and the incidence of generalized rash was higher (87.2% vs. 71.4%, $P < 0.05$) in the IVIG-resistant group than the IVIG-sensitive group. The conjunctival congestion, redness of lips and tongue, enlarged lymph nodes, and stiffness of hands and feet in children between the two groups did not differ statistically ($P > 0.05$, **Table 1**).

Laboratory Results Between Intravenous Immunoglobulin-Sensitive and Intravenous Immunoglobulin-Resistant Kawasaki Disease Children in Training Set

In the peripheral blood routine analysis, children with or without IVIG-resistant KD showed significant differences in the following indicators. The IVIG-resistant KD group had significantly lower peripheral blood monocyte (MO)% (3.70% vs. 5.90%, $P < 0.001$), eosinophil (EO)% (0.70% vs. 1.80%, $P < 0.01$) and PNI (46.5 vs. 54.8, $P < 0.001$) than the IVIG-sensitive KD group. In contrast, the IVIG-resistant KD group showed significantly larger peripheral blood NLR (6.4 vs. 4.4, $P < 0.001$) and higher hsCRP (105.0 mg/L vs. 68.2 mg/L, $P < 0.001$) than the IVIG-sensitive KD group. No significant differences were found in total peripheral blood white blood cell, hematocrit, mean corpuscular hemoglobin and hemoglobin ($P > 0.05$). In terms of biochemical parameters, the IVIG-resistant children showed much higher serum alanine aminotransferase (ALT) (59 U/L vs. 22 U/L, $P < 0.001$), aspartate aminotransferase (AST) (42 U/L vs. 29 U/L, $P < 0.01$), total bilirubin (TB) (15.2 μmol/L vs. 7.8 μmol/L, $P < 0.001$), direct bilirubin (DB) (7.2 μmol/L vs. 2.7 μmol/L, $P < 0.001$) and glutamyl transpeptidase (GGT) (106 U/L vs. 27 U/L, $P < 0.001$) than the IVIG-sensitive KD children did. In contrast, the IVIG-resistant KD children showed lower serum prealbumin (PAB) (51.6 g/L vs. 66.6 g/L, $P < 0.05$), sodium ion (Na) (137.1 mmol/L vs. 138.7 mmol/L, $P < 0.01$) and potassium ion (K) (4.3 mmol/L vs. 4.5 mmol/L, $P < 0.05$) than the IVIG-sensitive children. And there was no statistical difference in serum cardiac enzymes (lactate dehydrogenase and creatine kinase-MB) and ALB between the two groups ($P > 0.05$, **Table 2**).

Conversion of Continuous Variables to Dichotomous Variables in the Training Set

Before performing regression analysis, covariance diagnosis was first performed. Among the 15 variables (rash, duration of fever before IVIG, peripheral blood NLR, PNI, M%, E%, serum ALT, AST, TB, DB, GGT, PAB, Na, K, and hsCRP) which significantly differed between the IVIG-resistant and IVIG-sensitive KD groups as demonstrated by univariate analysis, serum TB and DB had significant covariance and thus the serum DB was deleted based on the frequency of clinical use. Of the remaining 14 variables, all 13 were continuous numerical variables, except for rash which was a categorical variable. For the convenience of the clinical use, the continuous variables were transformed into dichotomous variables based on the cutoff values obtained from the ROC curves. The results were illustrated in **Table 3**.

Constructing Predictive Scoring Model in the Training Set

The aforementioned 14 variables were incorporated into the binary logistic regression equation, and the backward conditional stepwise regression finally yielded three variables (serum TB, and peripheral blood NLR and PNI) as associated indicators to IVIG sensitivity. The OR (95% CI) values for diagnosing IVIG-resistant KD at serum TB $\geq$ 12.8 μmol/L were 4.273 (2.149, 8.323), peripheral blood NLR $\geq$ 5.0 for diagnosing IVIG-resistant KD were 4.761 (2.287, 9.913), and peripheral blood PNI $\leq$ 52.4 for diagnosing IVIG-resistant KD were 2.478 (1.081, 5.682).

With the reference to the abovementioned OR values, we defined 2 points for serum TB $\geq$ 12.8 μmol/L and 0 point for TB < 12.8 μmol/L, 2 points for peripheral blood NLR $\geq$ 5.0 and 0

TABLE 2 | Blood indicators between IVIG-sensitive and IVIG-resistant KD children in the training set.

Variable(s)	IVIG-sensitive KD	IVIG-resistant KD	Z/x^2	*P*-value
Peripheral blood WBC ($\times 10^9$/L)	13.38 (10.27–17.52)	14.15 (10.35–21.63)	−1.450	0.147
Peripheral blood NLR	4.4 (2.8–6.9)	6.4 (3.9–11.2)	−7.029	<0.001
Peripheral blood MO (%)	5.90 (4.40–8.30)	3.70 (2.60–6.00)	−4.857	<0.001
Peripheral blood EO (%)	1.80 (0.70–3.70)	0.70 (0.20–2.00)	−3.319	0.001
Peripheral blood HCT (%)	33.6 (31.1–35.9)	33.5 (31.5–35.8)	−0.139	0.890
Peripheral blood MCH (pg)	26.4 (25.3–27.3)	26.9 (25.8–27.7)	−1.863	0.062
Peripheral blood Hb (g/L)	106.0 (99.0–114.0)	104.0 (99.0–114.0)	−0.383	0.702
Serum hsCRP (mg/L)	68.2 (37.3–112.0)	105.0 (68.4–168.0)	−3.975	<0.001
Peripheral blood PNI	54.8 (48.5–61.2)	46.5 (40.6–52.0)	−5.687	<0.001
Serum ALT (U/L)	22 (12–54)	59 (22–189)	−4.188	<0.001
Serum AST (U/L)	29 (22–43)	42 (23–82)	−2.841	0.004
Serum ALB (g/L)	38.3 (35.8–41.0)	37.1 (34.0–40.8)	−1.758	0.079
Serum PAB (g/L)	66.6 (47.4–89.2)	51.6 (34.6–81.0)	−2.572	0.010
Serum TB (μmol/L)	7.8 (5.8–11.0)	15.2 (7.9–39.6)	−5.543	<0.001
Serum DB (μmol/L)	2.7 (2.0–4.4)	7.2 (3.1–27.0)	−5.684	<0.001
Serum GGT (U/L)	27 (12–97)	106 (18–194)	−4.061	<0.001
Serum Na (mmol/L)	138.7 (136.8–140.3)	137.1 (134.7–138.8)	−4.154	<0.001
Serum K (mmol/L)	4.5 (4.0–4.9)	4.3 (3.8–4.7)	−2.076	0.038
Serum LDH (U/L)	287 (242–350)	323 (251–416)	−1.767	0.077
Serum CK-MB (U/L)	26 (20–37)	28 (21–38)	−0.644	0.520

IVIG, intravenous immunoglobulin; KD, Kawasaki disease; WBC, white blood cell; NLR, neutrophil-to-lymphocyte ratio; MO, monocyte; EO, eosinophil; HCT, hematocrit; MCH, mean corpuscular hemoglobin; Hb, hemoglobin; hsCRP, high sensitivity C-reactive protein; PNI, prognostic nutritional index; ALT, alanine aminotransferase; AST, aspartate aminotransferase; ALB, albumin; PAB, prealbumin; TB, total bilirubin; DB, direct bilirubin; GGT, glutamyl transpeptidase; Na, sodium ion; K, potassium ion; LDH, lactate dehydrogenase; CK-MB, creatine kinase-MB.

TABLE 3 | The cutoff value of converting continuous variables to dichotomous variables in training set.

Cutoff value	AUC	*P*-value	Sensitivity	Specificity
Fever before IVIG ≤ 5 d	0.658	<0.001	0.660	0.597
Peripheral blood MO% ≤ 4.65%	0.713	<0.001	0.638	0.704
Peripheral blood EO% ≤ 0.55%	0.645	0.001	0.468	0.781
Serum hsCRP ≥ 65.8 mg/L	0.674	<0.001	0.787	0.491
Serum ALT ≥ 37.5 U/L	0.683	<0.001	0.702	0.663
Serum AST ≥ 37.5 U/L	0.624	0.005	0.596	0.679
Serum TB ≥ 12.8 μmol/L	0.743	<0.001	0.617	0.827
Serum GGT ≥ 80 U/L	0.678	<0.001	0.638	0.728
Serum Na ≤ 137.7 mmol/L	0.682	<0.001	0.638	0.646
Serum K ≤ 4.15 mmol/L	0.591	0.038	0.489	0.701
Peripheral blood NLR ≥ 5.0	0.808	< 0.001	0.702	0.813
Peripheral blood PNI ≤ 52.4	0.749	<0.001	0.809	0.592

AUC, area under curve; IVIG, intravenous immunoglobulin; KD, Kawasaki disease; MO, monocyte; EO, eosinophil; hsCRP, high sensitivity C-reactive protein; ALT, alanine aminotransferase; AST, aspartate aminotransferase; TB, total bilirubin; GGT, glutamyl transpeptidase; Na, sodium ion; K, potassium ion; NLR, neutrophil-to-lymphocyte ratio; PNI, prognostic nutritional index.

point for NLR < 5.0, and 1 point for peripheral blood PNI ≤ 52.4 and 0 point for PNI > 52.4. The constructed predictive scoring model contained the above three indicators, with a total score of 0 to 5 points for each patient. The total score was calculated for each child, and then the ROC curve revealed a cutoff value of three points with an AUC (95% CI) of 0.850 (0.798, 0.901, $P < 0.001$). When the score was ≥3 points, the sensitivity of this scoring model was 80.9% and the specificity was 77.6% in predicting IVIG-resistant KD (**Figure 2** and **Table 4**).

Validation of Scoring Model by Real Clinical Diagnosis in External Validation Set

To validate applicability of our scoring model, we calculated the points for each child in the validation set, and constructed a four-grid table (**Table 5**) based on the actual clinical diagnosis and the points of the predictive scoring model. The predicted diagnosis by the scoring prediction model was then compared with the actual clinical diagnosis of the patient, and the sensitivity, specificity, and accuracy of the predictive scoring model for identifying IVIG-resistant KD were 72.7%, 84.9%, and 83.9%, respectively. We also validated the scoring model for predicting IVIG therapeutic response in CKD and IKD cases separately in the validation set. We found that the sensitivity and specificity of this scoring model to predict the IVIG-resistant KD were 73.3% and 83.9% in CKD patients, respectively; while in IKD cases, the sensitivity and specificity were 66.7% and 88.2%, respectively.

DISCUSSION

In our training and validation studies in the central (Wuhan) and northern (Beijing) areas of China, we developed a predictive scoring model for the early IVIG-resistant KD prediction. The predictive scoring model consisted of three variables, serum TB and peripheral blood NLR and PNI. Among them, serum

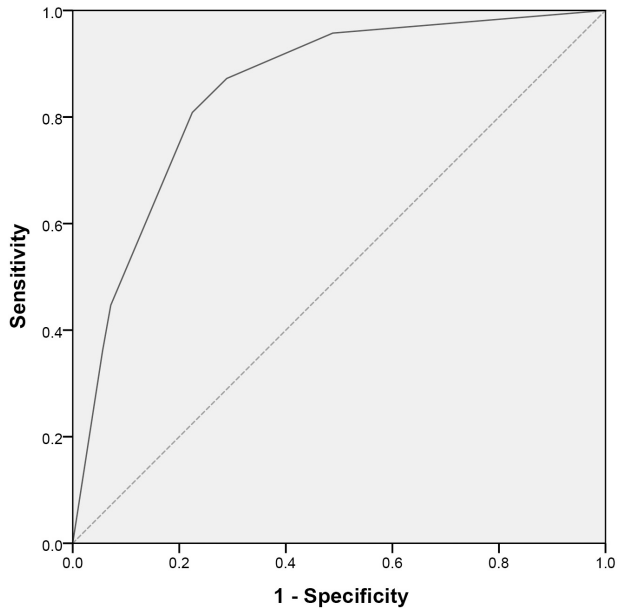

FIGURE 2 | ROC curve for scoring model between IVIG-resistant and IVIG-sensitive KD children. The X and Y axes of the curve represent the predicted false positive rate (1-specificity) and sensitivity, respectively. The dashed line indicates equal true and false positive rates, meaning no predictive value. The solid line is the ROC curve to predict IVIG-resistant KD. A region formed by the ROC curve and the X-axis is called the AUC and its value is 0.850 (95% CI: 0.798–0.901; $P < 0.001$). ROC, receiver operating characteristic; IVIG, intravenous immunoglobulin; KD, Kawasaki disease; AUC, area under the curve; CI, confidence interval.

TABLE 4 | Coefficients of binary logistic regression in training set.

Variable(s)	*P*-value	Odds ratio (95% CI)	Point
Serum TB ≥ 12.8 μmol/L	<0.001	4.273 (2.149, 8.323)	2
Peripheral blood NLR ≥ 5.0	<0.001	4.761 (2.287, 9.913)	2
Peripheral blood PNI ≤ 52.4	0.032	2.478 (1.081, 5.682)	1

CI, Confidence Interval; TB, total bilirubin; NLR, neutrophil-to-lymphocyte ratio; PNI, prognostic nutritional index.

TABLE 5 | Validation of the scoring model.

Score (point)	Clinical diagnosis		Total
	IVIG-resistant KD	IVIG-sensitive KD	
≥3	24	54	78
<3	9	304	313
Total	33	358	391

IVIG, intravenous immunoglobulin; KD, Kawasaki disease.

TB ≥ 12.8 μmol/L was scored by 2 points, peripheral blood NLR ≥ 5.0 scored 2 points and peripheral blood PNI ≤ 52.4 scored 1 point, with the total score being 5 points. The sensitivity of the prediction of IVIG-resistant KD was 80.9% and the specificity was 77.6% when a child had a total score of ≥3 points, which was externally validated at different area of China.

Serum TB was scored 2 points in the predictive scoring model and was shown to be an independent predictor. The higher level of TB in the IVIG-resistant KD group was also consistent with previous studies (25). However, the mechanisms by which serum TB was significantly increased in IVIG-resistant KD children have been unclear (32). IVIG-resistant KD has a severe immune-mediated inflammation of the blood vessels, which resulted in multiple organ damage including the liver function injury (33). We showed that serum ALT was more significantly elevated in IVIG-resistant KD than that of IVIG-sensitive KD children ($P < 0.001$), suggesting that IVIG-resistant KD children had severer liver function injury than those with IVIG-sensitive KD.

The peripheral blood NLR score was 2 points in the predictive scoring model. In clinical practice, some children with KD presented with a markedly elevated neutrophils and a decreased lymphocytes in number, and thereby a markedly elevated peripheral blood NLR. In the study, we revealed that children with IVIG-resistant KD had significantly higher peripheral blood NLR than those with IVIG-sensitive KD (6.4 vs. 4.4, $P < 0.001$). Peripheral blood routine indicators such as leukocytes, neutrophils and lymphocytes fluctuate in response to various factors such as inflammation and single indicators are highly variable and non-specific. However, the ratios of the above indicators could better reflect to some extent the inflammatory response (21). IVIG-resistant KD patients had a severe vascular inflammation compared to the IVIG-sensitive KD ones (18). In the study, we revealed that the peripheral blood NLR was an important variable in predicting IVIG resistance.

PNI was an index for nutritional assessment and risk prediction established by Japanese scholars Onodera et al. and was initially applied to the assessment after gastric and intestinal surgery (31). PNI also reflects the inflammatory condition of the body to some extent (34). Moreover, it has also been shown that low pre-treatment PNI levels (PNI < 55) can be used as an adjunctive predictor of CAL (35). In this scoring model, peripheral blood PNI was scored 1 point, where peripheral blood PNI consisted of two indicators, namely serum ALB and peripheral blood lymphocytes. It has been noted that low ALB levels were used in predicting IVIG-resistant KD (36). Another component of PNI is lymphocytes, a simple parameter that reflects the body's immune response and studies have shown significantly lower lymphocyte counts in IVIG-resistant KD patients (37, 38). However, the absolute lymphocyte value itself is influenced by the total number of leukocytes. Therefore, peripheral blood PNI would be useful to predict IVIG-resistant KD.

Our study successfully constructed a useful scoring model to predict IVIG-resistant KD patients consisting of three indicators: serum TB, peripheral blood NLR and PNI. This predictive scoring model is simple and easy to use and inexpensive. Whether a predictive scoring model can be externally validated in other medical institution is an important factor for the evaluation. The Japanese Egami or Kobayashi scoring model was the currently accepted scoring model with high sensitivity and applicability in Japanese children (16, 17). However, Song et al. found that the predictive sensitivity for IVIG-resistant KD patients

were unsatisfactory when the above two scoring models were used in children in Beijing, China (39). While, the predictive scoring model set up in the present study exhibited a high sensitivity and specificity in the validation set in another city in China, suggesting that our scoring model might have a good generalizability.

However, the present study also had some limitations. As a retrospective study, it would have a selective bias of the subjects. Therefore, a prospective randomized and controlled study is needed in the future to assist in predicting early optimization in children with IVIG-resistant KD.

CONCLUSION

Early identification and prediction of IVIG-resistant KD patients are extremely necessary in clinical pediatrics. In this study, we successfully constructed a helpful easy-to-perform and inexpensive predictive scoring model in different centers with a satisfactory predictive ability for IVIG-resistant KD cases. This model would be useful in assisting pediatricians in predicting the IVIG-resistant KD patients so as to provide reasonable therapeutic strategy for KD in children.

DATA AVAILABILITY STATEMENT

The raw data supporting the conclusions of this article will be made available by the authors, without undue reservation.

ETHICS STATEMENT

The studies involving human participants were reviewed and approved by the Ethics Committee of Wuhan Children's Hospital and Peking University First Hospital. Written informed consent from the participants' legal guardian/next of kin was not required to participate in this study in accordance with the national legislation and the institutional requirements.

AUTHOR CONTRIBUTIONS

JD, HJ, and YZ conceived and designed the project and directed the revision of the manuscript. CL, SW, YL, YS, JF, and DZ acquired the data. YYS, HY, and QZ directed the statistical methods, analyzed and interpreted the data. All authors wrote the manuscript, critically reviewed the manuscript, and approved the final version, access to the primary data and were responsible for the accuracy and completeness of the results.

FUNDING

The study was supported by the Key Project of Capital Clinical Characteristic Application Research (Z181100001718189) and Special Fund for Youth Clinical Research of Peking University First Hospital (2019CR20).

REFERENCES

1. McCrindle BW, Rowley AH, Newburger JW, Burns JC, Bolger AF, Gewitz M, et al. Diagnosis, treatment, and long-term management of Kawasaki disease: a scientific statement for health professionals from the American heart association. *Circulation.* (2017) 135:e927. doi: 10.1161/CIR.0000000000000484
2. Gordon JB, Kahn AM, Burns JC. When children with Kawasaki disease grow up: myocardial complications in adulthood. *J Am Coll Cardiol.* (2009) 54:1911–20. doi: 10.1016/j.jacc.2009.04.102
3. Vergara A, Monda E, Mautone C, Renon F, Di Masi A, Giordano M, et al. Rare case of Kawasaki disease with cardiac tamponade and giant coronary artery aneurysms. *Cardiol Young.* (2021) 31:865–6. doi: 10.1017/S1047951120004989
4. Shimahara Y, Fukushima S, Tadokoro N, Tsuda E, Hoashi T, Kitamura S, et al. Bilateral internal thoracic artery grafting in children under 5 years of age with Kawasaki disease: a case series. *Eur Heart J Case Rep.* (2020) 4:1–7. doi: 10.1093/ehjcr/ytaa390
5. Furusho K, Sato K, Soeda T, Matsumoto H, Okabe T, Hirota T, et al. High-dose intravenous gammaglobulin for Kawasaki disease. *Lancet.* (1983) 322:1359. doi: 10.1016/s0140-6736(83)91109-1
6. Ogawa S, Ayusawa M, Fukazawa R, Hamaoka K, Sonobe T. Guidelines for diagnosis and management of cardiovascular sequelae in Kawasaki disease (JCS 2013) – digest version. *Circ J.* (2014) 78:2521–62. doi: 10.1253/circj.cj-66-0096
7. Makino N, Nakamura Y, Yashiro M, Ae R, Tsuboi S, Aoyama Y, et al. Descriptive epidemiology of Kawasaki disease in Japan, 2011 – 2012; from the results of the 22nd nationwide survey. *J Epidemiol.* (2015) 25:239–45. doi: 10.2188/jea.JE20140089
8. Galeotti C, Kaveri SV, Cimaz R, Koné-Paut I, Bayry J. Predisposing factors, pathogenesis and therapeutic intervention of Kawasaki disease. *Drug Discov Today.* (2016) 21:1850–7. doi: 10.1016/j.drudis.2016.08.004
9. Miyata K, Kaneko T, Morikawa Y, Sakakibara H, Matsushima T, Misawa M, et al. Efficacy and safety of intravenous immunoglobulin plus prednisolone therapy in patients with Kawasaki disease (Post RAISE): a multicenter, prospective cohort study. *Lancet Child Adolesc Health.* (2018) 2:855–62. doi: 10.1016/S2352-4642(18)30293-1
10. Kobayashi T, Saji T, Otani T, Takeuchi K, Nakamura T, Arakawa H, et al. Efficacy of immunoglobulin plus prednisolone for prevention of coronary artery abnormalities in severe Kawasaki disease (RAISE study): a randomised, open-label, blinded-endpoints trial. *Lancet.* (2012) 379:1613–20. doi: 10.1016/S0140-6736(11)61930-2
11. Kato H, Koike S, Yokoyama T. Kawasaki disease: effect of treatment on coronary artery involvement. *Pediatrics.* (1979) 63:175–9. doi: 10.1203/00006450-197912000-00017
12. Sundel RP, Baker AL, Fulton DR, Newburger JW. Corticosteroids in the initial treatment of Kawasaki disease: report of a randomized trial. *J Pediatr.* (2003) 142:611–6. doi: 10.1067/mpd.2003.191
13. Newburger JW, Sleeper LA, McCrindle BW, Minich LL, Gersony W, Vetter VL, et al. Randomized trial of pulsed corticosteroid therapy for primary treatment of Kawasaki disease. *N Engl J Med.* (2007) 356:663–75. doi: 10.1056/NEJMoa061235
14. Ogata S, Ogihara Y, Honda T, Kon S, Akiyama K, Ishii M. Corticosteroid pulse combination therapy for refractory Kawasaki disease: a randomized trial. *Pediatrics.* (2012) 129:e17–23. doi: 10.1542/peds.2011-0148
15. Marchesi A, Rigante D, Cimaz R, Ravelli A, Tarissi de Jacobis I, Rimini A, et al. Revised recommendations of the Italian Society of Pediatrics about the general management of Kawasaki disease. *Ital J Pediatr.* (2021) 47:16. doi: 10.1186/s13052-021-00962-4
16. Kobayashi T, Inoue Y, Takeuchi K, Okada Y, Tamura K, Tomomasa T, et al. Prediction of intravenous immunoglobulin unresponsiveness in patients with Kawasaki disease. *Circulation.* (2006) 113:2606–12. doi: 10.1161/CIRCULATIONAHA.105.592865

17. Egami K, Muta H, Ishii M, Suda K, Sugahara Y, Iemura M, et al. Prediction of resistance to intravenous immunoglobulin treatment in patients with Kawasaki disease. *J Pediatr.* (2006) 149:237–40. doi: 10.1016/j.jpeds.2006.03.050
18. Sato S, Kawashima H, Kashiwagi Y, Hoshika A. Inflammatory cytokines as predictors of resistance to intravenous immunoglobulin therapy in Kawasaki disease patients. *Int J Rheum Dis.* (2013) 16:168–72. doi: 10.1111/1756-185X.12082
19. Hamada H, Suzuki H, Onouchi Y, Ebata R, Terai M, Fuse S, et al. Efficacy of primary treatment with immunoglobulin plus ciclosporin for prevention of coronary artery abnormalities in patients with Kawasaki disease predicted to be at increased risk of non-response to intravenous immunoglobulin (KAICA): a randomised controlled, open-label, blinded-endpoints, phase 3 trial. *Lancet.* (2019) 393:1128–37. doi: 10.1016/S0140-6736(18)32003-8
20. Piram M, Darce Bello M, Tellier S, Di Filippo S, Boralevi F, Madhi F, et al. Defining the risk of first intravenous immunoglobulin unresponsiveness in non-Asian patients with Kawasaki disease. *Sci Rep.* (2020) 10:3125. doi: 10.1038/s41598-020-59972-7
21. Kawamura Y, Takeshita S, Kanai T, Yoshida Y, Nonoyama S. The combined usefulness of the neutrophil-to-lymphocyte and platelet-to-lymphocyte ratios in predicting intravenous immunoglobulin resistance with Kawasaki disease. *J Pediatr.* (2016) 178:281–4. doi: 10.1016/j.jpeds.2016.07.035
22. Fu PP, Du ZD, Pan YS. Novel predictors of intravenous immunoglobulin resistance in Chinese children with Kawasaki disease. *Pediatr Infect Dis J.* (2013) 32:e319–23. doi: 10.1097/INF.0b013e31828e887
23. Tang Y, Yan W, Sun L, Huang J, Qian W, Ding Y, et al. Prediction of intravenous immunoglobulin resistance in Kawasaki disease in an East China population. *Clin Rheumatol.* (2016) 35:2771–6. doi: 10.1007/s10067-016-3370-2
24. Hua W, Sun Y, Wang Y, Fu S, Wang W, Xie C, et al. A new model to predict intravenous immunoglobin-resistant Kawasaki disease. *Oncotarget.* (2017) 8:80722–9. doi: 10.18632/oncotarget.21083
25. Yang S, Song R, Zhang J, Li X, Li C. Predictive tool for intravenous immunoglobulin resistance of Kawasaki disease in Beijing. *Arch Dis Child.* (2019) 104:262–7. doi: 10.1136/archdischild-2017-314512
26. Lin MT, Chang CH, Sun LC, Liu HM, Chang HW, Chen CA, et al. Risk factors and derived formosa score for intravenous immunoglobulin unresponsiveness in Taiwanese children with Kawasaki disease. *J Formos Med Assoc.* (2016) 115:350–5. doi: 10.1016/j.jfma.2015.03.012
27. Ayusawa M, Sonobe T, Uemura S, Ogawa S, Nakamura Y, Kiyosawa N, et al. Revision of diagnostic guidelines for Kawasaki disease (the 5th revised edition). *Pediatr Int.* (2005) 47:232–4. doi: 10.1111/j.1442-200x.2005.02033.x
28. Kobayashi T, Ayusawa M, Suzuki H, Abe J, Ito S, Kato T, et al. Revision of diagnostic guidelines for Kawasaki disease (6th revised edition). *Pediatr Int.* (2020) 62:1135–8. doi: 10.1111/ped.14326
29. Newburger JW, Takahashi M, Burns JC, Beiser AS, Chung KJ, Duffy CE, et al. The treatment of Kawasaki syndrome with intravenous gamma globulin. *N Engl J Med.* (1986) 315:341–7. doi: 10.1056/NEJM198608073150601
30. Fukazawa R, Kobayashi J, Ayusawa M, Hamada H, Miura M, Mitani Y, et al. JCS/JSCS 2020 Guideline on diagnosis and management of cardiovascular sequelae in Kawasaki disease. *Circ J.* (2020) 84:1348–407. doi: 10.1253/circj.CJ-19-1094
31. Onodera T, Goseki N, Kosaki G. Prognostic nutritional index in gastrointestinal surgery of malnourished cancer patients. *Nihon Geka Gakkai Zasshi.* (1984) 85:1001–5.
32. Park HM, Lee DW, Hyun MC, Lee SB. Predictors of nonresponse to intravenous immunoglobulin therapy in Kawasaki disease. *Korean J Pediatr.* (2013) 56:75–9. doi: 10.3345/kjp.2013.56.2.75
33. Cheng F, Kang L, Zhang F, Ma H, Wang X, Dong Y, et al. Analysis of hyperbilirubinemia in patients with Kawasaki disease. *Medicine.* (2020) 99:e21974. doi: 10.1097/MD.0000000000021974
34. Li T, Qi M, Dong G, Li X, Xu Z, Wei Y, et al. Clinical value of prognostic nutritional index in prediction of the presence and severity of neonatal sepsis. *J Inflamm Res.* (2021) 14:7181–90. doi: 10.2147/JIR.S343992
35. Tai IH, Wu PL, Guo MM, Lee J, Chu CH, Hsieh KS, et al. Prognostic nutrition index as a predictor of coronary artery aneurysm in Kawasaki disease. *BMC Pediatr.* (2020) 20:203. doi: 10.1186/s12887-020-02111-y
36. Kuo HC, Liang CD, Wang CL, Yu HR, Hwang KP, Yang KD. Serum albumin level predicts initial intravenous immunoglobulin treatment failure in Kawasaki disease. *Acta Paediatr.* (2010) 99:1578–83. doi: 10.1111/j.1651-2227.2010.01875.x
37. Takeshita S, Kanai T, Kawamura Y, Yoshida Y, Nonoyama S. A comparison of the predictive validity of the combination of the neutrophil-to-lymphocyte ratio and platelet-to-lymphocyte ratio and other risk scoring systems for intravenous immunoglobulin (ivig)-resistance in Kawasaki disease. *PLoS One.* (2017) 12:e0176957. doi: 10.1371/journal.pone.0176957
38. Liu X, Zhou K, Hua Y, Wu M, Liu L, Shao S, et al. Prospective evaluation of neutrophil-to-lymphocyte ratio and platelet-to-lymphocyte ratio for intravenous immunoglobulin resistance in a large cohort of Kawasaki disease patients. *Pediatr Infect Dis J.* (2020) 39:229–31. doi: 10.1097/INF.0000000000000256
39. Song R, Yao W, Li X. Efficacy of four scoring systems in predicting intravenous immunoglobulin resistance in children with Kawasaki disease in a children's hospital in Beijing, North China. *J Pediatr.* (2017) 184:120–4. doi: 10.1016/j.jpeds.2016.12.018

Conflict of Interest: The authors declare that the research was conducted in the absence of any commercial or financial relationships that could be construed as a potential conflict of interest.

frontiers | Frontiers in Pediatrics

ORIGINAL RESEARCH
published: 04 May 2022
doi: 10.3389/fped.2022.772142

A Pilot Study Characterizing Flow Patterns in the Thoracic Aorta of Patients With Connective Tissue Disease: Comparison to Age- and Gender-Matched Controls *via* Fluid Structure Interaction

Joseph A. Camarda[1], *Ronak J. Dholakia*[2], *Hongfeng Wang*[2], *Margaret M. Samyn*[1,2], *Joseph R. Cava*[1] *and John F. LaDisa Jr.*[1,2,3]*

[1] *Department of Pediatrics, Division of Cardiology, Herma Heart Institute, Children's Wisconsin and the Medical College of Wisconsin, Milwaukee, WI, United States,* [2] *Department of Biomedical Engineering, Marquette University the Medical College of Wisconsin, Milwaukee, WI, United States,* [3] *Departments of Medicine, Division of Cardiovascular Medicine and Physiology, Medical College of Wisconsin, Milwaukee, WI, United States*

OPEN ACCESS

Edited by:
Ruth Heying,
University Hospital Leuven, Belgium

Reviewed by:
Giuseppe De Nisco,
Polytechnic University of Turin, Italy
Weiguang Yang,
Stanford University, United States

***Correspondence:**
John F. LaDisa Jr.
jladisa@mcw.edu

Specialty section:
This article was submitted to Pediatric Cardiology, a section of the journal Frontiers in Pediatrics

Received: *07 September 2021*
Accepted: *25 March 2022*
Published: *04 May 2022*

Citation:
Camarda JA, Dholakia RJ, Wang H, Samyn MM, Cava JR and LaDisa JF Jr (2022) A Pilot Study Characterizing Flow Patterns in the Thoracic Aorta of Patients With Connective Tissue Disease: Comparison to Age- and Gender-Matched Controls via Fluid Structure Interaction. Front. Pediatr. 10:772142. doi: 10.3389/fped.2022.772142

Prior computational and imaging studies described changes in flow patterns for patients with Marfan syndrome, but studies are lacking for related populations. This pilot study addresses this void by characterizing wall shear stress (WSS) indices for patients with Loeys-Dietz and undifferentiated connective tissue diseases. Using aortic valve-based velocity profiles from magnetic resonance imaging as input to patient-specific fluid structure interaction (FSI) models, we determined local flow patterns throughout the aorta for four patients with various connective tissue diseases (Loeys-Dietz with the native aorta, connective tissue disease of unclear etiology with native aorta in female and male patients, and an untreated patient with Marfan syndrome, as well as twin patients with Marfan syndrome who underwent valve-sparing root replacement). FSI simulations used physiological boundary conditions and material properties to replicate available measurements. Time-averaged WSS (TAWSS) and oscillatory shear index (OSI) results are presented with localized comparison to age- and gender-matched control participants. Ascending aortic dimensions were greater in almost all patients with connective tissue diseases relative to their respective control. Differences in TAWSS and OSI were driven by local morphological differences and cardiac output. For example, the model for one twin had a more pronounced proximal descending aorta in the vicinity of the ductus ligamentum that impacted WSS indices relative to the other. We are optimistic that the results of this study can serve as a foundation for larger future studies on the connective tissue disorders presented in this article.

Keywords: Marfan syndrome, computational modeling, patient-specific modeling, wall shear stress, Loeys-Dietz syndrome

INTRODUCTION

Blood flow patterns in the aortic arch and descending thoracic aorta (dAo) are unique when compared with other portions of the arterial vasculature. For example, helical flow is present within the aortic arch under normal conditions and is thought to influence flow patterns at the origins of the carotid and subclavian arteries (1). Characterizing any deviations from these normal flow patterns may be important for optimal operative interventions involving the thoracic aorta with the goal of decreasing the likelihood of later, long-term aortic pathology. For instance, transient periods of turbulence during systole (due to modest differences in local vessel geometry from thoracic aortic diseases or surgery) could cause downstream flow disturbances. Such disturbances have been associated with local dilation (2, 3) and can subsequently impact indices of wall shear stress (WSS; defined as the tangential force per unit area exerted on a vessel wall as a result of flowing blood). Abnormal WSS has been related to pathology in the thoracic aorta. In a study of 10 middle-aged adults with preexisting plaques, areas of low time-averaged WSS (TAWSS) were found in a rotating pattern progressing down the dAo and correlated with areas of atherosclerosis (4). Excessively high WSS can also be deleterious by initiating platelet aggregation (5).

Marfan syndrome is one type of connective tissue disorder that impacts several tissues/organs, including the cardiovascular system, where it can lead to thoracic aortic aneurysms (6). Prior research indicates that thoracic aortic aneurysms are the leading cause of death for patients with Marfan syndrome (7). Despite the uniqueness and importance of flow patterns in the thoracic aorta, there are few studies characterizing local blood flow patterns for connective tissue diseases beyond Marfan syndrome (8). To date, most computational studies of patients with Marfan syndrome have employed rigid computational fluid dynamics (CFD) models, which have the potential to reveal detailed spatiotemporal quantification of hemodynamic indices, including WSS, based on magnetic resonance imaging (MRI) and blood pressure (BP) data (9–19). A recent report quantified several indices by CFD, including WSS, for patients with Marfan syndrome before and after surgery to implement personalized external aortic root support (20). Some local differences were noted after surgery, but values were largely similar. This investigation builds from this prior work by conducting fluid structure interaction (FSI) modeling that includes local wall deformation of the aorta for patients with Loeys-Dietz, connective tissue disease of unclear etiology, and native (i.e., untreated) Marfan syndrome, as well as fraternal (i.e., dichorionic) twin patients with Marfan syndrome who underwent valve sparing root repair. All results are interpreted relative to those from age- and gender-matched control patients. The approaches employed for this study assigned local tissue properties as well as physiological inflow profiles and outlet boundary conditions to replicate clinical measurements. With these advancements, we aim to more accurately replicate the physiological conditions for patients with these connective tissue anomalies, and therefore help to further reveal differences in WSS and related indices vs. control participants. Thus, this pilot investigation may aid future long-term studies of morbidity related to aortic vascular disease.

METHODS

Magnetic Resonance Imaging

Following Children's Wisconsin Institutional Review Board approval, MRI was performed for patients with connective tissue anomalies. MRI data from control participants with ages, genders, and Reynolds numbers aiming to closely match these patients were also obtained. Prior to protocol enrollment, verbal and written information was provided, and informed consent was obtained from participants. Details of the patients and control participants are shown in **Table 1** (10 men and two women aged 18–55 years). Patients had various connective tissue diseases (Loeys-Dietz with native aorta; connective tissue disease of unclear etiology with native aorta in female and male patients; and an untreated patient with Marfan syndrome). All imaging was conducted as part of clinically ordered sessions or ongoing research.

Gadolinium-enhanced (0.4 ml/kg; gadodiamide, Omniscan®, GE Healthcare, Waukesha, WI, USA) MR angiography (MRA) was performed with a breath-held 3D fast gradient echo sequence using a 1.5T Symphony® scanner (Siemens Healthcare, Erlangen, Germany). Slice thickness was 2.0 mm, with 56–60 sagittal slices per volume. A 384 × 192 acquisition matrix (reconstructed to 384 × 256) was used with a field of view (FoV) of 25 × 42 cm^2 (spatial resolution of 0.65 × 1.64 mm). Other parameters included a repetition time (TR) of 4.3 ms, echo time (TE) of 1.4 ms, and a flip angle of 25°.

Time-resolved, velocity-encoded two-dimensional anatomic and through-plane phase-contrast MRI (PC-MRI) was performed orthogonally in the ascending aorta (AscAo) near the main pulmonary artery, in the dAo at the level of the diaphragm, and orthogonal to the arch origins of the head and neck vessels. An additional PC-MRI scan was obtained through the aortic valve for all patients, and when possible for control participants. The data were used to create spatiotemporally varying computational model inlets delineated by the patient's aortic valve as previously described in detail (21, 22) and briefly summarized in the boundary conditions section below. Heart rates ranged from 82 to 92 bpm (with R-R ranging from 652 to 732 ms); 25 images were reconstructed for the average R-R interval. Imaging parameters included TR, TE, and flip angle of 46 ms, 3.8 ms, and 30°, respectively. The FoV was 30 × 22.5 cm^2 with an acquisition matrix of 256 × 192 and a slice thickness of 7 mm, resulting in a voxel size of 1.17 mm × 1.17 mm × 7 mm. Subjects breathed freely during PC-MRI acquisition, and data were retrospectively gated to the cardiac cycle. After scanning, supine, bilateral upper and lower extremity BP assessment was performed using a Dinamap BP system (GE Healthcare, Waukesha, WI, USA). Cardiac indexes, aortic dimensions, and mean Reynolds numbers are provided in **Table 1**. Dimensions are taken from the computational models created using MRA data according to the details below, which we understand to generally be a diastolic representation of vessel morphology.

TABLE 1 | Hemodynamic indices, diagnosis, and aortic dimensions.

Connective tissue disorder	Age	Gender	Diagnosis	Operation	Cardiac index (L/min/m^2)	AscAo diameter (mm)	dAo diameter (mm)	AscAo/dAo diameter ratio	Difference in AscAo/dAo diameter vs. control (%)	Reynolds number (dimension-less)
Loeys Dietz	55	M	Genetic-TGFBR 2 mutation	n/a	3.0	35.0	21.4	1.63	29.3	923
Control	57	M	-	-	2.5	32.2	25.5	1.26	-	910
Unknown etiology-male	38	M	Phenotypic diagnosis; Genetic-negative for FBN-1, TGFBR1, TGFBR 2	n/a	3.1	28.9	19.0	1.52	17.4	1,380
Control	32	M	-	-	4.5	26.9	20.7	1.30	-	1,520
Unknown etiology-female	24	F	Genetic-negative for FBN1, FBN1 del, TGFBR1, TGFBR2, MYLK, MYH11, ACTA 2	n/a	3.2	32.9	18.1	1.82	20.7	1,130
Control	23	F	-	-	2.0	22.0	14.6	1.51	-	823
Marfan syndrome–twin A	22	M	Genetic-FBN1 exon 30 mutation	Valve sparing root replacement	2.9	28.0	17.9	1.56	24.0	1,190
Control	26	M	-	-	2.5	26.3	20.9	1.26	-	1,190
Marfan syndrome–twin B	22	M	Genetic-FBN1 exon 30 mutation	Valve sparing root replacement	3.3	26.8	16.2	1.65	13.5	1,350
Control	24	M	-	-	3.5	28.8	19.8	1.46	-	1,550
Marfan syndrome-native	18	M	Phenotypic diagnosis	n/a	6.0	22.8	16.2	1.41	10.6	2,710
Control	18	M	-	-	3.2	25.1	19.7	1.28	-	1,520

Reynolds number calculations assume a blood density of 1.06 g/cm^3 and dynamic viscosity of 4 cP.

Computational Model Construction

Computational versions of the aorta and arteries of the head and neck were created from MRA imaging data using Simvascular (Simtk.org) software as discussed previously (15). Models were discretized using a commercially available, automatic mesh generation program (MeshSim, Simmetrix, Clifton Park, NY, USA). Meshes contained ∼4 million tetrahedral elements, and localized refinement was performed until results were independent of the mesh as discussed elsewhere (12) using an adaptive technique (23, 24) to deposit more elements near the luminal surface and in anatomical regions prone to flow disruption (14).

Inlet Boundary Conditions

PC-MRI data were used to calculate time-resolved volumetric blood flow as previously described (16, 25). A time-varying plug flow inlet based on the measured AscAo flow was created, but with a restricted cross section determined from time-varying PC-MRI magnitude data at the level of the valve (21). A normal trileaflet valve was assumed for control participants and confirmed using the imaging data mentioned above, when possible.

Outlet Boundary Conditions and Wall Deformation

Flow from the innominate, left common carotid artery, left subclavian artery, and dAo were used together with BP data to prescribe physiological outflow boundary conditions using three-element Windkessel approximations (26). The three-element Windkessel accounts for vessels distal to computational model branches using three parameters with physiological meaning, namely, characteristic resistance (R_c), capacitance (C), and distal resistance (R_d). The total arterial capacitance (TAC) for each patient was determined from inflow and BP data, assuming a characteristic to total resistance ratio of 6% (27). The TAC was then distributed among outlets according to their blood flow distributions (28). The terminal resistance ($R_t = R_c + R_d$) was then calculated from mean BP and PC-MRI flow measurements and distributed between the remaining resistance parameters by adjusting R_c to R_t ratios (6–10%) for each outlet using the

pulse pressure method, (29, 30) thereby replicating measured BP. An augmented-Lagrangian formulation (31) for constraining velocity profiles at model outlets was used to mitigate instabilities often occurring during flow deceleration and diastole. Vessel deformability (32) was included in FSI simulations as discussed elsewhere (15). Briefly, a wall thickness of 0.15 cm (33) was implemented from literature for all models and the Young's modulus was then adjusted iteratively until the AscAo mean luminal displacement was within 5% of the values obtained from PC-MRI magnitude measurements.

Computational Simulations

Simulations were performed using a novel stabilized finite element method to solve the conservation of mass (continuity), balance of fluid momentum (Navier-Stokes), and vessel wall elastodynamics equations (32). Simulations were run for 4–6 cardiac cycles until the flow rate and BP fields yielded periodic solutions.

Blood flow velocity, BP, and wall displacement were visualized using ParaView (Kitware, Clifton Park, NY, USA). TAWSS (34) and the oscillatory shear index (OSI) (25) was then calculated as previously described. Low TAWSS is generally thought to promote atherogenesis, as is elevated OSI, an index of directional changes in WSS. Low OSI indicates WSS is unidirectional, while a value of 0.5 is indicative of bidirectional WSS with a time-average value of zero. These indices were quantified in several ways. Values for TAWSS and OSI were extracted longitudinally along the inner and outer curvatures of the thoracic aorta, as well as along its anatomic right, and left sides as described previously (14, 35). This was done because prior imaging studies found that local values for these indices were statistically different from circumferential averages (36), thereby motivating the need to report detailed local WSS maps in computational studies. To visualize these indices locally, the surface of each vessel was unwrapped and mapped into a θ, l rectangular domain, where θ and l are the circumferential and longitudinal coordinates of each point on the vessel wall (37). Data presented represent an average of nearest-neighbor values in 2% increments along the length of the aorta. This distance was made consistent between patients and control participants using dimensional information from imaging data, and then normalized from 0 to 1. TAWSS values from 0 to 50 dyn/cm^2 are particularly interesting from the perspective of the vascular response to hemodynamics and are also highlighted in histograms (2 dyn/cm^2 bins) for values within this range. Histograms are also provided for the full range of OSI, 0–0.5 (0.2 unit bins) (22, 38).

RESULTS

Fluid structure interaction simulations for all patients, and their respective controls, yielded the TAWSS and OSI results shown in **Figures 1**, **3**, respectively. The size of the models shown is relative to each other using the descending aortic outlet dimension as reference. A summary of dimensions following model construction is also provided in **Table 1**. In nearly all cases, the AscAo dimension was greater in patients than the respective control participant. Conversely, with the exception of the female patient having connective tissue disease of unknown etiology, the dAo dimension was of smaller caliber compared to the age- and gender-matched control participant. The ratio of AscAo to dAo for patients was consequently 10.6–29.3% larger than AscAo:dAo ratio for control participants.

Patient With Loeys-Dietz Disease

The patient with Loeys-Dietz disease and corresponding control had the lowest overall distributions of TAWSS due primarily to the large AscAo dimensions in the setting of normal range cardiac output values (e.g., Loeys-Dietz = 3.0 L/min/m^2; control = 2.5 L/min/m^2). The histogram of TAWSS values shown in **Figure 2** reveals the similarity in distributions between the Loeys-Dietz and control models. The smaller caliber of the dAo relative to the AscAo in the patient with Loeys-Dietz disease relative to its control (mentioned above) also results in slightly higher distributions of TAWSS along the last half of the thoracic aorta quantified (distances from ∼0.5 to 1.0).

There were modest differences in OSI for the patient with Loeys-Dietz disease relative to the control participant (**Figure 3**). The histogram (**Figure 4**) shows similar amounts of elevated OSI values >0.4 for both models. The histogram from the patient with Loeys-Dietz disease showed that less of the luminal surface was exposed to elevated OSI (0.2–0.4) shown to be atherogenic in prior reports. The difference in OSI values within this region corresponded to the transverse arch of the control patient (**Figure 3**), which also seems to have slight out-of-plane morphology in this region compared to the more traditional arch of the patient with Loeys-Dietz disease. These differences can also be seen in the longitudinal plots (e.g., right, outer, and left surfaces at distances of ∼0.4–0.6).

Patients With Connective Tissue Disease of Unknown Etiology

The TAWSS histogram for the male patient with connective tissue disease of unknown etiology reveals a greater portion of the aorta and its branches were exposed to lower TAWSS, particularly in the ascending aorta, relative to control (**Figure 2**). This is clearly shown in longitudinal TAWSS plots along the outer and left luminal surfaces. Vascular dimensions and morphology were similar for both models, suggesting that these differences may primarily be due to a higher cardiac index for the control participant (e.g., 3.1 L/min/m^2 for the patient with connective tissue disease vs. 4.5 L/min/m^2 vs. for the control).

The ascending aorta of the male patient with connective tissue disease of unknown etiology was exposed to a greater area of elevated OSI values in the range of ∼0.1–0.4 (**Figure 3** and histogram of **Figure 4**), which occurred along nearly the full length of the left luminal surface and lasted 50–70% of the distance for the right and outer luminal surfaces (**Figure 4**).

The female patient with connective tissue disease of unknown etiology experienced higher TAWSS along the transverse arch and dAo (**Figure 1**). This is reflected in all longitudinal plots (**Figure 2**). This finding appears to correspond to a larger AscAo/dAo ratio for the patient compared to the control.

The larger caliber ascending aorta and its branches for the female patient with connective tissue disease of unknown

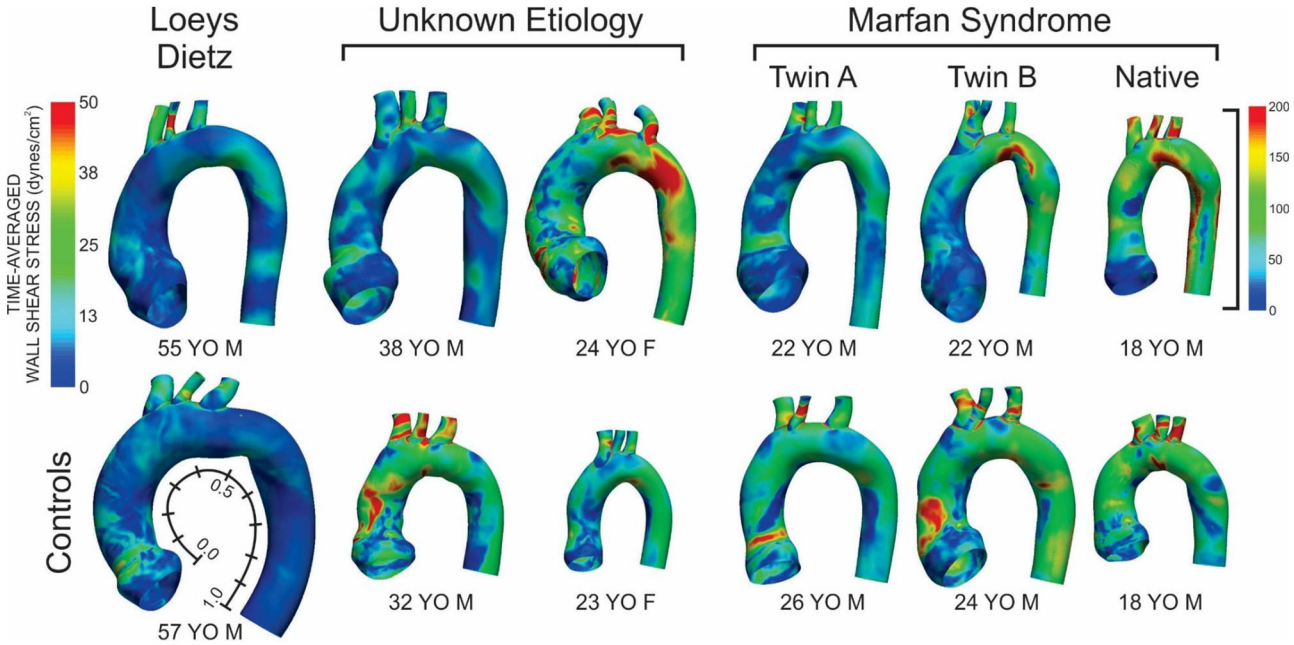

FIGURE 1 | Time-averaged wall shear stress (TAWSS) distributions for the six patients with the various connective tissue diseases studied (top row) and age- and gender-matched control participants to which each was compared (bottom row). The size of the models displaying the TAWSS results shown is relative to each other using the descending aortic outlet dimensions. Data in **Figures 2**, **4** are presented along the length of the aorta. This distance was made consistent between patients and control participants using dimensional information from imaging data and then normalized from 0 to 1 as shown beside the model and TAWSS from the leftmost control participant.

etiology resulted in a greater area of potentially deleterious OSI values in this region (**Figure 3**) and more area exposed to the full range of OSI compared to the corresponding control participant. Elevated OSI values were most pronounced along the left luminal surface (**Figure 4**).

Patients With Marfan Syndrome

TAWSS for the native (i.e., uncorrected) patient with Marfan syndrome was extremely high relative to the corresponding control participant primarily due to a cardiac index exceeding normal conditions (6.0 L/min/m^2 vs. 3.2 L/min/m^2 for the control). The distributions of OSI values were somewhat similar for values $>$ 0.2. By qualitative assessment, the AscAo of the native patient with Marfan syndrome had a greater area exposed to lower OSI (**Figure 3**), primarily along the inner and left luminal surfaces (**Figure 4**). Of note, the native patient with Marfan syndrome had the highest Reynolds number of all patients or participants studied (**Table 1**), and the value suggests flow was not laminar in the aorta of this patient, likely leading to spatial differences in OSI within the AscAo.

The twin patients with Marfan syndrome, who previously underwent aortic root replacement, had similar TAWSS distributions. The computational model labeled as Twin B for this study had a more dilated proximal descending aorta in the vicinity of the ductus ligamentum, which impacted indices of WSS. Differences between the computational models of each twin and their respective control model were mainly a function of cardiac index. TAWSS was generally lower in the dAo of both twins after surgery compared to their respective controls (**Figure 1**). This was most pronounced along the left luminal surface of the AscAo (**Figure 2**).

Distributions (**Figure 3**) and histograms (**Figure 4**) of OSI values for the twin patients with Marfan syndrome, who previously underwent aortic root replacement, were also similar with morphological differences in the vicinity of the ductus ligamentum mostly impacting the luminal surface at a normalized distance of ∼0.4–0.6. This area was not replaced in either subject and reflects their native aortic properties.

DISCUSSION

Blood flow patterns in the aortic arch and dAo are unique compared with other portions of the arterial vasculature. This is evident when considering the Reynolds number, a dimensionless index used to characterize fluid flow (2). Specifically, Reynolds number describes the ratio of convective inertial forces to viscous forces. In general, Reynolds number values $<$2,200 constitute laminar flow where adjacent layers of fluid move in layers without mixing, while those $>$2,200 may be characterized as transitional or turbulent depending on specific details of the local flow domain. Under normal conditions, the thoracic aorta experiences Reynolds numbers on the order of 1,500 (mean) as a result of its large caliber and high blood flow rates. These Reynolds number values indicate blood flow is generally laminar throughout the cardiac cycle, but there are undoubtedly portions

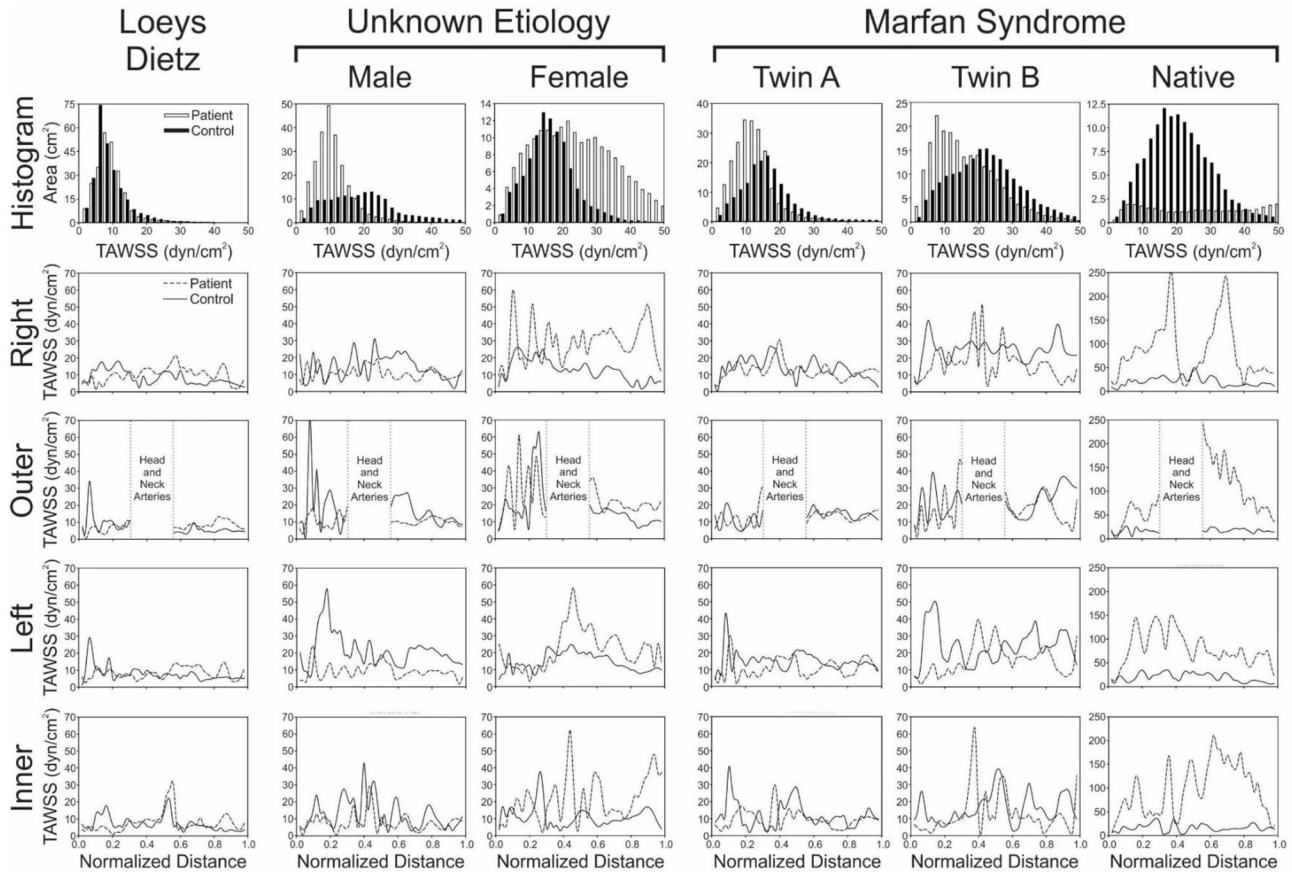

FIGURE 2 | Local quantification of TAWSS results. The top row shows histograms (2 dyn/cm^2 bins) of the area (cm^2) from each model surface exposed to TAWSS values from 0 to 50 dyn/cm^2 (connective tissue disease = solid bars; age- and gender-matched controls = hollow bars). Longitudinal TAWSS distributions along the outer, anatomic right, anatomic left, and inner curvatures of the aorta are also shown in subsequent rows for the patients with various connective tissue disease (dashed lines) vs. their associated age- and gender-matched controls (solid lines). Low TAWSS is generally thought to promote atherogenesis, so skewing of histogram results toward lower values could be interpreted as less ideal, as could overall lower values of TAWSS along the aortic surfaces.

of the cardiac cycle during which blood flow transiently becomes transitional and/or turbulent. Characterizing any deviations from these normal flow patterns may be important for optimal operative interventions for the thoracic aorta with the aim being to decrease the likelihood of later, long-term aortic pathology. For example, transient periods of turbulence during systole (due to modest differences in local vessel geometry from thoracic aortic diseases or surgery) could cause downstream disturbances.

This investigation builds upon prior work by conducting FSI, in contrast to rigid CFD, with modeling that includes local wall deformation of the aorta for patients with Loeys-Dietz, connective tissue disease of unclear etiology, and native (i.e., untreated) Marfan syndrome, as well as twin patients with Marfan syndrome who underwent valve sparing aortic root repair. We matched changes in dimension by PC-MRI measurements by assigning local tissue properties and iterating Young's modulus until the deformation matched that observed *in vivo*. Physiological inflow profiles are uniquely implemented by imposing a restricted cross-sectional flow determined from time-varying PC-MRI magnitude data at the level of the valve (21) and outlet boundary conditions for PC-MRI data are added to reflect clinical measurements (14, 15). Our goal with these model improvements was to more accurately replicate the physiological conditions for patients with these connective tissue anomalies, and therefore reveal differences in WSS and OSI vs. age- and gender-matched control participants in a pilot study.

In nearly all cases, the AscAo dimension was greater in patients with connective tissues diseases relative to their respective control. With the exception of the female patient with connective tissue disease of unknown etiology, the dAo dimension was of smaller caliber when compared to the corresponding control. Differences in TAWSS and OSI were driven by these local morphological differences and cardiac output. Unfortunately, it is difficult to speculate on the cause of smaller dAo dimensions in most patients relative to controls given the small sample size and heterogeneity. This finding should be validated in larger studies with groups of patients having similar genetic anomalies.

A unique presentation of the results of this study centers on the twin patients with Marfan syndrome who previously

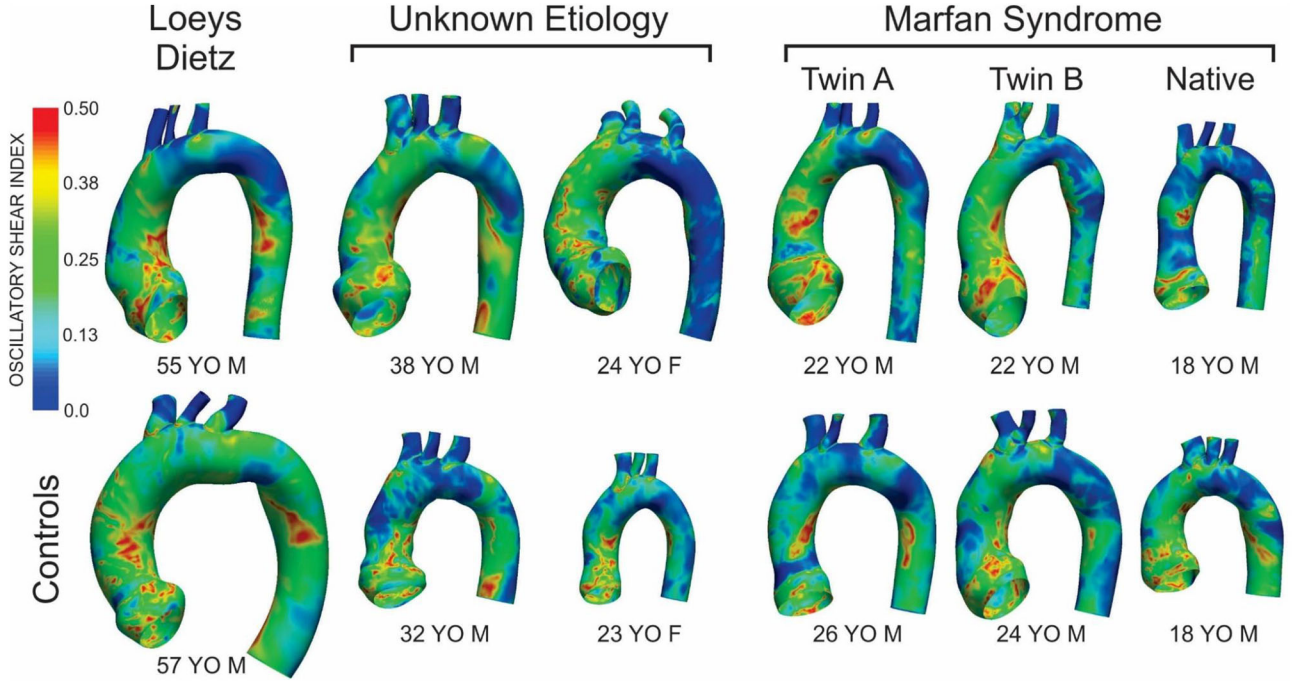

FIGURE 3 | Distributions of oscillatory shear index (OSI) for the six patients with the various connective tissue diseases studied (top row) and age- and gender-matched control participants to which each was compared (bottom row). The size of the models displaying the OSI results shown is relative to each other using the descending aortic outlet dimensions.

underwent aortic root replacement. The computational model labeled as Twin B for this study had a more pronounced proximal descending aorta in the vicinity of the ductus ligamentum that impacted indices of WSS relative to Twin A. As with the other patients studied here, differences between the computational results of each twin and their respective control were mainly a function of cardiac index. Nonetheless, TAWSS was generally lower in the AscAo of both twins after surgery compared to their respective controls (**Figure 1**). Interpretation of these findings prompted review of literature that may be applicable. With twin gestation, there is a higher incidence of congenital heart disease. For monozygotic twins (65% with one chorion), the incidence of congenital heart malformations may be six times that for a singleton. For monozygotic twins, twin-twin transfusion syndrome may play a role in the development of CHD (39). The twins in our cohort were fraternal twins (i.e., dichorionic) inheriting the gene mutation for Marfan syndrome. Marfan syndrome is almost exclusively inherited in an autosomal-dominant manner, although rare case reports have described recessive fibrillin 1 gene (FBN1) mutations (40). For these dichorionic twins, twin-twin transfusion does not explain the CHD, but rather genetic inheritance explains their clinical course. In other dichorionic twins with congenital heart diseases such a coarctation of the aorta, altered fetal-placental hemodynamics sometimes resulting from fetal growth restriction can contribute to the development of their congenital heart disease (41).

The results of this study build from and extend existing simulation results for these patient populations. For example, previous work has independently quantified stress and strain fields (42) for three patients with Marfan syndrome before and after surgery to implement personalized external aortic root support, as well as aortic flow patterns and resulting distributions of WSS using imposed flow and pressure waveforms allowing for qualitative comparison of velocity patterns to PC-MRI (20). Although the fluid flow version of the study used rigid wall CFD, the results are generally consistent with this study in that models created from data before personalized external aortic root support had larger AscAo diameters, leading to more flow disturbances (20). More recent work reported the ratio of circumferential to longitudinal WSS in idealized models informed by the data of patient with Marfan syndrome with stable or dilating aneurysms (43). To the best of our knowledge, there is a paucity of studies characterizing altered blood flow patterns for patients with connective tissue anomalies beyond Marfan syndrome. Despite the scarcity of such studies, there is a 2015 report that quantified aortic dimensions and indices of aortic stiffness in patients with connective tissue disorders using MRI (8). While the finding of elevated stiffness in patients with connective tissue disorders from this study suggests that rigid CFD models may be appropriate for this patient population,

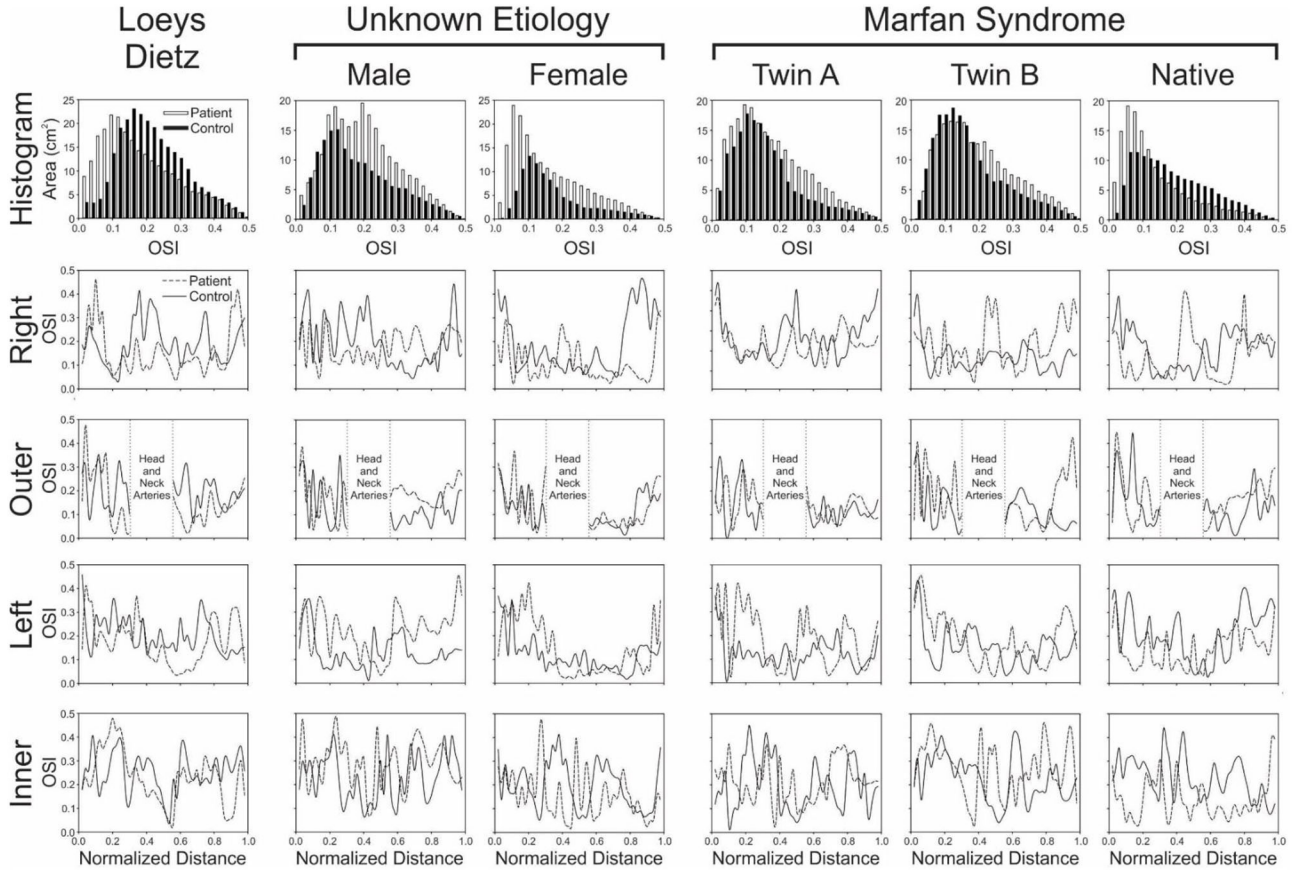

FIGURE 4 | Local quantification of oscillatory shear index (OSI) results. The top row shows histograms (0.2 unit bins) of the area (cm^2) from each model surface exposed to OSI values from 0 to 0.5 (connective tissue disease = solid bars; age- and gender-matched controls = hollow bars). Longitudinal OSI distributions along the outer, anatomic right, anatomic left, and inner curvatures of the aorta are also shown in subsequent rows for the patients with various connective tissue disease (dashed lines) vs. their associated age- and gender-matched controls (solid lines). Higher OSI values are generally thought to promote atherogenesis, so skewing of histogram results toward higher values could be interpreted as less ideal, as could overall higher values of OSI along the outer, anatomic right, anatomic left, and inner curvatures of the aorta.

it also points to the importance of accurately replicating deformation in patients with connective tissue disorders, who may not yet have experienced an increase in stiffness and associated adverse changes in WSS indices.

The results of this study should be considered relative to several potential limitations. Our investigation studied alterations in WSS indices locally in the proximal thoracic aorta and its branches given the hallmark capacitive function for this region of the arterial vasculature. There is evidence, however, that connective tissue disorders such as Marfan syndrome may also impact central aortic flow dynamics by virtue of altered distal resistance vessels (44). Although our outlet boundary conditions do account for downstream vascular resistance, the impact of changes in resistance vessel due to each connective tissue disease was not explicitly included in the outflow boundary conditions imposed for this study. To date, it is not known which specific, or combination of, WSS indices are directly linked to vascular pathologies for patients with connective tissue diseases. The influence of each index likely also depends on the patient population and its predominant pathology (e.g., stiffening, neointimal hyperplasia, and aneurysm rupture) (4, 45, 46). The small sample size for each connective tissue disease does undoubtedly present a limitation to extrapolating the results to the full population of patients with Loeys-Dietz, patients with connective tissue disease of unclear etiology, and those with Marfan syndrome (native and status post valve sparing root replacement). The cardiac index for the native (i.e., uncorrected) patient with Marfan syndrome was higher than expected based on elevated heart rate and hyperdynamic left ventricular ejection fraction. It is also possible that this patient had some anxiety during the MRI session. The goal of this study was to remain patient specific in terms of boundary conditions. However, when considering the results of this study, it may be interesting to conduct an idealized parameter-based study to quantify the impact of morphology and cardiac output independently. Such work is planned for the future. The Lagrangian multiplier

approach implemented for constraining outlet velocity profiles can be replaced in future work by a backflow stabilization treatment that is thought to be less intrusive to the flow field, computationally inexpensive, and has been implemented in Simvascular (47). While this study did impose a plug velocity profile at model inlets, it was restricted by the time-varying cross section determined from PC-MRI using novel methods previously developed in our lab (21). Upon implementation of these methods, we quantified the impact of valve morphology on aortic hemodynamics and identified regions most influenced by the inlet, including the ascending aorta that has previously been a site of dilation for patients with Marfan syndrome as a result of local flow patterns. Besides this approach, computational studies of the thoracic aorta to date have typically introduced blood flow in one of two ways. In one approach, PC-MRI is used to temporally sample the velocity profile downstream of the valve and input this measured profile directly into the model. While not directly including the valve, its impact can be manifested in the data that is obtained, but this requires appropriate through- and in-plane velocity encoding to adequately resolve flow features being input into the CFD model. This approach may be difficult to implement within the constraints of a clinical setting as it can require specialized sequences not routinely implemented and obtains data that are more detailed than those commonly used in clinical diagnosis. One alternative approach has been to construct CFD models with their inlet beginning just distal to the aortic sinuses, impose the blood flow waveform measured downstream as an assumed velocity profile at the model inlet, and allow the curvature of the arch to influence resulting flow patterns (14). While this technique does not use the complete spatial velocity information, it does not require specialized sequences, minimizes the introduction of noise at the model inflow due to inadequate velocity encoding, and allows for improved temporal resolution compared to 3-component PC-MRI (48). The methods of Wendell et al. used in this study (21) allow for more accurate representation of the impact of the aortic valve on computational studies of the thoracic aorta while still using data obtained as part of a routine clinical imaging session. The patients with connective tissue disorders of unknown etiology were suspected to have hereditary (or genetic) aortopathy, but negative testing for known genetic variants. The yield for current gene panels for thoracic aortic disease is only ∼30%, even in patients with high clinical suspicion. Hence, unfortunately, it is a common situation in our clinic to have suspected genetic etiology but a negative gene panel. This may be interpreted as not yet identifying the applicable gene(s) in that individual/family. We often pursue whole-exome sequencing in such patients, but even then the results often do not identify a causative genetic variant. This is a limitation that we are working to mitigate in the future as having complete genetic data for future cohorts would greatly enhance our understanding of the results presented for larger populations of patients.

CONCLUSION

The methods employed represent some of the most advanced vascular modeling tools available such as deformable walls, dynamically varying valvular area at the inlet of the model, physiological boundary conditions, and the use of age- and gender-matched controls. Despite some potential limitations outlined above in implementing these tools, the lack of computational modeling data for those patients with connective tissue diseases makes the current pilot data interesting and relevant. We are optimistic that the results of this study can serve as a foundation for larger future studies with the connective tissue disorders presented here.

DATA AVAILABILITY STATEMENT

The datasets presented in this article are not readily available because raw data supporting the conclusions of this article can only be available by the authors to the extent possible by the institutional approvals governing the research presented. Requests to access the datasets should be directed to jladisa@mcw.edu.

ETHICS STATEMENT

Ethical review and approval was obtained for the study using data from human participants in accordance with local legislation and institutional requirements. The patients/participants provided their written informed consent to participate in this study.

AUTHOR CONTRIBUTIONS

JAC: patient recruitment clinical expertise for manuscript development/review. HW and RD: computational simulations, analysis/interpretation of computational results, and approval of the article. MS and JRC: patient recruitment, supervision of MRI scanning, and clinical expertise for manuscript development/review. JL: concept/design, methodological developments, analysis/interpretation of computational results, drafting article, and approval of article. All authors contributed to the article and approved the submitted version.

FUNDING

Funding was provided through internal grant funding at the Medical College of Wisconsin (to MS) and an Educational Research Agreement between Children's Hospital of Wisconsin and Marquette University.

ACKNOWLEDGMENTS

The authors thank Mary Krolikowski and David C. Wendell PhD for their assistance with this study.

REFERENCES

1. Liu X, Sun A, Fan Y, Deng X. Physiological significance of helical flow in the arterial system and its potential clinical applications. *Ann Biomed Eng.* (2015) 43:3–15. doi: 10.1007/s10439-014-1097-2
2. Westerhof N, Stergiopulos N, Noble MIM. *Snapshots of hemodynamics an aid for clinical research and graduate education*. New York: Springer (2005).
3. Dobrin PB. Poststenotic dilatation. *Surg Gynecol Obstet.* (1991) 172:503–8.
4. Wentzel JJ, Corti R, Fayad ZA, Wisdom P, Macaluso F, Winkelman MO, et al. Does shear stress modulate both plaque progression and regression in the thoracic aorta? Human study using serial magnetic resonance imaging. *J Am Coll Cardiol.* (2005) 45:846–54. doi: 10.1016/j.jacc.2004.12.026
5. Hathcock JJ. Flow effects on coagulation and thrombosis. *Arterioscler Thromb Vasc Biol.* (2006) 26:1729–37. doi: 10.1161/01.ATV.0000229658.76797.30
6. Canadas V, Vilacosta I, Bruna I, Fuster V. Marfan syndrome. Part 1: pathophysiology and diagnosis. *Nat Rev Cardiol.* (2010) 7:256–65. doi: 10.1038/nrcardio.2010.30
7. Canadas V, Vilacosta I, Bruna I, Fuster V. Marfan syndrome. Part 2: treatment and management of patients. *Nat Rev Cardiol.* (2010) 7:266–76. doi: 10.1038/nrcardio.2010.31
8. Prakash A, Adlakha H, Rabideau N, Hass CJ, Morris SA, Geva T, et al. Segmental aortic stiffness in children and young adults with connective tissue disorders: relationships with age, aortic size, rate of dilation, and surgical root replacement. *Circulation.* (2015) 132:595–602. doi: 10.1161/CIRCULATIONAHA.114.014934
9. Coogan JS, Chan FP, Ladisa JF Jr, Taylor CA, Hanley FL, Feinstein JA. Computational fluid dynamic simulations for determination of ventricular workload in aortic arch obstructions. *J Thorac Cardiovasc Surg.* (2013) 145:489–95.e1. doi: 10.1016/j.jtcvs.2012.03.051
10. Figueroa CA, Taylor CA, Yeh V, Chiou AJ, Gorrepati ML, Zarins CK. Preliminary 3D computational analysis of the relationship between aortic displacement force and direction of endograft movement. *J Vasc Surg.* (2010) 51:1488–97. doi: 10.1016/j.jvs.2010.01.058
11. Kim HJ, Vignon-Clementel IE, Figueroa CA, LaDisa JF, Jansen KE, Feinstein JA, et al. On coupling a lumped parameter heart model and a three-dimensional finite element aorta model. *Ann Biomed Eng.* (2009) 37:2153–69. doi: 10.1007/s10439-009-9760-8
12. Kwon S, Feinstein JA, Dholakia RJ, LaDisa JF Jr. Quantification of local hemodynamic alterations caused by virtual implantation of three commercially available stents for the treatment of aortic coarctation. *Pediatr Cardiol.* (2014) 35:732–40. doi: 10.1007/s00246-013-0845-7
13. LaDisa JF Jr, Bowers M, Harmann L, Prost R, Doppalapudi AV, Mohyuddin T, et al. Time-efficient patient-specific quantification of regional carotid artery fluid dynamics and spatial correlation with plaque burden. *Medical physics.* (2010) 37:784–92. doi: 10.1118/1.3292631
14. LaDisa JF Jr, Dholakia RJ, Figueroa CA, Vignon-Clementel IE, Chan FP, Samyn MM, et al. Computational simulations demonstrate altered wall shear stress in aortic coarctation patients treated by resection with end-to-end anastomosis. *Congenit Heart Dis.* (2011) 6:432–43. doi: 10.1111/j.1747-0803.2011.00553.x
15. LaDisa JF Jr, Figueroa CA, Vignon-Clementel IE, Kim HJ, Xiao N, Ellwein LM, et al. Computational simulations for aortic coarctation: representative results from a sampling of patients. *J Biomech Eng.* (2011) 133:091008. doi: 10.1115/1.4004996
16. Les AS, Shadden SC, Figueroa CA, Park JM, Tedesco MM, Herfkens RJ, et al. Quantification of hemodynamics in abdominal aortic aneurysms during rest and exercise using magnetic resonance imaging and computational fluid dynamics. *Ann Biomed Eng.* (2010) 38:1288–313. doi: 10.1007/s10439-010-9949-x
17. Marsden AL, Bernstein AJ, Reddy VM, Shadden SC, Spilker RL, Chan FP, et al. Evaluation of a novel Y-shaped extracardiac Fontan baffle using computational fluid dynamics. *J Thorac Cardiovasc Surg.* (2009) 137:394–403.e2. doi: 10.1016/j.jtcvs.2008.06.043
18. Tang BT, Fonte TA, Chan FP, Tsao PS, Feinstein JA, Taylor CA. Three-dimensional hemodynamics in the human pulmonary arteries under resting and exercise conditions. *Ann Biomed Eng.* (2011) 39:347–58. doi: 10.1007/s10439-010-0124-1
19. Vignon-Clementel IE, Figueroa CA, Jansen KE, Taylor CA. Outflow boundary conditions for 3D simulations of non-periodic blood flow and pressure fields in deformable arteries. *Comput Methods Biomech Biomed Engin.* (2010) 13:625–40. doi: 10.1080/10255840903413565
20. Singh SD, Xu XY, Wood NB, Pepper JR, Izgi C, Treasure T, et al. Aortic flow patterns before and after personalised external aortic root support implantation in Marfan patients. *J Biomech.* (2016) 49:100–11. doi: 10.1016/j.jbiomech.2015.11.040
21. Wendell DC, Samyn MM, Cava JR, Ellwein LM, Krolikowski MM, Gandy KL, et al. Including aortic valve morphology in computational fluid dynamics simulations: initial findings and application to aortic coarctation. *Med Eng Phys.* (2013) 35:723–35. doi: 10.1016/j.medengphy.2012.07.015
22. Wendell DC, Samyn MM, Cava JR, Krolikowski MM, LaDisa JF Jr. The impact of cardiac motion on aortic valve flow used in computational simulations of the thoracic aorta. *J Biomech Eng.* (2016) 138:0910011–111. doi: 10.1115/1.4033964
23. Sahni O, Muller J, Jansen KE, Shephard MS, Taylor CA. Efficient anisotropic adaptive discretization of the cardiovascular system. *Comput Methods Biomech Biomed Engin.* (2006) 195:5634–55. doi: 10.1016/j.cma.2005.10.018
24. Muller J, Sahni O, Li X, Jansen KE, Shephard MS, Taylor CA. Anisotropic adaptive finite element method for modeling blood flow. *Comput Methods Biomech Biomed Engin.* (2005) 8:295–305. doi: 10.1080/10255840500264742
25. Tang BT, Cheng CP, Draney MT, Wilson NM, Tsao PS, Herfkens RJ, et al. Abdominal aortic hemodynamics in young healthy adults at rest and during lower limb exercise: quantification using image-based computer modeling. *Am J Physiol Heart Circ Physiol.* (2006) 291:H668–76. doi: 10.1152/ajpheart.01301.2005
26. Vignon-Clementel IE, Figueroa CA, Jansen KE, Taylor CA. Outflow boundary conditions for three-dimensional finite element modeling of blood flow and pressure in arteries. *Comput Methods Appl Mech Eng.* (2006) 195:3776–96. doi: 10.1016/j.cma.2005.04.014
27. Laskey WK, Parker HG, Ferrari VA, Kussmaul WG, Noordergraaf A. Estimation of total systemic arterial compliance in humans. *J Appl Physiol.* (1990) 69:112–9. doi: 10.1152/jappl.1990.69.1.112
28. Stergiopulos N, Young DF, Rogge TR. Computer simulation of arterial flow with applications to arterial and aortic stenoses. *J Biomech.* (1992) 25:1477–88. doi: 10.1016/0021-9290(92)90060-E
29. O'Rourke MF, Safar ME. Relationship between aortic stiffening and microvascular disease in brain and kidney: cause and logic of therapy. *Hypertension.* (2005) 46:200–4. doi: 10.1161/01.HYP.0000168052.00426.65
30. Stergiopulos N, Segers P, Westerhof N. Use of pulse pressure method for estimating total arterial compliance *in vivo*. *Am J Physiol Heart Circ Physiol.* (1999) 276:H424–8. doi: 10.1152/ajpheart.1999.276.2.H424
31. Kim HJ, Figueroa CA, Hughes TJR, Jansen KE, Taylor CA. Augmented Lagrangian method for constraining the shape of velocity profiles at outlet boundaries for three-dimensional Finite Element simulations of blood flow. *Comput Methods Appl Mech Eng.* (2009) 198:3551–66. doi: 10.1016/j.cma.2009.02.012
32. Figueroa CA, Vignon-Clementel IE, Jansen KE, Hughes TJR, Taylor CA. A coupled momentum method for modeling blood flow in three-dimensional deformable arteries. *Comput Methods Appl Mech Eng.* (2006) 195:5685–706. doi: 10.1016/j.cma.2005.11.011
33. Westerhof N, Bosman F, De Vries CJ, Noordergraaf A. Analog studies of the human systemic arterial tree. *J Biomech.* (1969) 2:121–43. doi: 10.1016/0021-9290(69)90024-4
34. Eslami P, Tran J, Jin Z, Karady J, Sotoodeh R, Lu MT, et al. Effect of wall elasticity on hemodynamics and wall shear stress in patient-specific simulations in the coronary arteries. *J Biomech Eng.* (2020) 142: 0245031–310. doi: 10.1115/1.4043722
35. Samyn MM, Dholakia R, Wang H, Co-Vu J, Yan K, Widlansky ME, et al. Cardiovascular magnetic resonance imaging-based computational fluid dynamics/fluid-structure interaction pilot study to detect early vascular changes in pediatric patients with type 1 diabetes. *Pediatr Cardiol.* (2015) 36:851–61. doi: 10.1007/s00246-014-1071-7
36. Frydrychowicz A, Stalder AF, Russe MF, Bock J, Bauer S, Harloff A, et al. Three-dimensional analysis of segmental wall shear stress in the aorta by flow-sensitive four-dimensional-MRI. *J Magn Reson Imaging.* (2009) 30:77–84. doi: 10.1002/jmri.21790

37. Gundert TJ, Shadden SC, Williams AR, Koo BK, Feinstein JA, Ladisa JF Jr. A rapid and computationally inexpensive method to virtually implant current and next-generation stents into subject-specific computational fluid dynamics models. *Ann Biomed Eng.* (2011) 39:1423–37. doi: 10.1007/s10439-010-0238-5
38. Ellwein L, M. SM, M. D, Schindler-Ivens S, Liebham S, LaDisa JF, Jr. Toward translating near-infrared spectroscopy oxygen saturation data for the noninvasive prediction of spatial and temporal hemodynamics during exercise. *Biomech Model Mechanobiol.* (2017) 16:75–96. doi: 10.1007/s10237-016-0803-4
39. Balasubramanian R, Vuppalapati S, Avanthika C, Jhaveri S, Peddi NC, Ahmed S, et al. Epidemiology, genetics and epigenetics of congenital heart diseases in twins. *Cureus.* (2021) 13:e17253. doi: 10.7759/cureus.17253
40. Hilhorst-Hofstee Y, Rijlaarsdam ME, Scholte AJ, Swart-van den Berg M, Versteegh MI, van der Schoot-van Velzen I, et al. The clinical spectrum of missense mutations of the first aspartic acid of cbEGF-like domains in fibrillin-1 including a recessive family. *Hum Mutat.* (2010) 31:E1915–27. doi: 10.1002/humu.21372
41. Piacentini G, Mastromoro G, Bottoni A, Romano V, Riccardi R, Orfeo L. Pathophysiology of coarctation of the aorta in dichorionic twins with growth discordance. *Ultrasound Obstet Gynecol.* (2022) 59:124–5. doi: 10.1002/uog.23717
42. Singh SD, Xu XY, Pepper JR, Treasure T, Mohiaddin RH. Biomechanical properties of the Marfan's aortic root and ascending aorta before and after personalised external aortic root support surgery. *Med Eng Phys.* (2015) 37:759–66. doi: 10.1016/j.medengphy.2015.05.010
43. Pons R, Guala A, Rodriguez-Palomares JF, Cajas JC, Dux-Santoy L, Teixido-Tura G, et al. Fluid-structure interaction simulations outperform computational fluid dynamics in the description of thoracic aorta haemodynamics and in the differentiation of progressive dilation in Marfan syndrome patients. *R Soc Open Sci.* (2020) 7:191752. doi: 10.1098/rsos.191752
44. Syyong HT, Chung AW, Yang HH, van Breemen C. Dysfunction of endothelial and smooth muscle cells in small arteries of a mouse model of Marfan syndrome. *Br J Pharmacol.* (2009) 158:1597–608. doi: 10.1111/j.1476-5381.2009.00439.x
45. Meng H, Tutino VM, Xiang J, Siddiqui A. High WSS or low WSS? Complex interactions of hemodynamics with intracranial aneurysm initiation, growth, and rupture: toward a unifying hypothesis. *AJNR Am J Neuroradiol.* (2014) 35:1254–62. doi: 10.3174/ajnr.A3558
46. LaDisa JF Jr, Olson LE, Molthen RC, Hettrick DA, Pratt PF, Hardel MD, et al. Alterations in wall shear stress predict sites of neointimal hyperplasia after stent implantation in rabbit iliac arteries. *Am J Physiol Heart Circ Physiol.* (2005) 288:H2465–75. doi: 10.1152/ajpheart.01107.2004
47. Moghadam ME, Bazilevs Y, Hsia TY, Vignon-Clementel IE, Marsden AL, Allianc MCH, et al. Comparison of outlet boundary treatments for prevention of backflow divergence with relevance to blood flow simulations. *Comput Mech.* (2011) 48:277–91. doi: 10.1007/s00466-011-0599-0
48. Lotz J, Meier C, Leppert A, Galanski M. Cardiovascular flow measurement with phase-contrast MR imaging: basic facts and implementation. *Radiographics.* (2002) 22:651–71. doi: 10.1148/radiographics.22.3.g02ma11651

Conflict of Interest: The authors declare that the research was conducted in the absence of any commercial or financial relationships that could be construed as a potential conflict of interest.

Publisher's Note: All claims expressed in this article are solely those of the authors and do not necessarily represent those of their affiliated organizations, or those of the publisher, the editors and the reviewers. Any product that may be evaluated in this article, or claim that may be made by its manufacturer, is not guaranteed or endorsed by the publisher.

frontiers | Frontiers in Pediatrics

REVIEW
published: 16 May 2022
doi: 10.3389/fped.2022.876742

Cardiac Imaging in Patients After Fontan Palliation: Which Test and When?

Paolo Ciliberti[1], Paolo Ciancarella[2], Pasqualina Bruno[1], Davide Curione[2], Veronica Bordonaro[2], Veronica Lisignoli[1], Mario Panebianco[1], Marcello Chinali[1], Aurelio Secinaro[2], Lorenzo Galletti[1] and Paolo Guccione[1]*

[1] Department of Cardiac Surgery, Cardiology, Heart and Lung Transplantation Bambino Gesu' Children's Hospital, IRCCS, Rome, Italy, [2] Advanced Cardiothoracic Imaging Unit, Bambino Gesù Children's Hospital, IRCCS, Rome, Italy

The Fontan operation represents the final stage of a series of palliative surgical procedures for children born with complex congenital heart disease, where a "usual" biventricular physiology cannot be restored. The palliation results in the direct connection of the systemic venous returns to the pulmonary arterial circulation without an interposed ventricle. In this unique physiology, systemic venous hypertension and intrathoracic pressures changes due to respiratory mechanics play the main role for propelling blood through the pulmonary vasculature. Although the Fontan operation has dramatically improved survival in patients with a single ventricle congenital heart disease, significant morbidity is still a concern. Patients with Fontan physiology are in fact suffering from a multitude of complications mainly due to the increased systemic venous pressure. Consequently, these patients need close clinical and imaging monitoring, where cardiac exams play a key role. In this article, we review the main cardiac imaging modalities available, summarizing their main strengths and limitations in this peculiar setting. The main purpose is to provide a practical approach for all clinicians involved in the care of these patients, even for those less experienced in cardiac imaging.

Keywords: congenital heart disease, Fontan operation, echocardiography, cardiac CT, cardiac MRI

OPEN ACCESS

Edited by:
Antonio Francesco Corno, Children's Memorial Hermann Hospital, United States

Reviewed by:
Michal Odermarsky, Skåne University Hospital, Sweden
Santosh Uppu, University of Texas Health Science Center at Houston, United States

****Correspondence:***
Paolo Ciliberti
paolo.ciliberti@opbg.net

Specialty section:
This article was submitted to Pediatric Cardiology, a section of the journal Frontiers in Pediatrics

Received: *15 February 2022*
Accepted: *13 April 2022*
Published: *16 May 2022*

Citation:
Ciliberti P, Ciancarella P, Bruno P, Curione D, Bordonaro V, Lisignoli V, Panebianco M, Chinali M, Secinaro A, Galletti L and Guccione P (2022) Cardiac Imaging in Patients After Fontan Palliation: Which Test and When? Front. Pediatr. 10:876742. doi: 10.3389/fped.2022.876742

BACKGROUND

The Fontan operation represents the final stage of a series of palliative surgical procedures for children born with complex congenital heart disease, where a "usual" biventricular physiology cannot be restored (1). Unlike the normal cardiovascular system, where pulmonary and systemic circuits are connected in series with a double propelling pump (the right and left ventricles), after this surgical palliation there is a direct connection of the systemic venous returns to the pulmonary arterial circulation without an interposed ventricle (2). In this unique physiology, the absence of a subpulmonary ventricle results in systemic venous hypertension for propelling blood through the pulmonary vasculature (2, 3). Therefore pulmonary vasculature resistance has a key role in determining adequate ventricular preload and maintaining an adequate cardiac output in these patients (2, 4). In effect modulation of PVR may provide a benefit in this peculiar setting (3, 5).

Although the Fontan operation has dramatically improved survival in patients with a single ventricle congenital heart disease (6–8), significant morbidity is still a concern (9, 10).

Chronic elevation of systemic venous pressure, required to maintain transpulmonary blood flow, leads to a multitude of complications. Furthermore, these patients experience a decreased exercise capacity due to chronic low cardiac output as a consequence of inability to adequately increase it during exercise mainly because of chronotropic incompetence (11).

In addition, as a consequence of improved survival of these patients, the incidence of the so-called "Failing Fontan" is increasing. The "Failing Fontan" is a status characterized by progressive clinical deterioration and reduced health-related quality of life (10). Multiorgan dysfunction, peripheral edema, ascites, abnormal protein turnover and liver dysfunction are in fact the main features of Fontan Failure. Its pathogenesis is still not completely understood, and once established, the outcome is poor and heart transplant is the only possible treatment. Hence, early diagnosis and cardiac transplant listing are crucial in this setting.

Due to these significant possible complications, patients who undergo the Fontan procedure need close clinical and imaging monitoring, where cardiac exams play a key role (12, 13).

The aim of this review is to highlight the information that can be obtained with each imaging modality and to illustrate their weaknesses in this peculiar setting.

WHAT IS THE FONTAN CIRCULATION?

Nearly 10% of congenital heart defects belong to the group of functionally univentricular hearts (3). This condition is usually characterized by the presence of only one well-developed ventricle able to sustain cardiac output. Less frequently, there could be two well-developed ventricles but with a major intracardiac shunt that makes their separation not achievable. In any case, there is a "single" available ventricle that has to maintain both the systemic and the pulmonary circulations, which are not connected as usual in series but in parallel. Such a circuit has two major handicaps: arterial desaturation and a chronic ventricular volume overload (1).

The Fontan operation represents the final surgical stage in the strategy of palliation for the management of patients born with an anatomical or functional univentricular heart (1).

The idea behind this palliation is to use the only ventricle available to sustain the systemic circulation by connecting it to the aorta, while ensuring an acceptable blood flow into the lungs in a passive way, without any additional propelling source, by connecting directly the systemic veins to the pulmonary arteries. The major advantage of this strategy is the separation between the systemic and pulmonary circulation with normalization of oxygen saturation.

Since the original description (14) in the early 70s, when Fontan and Baudet performed the anastomosis of the superior caval vein to the right pulmonary artery (Glenn shunt) and the direct suture of the right atrial appendage onto the proximal right pulmonary artery in a patient with Tricuspid Atresia, several modifications have led to the contemporary total cavo-pulmonary connection (TCPC).

Currently, TCPC is achieved by a multistage surgical approach where the Fontan operation represents the last step.

In early life, the goal of the initial surgical operation (first step) is to allow for survival, providing an unobstructed systemic outlet and a controlled pulmonary blood flow. Later, total cavopulmonary connection is usually achieved using a two-stage operation. A superior cavopulmonary connection (the superior vena cava is anastomosed to the pulmonary arteries) is performed at about 6 months of age (second step). The patient remains cyanotic after this stage, because desaturated blood flow coming from the inferior caval vein is still directed to the main ventricle and then to the aorta, but ventricle loading is significantly decreased. Total cavopulmonary connection (third and last step) is performed ordinarily between 3 and 5 years of age (depending on single center preference, patient saturation, growth of vessels), connecting the inferior vena cava to the pulmonary arteries, usually by interposition of an extracardiac conduit. This leads to complete separation of the systemic and pulmonary circulations and to normalization of oxygen saturation.

In patients at high risk of system failure due to small pulmonary arteries or ventricular dysfunction, a little communication (fenestration) between the extracardiac conduit and the systemic atrium can be created, allowing a protective "right-to-left shunt", which limits systemic venous congestion, increases ventricular preload and output, with the unavoidable drawback of some degree of arterial desaturation (15). Later, the fenestration can be closed with a device using a transcatheter approach, even if a substantial number of small fenestrations also close spontaneously during follow-up (16).

MAIN LONG-TERM COMPLICATIONS IN PATIENTS WITH FONTAN PALLIATION

Although when assessing long-term results of the Fontan operation several confounding factors may occur in relation to the different underlying defects and to the evolution of surgical management, long term follow-up data indicates that this operation has incredibly improved survival in patients born with "functionally univentricular hearts". Without surgery, these patients only had a 10% chance of survival beyond the first year of life (17), whilst current survival rate after Fontan surgery seems to be of 74, 61, and 43% at 10-, 20-, and 30-years, respectively (6).

Therefore, nowadays the main issue in these patients is the significant morbidity consequent to the Fontan operation. Several complications occur late after surgery, and are almost unavoidable, mainly due to the systemic venous hypertension required to propel blood into the system (3). Potential complications are various and the most frequent are arrhythmias, thromboembolic events, cyanosis, hepatic dysfunction/cirrhosis, protein-losing enteropathy (PLE), and plastic bronchitis (10).

With the "Classic Fontan" operation, where the right atrium was incorporated in the Fontan circulation, progressive atrial dilatation was a major issue, causing atrial arrhythmias and thromboembolic events. The incidence of these adverse events has been significantly reduced by the evolution of the surgical technique. Nevertheless, arrhytmias can still occur even with

TCPC, in particular supraventricular tachycardia, which is more frequent with the aging of patients and may negatively affect the hemodynamics of the Fontan circulation, also predisposing to thrombotic events. The main mechanism of formation are atrial re-entry microcircuits (18) which can be favored both by intrinsic alterations of myocardial tissue (19) and by the presence of multiple atrial sutures and surgical anastomoses.

Thromboembolic events can also occur and remain one the main causes of death in this setting (20). Predisposing factors are reduced cardiac output, abnormal flow in the systemic and pulmonary veins, atrial dilation and arrhythmias. At the same time, a reduction of coagulation factors, due to liver failure and PLE, can sometimes induce an increased hemorrhagic risk.

The increased systemic venous pressure leads to elevated pressure and congestion in the hepatic veins as well, causing pathological changes in the liver. Congestion, dilation of bile ducts, fibrosis, and cirrhosis can occur, exposing these patients even to liver malignancy (21, 22).

Additionally, the increased central venous pressure may induce recanalization of embryologically preformed and obliterated vessels, with the development of systemic to pulmonary venous collaterals that can lead to systemic desaturation and worsening of ventricular function (3).

The elevated pressure in the superior vena cava is transmitted to the thoracic duct as well, leading to impaired and abnormal lymphatic drainage, which can cause two rare but extremely dangerous complications: PLE and plastic bronchitis. Leakage into the intestine causes PLE, which represents the most frequent lymphatic problem in this setting (23). PLE implies an abnormal loss of proteins in the intestinal lumen secondary to intestinal lymphangiectasia with leakage of lymphocytes, chylomicrons and serum proteins, such as albumin and immunoglobulin, resulting in edema, ascites and immunodeficiency. Lymphatic leakage into the bronchi leads to the development of plastic bronchitis (3). This is an extremely uncommon but dreadful complication, where the formation of bronchial casts in the airway can cause bronchial obstruction and asphyxia. Casts are made up of cells and inflammatory products or of mucin and fibrin. The exact mechanism of cast formation, which is anyway driven by increased lymphatic pressure, is quite unclear.

Moreover, over time the systemic ventricle may develop systolic and/or diastolic dysfunction because of the abnormal hemodynamic condition and ventricular morphology (24). Ventricular dysfunction can be triggered both by the congenital malformation itself, even before surgical treatment, and by the abnormal working and loading ventricle conditions at the different stages of palliation. The congenital malformation itself may predispose to ventricular dysfunction especially in the presence of a morphologic right ventricle, which is not suited for and may fail after some years of systemic loading. In addition, a tricuspid valve often poorly tolerates the initial volume overload and the systemic afterload, leading to valve regurgitation and further volume overload (1). During the first months after birth, the single ventricle is always subjected to volume overload, having to sustain both the systemic and pulmonary circulations. This volume overload leads to dilation, spherical remodeling and eccentric hypertrophy. The preload to the ventricle is then acutely reduced, firstly at the time of the Glenn shunt and later at the time of the Fontan operation. The ventricle thus goes from being overloaded and overstretched to being significantly underloaded. This change in loading conditions can lead to systolic and diastolic dysfunction. Furthermore, the ventricle may enter a vicious cycle whereby diastolic impairment can further increase pulmonary vascular resistance, resulting in worsening of ventricular filling and therefore declining systolic function and cardiac output (24).

HOW TO IMAGE THE FONTAN CIRCUIT?

What We Need to Know?

In a patient who underwent the Fontan operation, routine follow up must check that the palliation system is working properly. Early signals of failing should be promptly detected by imaging, both for planning a circuit optimization if possible and to lead to an early transplant listing when perfectioning can not be achieved.

The main goals of a comprehensive assessment are the ventricle and atrioventricular valve function, the patency of the Fontan pathway (IVC to PA conduit, Glenn Shunt and pulmonary arteries), and the presence of collateral flow (12). Ruling out an increase in pulmonary vascular resistance, and the presence of extracardiac issues (in particular liver dysfunction/malignancy and lymphatic disorders) are the other targets of a complete evaluation (12). Any other anatomical issue such as residual systemic obstruction (residual coarctation, ventricular septal defect stenosis, pulmonary veins compression or stenosis) must also be identified. If these lesion are amenable to correction, the palliation system efficiency may be significantly improved.

The different modalities have have their own strengths and weaknesses (**Table 1**) and they should be used in a complementary fashion to accurately assess anatomy, hemodynamics, and prognosis in these patients.

Strenghts and Weaknesses of the Main Imaging Modalities

Echocardiography

Echocardiography (ECHO) is the most used imaging modality in patients with congenital heart disease. It is an unequaled image modality in terms of availability, cost and ease of use, being

TABLE 1 | Schematic summary of main strenghts and weaknesses of each imaging modality.

	ECHO	CMR	CCT	CATH
Easiness of use	++++	++	+++	+
Invasiveness/harmfulness	+	++	+++	++++
Anatomical assessment	++	+++	++++	+++
Functional assessment	++	+++	++	++++
Possibility of intervention	/	/	/	++++
Extracardiac assessment	+	++++	+++	+

possible even at the patient's bedside.Therefore, it remains the first-line imaging modality even in this peculiar setting (25).

Nevertheless, as patients grow into adulthood, image quality is often limited due to diminishing acoustic windows. Multiple factors may be implicated, such as higher BMIs and chest wall deformity, particularly in patients who underwent multiple cardiac surgical operations (26). As a consequence, in adult Fontan patients ECHO may provide incomplete information, often targeted to ventricular and valvular function.

Fontan pathway and pulmonary arteries may sometimes be visualized in case of good acoustic windows. Nevertheless, CCT or CMR should be performed to rule out any issues with certainty, allowing for unrestricted visualization of all structures (13).

Regarding ventricular function, it is well known that single ventricle function is not easy to assess, particularly when the single ventricle is a morphologic right ventricle. Agreement between echocardiographic and CMR evaluation of systolic function improves with experience in this setting but remains suboptimal. Especially when used as a test for assessing poor RV function, ECHO shows a high sensitivity, but specificity is heavily influenced by operator experience, with the risk of a relatively high rate of false positives (27). Regarding diastolic function, which is frequently impaired in these patients, it is important to know that the interpretation of standard parameters (mitral valve inflow velocities, and E/E′ ratio using tissue doppler modality) in single ventricle physiology may be challenging, and standard values are generally not available (28). Atrial size as well, which is a commonly used parameter of diastolic function in normal heart physiology, is typically not applicable in Fontan patients. Therefore, although it is technically feasible to utilize standard parameters, assessing diastolic function in single ventricle is extremely challenging (29). Further studies are required for verification of specific parameters in this setting.

Atrio-Ventricular (AV) valve regurgitation is a common long-term complication in single ventricle circulation and ECHO remains the main imaging modality to routinely investigate valvar function. It can be performed using several imaging and Doppler parameters such as regurgitation jet area, vena contracta width, in addition to qualitative jet assessment (28).

In summary, ECHO remains the first line imaging and a reliable method for systolic ventricular function (**Supplementary Video 1**) and valve assessment. A full echocardiographic study should be part of every outpatient check-up, at intervals of no more than 12 months.

Cardiovascular Magnetic Resonance

Cardiovascular Magnetic Resonance (CMR) is the only method able to simultaneously obtain a comprehensive anatomical and functional assessment.

The advantages of this imaging modality are well recognized: the lack of invasiveness and ionizing radiation, the ability to visualize the entire cardio-thoracic anatomy with high spatial resolution and without acoustic window limitations, the opportunity to obtain hemodynamic and functional information thanks to the assessment of flows in any target vessel and to the accurate quantification of ventricular function (30). Excellent tissue characterization of the ventricular myocardium can also be achieved (30).

However, CMR also has some drawbacks, mainly represented by the long scanning times, which necessitate general anesthesia in uncooperative patients (such as under 7–8 years of age) and make the exam difficult to perform in clinically unwell subjects. In addition, image quality can be limited by arrhythmia and CMR is not suitable in patients suffering from claustrophobia and in the presence of unsafe metallic devices (13).

Anatomical Vascular Assessment

The entire cardio-thoracic anatomy is well depicted with contrast-enhanced magnetic resonance angiogram (MRA) and with non-contrast ECG-gated 3D sequences. Also, cine bright-blood sequences offer a good representation of vascular anatomy thanks to high blood-tissue contrast and dynamic visualization of vessels during the cardiac cycle (**Figures 1**, **2**). Black-blood imaging is useful when ferromagnetic devices are present, due to its lesser sensitivity to magnetic field inhomogeneity.

The Fontan pathway and branch pulmonary arteries (PAs) are carefully evaluated to rule out stenoses that could be detrimental to flow dynamics in a circulatory system without a subpulmonary pump. Central PAs can be compressed and stretched by vessel roots and neo-aorta dilatation after the Norwood operation. Residual/recurrent coarctation of the aorta after aortic arch reconstruction is another complication that occurs in these patients and can promote ventricular hypertrophy and dysfunction. Pulmonary vein compression can be harmful to passive pulmonary flow circulation and need to be

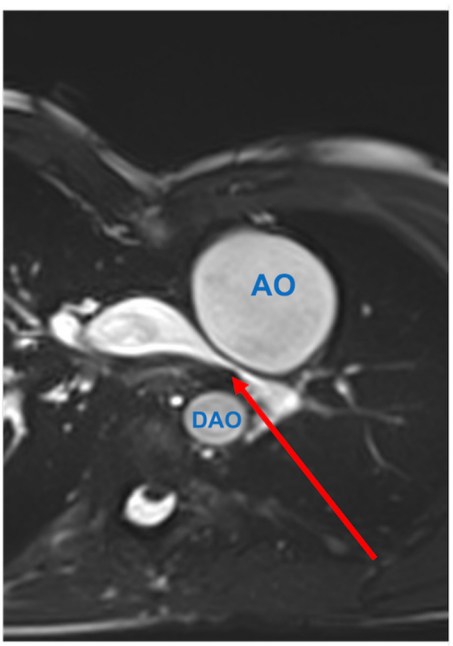

FIGURE 1 | Pulmonary artery stenosis (red arrow) seen by CMR. Axial SSFP-cine view shows the left pulmonary artery is compressed between the dilated aortic root (AO) and the descending aorta (DAO).

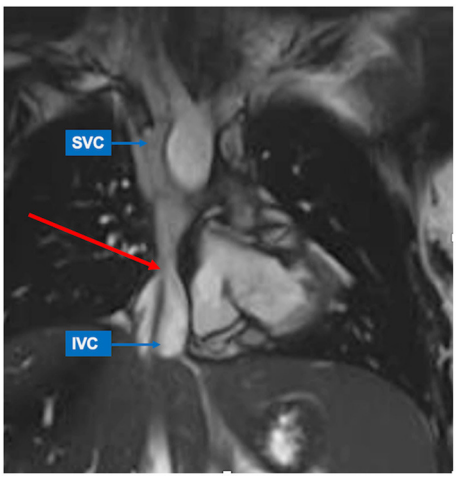

FIGURE 2 | Inferior caval vein (IVC)-to-pulmonary artery stenosis (red arrow) seen by CMR. SSFP-coronal view demonstrates focal stenosis of the IVC-to-pulmonary artery pathway (red arrow). The superior caval vein (SVC) shows normal size.

excluded, especially in patients with enlarged right atrium after atriopulmonary Fontan.

Ventricular Evaluation and Tissue Characterization

CMR is the gold standard for the assessment of ventricular size and function in univentricular hearts (31) regardless the "original anatomy" and ventricle type (**Figure 3**). Global and regional functional evaluation is obtained with standard cine SSFP sequences in short and long axis views. Morpho-functional parameters are calculated with dedicated post-processing software by tracing endocardial contours on a contiguous stack of short axis slices at end-diastole and end-systole, using Simpson's method. Hypoplastic ventricular chambers should be included if they contribute to systemic output, paying attention to exclude the interventricular septum from the blood pool.

Although a normal reference range for ventricular volumes in UVH has not been universally defined, serial assessment of ventricular dimensions is important because dilatation of systemic ventricle is an independent risk factor for death and transplant after Fontan palliation (32), and echocardiography systematically underestimates ventricular volumes by 30% compared to CMR (33).

Tissue characterization with late gadolinium enhancement technique allows to identify the presence and extent of myocardial fibrosis, which correlates with decreased ventricular function, increased EDVi and incidence of ventricular tachyarrhythmia (32).

Flow Assessment

Vessel flow analysis is routinely performed with conventional through-plane 2D phase-contrast (PC) sequences. PC can be used to assess cardiac index, calculate semilunar valve regurgitation by direct quantification or estimate atrioventricular valve regurgitation by matching antegrade systemic flow and ventricular stroke volume. Hemodynamic magnitude of a unilateral branch pulmonary artery stenosis can be evaluated by calculating disproportion of pulmonary blood flow distribution.

Flow analysis includes quantification of systemic-to-pulmonary collaterals. Elevation of central venous pressure promotes development of veno-venous collaterals which arise from superior or inferior vena cava and innominate veins, and connect to pulmonary veins or directly to the atria, thus bypassing pulmonary vascular bed with consequent cyanosis.

Aorto-pulmonary collaterals (APCs) are a response to systemic desaturation: they originate from systemic arteries (descending aorta and its branches), and supply the pulmonary circulation with high pressure flow which compete and limit deoxygenated blood flow from cavo-pulmonary connection. APCs also represent a right-to-left shunt and contribute to ventricular volume overload (34). With PC sequences, the burden of systemic-to-pulmonary collaterals can be calculated by subtracting the pulmonary arterial flow from the pulmonary venous flow or by subtracting the sum of caval flows from the aortic flow (35). Angiographic imaging can also help to identify major collateral vessels, which can represent the target for interventional procedures.

Extra-Cardiac Complications

Fontan-associated liver disease (FALD) represents a major non-cardiac determinant of mortality following the Fontan procedure and an emerging concern in patients with univentricular pathophysiology. Hemodynamic changes with elevated central venous pressure and diminished cardiac output promote congestive hepatopathy, resulting in progressive fibrosis/cirrhosis in response to chronic liver injury, with multiple regenerative nodules which may finally degenerate to hepatocellular carcinoma. The staging and surveillance of liver fibrosis in FALD requires a multi-modality approach, including radiological imaging. US elastography is a valuable screening investigation in identifying features of FALD and may be useful in identifying progression of FALD before biochemical hepatic dysfunction. Both magnetic resonance imaging and computed tomography provide more detailed information in delineating liver injury in FALD (**Figure 4**), and are more appropriate to detect and characterize focal liver lesions (36). Although there is no consensus on the surveillance plan of patients with FALD, serial follow-up of liver fibrosis and monitoring of hypervascular hepatic nodules is recommended (37).

Increased systemic venous pressure is also associated with impaired lymphatic drainage and engorgement of the lymphatic system. Patients with lymphatic perfusion abnormalities develop significant more early and late complications after Fontan completion, even in the absence of obstruction in the Fontan pathway or ventricular dysfunction. Various manifestations can occur such as protein losing enteropathy (PLE), plastic bronchitis (PB), interstitial pulmonary edema, pleuro-pericardial effusion and ascites.

PLE and PB are among the most serious complications that can occur late after Fontan Palliation. MR is able

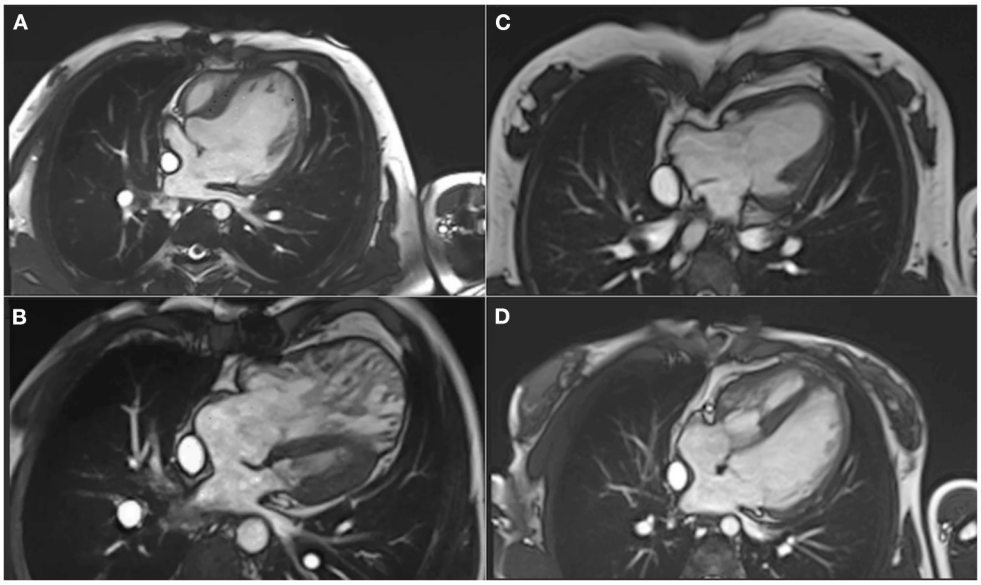

FIGURE 3 | Different types of ventricle anatomy in patients with Fontan Palliation seen by CMR (4-chamber views). **(A)** Tricuspid Atresia. **(B)** Hypoplastic Left Heart Syndrome. **(C)** Double Inlet Left Ventricle. **(D)** Pulmonary Atresia and intact Ventricular Septum with hypoplastic right ventricle.

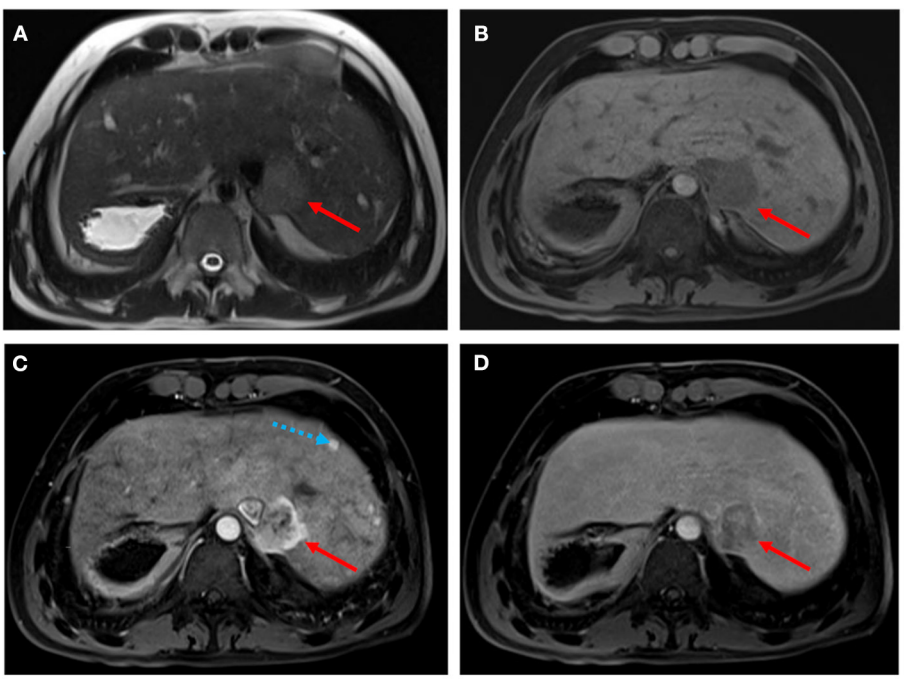

FIGURE 4 | Hepatocellular carcinoma in a 30-year-old man with Fontan palliation. Axial T2- and T1-weighted MR images **(A,B)** show a 4 cm paracaval solid lesion with smooth margins and posterior hepatic capsule bulge (arrows). The tumor shows heterogeneous hyperintensity in the arterial phase of the dynamic contrast-enhanced sequence **(C)**, and typical washout in the delayed phase **(D)**. The background liver is diffusely heterogeneous after contrast injection, with multiple small arterial-enhancing foci [dotted blue arrow in **(C)**] without delayed washout, in keeping with hypervascular regenerative hepatic nodules.

to characterize lymphatic perfusion abnormalities using static and dynamic sequences (**Figure 5**). Heavily T2-weighted static lymphangiography is a fast and noninvasive method to visualize the lymphatic system, define perfusion abnormalities in the thoracic and mesenteric regions and identify impaired lymphatic drainage with thoracic duct dilatation (38). Pre-Fontan assessment with T2 imaging help to identify patients with higher-grade lymphatic perfusion abnormalities who are more likely to develop post-surgical complications, improving pre-surgical risk stratification and identifying the subjects who could benefit from a lymphatic treatment (39).

Dynamic contrast-enhanced magnetic resonance lymphangiography (DCMRL) is a recently developed technique which allows a minimally invasive evaluation of the lymphatic flow pathways and their anomalies, using time-resolved MR angiography sequence after intranodal injection of gadolinium-based contrast material (40). DCMRL demonstrates abnormal pulmonary lymphatic streaming toward the peribronchial lymphatics and lung parenchyma and can be useful for planning interventional strategies of thoracic duct embolization (41).

Cardiac Computed Tomography

Cardiac Computed Tomography (CCT) is an alternative imaging modality to assess Fontan anatomy and ventricular function when CMR is contraindicated or in specific clinical conditions such as unstable and uncooperative patients, stent evaluation and acute setting (**Figure 6**). Thanks to its high spatial resolution and short acquisition time, CCT represents a powerful tool for a comprehensive anatomical evaluation of cardiac and extra-cardiac vascular structures, thus reducing the need for diagnostic catheterization. The main weaknesses of CCT are the lack of flow assessment, which limits functional information, relatively low temporal resolution, poor tissue contrast, and exposition to ionizing radiation (quite low with recent systems) and contrast administration (potentially causing allergic reactions and nepropathy) (42).

CCT scan in this setting can be challenging to perform. The main issue in evaluating these patients is to obtain a uniform opacification of the venous pathway and the pulmonary arteries. Typically, blood flow from the superior vena cava is directed to right lung, whereas flow from the inferior vena cava is mostly directed to the left lung. The result is a different timing of opacification of the caval veins and the pulmonary arteries. Hence, conventional contrast administration into the upper arms and first pass through the SVC and PAs generates streak artifacts and pseudo-filling defects which can mimic thrombosis (**Figure 7**). Various protocols have been proposed to avoid these pitfalls, such as single-injection single-phase technique with a late acquisition after 80–90 s, or a dual-injection dual-phase technique that requires contemporary use of two peripheral venous accesses (both upper and lower extremities) (43). The latter may be the preferred strategy for the assessment of pulmonary thromboembolic complications because it offers simultaneous opacification of the pulmonary arteries in the same vascular phase (44).

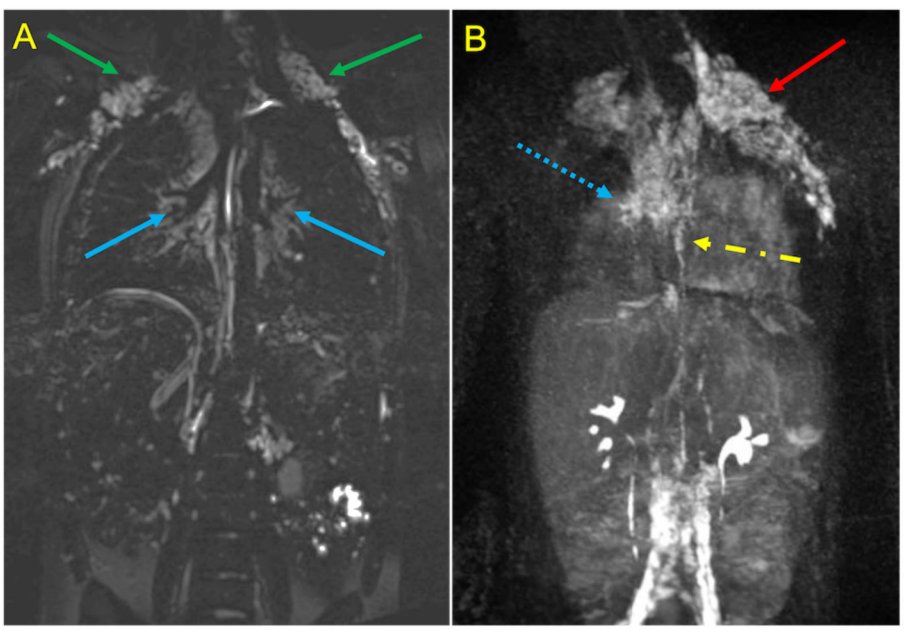

FIGURE 5 | MR Lymphangiography in a Patient treated with TCPC palliation complicated by plastic bronchitis. Static T2-SPACE coronal image **(A)** demonstrates abnormal supraclavicular (green arrows) and peri-hilar (blue arrows) lymphostasis. Dynamic contrast-enhanced MIP coronal image **(B)** after intranodal contrast injection shows rapid filling of retroperitoneal lymphatics and of the thoracic duct (yellow arrow), with marked reflow into supraclavicular (red arrow) and mediastinal channels (dotted blue arrow).

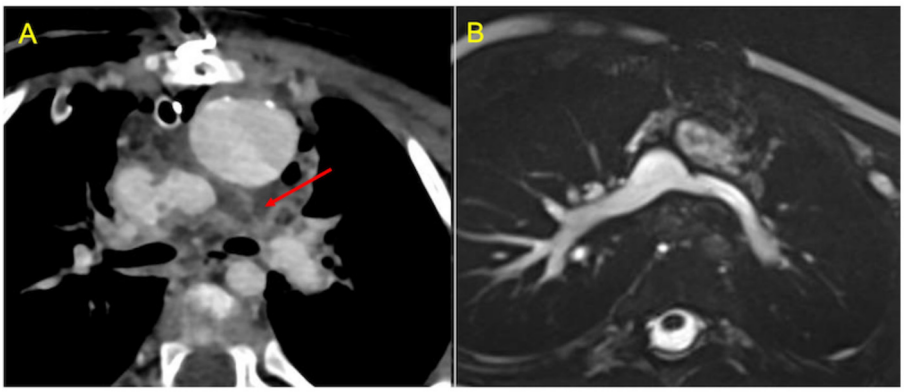

FIGURE 6 | Use of CCT in the acute setting. **(A)** contrast-enhanced axial image shows early post-operative left pulmonary artery thrombosis with a filling defect extended from the cavo-pulmonary anastomosis to the left hilum (red arrow). **(B)** CMR axial SSFP view performed 2 months after surgical reintervention demonstrates vessel patency.

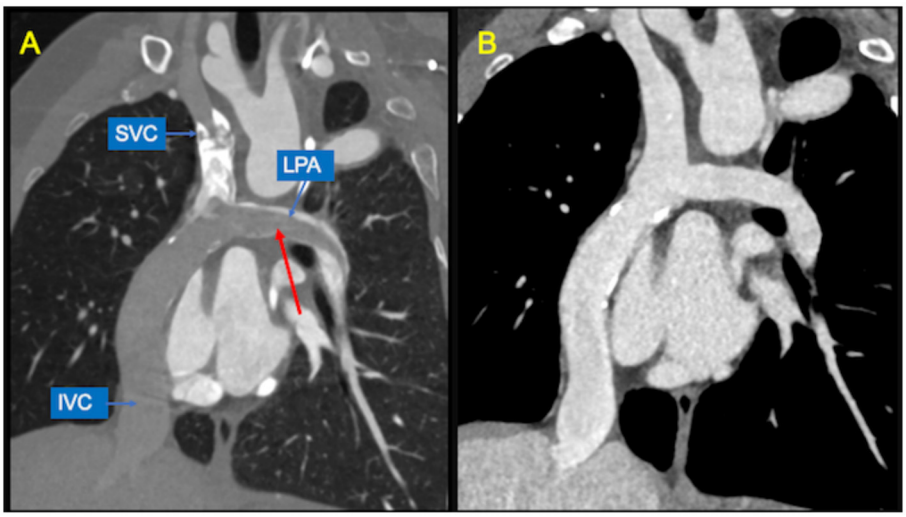

FIGURE 7 | Potential pitfalls of CCT with single-injection protocol. **(A)** Coronal image shows mixing of contrast material from the superior vena cava (SVC) and unopacified blood from inferior vena cava (IVC), generating pseudo-filling defects in the left pulmonary artery (LPA) during the early arterial phase (red arrow). **(B)** The same image obtained during venous recirculation of contrast reveals regular patency of the Fontan circuit.

A systemic arterial phase acquisition is generally indicated for coronary artery imaging or when functional assessment is requested (43). Volumetric and functional data obtained with ECG-gated scan protocol shows good agreement with CMR measurement, at the expense of a substantial increase in radiation burden (45).

Assessment of vascular stents (**Figure 8**) represents another specific indication for CCT. However, beam-hardening artifacts generated by metallic material could limit the evaluation of lumen patency and in-stent restenosis caused by neo-intimal hyperplasia or stent thrombosis.

Cardiac Catheterization

In recent years, the use of cardiac catheterization as diagnostic imaging modality has significantly decreased, because of the advent of new non-invasive advanced imaging techniques, such as CCT and CMR.

Nevertheless, catheterization remains crucial when the likelihood of an intervention for circuit optimization is high and when specific hemodynamic parameters are needed, such as assessment of PVR, ventricular diastolic function (including constrictive and restrictive physiology) and pressure gradients (25).

Cardiac catheterization is the only method able to accurately measure end diastolic ventricular pressure, Fontan system pressure and transpulmonary gradient (46). In addition, in case of anatomical issues, such as residual aortic coartaction, or pulmonay branches or conduit stenosis, catheterization is the only technique for assessing real pressure gradients and thus the real hemodynamic significance of a lesion.

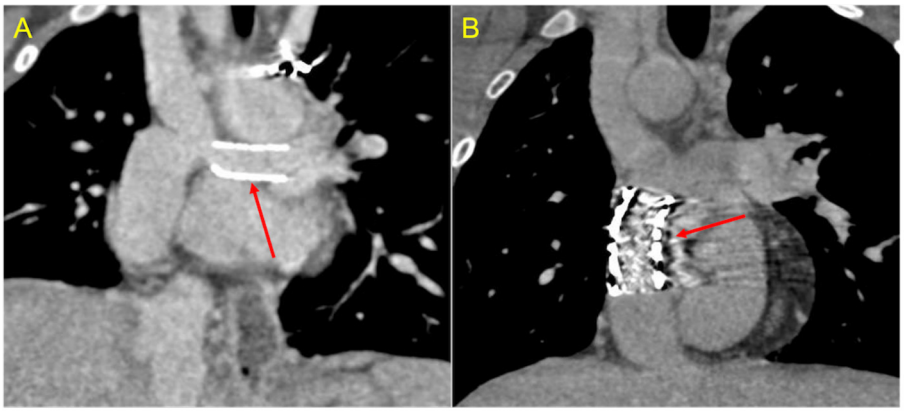

FIGURE 8 | Stent assessment with CCT. **(A)** Coronal image in a Fontan patient with left pulmonary artery stenting (red arrow) illustrates how stent lumen patency can be evaluated during the venous phase with a homogeneous opacification of all vessels. **(B)** Coronal image in a Fontan patient with IVC-to-pulmonary artery conduit stenting (red arrow) demonstrates that ruling out in-stent restenosis can sometimes be difficult due to beam-hardening artifacts.

As catheter evaluation of estimated flows using the Fick principle and assumed oxygen consumption is limited and potentially incorrect (46), combined invasive catheter hemodynamics and simultaneous CMR evaluation is used in some centers to optimize vascular resistance evaluation (47, 48). This is the best method for measuring real pulmonary vascular resistance in clinical practice, especially in patients who are listed for transplantation because of a failing Fontan palliation (46). Moreover, radiation exposure remains a major drawback of pediatric and congenital cardiac catheterization. Over the recent years, many technological advances have led to faster CMR scanning time and real-time magnetic resonance imaging, allowing CMR guided cardiac catheterization (49, 50). The initial in-man experience of MRI-guided cardiac catheter interventions was halted due to MRI-compatible guidewire limitations (51). Ongoing investment and research on MRI-compatible guidewires may lead to MRI-guided diagnostic and interventional catheterization coming into the mainstream, avoiding all radiation exposure and improving soft tissue imaging (49, 51).

Cardiac catheterization can perform treatment at almost any levels of the Fontan system, (extracardiac conduit, pulmonary arteries, superior caval vein), with angioplasty or stent placement. It is also possible to percutaneously close (if no longer needed) or create (in failing systems) a fenestration (52). If significant collateral vessels are present (**Figure 9**), it is possible to close them through coil injection. Treatment of these vessels increases short and medium-term survival in Fontan candidates and reduces system failure in patients after total cavo-pulmonary anastomosis.

Lymphangiography could play an important role in case of complications with a suspected lymphatic etiopathology such as protein-losing enteropathy or plastic bronchitis. Some high-volume centers are developing techniques for embolizing these periportal/peritracheal dilated lymphatic vessels with good results (53).

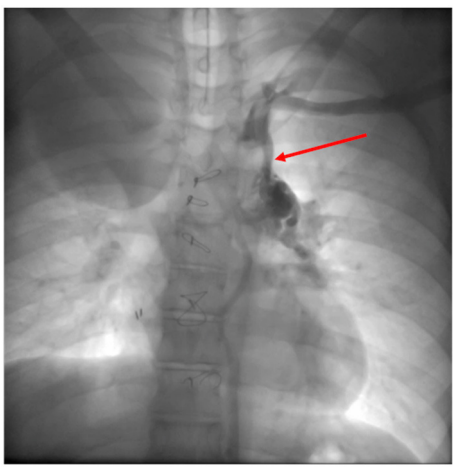

FIGURE 9 | Veno-venous collateral vessel seen by Cardiac Catheterization. After injection in the left arm a large vessel (red arrow) arising from the left brachiocephalic venous system is visualized. The vessel courses inferiorly connecting to the left pulmonary veins.

In summary, the main strengths of cardiac catheterization are the possibility of intracavitary pressure measurement and the possibility of interventions during the same procedure if needed. The main drawbacks include the invasive nature often requiring anesthesia or sedation, ionizing radiation exposure and contrast nephrotoxicity. Recent ESC GUCH Guidelines recommend Cardiac catheterization at a low threshold in cases of unexplained oedema, exercise deterioration, new-onset arrhythmia, cyanosis, and haemoptysis (25).

CONCLUSION

Patients with Fontan physiology suffer from a multitude of unavoidable complications mainly due to the increased systemic venous pressure. Consequently, these patients need close clinical

and imaging monitoring, since early recognition of failing hemodynamics can be essential to secure long-term survival.

ECHO remains the first-line method, and is mainly used for routine follow-up.

Nevertheless, nowadays cross-sectional imaging has become an essential tool in the evaluation of these patients. CMR in particular has acquired a key role in providing anatomic and functional information at the same time, overcoming the limitations of poor acoustic ECHO windows as patients become adults. CMR is also able to provide essential information about extra-cardiac complications such as liver dysfunction and abnormal lymphatic drainage. CCT may be useful when CMR is contraindicated or for anatomical assessment in uncooperative patients. Cardiac catheterization is currently reserved for measuring specific hemodynamic parameters and for those patients where an intervention during the same procedure is expected.

AUTHOR CONTRIBUTIONS

PCil, LG, and AS contributed to conception of the review. PCia, MC, VB, DC, PG, MP, PB, and VL wrote sections of the manuscript. PCil wrote the first draft of the manuscript. All authors contributed to manuscript revision, read, and approved the submitted version.

SUPPLEMENTARY MATERIAL

The Supplementary Material for this article can be found online at: https://www.frontiersin.org/articles/10.3389/fped.2022.876742/full#supplementary-material

Supplementary Video 1 | Echocardiographic 4 chamber view in a patient born with Tricuspid Atresia who underwent Fontan Palliation, showing significant global systolic dysfunction.

REFERENCES

1. Gewillig M. The Fontan circulation. *Heart Br Card Soc.* (2005) 91:839–46. doi: 10.1136/hrt.2004.051789
2. Gewillig M, Brown SC, Eyskens B, Heying R, Ganame J, Budts W, et al. The Fontan circulation: who controls cardiac output? *Interact Cardiovasc Thorac Surg.* (2010) 10:428–33. doi: 10.1510/icvts.2009.218594
3. Ciliberti P, Schulze-Neick I, Giardini A. Modulation of pulmonary vascular resistance as a target for therapeutic interventions in Fontan patients: focus on phosphodiesterase inhibitors. *Future Cardiol.* (2012) 8:271–84. doi: 10.2217/fca.12.16
4. Egbe AC, Connolly HM, Miranda WR, Ammash NM, Hagler DJ, Veldtman GR, et al. Hemodynamics of Fontan failure: the role of pulmonary vascular disease. *Circ Heart Fail.* (2017) 10:e004515. doi: 10.1161/CIRCHEARTFAILURE.117.004515
5. Ciliberti P, Giardini A. Impact of oral chronic administration of sildenafil in children and young adults after the Fontan operation. *Future Cardiol.* (2011) 7:609–12. doi: 10.2217/fca.11.52
6. Pundi KN, Johnson JN, Dearani JA, Pundi KN Li Z, Hinck CA, Dahl SH, et al. 40-year follow-up after the fontan operation: long-term outcomes of 1,052 patients. *J Am Coll Cardiol.* (2015) 66:1700–10. doi: 10.1016/j.jacc.2015.07.065
7. Fuchigami T, Nagashima M, Hiramatsu T, Matsumura G, Tateishi M, Masuda N, et al. Long-term follow-up of Fontan completion in adults and adolescents. *J Card Surg.* (2017) 32:436–42. doi: 10.1111/jocs.13157
8. Khairy P, Fernandes SM, Mayer JE Jr, Triedman JK, Walsh EP, Lock JE, et al. Long-term survival, modes of death, and predictors of mortality in patients with Fontan surgery. *Circulation.* (2008) 117:85–92. doi: 10.1161/CIRCULATIONAHA.107.738559
9. Gentles TL, Gauvreau K, Mayer JE Jr, Fishberger SB, Burnett J, Colan SD, et al. Functional outcome after the Fontan operation: factors influencing late morbidity. *J Thorac Cardiovasc Surg.* (1997) 114:392–403; discussion 404–5. doi: 10.1016/S0022-5223(97)70184-3
10. Trojnarska O, Ciepłucha A. Challenges of management and therapy in patients with a functionally single ventricle after Fontan operation. *Cardiol J.* (2011) 18:119–27.
11. Gewillig M, Goldberg DJ. Failure of the fontan circulation. *Heart Fail Clin.* (2014) 10:105–16. doi: 10.1016/j.hfc.2013.09.010
12. Hauser JA, Taylor AM, Pandya B. How to image the adult patient with Fontan circulation. *Circ Cardiovasc Imaging.* (2017) 10:e004273. doi: 10.1161/CIRCIMAGING.116.004273
13. Ciancarella P, Ciliberti P, Santangelo TP, Secchi F, Stagnaro N, Secinaro A. Noninvasive imaging of congenital cardiovascular defects. *Radiol Med.* (2020) 125:1167–85. doi: 10.1007/s11547-020-01284-x
14. Fontan F, Baudet E. Surgical repair of tricuspid atresia. *Thorax.* (1971) 26:240–8. doi: 10.1136/thx.26.3.240
15. Bridges ND, Mayer JE Jr, Lock JE, Jonas RA, Hanley FL, Keane JF, et al. Effect of baffle fenestration on outcome of the modified Fontan operation. *Circulation.* (1992) 86:1762–9. doi: 10.1161/01.CIR.86.6.1762
16. Atz AM, Travison TG, McCrindle BW, Mahony L, Quartermain M, Williams RV, et al. Late status of Fontan patients with persistent surgical fenestration. *J Am Coll Cardiol.* (2011) 57:2437–43. doi: 10.1016/j.jacc.2011.01.031
17. Dick M, Fyler DC, Nadas AS. Tricuspid atresia: clinical course in 101 patients. *Am J Cardiol.* (1975) 36:327–37. doi: 10.1016/0002-9149(75)90484-1
18. Weipert J, Noebauer C, Schreiber C, Kostolny M, Zrenner B, Wacker A, et al. Occurrence and management of atrial arrhythmia after long-term Fontan circulation. *J Thorac Cardiovasc Surg.* (2004) 127:457–64. doi: 10.1016/j.jtcvs.2003.08.054
19. Deal BJ, Mavroudis C, Backer CL. Arrhythmia management in the Fontan patient. *Pediatr Cardiol.* (2007) 28:448–56. doi: 10.1007/s00246-007-9005-2
20. Jacobs ML, Pourmoghadam KK. Thromboembolism and the role of anticoagulation in the Fontan patient. *Pediatr Cardiol.* (2007) 28:457–64. doi: 10.1007/s00246-007-9006-1
21. Ghaferi AA, Hutchins GM. Progression of liver pathology in patients undergoing the Fontan procedure: chronic passive congestion, cardiac cirrhosis, hepatic adenoma, and hepatocellular carcinoma. *J Thorac Cardiovasc Surg.* (2005) 129:1348–52. doi: 10.1016/j.jtcvs.2004.10.005
22. Kiesewetter CH, Sheron N, Vettukattill JJ, Hacking N, Stedman B, Millward-Sadler H, et al. Hepatic changes in the failing Fontan circulation. *Heart.* (2007) 93:579–84. doi: 10.1136/hrt.2006.094516
23. Mertens L, Hagler DJ, Sauer U, Somerville J, Gewillig M. Protein-losing enteropathy after the Fontan operation: an international multicenter study. *J Thorac Cardiovasc Surg.* (1998) 115:1063–73. doi: 10.1016/S0022-5223(98)70406-4
24. Gewillig M, Brown SC. The Fontan circulation after 45 years: update in physiology. *Heart.* (2016) 102:1081–6. doi: 10.1136/heartjnl-2015-307467
25. *ESC Guidelines on Grown-Up Congenital Heart Disease (GUCH) (Management of)*. Available online at: https://www.escardio.org/Guidelines/Clinical-Practice-Guidelines/Grown-Up-Congenital-Heart-Disease-Management-of, https://www.escardio.org/Guidelines/Clinical-Practice-Guidelines/Grown-Up-Congenital-Heart-Disease-Management-of (accessed January 31, 2022).
26. Prakash A, Powell AJ, Geva T. Multimodality noninvasive imaging for assessment of congenital heart disease. *Circ Cardiovasc Imaging.* (2010) 3:112–25. doi: 10.1161/CIRCIMAGING.109.875021
27. Bellsham-Revell HR, Simpson JM, Miller OI, Bell AJ. Subjective Evaluation of Right Ventricular systolic function in hypoplastic left heart syndrome: how accurate is it? *J Am Soc Echocardiogr.* (2013) 26:52–6. doi: 10.1016/j.echo.2012.09.020

28. Kheiwa A, Harris IS, Varadarajan P. A practical guide to echocardiographic evaluation of adult Fontan patients. *Echocardiogr Mt Kisco N.* (2020) 37:2222–30. doi: 10.1111/echo.14819
29. Margossian R, Sleeper LA, Pearson GD, Barker PC, Mertens L, Quartermain MD, et al. Assessment of diastolic function in single-ventricle patients after the fontan procedure. *J Am Soc Echocardiogr Off Publ Am Soc Echocardiogr.* (2016) 29:1066–73. doi: 10.1016/j.echo.2016.07.016
30. Muscogiuri G, Secinaro A, Ciliberti P, Fuqua M, Nutting A. Utility of cardiac magnetic resonance imaging in the management of adult congenital heart disease. *J Thorac Imaging.* (2017) 32:233. doi: 10.1097/RTI.0000000000000280
31. Yeong M, Loughborough W, Hamilton M, Manghat N. Role of cardiac MRI and CT in Fontan circulation. *J Congenit Cardiol.* (2017) 1:8. doi: 10.1186/s40949-017-0010-x
32. Rathod RH, Prakash A, Kim YY, Germanakis IE, Powell AJ, Gauvreau K, et al. Cardiac magnetic resonance parameters predict transplantation-free survival in patients with fontan circulation. *Circ Cardiovasc Imaging.* (2014) 7:502–9. doi: 10.1161/CIRCIMAGING.113.001473
33. Kutty S, Rathod RH, Danford DA, Celermajer DS. Role of imaging in the evaluation of single ventricle with the Fontan palliation. *Heart Br Card Soc.* (2016) 102:174–83. doi: 10.1136/heartjnl-2015-308298
34. Balasubramanian S, Joshi A, Lu JC, Agarwal PP. Advances in noninvasive imaging of patients with single ventricle following fontan palliation. *Semin Roentgenol.* (2020) 55:320–9. doi: 10.1053/j.ro.2020.06.014
35. Ibe DO, Rapp JB, Whitehead KK, Otero HJ, Smith CL, Fogel MA, et al. Pearls and pitfalls in pediatric Fontan operation imaging. *Semin Ultrasound CT MR.* (2020) 41:442–50. doi: 10.1053/j.sult.2020.05.009
36. Gordon-Walker TT, Bove K, Veldtman G. Fontan-associated liver disease: a review. *J Cardiol.* (2019) 74:223–32. doi: 10.1016/j.jjcc.2019.02.016
37. Daniels CJ, Bradley EA, Landzberg MJ, Aboulhosn J, Beekman RH, Book W, et al. Fontan-associated liver disease: proceedings from the American college of cardiology stakeholders meeting, october 1 to 2, 2015, Washington DC. *J Am Coll Cardiol.* (2017) 70:3173–94. doi: 10.1016/j.jacc.2017.10.045
38. Dittrich S, Weise A, Cesnjevar R, Rompel O, Rüffer A, Schöber M, et al. Association of lymphatic abnormalities with early complications after Fontan operation. *Thorac Cardiovasc Surg.* (2021) 69:e1–9. doi: 10.1055/s-0040-1722178
39. Ghosh RM, Griffis HM, Glatz AC, Rome JJ, Smith CL, Gillespie MJ, et al. Prevalence and cause of early fontan complications: does the lymphatic circulation play a role? *J Am Heart Assoc.* (2020) 9:e015318. doi: 10.1161/JAHA.119.015318
40. Bordonaro V, Ciancarella P, Ciliberti P, Curione D, Napolitano C, Santangelo TP, et al. Dynamic contrast-enhanced magnetic resonance lymphangiography in pediatric patients with central lymphatic system disorders. *Radiol Med.* (2021) 126:737–43. doi: 10.1007/s11547-020-01309-5
41. Itkin MG, McCormack FX, Dori Y. Diagnosis and treatment of lymphatic plastic bronchitis in adults using advanced lymphatic imaging and percutaneous embolization. *Ann Am Thorac Soc.* (2016) 13:1689–96. doi: 10.1513/AnnalsATS.201604-292OC
42. Secinaro A, Curione D. Congenital heart disease in children. In: Nikolaou K, Bamberg F, Laghi A, Rubin GD, editors. *Multislice CT*. Cham: Springer International Publishing (2019). p. 987–1009.
43. Secinaro A, Curione D, Mortensen KH, Santangelo TP, Ciancarella P, Napolitano C, et al. Dual-source computed tomography coronary artery imaging in children. *Pediatr Radiol.* (2019) 49:1823–39. doi: 10.1007/s00247-019-04494-2
44. Ghadimi Mahani M, Agarwal PP, Rigsby CK, Lu JC, Fazeli Dehkordy S, Wright RA, et al. for Assessment of thrombosis and pulmonary embolism in multiple stages of single-ventricle palliation: challenges and suggested protocols. *RadioGraphics.* (2016) 36:1273–84. doi: 10.1148/rg.2016150233
45. Yamamuro M, Tadamura E, Kubo S, Toyoda H, Nishina T, Ohba M, et al. Cardiac functional analysis with multi-detector row CT and segmental reconstruction algorithm: comparison with echocardiography, SPECT, and MR imaging. *Radiology.* (2005) 234:381–90. doi: 10.1148/radiol.2342031271
46. Stumper O, Penford G. Catheter hemodynamic assessment of the univentricular circulation. *Ann Pediatr Cardiol.* (2017) 10:167–74. doi: 10.4103/apc.APC_160_16
47. Razavi R, Hill DLG, Keevil SF, Miquel ME, Muthurangu V, Hegde S, et al. Cardiac catheterisation guided by MRI in children and adults with congenital heart disease. *Lancet Lond Engl.* (2003) 362:1877–82. doi: 10.1016/S0140-6736(03)14956-2
48. Muthurangu V, Taylor A, Andriantsimiavona R, Hegde S, Miquel ME, Tulloh R, et al. Novel method of quantifying pulmonary vascular resistance by use of simultaneous invasive pressure monitoring and phase-contrast magnetic resonance flow. *Circulation.* (2004) 110:826–34. doi: 10.1161/01.CIR.0000138741.72946.84
49. Moore P. MRI-guided congenital cardiac catheterization and intervention: the future? *Catheter Cardiovasc Interv Off J Soc Card Angiogr Interv.* (2005) 66:1–8. doi: 10.1002/ccd.20485
50. Veeram Reddy SR, Arar Y, Zahr RA, Gooty V, Hernandez J, Potersnak A, et al. Invasive cardiovascular magnetic resonance (iCMR) for diagnostic right and left heart catheterization using an MR-conditional guidewire and passive visualization in congenital heart disease. *J Cardiovasc Magn Reson Off J Soc Cardiovasc Magn Reson.* (2020) 22:20. doi: 10.1186/s12968-020-0605-9
51. Pushparajah K, Chubb H, Razavi R. MR-guided cardiac interventions. *Top Magn Reson Imaging TMRI.* (2018) 27:115–28. doi: 10.1097/RMR.0000000000000156
52. Bouhout I, Ben-Ali W, Khalaf D, Raboisson MJ, Poirier N. Effect of fenestration on Fontan procedure outcomes: a meta-analysis and review. *Ann Thorac Surg.* (2020) 109:1467–74. doi: 10.1016/j.athoracsur.2019.12.020
53. Dori Y, Keller MS, Rome JJ, Gillespie MJ, Glatz AC, Dodds K, et al. Percutaneous lymphatic embolization of abnormal pulmonary lymphatic flow as treatment of plastic bronchitis in patients with congenital heart disease. *Circulation.* (2016) 133:1160–70. doi: 10.1161/CIRCULATIONAHA.115.019710

Conflict of Interest: The authors declare that the research was conducted in the absence of any commercial or financial relationships that could be construed as a potential conflict of interest.

frontiers | Frontiers in Cardiovascular Medicine

ORIGINAL RESEARCH
published: 23 May 2022
doi: 10.3389/fcvm.2022.885140

Echocardiography-Guided Percutaneous Patent Ductus Arteriosus Closure: 1-Year Single Center Experience in Indonesia

Sisca Natalia Siagian[1], Radityo Prakoso[1], Bayushi Eka Putra[1], Yovi Kurniawati[1], Olfi Lelya[1], Aditya Agita Sembiring[1], Indriwanto Sakidjan Atmosudigdo[1], Poppy Surwianti Roebiono[1], Anna Ulfah Rahajoe[1], Ganesja Moelia Harimurti[1], Brian Mendel[1], Christianto Christianto[2], Moira Setiawan[2] and Oktavia Lilyasari[1]*

[1] Division of Pediatric Cardiology and Congenital Heart Disease, Department of Cardiology and Vascular Medicine, National Cardiovascular Center Harapan Kita, Universitas Indonesia, Jakarta, Indonesia, [2] Faculty of Medicine, Universitas Indonesia, Jakarta, Indonesia

OPEN ACCESS

Edited by:
Ruth Heying,
University Hospital Leuven, Belgium

Reviewed by:
Omar R. J. Tamimi,
King Fahd Medical City, Saudi Arabia
Mario Carminati,
IRCCS San Donato Polyclinic, Italy

***Correspondence:**
Sisca Natalia Siagian
sisca.ped.car@gmail.com

Specialty section:
This article was submitted to Pediatric Cardiology, a section of the journal Frontiers in Cardiovascular Medicine

Received: *27 February 2022*
Accepted: *20 April 2022*
Published: *23 May 2022*

Citation:
Siagian SN, Prakoso R, Putra BE, Kurniawati Y, Lelya O, Sembiring AA, Atmosudigdo IS, Roebiono PS, Rahajoe AU, Harimurti GM, Mendel B, Christianto C, Setiawan M and Lilyasari O (2022) Echocardiography-Guided Percutaneous Patent Ductus Arteriosus Closure: 1-Year Single Center Experience in Indonesia. Front. Cardiovasc. Med. 9:885140. doi: 10.3389/fcvm.2022.885140

Introduction: Since the first successful percutaneous closure under transesophageal echocardiographic (TEE) guidance, many centers explored transcatheter procedures without fluoroscopy. This single-center study is aimed to show the feasibility and safety of percutaneous patent ductus arteriosus (PDA) closure under echocardiography-only guidance during our 1-year experience.

Methods: Patients with PDA were recruited for percutaneous PDA closure guided by either fluoroscopy or echocardiography-only in National Cardiovascular Center Harapan Kita (ClinicalTrials.gov Identifier: NCT05321849, clinicaltrials.gov/ct2/show/NCT05321849). Patients were evaluated clinically and radiologically using transthoracic echocardiography (TTE) at 6, 24, and 48 h after the procedure. The primary endpoint was the procedural success. Secondary endpoints were the procedural time and the rate of adverse events.

Results: A total of 60 patients underwent transcatheter PDA closure, 30 patients with fluoroscopy and 30 patients with echocardiography guidance. All patients had successful PDA closure. There were only residual shunts, which were disappeared after follow-up in both groups, but one patient with a fluoroscopy-guided procedure had moderate tricuspid regurgitation with suspected thrombus in the tricuspid valve. The procedural time was not significantly different between the fluoroscopy and echocardiography groups.

Keywords: congenital heart disease, fluoroscopy, patent ductus arteriosus, percutaneous, echocardiography

INTRODUCTION

Percutaneous patent ductus arteriosus (PDA) closure has become the preferred therapeutic alternative since its introduction more than three decades ago, where it is also recommended by the American Heart Association/American College of Cardiology (AHA/ACC) and the European Society of Cardiology (ESC). Even though the occluder and device delivery systems have been

modified throughout the years, fluoroscopy has been utilized as the gold standard for guidance modality (1, 2). With the advancement of technology, it is now feasible to be performed with limited fluoroscopic exposure. However, the detrimental effects of radiation should not be overlooked, especially for both pediatric patients and interventional cardiologists (3, 4). Pediatric patients are more sensitive toward radiation when compared to adult patients, and they have a longer life expectancy, increasing the chances of lifetime attributable risks of radiation (5). Interventional cardiologists are repeatedly exposed to radiation, thus accumulating the risks of radiation (6). Since Ewert et al. reported the first successful transcatheter closure of atrial septal defect (ASD) under transesophageal echocardiographic (TEE) guidance, many centers explored transcatheter procedures without fluoroscopy, such as ours (7). Our center has been routinely performing transcatheter closure under echocardiographic guidance in 220 patients with ASD or ventricular septal defects (VSDs) with satisfactory outcomes (8). Therefore, this single-center study is aimed to show the feasibility and safety of percutaneous PDA closure under echocardiography-only guidance during our 1-year experience.

METHODS

Study Design and Setting

From March 2019 to April 2020, a total of 60 patients with PDA were recruited as participants for this prospective, single-center, and non-randomized clinical trial. They were divided equally into two groups: the fluoroscopy group, which underwent percutaneous PDA guided by fluoroscopy and the echocardiography group, which underwent percutaneous PDA closures guided by transthoracic echocardiography (TTE) and TEE at the National Cardiovascular Centre Harapan Kita, Jakarta, Indonesia. Patients with stable hemodynamic and clinically asymptomatic PDA were evaluated and considered for transcatheter PDA closure. Significant chamber enlargement and mild to moderate pulmonary hypertension were also the indications for transcatheter closure. Ductal morphology was evaluated using multiplanar TTE and TEE imaging.

After the procedures, patients were evaluated and followed up after 6, 24, and 48 h to observe any residual shunts and complications. This study protocol conforms to the ethical guidelines of the Declaration of Helsinki and the Nuremberg Code with approval from the Research Ethics Committee of National Cardiovascular Center Harapan Kita No LB.02.01/VII/475/KEP076/2020. Written consent to perform the procedure and to use the patients' medical records for this study was obtained from the patients or their parents.

Study Population

The inclusion criteria for this study are children under 18 years old with type-A PDA who were planned for PDA closure. We only conducted this treatment in type A patients with PDA in our 1-year experience since, according to the literature, isolated patients with PDA are mostly type A PDA. The exclusion criteria include the coexistence of other associated congenital heart diseases requiring surgical intervention and PDA patients with irreversible high pulmonary vascular resistance (PVR) unreactive with the oxygen test.

Pre-procedural Preparation and Device Selection

All recruited patients received pre-procedural examinations consisting of a standard electrocardiogram, a chest X-ray, and blood tests. Device size selection was based on the measurement of the diameter of the PDA isthmus during echocardiography assessment. We prefer to utilize Amplatzer Duct Occluder II (AGA) or Konar Multifunctional VSD Occluder (LifeTech) if the PDA is rather small. We utilized Amplatzer Duct Occluder I (AGA), Konar Multifunctional VSD Occluder (LifeTech), or PDA Occluder Device (MemoPart) if the PDA was rather large. We use a device that can be utilized retrogradely or antegradely in specific circumstances where the PDA size is large but can still be conducted retrogradely. The selection of the occluders from the available types, Amplatzer Duct Occluder I (AGA), Amplatzer Duct Occluder II (AGA), PDA Occluder Device (MemoPart), PDA Occluder Device (LifeTech), Konar Multifunctional VSD Occluder (LifeTech), Multifunctional Occluder (LifeTech), and HeartR PDA Occluder (LifeTech), was determined by the operator according to the size of PDA.

Instrumentation and Percutaneous Approach

The patients were sedated under general anesthesia (GA) and intubated with an endotracheal tube. At our institution, all pediatric catheterization procedures are performed under general anesthetic. This is because pediatric patients are sometimes uncooperative and may throw a tantrum during the treatment, complicating the procedure. Evaluation of the morphology and diameter of the PDA isthmus and ampulla were measured with the assistance of TTE high parasternal view and/or TEE high esophageal aortic long-axis view (**Figure 1**). Asepsis and antisepsis in right and left inguinal regions and local anesthesia with 2% lidocaine injection were performed in the femoral region. Venous or arterial access was made by puncturing the femoral vein or artery. A 4–6 French percutaneous sheath with an introducer set was inserted using the Seldinger technique. For diagnostic and interventional purposes, a 4–6 French Judkins Right (JR) guiding, or multipurpose (MP) catheter was used with a 0.025 or 0.035 standard guidewire. Meanwhile, a 7–12 French JR guiding catheter and delivery sheath were used for device implantation. A stepwise approach to antegrade and retrograde percutaneous PDA closure can be seen in **Figures 2**, **3**. The dose of anticoagulant used in our procedure was heparin 50–100 IU/kgBW. While there is no difference in heparin doses for antegrade and retrograde approaches, we would add additional doses if the duration of the procedure exceeds 1 h. Antibiotic cefazolin was given 50 mg/kgBW IV before the occluder device was implanted. Evaluation of the device position,

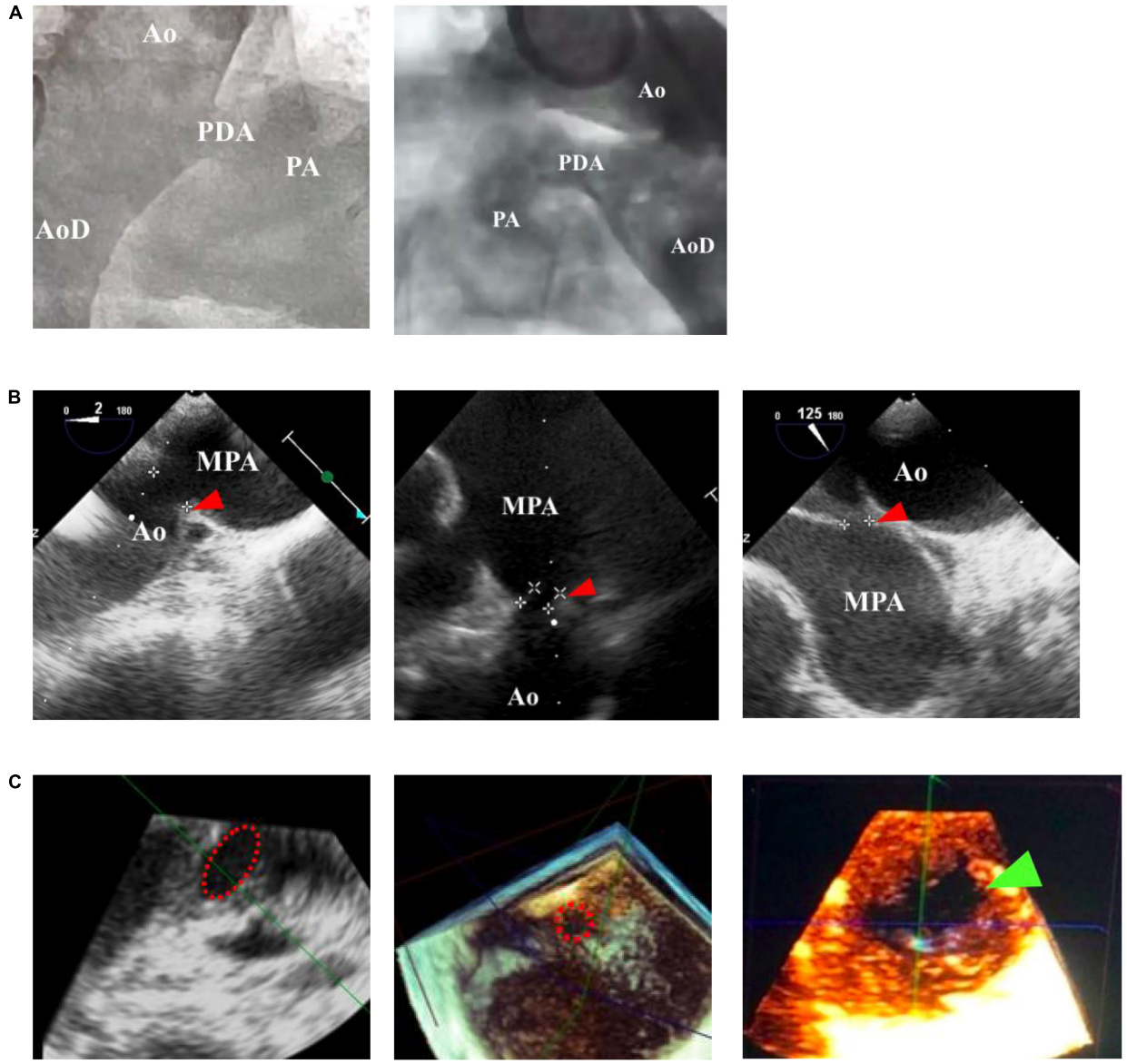

FIGURE 1 | Comparison of patent ductus arteriosus (PDA) size and morphology measurements using fluoroscopy and echocardiography guidance. **(A)** Fluoroscopy can only provide a 2-dimensional image, whereas **(B)** transthoracic echocardiography (TTE) and transesophageal echocardiography (TEE) can provide a 3-dimensional structure as shown by the red arrowhead. **(C)** Cross-sectional PDA morphology measured by using transesophageal echocardiography (TEE), indicated by the dotted red circle. Green arrowhead showed oval-shaped PDA. Ao, aorta; AoD, descending aorta; MPA, main pulmonary artery; PA, pulmonary artery.

residual shunt, and turbulence in the aorta and pulmonary artery (PA) was made before and after the device detachment from the delivery cable.

Follow-Up and Outcome

Patients were evaluated clinically and through imaging by TTE at 6, 24, and 48 h after the procedure. The primary endpoint was the outcome of the procedural success. Successful closure was defined as successful device implantation, without device migration, and no residual shunt or central mild shunt was detected by TTE at the time of post-discharge follow-up.

The secondary endpoints were procedural times and the rate of adverse events. The procedural time was measured from the initiation of GA to the post-procedural evaluation using TTE. Adverse events were defined as any complications, such as occluder migration, hemolysis, peripheral vascular complications, and residual shunt (except central mild shunt), detected during the procedures, immediately after the procedures, or at post-discharge follow-up. Data acquired from the patients' medical records were patient demographics (age, gender, and weight), the size of the PDA, the type and size of the device, the crossing catheter, and the technical approaches.

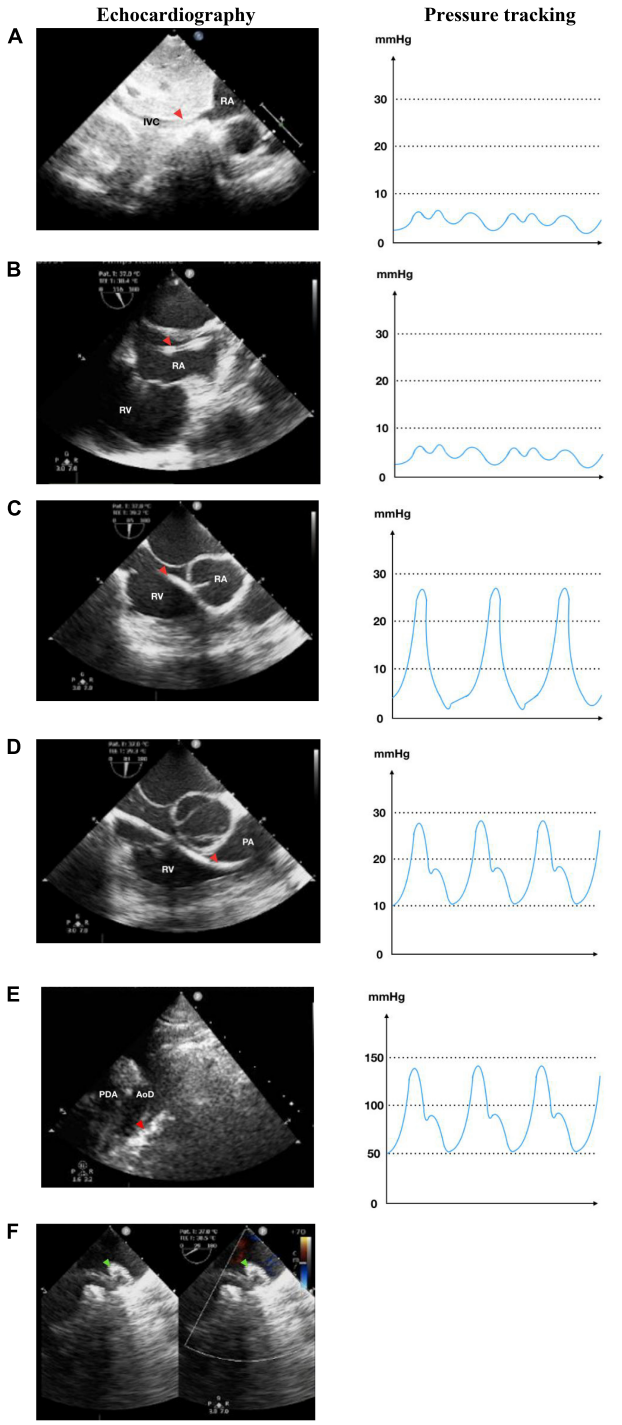

FIGURE 2 | Antegrade transvenous approach of percutaneous patent ductus arteriosus (PDA) closure. **(A)** Catheter is seen in IVC in transthoracic echocardiography (TTE) subxiphoid view. **(B)** Catheter is seen in RA in TEE bicaval view (90–110°). **(C)** Catheter in RV TEE 90° view. **(D)** Catheter enters PA in TEE 90° view. **(E)** Catheter crossed from PA towards AoD through PDA in TTE arch view. **(F)** The device is stowed in place in TEE (40–50°). IVC, inferior vena cava; RA, right atrium; RV, right ventricle; PA, pulmonary artery; Ao, aorta; LA, left atrium; LV, left ventricle; AoD, descending aorta; PDA, patent ductus arteriosus. Red arrowhead shows the catheter head. Green arrowhead indicates the occluder device.

Statistical Analysis

The analysis was performed on an intention to treat basis, with outcomes related to the initial treatment decision. The Shapiro-Wilk test was used as normality test for numerical data where the data were represented as mean (SD) for normally distributed data and median (range) for skewed data. The independent *t*-test was used for comparison of numerical data between the two groups for normally distributed data, while the Mann-Whitney test was used for skewed data. All data analyses were carried out using Statistical Package for Social Science (SPSS) 26.0 software. Values of p lower than 0.05 were considered significant.

RESULTS

This study included 60 patients in total, where 30 patients were allocated to the echocardiography (test) group and 30 patients were allocated to the fluoroscopy (control) group. The summarized baseline characteristics of subjects and the approaches used, time taken for the procedures, crossing catheter, and devices used can be seen in **Table 1**.

Study Primary Endpoint

All the procedures were successful with no device dislodgement in both groups. From the echocardiography group, 13 out of 30 patients had mild residual central shunt, which was eventually resolved during follow-up. On the other hand, there were 17 out of 30 patients with mild residual central shunt after the procedures in which fluoroscopy was used, which was also resolved during follow-up. From these results, we can conclude that the echocardiography group is non-inferior to the fluoroscopy group.

Study Secondary Endpoint

The procedures were conducted using either antegrade approach or retrograde approach. The median procedural time of using an antegrade approach for the test and control group was 28.5 (20.3–48.3) and 36 (34–59.5) min, respectively ($p = 0.113$), while the median procedural time of using a retrograde approach for the test and control group was 61 (53–80) and 61.5 (36.5–79.8) min, respectively ($p = 0.575$). Without taking into account the approach, the procedural time was not significantly different in the echocardiography group and the fluoroscopy group [50 (25–58) min vs. 53 (36–77), $p = 0.09$].

During the procedure, after the procedure, and after discharge of the patients, there were no adverse events, such as major procedural complications (death, peripheral vascular injury, pericardial effusion, and pericardial tamponade). All patients neither required blood transfusion nor any inotropic support. An echocardiographic assessment conducted during follow-up showed complete closure in all patients with no left PA stenosis and aortic arch obstruction identified. All patients had successful closures with no residual shunts and recovered well. There were no post-procedural unresolved residual shunts, thrombosis, or any valvular regurgitations observed during follow-up, except in one patient from the fluoroscopy group who had moderate

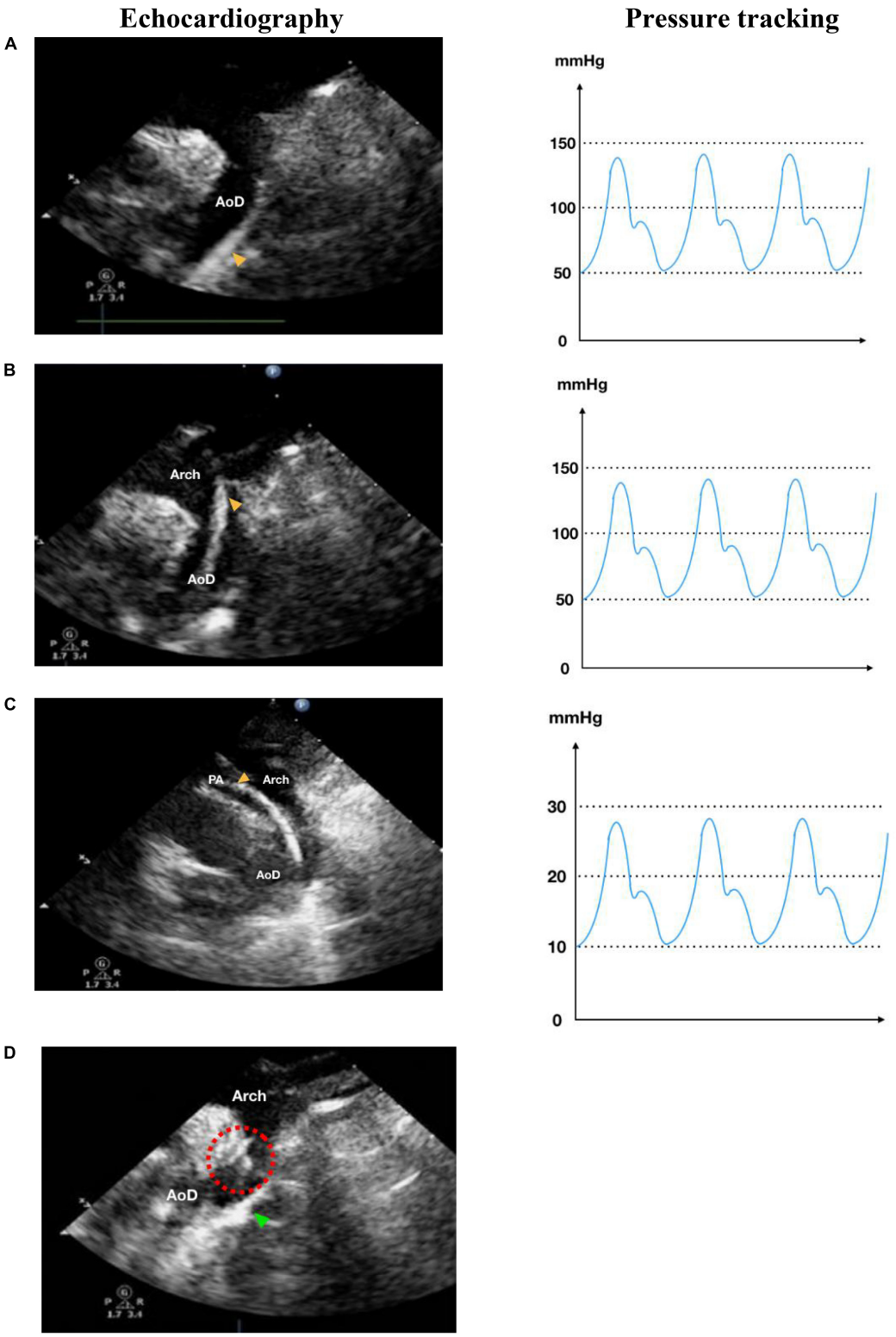

FIGURE 3 | Retrograde transarterial approach of percutaneous patent ductus arteriosus (PDA) closure. **(A)** Catheter is seen in AoD in TTE arch view. **(B)** Catheter is pushed towards the aortic arch in TTE arch view. **(C)** In parasternal short axis TTE view as high as the great arteries, the catheter is seen in PA through PDA from AoD. **(D)** In TTE arch view, the device is stowed in place (shown by red dotted circle) after being delivered from the delivery cable. IVC, inferior vena cava; RA, right atrium; RV, right ventricle; PA, pulmonary artery; Ao, aorta; LA, left atrium; LV, left ventricle; AoD, descending aorta; PDA, patent ductus arteriosus. Orange arrowhead shows the catheter head. Green arrowhead indicates the occluder device.

TABLE 1 | Summary of baseline characteristics of patients and procedures.

Variables	Echocardiography group (*n* = 30)	Fluoroscopy group (*n* = 30)	*P*-value
Age, years	6.0 (2.4–9.0)	2.8 (1.8–20.3)	0.942
Sex (male/female)	14/16	6/24	
Weight, kg	17.0 (12.2–23.0)	12.9 (8.0–40.3)	0.554
PDA size, mm	5.07 ± 2.25	5.58 ± 1.97	0.465
Approach			
Retrograde	23	8	
Antegrade	7	22	
Procedural time	50 (25–58)	53 (36–77)	0.090
Retrograde	28.5 (20.3–48.3)	36 (34–59.5)	0.113
Antegrade	61 (53–80)	61.5 (36.5–79.8)	0.575
Crossing catheter			
JR guiding catheter	30	6	
Multipurpose guiding catheter	0	24	
Device type			
PDA Occluder Device (Memopart)	1	16	
PDA Occluder Device (LifeTech)	4	0	
Konar MF VSD Occluder (Lifetech)	8	8	
HeartR PDA Occluder (Lifetech)	0	3	
ADO I (AGA)	0	2	
ADO II (AGA)	10	1	
MF Occluder (LifeTech)	7	0	
Device size, mm	13.4 ± 3.5	16.5 ± 3.7	0.920

PDA, patent ductus arteriosus; JR, Judkins Right; MF, Multifunctional; VSD, ventricular septal defect; ADO, Amplatzer Duct Occluder.

tricuspid regurgitation with suspected thrombus in the tricuspid valve, which was detected during follow-up.

DISCUSSION

Transcatheter closure has become the main approach for most PDA closures as it has lower complications and shorter hospital stay when compared to the surgical approach (1, 9). The 2018 AHA/ACC and the 2020 ESC guidelines for the management of congenital heart disease recommend transcatheter closure for all PDAs with evidence of LV volume overload regardless of symptoms, except in patients with Eisenmenger physiology, lower limb desaturation on exercise, PA systolic pressure greater than two-thirds of systemic systolic pressure or PVR greater than two-thirds of systemic vascular resistance adults (10, 11). For the last four decades, transcatheter PDA closure under fluoroscopy guidance has been the most popular choice due to its convenience as it can localize the wire and device accurately (12). Since the success of the first echocardiography-guided balloon atrial septostomy, which was performed by Rashkind in 1966 (13), many cardiologists have been experimenting with using echocardiography as guidance for many procedures, such as PDA closure (8, 14).

The frequent use of fluoroscopy may cause long-term side effects, depending on the dosage and duration of radiation exposure. In addition, the complexity of a procedure also adds to the duration of exposure, as in transcatheter PDA closure (15). Prolonged radiation not only harms pediatric patients who are more sensitive to radiation than adults (5), but it is also a risk to interventionists, especially those who routinely perform these procedures. While the advancement of technology allows for minimal fluoroscopic exposure through non-ionic contrast, the accumulated exposure on interventionists should not be overlooked (6), where side effects may show as late as the 70–90 s (16). Studies have shown that radiation increases the risks of skin injuries, cataracts, hair loss, and neoplasms (17). A study by Roguin et al. reported 44 interventional cardiologists with brain and neck cancer on their left side as it is exposed to more radiation than the right (18, 19).

In this study, we compared the time taken for PDA closure procedures using fluoroscopy and echocardiography. The median procedural time of using both antegrade and retrograde approaches for the test and control groups was insignificant ($p = 0.575$). The retrograde approach had a shorter procedural time in comparison to the antegrade approach where the catheter needs more manipulation to be directed into the right ventricle and PA to reach the PDA (see **Figures 2C,D**). However, the retrograde approach is limited to patients with low body weight or large PDA since complications might occur through arterial access, such as thrombosis at the access site. Regardless of the approach, the difference in procedural time between the echocardiography group and the fluoroscopy group was insignificant ($p = 0.09$). These results mean that using only echocardiography did not compromise procedural time.

Binobaidan et al. (12), Cao et al. (20), and Ye et al. (21) showed success rates of 100% in PDA closure, while only Zhang et al. (22) showed a success rate of 97.1%. These results

were similar to our study in which all the procedures were successful in both echocardiography and fluoroscopy groups. Most studies showed no residual shunt and severe complications after 1 month to 2 years of follow-up (12, 20–22). Pan et al. had 8 cases of small residual shunts in 24 h but resolved afterward (6). The minor complications in these studies include device embolization, acute occluder dislodgement, and small residual shunts (6, 12, 20–22). In our study, there were no complications following echocardiography-guided PDA closures with most of the patients only experiencing residual shunts, which disappeared during follow-up. However, one fluoroscopy-guided procedure resulted in moderate tricuspid regurgitation with a thrombus in the tricuspid valve. This may be due to variable confounding factors, such as the complexity of the PDA, operator experience, or the length of the procedure, which may contribute to the complications despite better visualization in the fluoroscopy group. These results showed that the echocardiography-guided procedure is not inferior to the fluoroscopy-guided procedure.

Based on pre-catheterization data, TTE or TEE showed similarities in assessing the defect size. Shyu et al. showed that TEE provided greater sensitivity to TTE in confirming PDA size (97 vs. 42%) (23). The selection of devices in 38 subjects is based on the size of the PDA. The addition of 2–4 mm from the diameter of the smallest PDA was done in device selection, but the device size would be twice the size of the PDA if it presents with pulmonary hypertension (24). Devices, such as Amplatzer Duct Occluder (ADO II) and Multifunctional (MF) Occluder, could be performed both antegradely and retrogradely. However, ADO II could only be used in patients with small PDAs. MF Occluder is now a better choice since it could be used on a large size PDA with a smaller delivery sheath. In our center, the post-procedural residual shunt is commonly found when using MF Occluder, which disappeared within 24–48 h, possibly due to the soft nature of the device. We recommend choosing devices according to the type and size of the PDA, availability, and convenience of the operators (1).

In comparison to fluoroscopic guidance, the largest hurdle of echocardiography-guided closure is to track the guidewire, catheter, and delivery sheath in the two-dimensional echocardiographic view plane, which is related to safety and procedural time. Conventional intervention techniques emphasize simplicity to determine the catheter location as fluoroscopy detects it through projection. A vast understanding of cardiac anatomy and physiology, along with the utilization of the appropriate guidewire, catheter, delivery sheath, and the positioning of the ultrasound probe, would exceedingly increase accuracy. Interventionists with insufficient experience should go for the standard procedure. Future efforts should be directed toward pre-procedural selection criteria for echocardiography-guided transcatheter PDA closure with devices based on the PDA size and surrounding structures.

LIMITATION

The small number of subjects is an unavoidable limitation as this is the first pilot study of echocardiography-guided PDA closure to be conducted in Indonesia. The procedures were conducted by different operators, which may affect results concerning procedural times and complications as the procedures were highly dependent on the operators. Therefore, we recommend further studies with more subjects and skilled operators to validate the feasibility and safety of echocardiography-guided PDA closure.

CONCLUSION

Echocardiography-guided PDA closure is non-inferior, even with a limited window view when compared to using fluoroscopy. The procedural time for echocardiography-guided PDA closure was also not significantly different from fluoroscopy-guided PDA closure, which means that using only echocardiography did not compromise procedural time. However, as this is a new technique, this method is especially operator dependent and requires an experienced team for it to be performed successfully. Unfortunately, it would still require years for this method to be widely used.

DATA AVAILABILITY STATEMENT

The original contributions presented in the study are included in the article/supplementary material, further inquiries can be directed to the corresponding author.

ETHICS STATEMENT

The studies involving human participants were reviewed and approved by the Research Ethics Committee of National Cardiovascular Center Harapan Kita. Written informed consent to participate in this study was provided by the participants' legal guardian/next of kin.

AUTHOR CONTRIBUTIONS

SS conceived the original idea of the manuscript. SS, RP, BP, YK, OLe, AS, IA, PR, AR, GH, and OLi contributed in collecting data and writing the main text of the manuscript. BM, CC, and MS performed statistical analyses and also helped in writing the manuscript. All authors discussed and agreed with the idea of the manuscript and accepted the proofread manuscript.

ACKNOWLEDGMENTS

We would like to thank those who have supported us in the making of this study. We are especially grateful to the Department of Cardiology and Vascular Medicine, Faculty of Medicine Universitas Indonesia, for their guidance and assistance in teaching the authors about research methodology and for proofreading this article.

REFERENCES

1. Baruteau AE, Hascoët S, Baruteau J, Boudjemline Y, Lambert V, Angel CY, et al. Transcatheter closure of patent ductus arteriosus: past, present and future. *Arch Cardiovasc Dis.* (2014) 107:122–32. doi: 10.1016/j.acvd.2014.01.008
2. Hamrick SEG, Hansmann G. Patent ductus arteriosus of the preterm infant. *Pediatrics.* (2010) 125:1020–30. doi: 10.1542/peds.2009-3506
3. Meinel FG, Nance JW, Harris BS, De Cecco CN, Costello P, Schoepf UJ, et al. Radiation risks from cardiovascular imaging tests. *Circulation.* (2014) 130:442–5. doi: 10.1161/CIRCULATIONAHA.113.005340
4. Johnson JN, Sathanandam S, Naik R, Philip R. Echocardiographic guidance for transcatheter patent ductus arteriosus closure in extremely low birth weight infants. *Congenit Heart Dis.* (2019) 14:74–8. doi: 10.1111/chd.12725
5. Baysson H, Nkoumazok B, Barnaoui S, Réhel L, Girodon B, Milani G, et al. Follow-up of children exposed to ionising radiation from cardiac catheterisation: the Coccinelle study. *Radiat Prot Dosimetry.* (2015) 165:13–6. doi: 10.1093/rpd/ncv039
6. Pan XB, Ouyang WB, Wang SZ, Liu Y, Zhang DW, Zhang FW, et al. Transthoracic echocardiography-guided percutaneous patent ductus arteriosus occlusion: a new strategy for interventional treatment. *Echocardiography.* (2016) 33:1040–5. doi: 10.1111/echo.13207
7. Ewert P, Berger F, Daehnert I, van Wees J, Gittermann M, Abdul-Khaliq H, et al. Transcatheter closure of atrial septal defects without fluoroscopy: feasibility of a new method. *Circulation.* (2000) 101:847–9. doi: 10.1161/01.cir.101.8.847
8. Mendel B, Laurentius A, Ulfiarakhma D, Prakoso R. Safety and feasibility of transesophageal echocardiography in comparison to transthoracic echocardiography-guided ventricular septal defect percutaneous closure: an evidence-based case report. *World Heart J.* (2020) 12:199–207.
9. Amrousy DE, Zoair AM. Pediatric patients: a systematic review with meta-analysis. *Artic J Pediatr Surg.* (2017) 3:1054.
10. Stout KK, Daniels CJ, Aboulhosn JA. 2018 AHA/ACC guideline for the management of adults with congenital heart disease: a report of the American College of Cardiology/American Heart Association Task Force on Clinical Practice Guidelines. *Circulation.* (2019) 139:e698–800.
11. Baumgartner H, De Backer J, Babu-Narayan SV, Budts W, Chessa M, Diller GP, et al. 2020 ESC Guidelines for the management of adult congenital heart disease. *Eur Heart J.* (2021) 42:563–645. doi: 10.1093/eurheartj/ehaa554
12. Binobaidan M, Al Issa M, Alonazi A, Abdulhameed J. Transthoracic echocardiographic guidance for percutaneous patent ductus arteriosus closure in pediatric patients. *J Cardiol Cardiovasc Ther.* (2016) 2:55–9. doi: 10.19080/JOCCT.2016.02.555590
13. Rashkin WJ. Miller WW. Creation of atrial septal defect without thoracotomy. A palliative approach towards transposition of the great arteries. *JAMA*. (1966) 196:991–2.
14. Hascoët S, Warin-Fresse K, Baruteau AE, Hadeed K, Karsenty C, Petit J, et al. Cardiac imaging of congenital heart diseases during interventional procedures continues to evolve: pros and cons of the main techniques. *Arch Cardiovasc Dis.* (2016) 109:128–42. doi: 10.1016/j.acvd.2015.11.011
15. Villemain O, Malekzadeh-Milani S, Sitefane F, Mostefa-Kara M, Boudjemline Y. Radiation exposure in transcatheter patent ductus arteriosus closure: time to tune? *Cardiol Young.* (2018) 28:653–60. doi: 10.1017/s1047951117002839
16. Venneri L, Rossi F, Botto N, Andreassi MG, Salcone N, Emad A, et al. Cancer risk from professional exposure in staff working in cardiac catheterization laboratory: insights from the National Research Council's Biological Effects of Ionizing Radiation VII Report. *Am Heart J.* (2009) 157:118–24. doi: 10.1016/j.ahj.2008.08.009
17. Mettler FAJ, Koenig TR, Wagner LK, Kelsey CA. Radiation injuries after fluoroscopic procedures. *Semin Ultrasound CT MR.* (2002) 23:428–42. doi: 10.1016/s0887-2171(02)90014-4
18. Roguin A, Goldstein J, Bar O, Goldstein JA. Brain and neck tumors among physicians performing interventional procedures. *Am J Cardiol.* (2013) 111:1368–72. doi: 10.1016/j.amjcard.2012.12.060
19. Reeves RR, Ang L, Bahadorani J, Naghi J, Dominguez A, Palakodeti V, et al. Invasive cardiologists are exposed to greater left sided cranial radiation: the BRAIN study (Brain Radiation Exposure and Attenuation During Invasive Cardiology Procedures). *JACC Cardiovasc Interv.* (2015) 8:1197–206. doi: 10.1016/j.jcin.2015.03.027
20. Cao H, Chen Q, Zhang GC, Chen LW, Xu F, Zhang JX, et al. Clinical study of stand-alone transthoracic echocardiography-guided percutaneous occlusion of patent ductus arteriosus. *Anatol J Cardiol.* (2018) 20:30–4. doi: 10.14744/AnatolJCardiol.2018.90001
21. Ye Z, Li Z, Yi H, Zhu Y, Sun Y, Li P, et al. Percutaneous device closure of pediatirc patent ductus arteriosus through femoral artery guidance by transthoracic echocardiography without radiation and contrast agents. *J Cardiothorac Surg.* (2020) 15:107. doi: 10.1186/s13019-020-01119-w
22. Zhang W, Gao L, Jin W, Wu Q, Hu S, Yang Y, et al. Echocardiography-guided percutaneous closure of patent ductus arteriosus without arterial access: feasibility and safety for a new strategy. *J Cent South Univ Med Sci.* (2018) 43:1000–6. doi: 10.11817/j.issn.1672-7347.2018.09.011
23. Shyu KG, Lai LP, Lin SC, Chang H, Chen JJ. Diagnostic accuracy of transesophageal echocardiography for detecting patent ductus arteriosus in adolescents and adults. *Chest.* (1995) 108:1201–5. doi: 10.1378/chest.108.5.1201
24. Shah J, Bhalodiya D, Rawal A, Nikam TS. Long-term results of transcatheter closure of large patent ductus arteriosus with severe pulmonary arterial hypertension in pediatric patients. *Int J Appl Basic Med Res.* (2020) 10:3–7. doi: 10.4103/ijabmr.IJABMR_192_19

Conflict of Interest: The authors declare that the research was conducted in the absence of any commercial or financial relationships that could be construed as a potential conflict of interest.

frontiers | Frontiers in Pediatrics

POLICY AND PRACTICE REVIEWS
published: 09 June 2022
doi: 10.3389/fped.2022.873421

Practical Workflow for Cardiovascular Assessment and Follow-Up in Kawasaki Disease Based on Expert Opinion

Diana van Stijn[1], R. Nils Planken[2], Maarten Groenink[2,3], Nico Blom[4], Robbert J. de Winter[3], Taco Kuijpers[1†] and Irene Kuipers[4†]*

[1] Department of Pediatric Immunology, Rheumatology and Infectious Diseases, Emma Children's Hospital, Amsterdam University Medical Center (UMC), University of Amsterdam, Amsterdam, Netherlands, [2] Department of Radiology and Nuclear Medicine, Amsterdam University Medical Center (UMC), University of Amsterdam, Amsterdam, Netherlands, [3] Department of Cardiology, Amsterdam University Medical Center (UMC), University of Amsterdam, Amsterdam, Netherlands, [4] Department of Pediatric Cardiology, Emma Children's Hospital, Amsterdam University Medical Center (UMC), University of Amsterdam, Amsterdam, Netherlands

OPEN ACCESS

Edited by:
Ruth Heying,
University Hospital Leuven, Belgium

Reviewed by:
Andre Jakob,
Ludwig Maximilian University of Munich, Germany
Laura Muiño Mosquera,
Ghent University Hospital, Belgium

***Correspondence:**
Diana van Stijn
d.vanstijn@amsterdamumc.nl

† These authors share senior authorship

Specialty section:
This article was submitted to Pediatric Cardiology, a section of the journal Frontiers in Pediatrics

Received: *10 February 2022*
Accepted: *16 May 2022*
Published: *09 June 2022*

Citation:
van Stijn D, Planken RN, Groenink M, Blom N, de Winter RJ, Kuijpers T and Kuipers I (2022) Practical Workflow for Cardiovascular Assessment and Follow-Up in Kawasaki Disease Based on Expert Opinion. Front. Pediatr. 10:873421. doi: 10.3389/fped.2022.873421

Background: Approximately 25% of the patients with a history of Kawasaki disease (KD) develop coronary artery pathology if left untreated, with coronary artery aneurysms (CAA) as an early hallmark. Depending on the severity of CAAs, these patients are at risk of myocardial ischemia, infarction and sudden death. In order to reduce cardiac complications it is crucial to accurately identify patients with coronary artery pathology by an integrated cardiovascular program, tailored to the severity of the existing coronary artery pathology.

Methods: The development of this practical workflow for the cardiovascular assessment of KD patients involve expert opinions of pediatric cardiologists, infectious disease specialists and radiology experts with clinical experience in a tertiary KD reference center of more than 1000 KD patients. Literature was analyzed and an overview of the currently most used guidelines is given.

Conclusions: We present a patient-specific step-by-step, integrated cardiovascular follow-up approach based on expert opinion of a multidisciplinary panel with expertise in KD.

Keywords: Kawasaki disease, mucocutaneous lymph node syndrome, imaging, coronary artery aneurysms, cardiovascular assessment

INTRODUCTION

Kawasaki disease (KD) is a pediatric systemic vasculitis of unknown etiology, which mainly affects children under the age of 5 years. KD is generally a self-limiting acute inflammatory disease that predominantly affects the coronary arteries. Inflammation of the coronary arteries may lead to coronary artery aneurysms (CAAs) which can lead to adverse cardiac complications. CAAs develop in approximately 25% of untreated patients and can be reduced to 9% if treated timely (1–4). Some risk factors have been identified for the development of CAAs such as: resistance to treatment, delayed treatment (later than 10 days after fever onset), male gender, incomplete KD and an age at the end-spectrum of the classical age for KD (5, 6). Studies have shown that CAA regression mainly occurs within the first 2 years after onset of disease (7). Regression seems to occur with

a predilection for some conditions: when aneurysms do not show calcification, have a smaller diameter, or have an ectatic shape (1).

Pediatric cardiologists use echocardiography to diagnose and monitor KD patients. Currently *Z* scores are most commonly used for risk assessment and clinical decision making whereas in the past, luminal diameters were used. CAAs can be classified according to their *Z* score; small aneurysms: $\geq 2.5 < 5.0$, medium aneurysms: $\geq 5.0 < 10.0$, large/giant aneurysms: ≥ 10.0. Patients in the last category and even more so in case of a *Z* score $\geq$ 20.0, are at the highest risk for the development of stenosis and formation of coronary thrombus, which may lead to myocardial ischemia, infarction and sudden death (8). Multiple *Z* score calculators are used and inter-variability in *Z* score calculation has been reported, especially larger dimensions of the coronary arteries show larger discrepancies between different calculators (9). These discrepancies between *Z* score systems can lead to variation in diagnosis and management (10), more research is required to identify the ideal *Z* scoring system.

CAAs in the right coronary artery (RCA), in the left anterior descending coronary artery (LAD), in the circumflex (Cx) and CAAs with complicated architecture also have an increased risk for luminal narrowing and thrombosis. In previous reports perivascular brightness was considered an early sign for CAA formation (11), but more recent studies showed that perivascular brightness and lack of tapering were non-specific findings that could also be found in healthy children and children with fever without KD (12, 13).

While striving toward a uniform and realistic monitoring schedule for KD patients, we had previously set up a practical workflow at our center (14). Since our previous report, we obtained experience with state-of-the art coronary CT angiography (cCTA) (15, 16), which can assess the coronary artery tree at great detail with reduced radiation exposure. Therefore, cCTA is now fully integrated into our updated cardiovascular follow-up workflow, to avoid underreporting CAAs and prevent cardiac ischemia. This update gives an overview of the most current guidelines with practical recommendations based on the clinical experience from our single center in over 1,000 KD patients.

Echocardiography

Coronary Artery Pathology

Echocardiography is the cornerstone of the acute and long-term cardiovascular assessment in KD patients during adolescence. When visualizing the coronary arteries, it is important at which location the luminal diameters are measured (**Figure 1**); after which these diameters are calculated to *Z* scores with the Body Surface Area (BSA). *Z* scores are acquired by echocardiography and not validated for other imaging modalities. Each coronary artery has a different echocardiographic view for best visualization (**Figure 1**). Echocardiography is limited in visualizing the distal sections of the coronary artery tree due to limited ultrasound windows, and diagnostic accuracy has been questioned (9, 15). Therefore, complementary imaging modalities should be considered. However, there is minimal risk for distal involvement without proximal involvement (15, 17).

Non-coronary Cardiac Involvement

Cardiac manifestations in KD can occur independently of coronary artery lesions. Therefore, not only coronary artery assessment but also echocardiographic assessment of the cardiac chamber size and function in the acute phase is necessary. The inflammatory process in KD can affect the pericardium, myocardium, endocardium and the valves. (Peri) myocardial inflammation occurs allegedly in all KD patients and very likely even before the development of coronary arteritis (18). It can cause transient cardiac dysfunction, often described as inflammatory myocarditis, but only a minority of patients exhibit heart failure symptoms (19, 20). Echocardiographic findings indicating perimyocardial inflammation in the acute stage of the disease are: decreased left ventricular fractional shortening or ejection fraction, mitral valve regurgitation, and pericardial effusion (21, 22). Myocardial inflammation is known to mainly cause edema without permanent cell damage (18). Apart from the acute phase, echocardiography continues to be of additional value during follow-up to monitor potential evolving complications such as reduced ventricular wall movements as signs of ischemia or (missed) infarction. Aneurysms of the aortic root (*Z* score $\geq$ 2) are present in 10% of KD patients (23), which does not seem to regress 1 year after onset of disease (24). Long-term surveillance is necessary to determine the importance of this finding, which is unclear to date. Aortic dissection has not been reported in KD patients thus far.

Electrocardiography

Electrocardiography is generally used to exclude myocardial ischemia and infarction. Atrioventricular (AV) block, repolarization abnormalities and arrhythmias may occur as a result of the inflammation as well. Due to stenotic or thrombotic CAAs, KD patients can exhibit abnormal electrocardiography, indicating ischemia or myocardial infarction. Such signs must have immediate dollow-up imaging and biochemical check in plasma for cardiac enzymes.

Coronary Artery Angiography

Initially, coronary artery angiography (CAG) has been advocated to be performed regularly depending on the size of CAA or strongly suspected risk of ischemia. CAG is still considered the "gold standard", if necessary complemented with intracoronary imaging. Several adverse cardiac events haven been described when CAG is performed in the acute phase of KD (25). Furthermore, patients are exposed to a relatively high radiation dose and in children the procedure needs to be performed under general anesthesia. This has caused clinicians to consider alternative imaging techniques. Studies have shown that the cCTA, compared to CAG is reliable and useful in the complete

Abbreviations: AHA, American Heart Association; AV, atrioventricular; BSA, body surface area; CAA, coronary artery aneurysm; CABG, coronary artery bypass grafting; CAG, coronary artery angiography; cCTA, coronary computed tomographic angiography; CMR, cardiac magnetic resonance imaging; Cx, circumflex; IVIG, intravenous immunoglobulin; JCS, Japanese Circulation Society; KD, Kawasaki disease; LAD, left anterior descending coronary artery; LMCA, left main coronary artery; LMP, luminal myofibroblastic process proliferation; PTCA, percutaneous transluminal coronary angioplasty; RCA, right coronary artery.

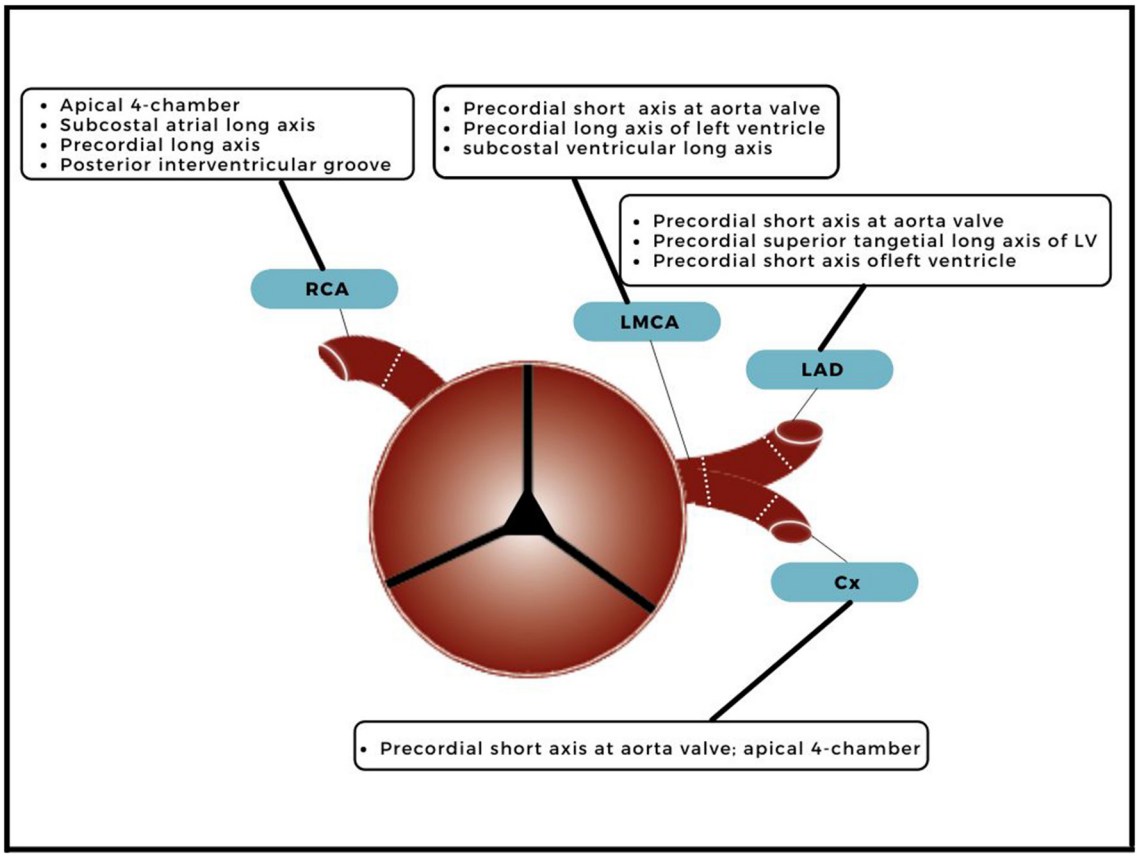

FIGURE 1 | Echocardiographic view and measuring points. A transverse plane of the ascending aorta, just above the aortic valve, with branching of the right coronary artery (RCA), left main coronary artery (LMCA), left anterior descending artery (LAD) and circumflex (Cx). The dotted lines indicate the measuring points and echocardiographic views for best visualization measurement are included.

visualization of the coronary arteries and accurate measurement of possible CAAs (26). Invasive angiography should only be considered when revascularization by either interventional approach or surgery is indicated based on non-invasive imaging.

Coronary Computed Tomographic Angiography

cCTA is a non-invasive anatomical imaging modality that is ideal for overall detailed 3D coronary artery assessment. It can detect aneurysms, stenosis, thrombosis and calcification at a much greater detail than echocardiography (15). Echocardiography can miss pathology in the distal segments of the coronary artery tree due to a limited ultrasound window, whereas cCTA does not have that limitation and gives a total overview. Moreover, and indicated in our previous study, the circumflex (Cx) most often cannot be detected by echocardiography, but is properly visualized in all patients by cCTA and may contain large CAAs as well (15). Motion artifacts are infrequent in cCTA imaging but may occur (16).

In the past, radiation exposure has been a limiting factor for the application of cCTA in pediatric patients. State-of-the-art CT scanners enable imaging of the coronary artery tree at acceptable radiation exposure and is generally considered an alternative to CAG, as non-invasive anatomical imaging modality in KD (15). Between 1996–2010 a mean radiation exposure acquired by chest CT in children <5 years, 5–9 years and 10–14 years has been 5.3 mSv, 7.5 mSv, 6.4 mSv, respectively (27). By optimization, radiation exposure can be reduced, substantially lowering the risk of radiation induced cancers (27). With a third generation dual-source CT scanner we reached a median effective dose (ED) of 1.5 mSv in KD patients for the evaluation of the coronary arteries (15), while natural background radiation has been estimated at 3 mSv per year for adults and a chest X-ray at 0.01 mSv (28). Apart from the actual exposure dose per procedure, the exposure is also determined by the heart rate. At irregular and high heart rates the acquisition window is widened resulting in a higher radiation dose. Furthermore, a higher heart rate is associated with more motion artifacts.

To reduce motion artifacts, if appropriate, beta-blockers should be prescribed if the heart rate exceeds 72 beats per min. When using a dual-source scanner, good quality acquisitions at higher heart-rates are possible by applying a prospective ECG-triggered sequential scan, instead of a

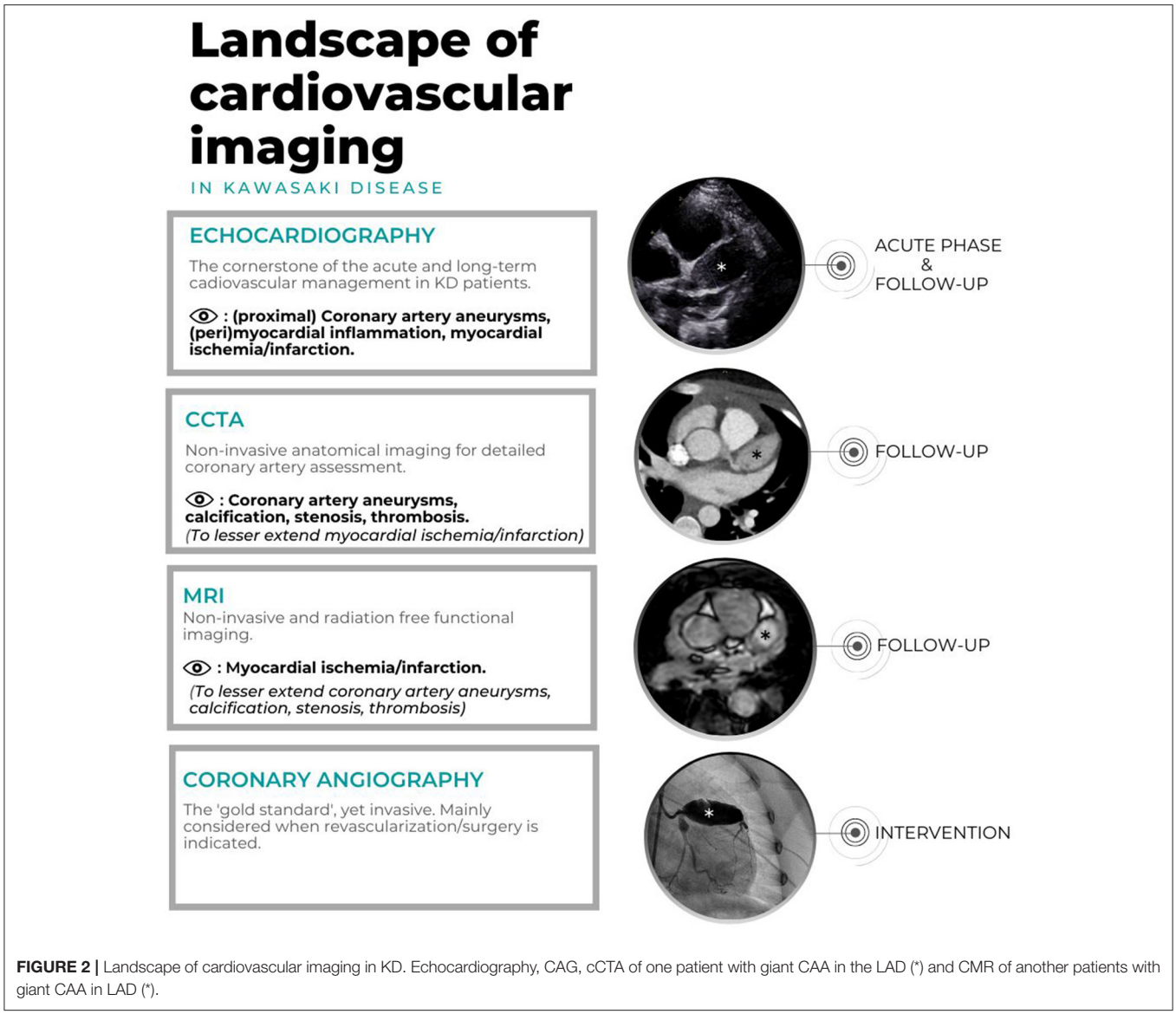

FIGURE 2 | Landscape of cardiovascular imaging in KD. Echocardiography, CAG, cCTA of one patient with giant CAA in the LAD (*) and CMR of another patients with giant CAA in LAD (*).

high-pitch spiral scan. To avoid motion artifacts, children between the age of 18 months and 4 years are scanned under general anesthesia. Children younger than 18 months are scanned with a "feed and wrap" method, where the child is first fed then swaddled to induce natural sleep during scanning.

If patients are to transition to the adult cardiologist, cCTA in the late adolescence can give a starting point for further follow-up.

Cardiac Magnetic Resonance Imaging

CMR is a non-invasive and radiation free functional imaging modality. Before the arrival of the dual-source CT scanners, CMR was the preferred imaging method for the coronary artery assessment in addition to echocardiography. However, studies have shown that CMR is not as accurate as the cCTA for the detection of CAAs, thrombosis, calcification and stenosis (16). Nevertheless, CMR does offer the evaluation of the cardiac function, volumes and myocardial perfusion with pharmacological stress testing which is essential to assess reversible ischemia and visualization of myocardial scarring with delayed contrast enhancement (29–31).

The disadvantage of MRI is that imaging is more sensitive to motion artifacts due to the long scan time that is required to acquire all the proper image sequences. Involuntary subject motion and cardio/respiratory motions including high and variable heart rate, can significantly affect image quality. Children under the age of +/- 10 years (depending on compliance) often require anesthesia because they are unable to stay motionless and compliant for the duration that the CMR requires to obtain high-quality images.

TABLE 1 | Summary of AHA guidelines echocardiography during acute and subacute an convalescent phase (<3 months).

	Detection of	Interval echocardiography	Other
Uncomplicated patients	CAA	At diagnosis, 1–2 weeks after treatment, 4–6 weeks after treatment	
Z score > 2.5	CAA	At least 2x per week until progression stopped	
If expanding or giant CAA	Coronary artery thrombosis	- 1x per week in 1st 45 days - 2x per week while expanding, otherwise: monthly until 3rd month	In case of giant CAA consider cCTA/CMR/CAG at baseline (within 2–6 months)

Stress Testing for Inducible Myocardial Ischemia

Echocardiography, MRI or single-photon emission computed tomography (SPECT) stress testing is a noninvasive procedure that can detect inducible ischemia in KD patients. In general, exercise stress is preferred over pharmacologically induced stress (32); therefore, the success rate depends highly on the ability of the child to cooperate. Stress testing does not have a fixed place in our practical workflow but is performed on indication (when thrombosis and/or stenosis is suspected, when having clinical symptoms such as chest pain, ECG changes and/or severe abnormalities on previous imaging). Little research has been performed thus far to determine the clinical benefits (treatment and management) of stress testing in addition to CMR and/or CT.

Future Imaging Perspectives: Hemodynamics

Not only the *Z* score of the CAA matters for risk stratification, also shape, number of CAAs should be examined because they influence hemodynamics. Hemodynamics are relevant in the development of thrombosis. Insight into the changes in blood flow and shear stress might be useful in developing a more specific risk assessment for patients with aneurysms. Invasive studies (doppler flow wire measurements) suggest that stagnation of flow and low shear stress is associated with the risk of thrombus formation (33, 34). Image-based modeling to quantify hemodynamics and shear stress showed that hemodynamic parameters can identify aneurysms at risk for thrombotic lesions (35, 36).

Echocardiography, cCTA, CMR and CAG are of importance for the risk assessment of aneurysmatic lesions, to further optimize anticoagulant treatment and assess the timing of coronary artery bypass grafting or percutaneous transluminal coronary angioplasty (PTCA). **Figure 2** shows the landscape of cardiovascular imaging modalities in KD patients.

Assessment of Guidelines

Acute, Subacute and Convalescent Phase Until 3 Months After Onset of Disease

American Heart Association

The American Heart Association (AHA) guidelines (17) recommend echocardiography as the first choice imaging modality, the frequency depends on the presence of CAA, stability and size (**Table 1**). ECG is not routinely adopted in the AHA cardiovascular assessment guidelines of the acute phase.

Japanese Circulation Society

Interestingly, the guidelines of the Japanese Circulation Society (JCS) (37) do not define a CAA in the first month of disease, only if the lesions persists after 1 month of disease. If the CAA, independent of its size, resolves within 1 month it will be classified as a transient dilation. KD patients categorized with no dilation or transient dilation are recommended to have an ECG and echocardiogram at 1 and 2 months. For the patients with a remaining CAA, with a stenotic lesion confirmed by CAG (with or without ischemia), the JCS recommends to consider cCTA, CMR or CAG in the convalescent phase. The JCS does not have step-by-step recommendations for the acute phase (i.e., the first 3 months) other than the last mentioned.

Long-Term Follow-Up (From 3 Months Onward)

Both guidelines propose their long-term cardiovascular assessment based on the findings by echocardiography during the first 3 months. Both guidelines have recommendations for regressed CAAs over time, for the long-term follow-up. The long-term cardiovascular assessment of the AHA and JCS are summarized in **Tables 2**, **3**, respectively.

The Japanese guidelines consider additional imaging modalities (cCTA, CMR or CAG). The JCS mentions that stress testing is important for myocardial ischemia detection. Stress echocardiography or CMR using either pharmacological stress or exercise could be valuable in addition to the exercise ECG. The JCS describes "periodic check-ups" in regressed medium and giant CAAs, but it is unclear what these check-ups should encompass as a minimum. In addition, the JCS mentions that it is desirable to perform CAG at least once in patients with coronary artery dilation, due to discrepancies between echocardiography and CAG.

CARDIOVASCULAR ASSESSMENT: ACTIONABLE WORKFLOW BASED ON EXPERT OPINION FROM A TERTIARY KD CLINIC

Acute, Subacute and Convalescent Phase (Up to 3 Months)

Based on our experience and more or less similar to the AHA, we apply echocardiography in uncomplicated patients

TABLE 2 | Summary of AHA guidelines for the long-term cardiovascular assessment (> 3 months).

Classification	Interval echocardiography + ECG	cCTA, CMR, CAG	Inducible myocardial ischemia (stress echocardiography MRI, stress nuclear medicine, positron emission tomography (PET))
No Dilation and dilation	Consider: up to 12 months*		
Regression small CAA to normal/dilation	Every 1–3 years, not performing routine echocardiography may be considered unless patient has symptoms or signs of ventricular dysfunction/myocardial ischemia	Consider: if inducible ischemia/ventricular dysfunction	Consider: every 3–5 years or if patient has symptoms**
Regression medium CAA to small CAA	Yearly	Consider: 3–5 years	Every 2–3 years or if patient has symptoms**
Regression medium CAA to normal/dilation	Every 1–2 years, not performing routine echocardiography may be considered unless patient has symptoms or signs of ventricular dysfunction/myocardial ischemia	Consider: if inducible ischemia	Every 2–5 years if patient has symptoms**
Regression giant CAA to medium CAA	Every 6–12 months	Consider: 2–5 years	Every year if patient has symptoms**
Regression giant CAA to small CAA	Every 6–12 months	Consider: 2–5 years	Every 1–2 years or if patient has symptoms**
Regression giant CAA to normal/dilation	Every 1–2 years, not performing routine echocardiography may be considered unless patient has symptoms or signs of ventricular dysfunction	Consider: 2–5 years	Every 2–5 years or if the patient has symptoms**
Remaining small CAA	6 months, 1 year, every year onward is reasonable	Consider: 3–5 years	Every 2–3 years or if patient has symptoms**
Remaining medium CAA	3 months, 6 months, 1 year. Every 6–12 months onward is reasonable	Consider: 2–5 years	Every 1–3 years or if patient has symptoms**
Remaining giant CAA	6, 9, 12 months in 1st year and every 3–6 months onward	Consider: Baseline within 2–6 months or in 1st year, consider every 1–5 years onward	Every 6–12 months if patient has symptoms**

Dilation is a CAA with Z score ≥2–< 2.5.
**Ongoing follow-up to 12 months may be considered, if dilation is persistent after 4–6 weeks then it is reasonable to continue follow up to 12 months or even every 2–5 years.*
***Suggestive for ischemia or signs of ventricular dysfunction.*

TABLE 3 | Summary of JCS guidelines for the long-term cardiovascular assessment (> 3 months).

Classification	Interval echocardiography + ECG	cCTA, CMR, CAG
No Dilation and transient dilation*	6, 12 months and 5 years (or yearly) until 5 years old	
Regression small CAA (normalization)	Yearly	Consider: 1 year/when CAA regresses, recommended when finishing high school**
Regression medium/giant CAA (normalization)	Every 6–12 months	Consider: 1 year then 3–5 years**
Remaining small CAA	Yearly	Consider: 1 year then 3–5 years, desirable to perform CAG at least once***
Remaining medium CAA	Every 6–12 months	Consider: 1 year then 2–5 years, desirable to perform CAG at least once ***
Remaining giant CAA	Every 6–12 months	Consider: 1 year then 1–5 years, desirable to perform CAG at least once ***
Coronary artery stenotic lesion + ischemia	Consider timely	Consider timely
Coronary artery stenotic lesion	Every 6–12 months	Consider: 1 year then 1–5 years

**Transient dilation is defined as any CAA in the first month.*
***Periodic check-ups are advised due to the potential progression with calcification or stenosis after 10–20 years.*
****According to the JCS, it is desirable to perform CAG at least once in patients with dilation and CAAs because of discrepancies between echocardiography and CAG.*

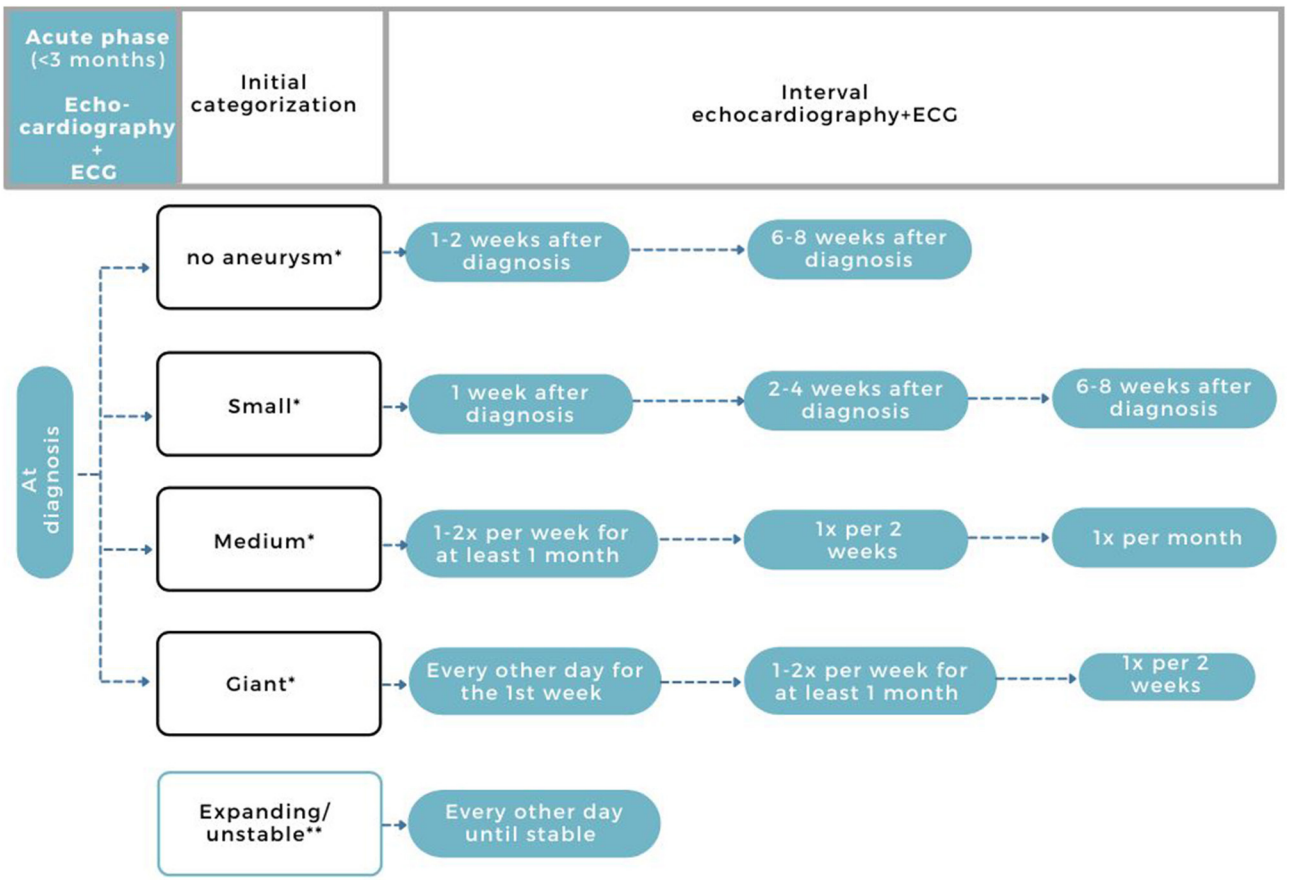

FIGURE 3 | Current practice for cardiovascular assessment in the acute phase of KD (< 3 months).

in the acute phase: at diagnosis, week 1-2, and week 6-8 (**Figure 3**). In patients with expanding/unstable CAAs upon the first echocardiographies, or with signs of ongoing inflammation (fever or persistent/slowly decreasing CRP), we strongly recommend more frequent echocardiographic imaging (**Figure 3**). When echocardiography results are indefinite and/or more complications are suspected, additional imaging can be of additional value, also in the acute phase.

LONG-TERM FOLLOW-UP

Our current practice for the long-term follow-up is divided in a stable situation (**Figure 4**) and one of regression of the aneurysmatic lesion (**Figure 5**).

Stable Situation

No Aneurysm

Similar to AHA and JCS guidelines for KD patients with no coronary artery involvement on echocardiography, we do not recommend any additional imaging methods. We follow a different frequency of echocardiography, encompassing a follow-up at 6 months, 12 months, 5 years, and at 14 years (**Figure 4**).

At the final check we offer an extensive risk factor evaluation for the detection of additional risk factors on top of KD (including lipid profile, familial cardiovascular disease and atherosclerosis risk interpretation). We combine lipid profiles with cCTA for plaque, CAA and thrombosis detection (**Figure 4**). When repeatedly abnormal lipid profiles are detected (increased LDLc, total cholesterol, LpA), we perform a targeted next-generation sequencing panel of 30 genes to exclude familial dyslipidemia). If abnormal, life style advice and cholesterol lowering medication is provided with patient-tailored follow-up.

Small Aneurysm (Z Score ≥ 2.5 < 5.0)

At our center, we offer patients with small aneurysms echocardiographic follow-up combined with ECG similar to the AHA guidelines, at 6 months, 12 months, and every 1–3 years until the age of 14 where we combine imaging with extensive assessment of risk factors, essentially as mentioned above. Based on current experience with state-of-the-art cCTA,

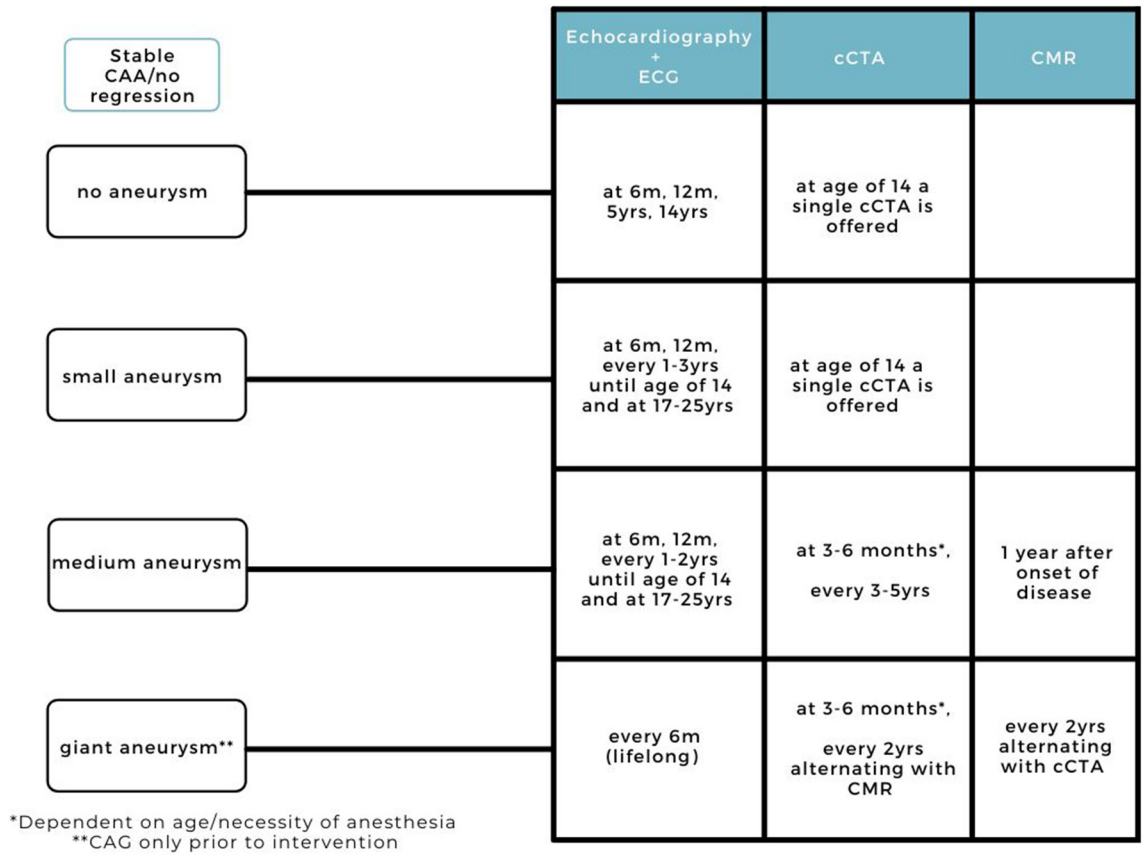

FIGURE 4 | Current practice for long-term cardiovascular follow-up (>3 months) in KD patients (stable CAAs, without regression).

we recommend additional imaging in KD patients with coronary artery involvement. By detecting missed aneurysms, a more accurate CAA classification can be established and possible complications due to under-treatment can be prevented. We suggest this additional imaging at the age of 14 to avoid motion artifacts and higher radiation exposure.

Depending on the imaging results, and additional (chemical) laboratory findings, transition to adult care is being discussed with the patients (and their parents) around this time (**Figure 4**). We combine lipid profiles with cCTA for plaque, CAA and thrombosis detection. Between the age of 17 and 25 we offer an extra visit if additional risk factors are present (blood tests, adipositas, familial cardiovascular disease).

Medium Aneurysm (Z Score ≥ 5.0 < 10.0)

At our center, patients with medium aneurysms are offered more frequent echocardiographic follow-up than the AHA guidelines, but less frequent than the JCS guidelines. For additional imaging we have a clear schedule in which cCTA and CMR both have a distinct role and place in time. The first cCTA for the coronary artery assessment is performed at 3–6 months (depending on the age and necessity of anesthesia) and every 3–5 years (**Figure 4**). We do not perform additional imaging immediately after diagnosis, as the first weeks are known for diameter changes of the aneurysms also the patient can be more agitated/with tachycardia in the acute phase which can be challenging for high quality imaging therefore we wait until the 3rd month. We suggest to perform CMR 1 year after onset of disease to evaluate the cardiac function, volumes and fibrosis.

Giant Aneurysm Z Score ≥ 10

Patients with a CAA classification of a giant CAA (and even more so patients with a Z score > 20), have a risk of luminal narrowing, formation of thrombosis and major adverse cardiovascular events especially in patients with a CAA in the LAD and RCA (8). Therefore, we suggest to perform additional cardiovascular assessment at 3–6 months and thereafter every year, alternating CMR for cardiac function analysis and ischemia detection, and cCTA for assessment of the coronary artery tree and evaluation of diameter, calcification, formation of thrombosis, plaque deposition, and arterial stenosis (**Figure 4**), together with lipid profiles as mentioned above, including repeated monitoring for blood parameters because of the double (or triple) anticoagulant medication.

Regression

When regression is suggested upon echocardiography, and confirmed by cCTA, we suggest an adjusted follow-up routine

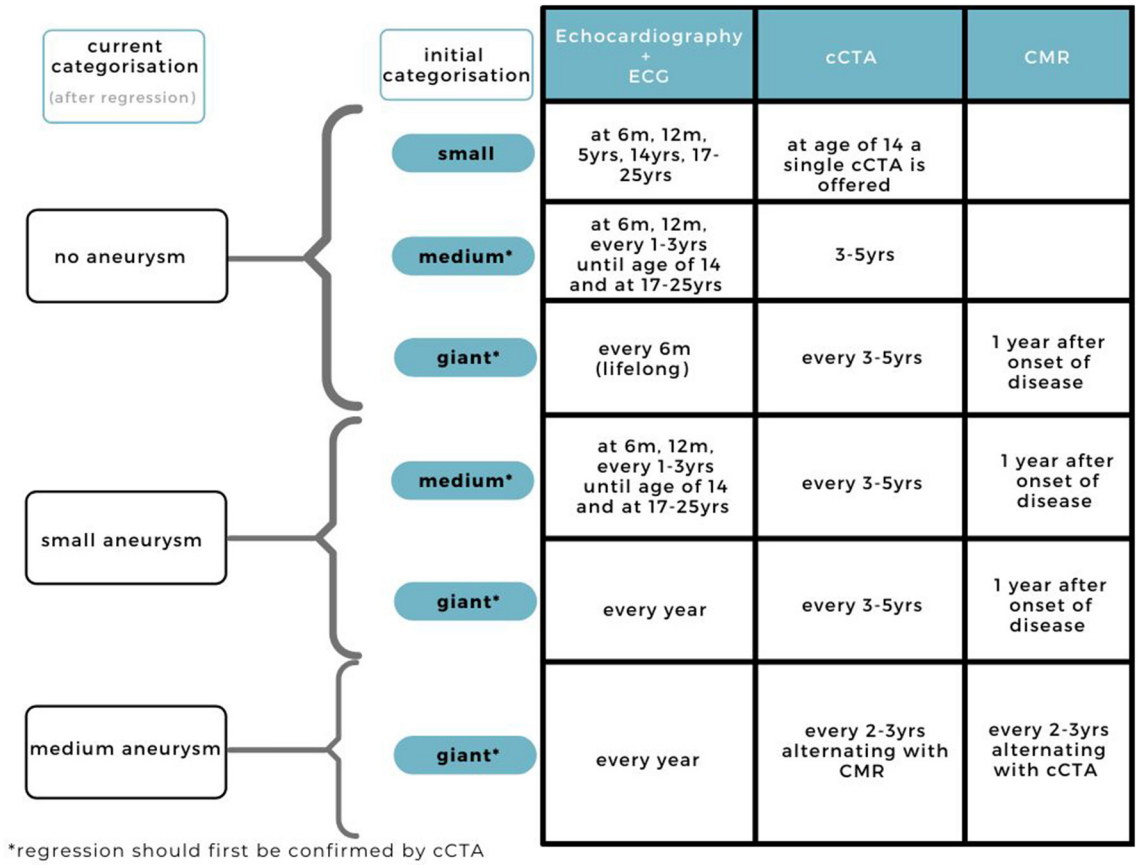

FIGURE 5 | Current practice for cardiovascular assessment during follow-up in KD patients with regressed CAAs.

depending on the change in *Z* score classification (**Figure 5**). Giant and medium aneurysms that have regressed are at risk for stenosis, therefore frequent imaging, especially during the regression, is advised. Depending on the stability of the regressed CAA and parents, it may be decided to deviate from this imaging frequency based on the doctor's own discretion.

DISCUSSION

Based on our experience in practice, combined with the current guidelines, we have presented our patient-specific follow-up workflow for the cardiovascular assessment in KD patients.

The first 3 months since the onset of disease is a precarious time and the frequency of echocardiography is dependent on a few factors: presence or absence of fever, expanding/unstable or stable luminal diameter of the coronary arteries and the *Z* score category in case of an aneurysm. Especially patients with ongoing inflammation such as IVIG resistance rechute or persistent fever are at risk for complications. Long-term follow-up is dependent on the initial CAA classification and extent of regression.

CONCLUSION

Based on our experience in a tertiary single center KD center, and the current guidelines we have presented our cardiovascular assessment flowchart during the acute phase and long-term follow-up. With the current acceptable radiation exposures, cCTA now plays a significant role in patients positive for coronary artery involvement and CMR for cardiac function and infarction size.

AUTHOR CONTRIBUTIONS

DS conceptualized the study and drafted the initial manuscript. TK and IK contributed equally as co-senior authors and conceptualized the study, coordinated, supervised and reviewed the manuscript for important intellectual content, and revised the manuscript. RP, MG, NB, and RW conceptualized the study and reviewed for important intellectual content and revised the manuscript. All authors approved the final manuscript as submitted and agree to be accountable for all aspects of the work.

FUNDING

Funding was made available by the foundation "Kind en Handicap" and an anonymous donor through the AMC foundation.

ACKNOWLEDGMENTS

We gratefully appreciate the echocardiogram technicians, Ari Widyanti, Ewoudt Straat and Natasja Pilot for their work and Marije Reijgersberg for the organization of the outpatient clinic.

REFERENCES

1. Newburger JW, Takahashi M, Burns JC, Beiser AS, Chung KJ, Duffy CE, et al. The treatment of Kawasaki syndrome with intravenous gamma globulin. *N Engl J Med.* (1986) 315:341–7. doi: 10.1056/NEJM198608073150601
2. Terai M, Shulman ST. Prevalence of coronary artery abnormalities in Kawasaki disease is highly dependent on gamma globulin dose but independent of salicylate dose. *J Pediatr.* (1997) 131:888–93. doi: 10.1016/S0022-3476(97)70038-6
3. Nagashima M, Matsushima M, Matsuoka H, Ogawa A, Okumura N. High-dose gammaglobulin therapy for Kawasaki disease. *J Pediatr.* (1987) 110:710–2. doi: 10.1016/S0022-3476(87)80007-0
4. Furusho K, Sato K, Soeda T, Matsumoto H, Okabe T, Hirota T, et al. High-dose intravenous gammaglobulin for Kawasaki disease. *Lancet.* (1983) 2:1359. doi: 10.1016/S0140-6736(83)91109-1
5. Muta H, Ishii M, Sakaue T, Egami K, Furui J, Sugahara Y, et al. Older age is a risk factor for the development of cardiovascular sequelae in Kawasaki disease. *Pediatrics.* (2004) 114:751–4. doi: 10.1542/peds.2003-0118-F
6. Mastrangelo G, Cimaz R, Calabri GB, Simonini G, Lasagni D, Resti M, et al. Kawasaki disease in infants less than one year of age: an Italian cohort from a single center. *BMC Pediatr.* (2019) 19:321. doi: 10.1186/s12887-019-1695-0
7. Dietz SM, Kuipers IM, Koole JCD, Breur J, Fejzic Z, Frerich S, et al. Regression and complications of z-score-based giant aneurysms in a dutch cohort of kawasaki disease patients. *Pediatr Cardiol.* (2017) 38:833–9. doi: 10.1007/s00246-017-1590-0
8. McCrindle BW, Manlhiot C, Newburger JW, Harahsheh AS, Giglia TM, Dallaire F, et al. Medium-term complications associated with coronary artery aneurysms after kawasaki disease: a study from the international kawasaki disease registry. *J Am Heart Assoc.* (2020) 9:e016440. doi: 10.1161/JAHA.119.016440
9. Ronai C, Hamaoka-Okamoto A, Baker AL, de Ferranti SD, Colan SD, Newburger JW, et al. Coronary artery aneurysm measurement and Z Score variability in kawasaki disease. *J Am Soc Echocardiogr.* (2016) 29:150–7. doi: 10.1016/j.echo.2015.08.013
10. Lorenzoni RP, Elkins N, Quezada M, Silver EJ, Mahgerefteh J, Hsu DT, et al. Impact of Z score system on the management of coronary artery lesions in Kawasaki disease. *Cardiol Young.* (2021) 1–8. doi: 10.1017/S1047951121003437
11. Takahashi M, Mason WH, Acherman RJ, Lewis AB, Szmuszkovicz JR, Wong PC, et al. Is Perivascular echo brightness a reliable marker of coronary arteritis in acute kawasaki syndrome? *Pediatr Res.* (2003) 53:177–177. doi: 10.1203/00006450-200301000-00139
12. Rabinowitz EJ, Rubin LG, Desai K, Hayes DA, Tugertimur A, Kwon EN, et al. Examining the utility of coronary artery lack of tapering and perivascular brightness in incomplete kawasaki disease. *Pediatr Cardiol.* (2019) 40:147–53. doi: 10.1007/s00246-018-1971-z
13. Yu JJ, Jang WS, Ko HK, Han MK, Kim YH, Ko JK, et al. Perivascular brightness of coronary arteries in Kawasaki disease. *J pediatr.* (2011) 159:454–7.e451. doi: 10.1016/j.jpeds.2011.02.029
14. Dietz SM, Tacke CE, Kuipers IM, Wiegman A, de Winter RJ, Burns JC, et al. Cardiovascular imaging in children and adults following Kawasaki disease. *Insights Imaging.* (2015) 6:697–705. doi: 10.1007/s13244-015-0422-0
15. van Stijn D, Planken RN, Groenink M, Streekstra GJ, Kuijpers TW, Kuipers IM. Coronary artery assessment in Kawasaki disease with dual-source CT angiography to uncover vascular pathology. *Eur Radiol. (*2019) 30:432–41. doi: 10.1007/s00330-019-06367-6
16. van Stijn D, Planken N, Kuipers I, Kuijpers T, CT. Angiography or cardiac MRI for detection of coronary artery aneurysms in kawasaki disease. *Front Pediatr.* (2021) 9:630462. doi: 10.3389/fped.2021.630462
17. McCrindle BW, Rowley AH, Newburger JW, Burns JC, Bolger AF, Gewitz M, et al. Diagnosis, treatment, and long-term management of kawasaki disease: a scientific statement for health professionals from the American Heart Association. *Circulation.* (2017) 135:e927–99. doi: 10.1161/CIR.0000000000000484
18. Harada M, Yokouchi Y, Oharaseki T, Matsui K, Tobayama H, Tanaka N, et al. Histopathological characteristics of myocarditis in acute-phase Kawasaki disease. *Histopathology.* (2012) 61:1156–67. doi: 10.1111/j.1365-2559.2012.04332.x
19. Dionne A, Dahdah N. Myocarditis and Kawasaki disease. *Int J Rheum Dis.* (2018) 21:45–9. doi: 10.1111/1756-185X.13219
20. Takahashi M. Myocarditis in Kawasaki syndrome. A minor villain? *Circulation.* (1989) 79:1398–400. doi: 10.1161/01.CIR.79.6.1398
21. Anderson TM, Meyer RA, Kaplan S. Long-term echocardiographic evaluation of cardiac size and function in patients with Kawasaki disease. *Am Heart J.* (1985) 110:107–15. doi: 10.1016/0002-8703(85)90523-X
22. Pilania RK, Jindal AK, Bhattarai D, Naganur SH, Singh S. Cardiovascular involvement in Kawasaki disease is much more than mere coronary arteritis. *Front Pediatr.* (2020) 8:526969. doi: 10.3389/fped.2020.526969
23. Printz BF, Sleeper LA, Newburger JW, Minich LL, Bradley T, Cohen MS, et al. Noncoronary cardiac abnormalities are associated with coronary artery dilation and with laboratory inflammatory markers in acute Kawasaki disease. *J Am Coll Cardiol.* (2011) 57:86–92. doi: 10.1016/j.jacc.2010.08.619
24. Ravekes WJ, Colan SD, Gauvreau K, Baker AL, Sundel RP, van der Velde ME, et al. Aortic root dilation in Kawasaki disease. *Am J Cardiol.* (2001) 87:919–22. doi: 10.1016/S0002-9149(00)01541-1
25. Gurofsky RC, Sabharwal T, Manlhiot C, Redington AN, Benson LN, Chahal N, et al. Arterial complications associated with cardiac catheterization in pediatric patients with a previous history of Kawasaki disease. *Catheter Cardiovasc Interv.* (2009) 73:809–13. doi: 10.1002/ccd.21892
26. Tsujii N, Tsuda E, Kanzaki S, Kurosaki K. Measurements of coronary artery aneurysms due to Kawasaki disease by dual-source computed tomography (DSCT). *Pediatr Cardiol.* (2016) 37:442–7. doi: 10.1007/s00246-015-1297-z
27. Miglioretti DL, Johnson E, Williams A, Greenlee RT, Weinmann S, Solberg LI, et al. The use of computed tomography in pediatrics and the associated radiation exposure and estimated cancer risk. *JAMA Pediatr.* (2013) 167:700–7. doi: 10.1001/jamapediatrics.2013.311
28. Loftus ML, Sanelli PC, Frush DP, Applegate KE. Radiation exposure from medical imaging. In: Medina LS, Sanelli PC, Jarvik JG, editors. *Evidence-Based Neuroimaging Diagnosis and Treatment: Improving the Quality of Neuroimaging in Patient Care*. New York, NY: Springer New York (2013). p. 63–79.
29. Wagner A, Mahrholdt H, Holly TA, Elliott MD, Regenfus M, Parker M, et al. Contrast-enhanced MRI and routine single photon emission computed tomography (SPECT) perfusion imaging for detection of subendocardial myocardial infarcts: an imaging study. *Lancet.* (2003) 361:374–9. doi: 10.1016/S0140-6736(03)12389-6
30. Schwitter J, Wacker CM, van Rossum AC, Lombardi M, Al-Saadi N, Ahlstrom H, et al. MR-IMPACT: comparison of perfusion-cardiac magnetic resonance with single-photon emission computed tomography for the detection of coronary artery disease in a multicentre, multivendor, randomized trial. *Eur Heart J.* (2008) 29:480–9. doi: 10.1093/eurheartj/ehm617
31. Kim RJ, Wu E, Rafael A, Chen EL, Parker MA, Simonetti O, et al. The use of contrast-enhanced magnetic resonance imaging to identify reversible myocardial dysfunction. *N Engl J Med.* (2000) 343:1445–53. doi: 10.1056/NEJM200011163432003
32. Pellikka PA, Arruda-Olson A, Chaudhry FA, Chen MH, Marshall JE, Porter TR, et al. Guidelines for performance, interpretation, and application of stress echocardiography in ischemic heart disease: from the american

society of echocardiography. *J Am Soc of Echocardiogr*. (2020) 33:1–41.e48. doi: 10.1016/j.echo.2019.07.001
33. Kuramochi Y, Ohkubo T, Takechi N, Fukumi D, Uchikoba Y, Ogawa S. Hemodynamic factors of thrombus formation in coronary aneurysms associated with Kawasaki disease. *Pediatr Int.* (2000) 42:470–5. doi: 10.1046/j.1442-200x.2000.01270.x
34. Ohkubo T, Fukazawa R, Ikegami E, Ogawa S. Reduced shear stress and disturbed flow may lead to coronary aneurysm and thrombus formations. *Pediatr Int.* (2007) 49:1–7. doi: 10.1111/j.1442-200X.2007.02312.x
35. Sengupta D, Kahn AM, Burns JC, Sankaran S, Shadden SC, Marsden AL. Image-based modeling of hemodynamics in coronary artery aneurysms caused by Kawasaki disease. *Biomech Model Mechanobiol.* (2012) 11:915–32. doi: 10.1007/s10237-011-0361-8
36. Sengupta D, Kahn AM, Kung E, Esmaily Moghadam M, Shirinsky O, Lyskina GA, et al. Thrombotic risk stratification using computational modeling in patients with coronary artery aneurysms following Kawasaki disease. *Biomech Model Mechanobiol.* (2014) 13:1261–76. doi: 10.1007/s10237-014-0570-z
37. Fukazawa R, Kobayashi J, Ayusawa M, Hamada H, Miura M, Mitani Y, et al. JCS/JSCS 2020 guideline on diagnosis and management of cardiovascular sequelae in Kawasaki disease. *Circ J.* (2020) 84:1348–407. doi: 10.1253/circj.CJ-19-1094

Conflict of Interest: The authors declare that the research was conducted in the absence of any commercial or financial relationships that could be construed as a potential conflict of interest.

Publisher's Note: All claims expressed in this article are solely those of the authors and do not necessarily represent those of their affiliated organizations, or those of the publisher, the editors and the reviewers. Any product that may be evaluated in this article, or claim that may be made by its manufacturer, is not guaranteed or endorsed by the publisher.

frontiers | Frontiers in Cardiovascular Medicine

ORIGINAL RESEARCH
published: 24 June 2022
doi: 10.3389/fcvm.2022.855118

Isolating the Effect of Arch Architecture on Aortic Hemodynamics Late After Coarctation Repair: A Computational Study

Vahid Goodarzi Ardakani[1], *Harshinee Goordoyal*[1], *Maria Victoria Ordonez*[2], *Froso Sophocleous*[2,3], *Stephanie Curtis*[2], *Radwa Bedair*[2], *Massimo Caputo*[2,3], *Alberto Gambaruto*[1] *and Giovanni Biglino*[2,3,4]*

[1] Department of Mechanical Engineering, University of Bristol, Bristol, United Kingdom, [2] University Hospitals Bristol and Weston, NHS Foundation Trust, Bristol, United Kingdom, [3] Bristol Medical School, University of Bristol, Bristol, United Kingdom, [4] National Heart and Lung Institute, Imperial College London, London, United Kingdom

Objectives: Effective management of aortic coarctation (CoA) affects long-term cardiovascular outcomes. Full appreciation of CoA hemodynamics is important. This study aimed to analyze the relationship between aortic shape and hemodynamic parameters by means of computational simulations, purposely isolating the morphological variable.

Methods: Computational simulations were run in three aortic models. MRI-derived aortic geometries were generated using a statistical shape modeling methodology. Starting from $n = 108$ patients, the mean aortic configuration was derived in patients without CoA ($n = 37$, "no-CoA"), with surgically repaired CoA ($n = 58$, "r-CoA") and with unrepaired CoA ($n = 13$, "CoA"). As such, the aortic models represented average configurations for each scenario. Key hemodynamic parameters (i.e., pressure drop, aortic velocity, vorticity, wall shear stress WSS, and length and number of strong flow separations in the descending aorta) were measured in the three models at three time points (peak systole, end systole, end diastole).

Results: Comparing no-CoA and CoA revealed substantial differences in all hemodynamic parameters. However, simulations revealed significant increases in vorticity at the site of CoA repair, higher WSS in the descending aorta and a 12% increase in power loss, in r-CoA compared to no-CoA, despite no clinically significant narrowing (CoA index >0.8) in the r-CoA model.

Conclusions: Small alterations in aortic morphology impact on key hemodynamic indices. This may contribute to explaining phenomena such as persistent hypertension in the absence of any clinically significant narrowing. Whilst cardiovascular events in these patients may be related to hypertension, the role of arch geometry may be a contributory factor.

Keywords: aortic coarctation, aortic hemodynamics, computational modeling, computational fluid dynamics, power loss, wall shear stress

OPEN ACCESS

Edited by:
Ruth Heying,
University Hospital Leuven, Belgium

Reviewed by:
Mario Carminati,
IRCCS San Donato Polyclinic, Italy
Daniel De Wolf,
Ghent University Hospital, Belgium

***Correspondence:**
Giovanni Biglino
g.biglino@bristol.ac.uk

Specialty section:
This article was submitted to Pediatric Cardiology, a section of the journal Frontiers in Cardiovascular Medicine

Received: *14 January 2022*
Accepted: *30 May 2022*
Published: *24 June 2022*

Citation:
Goodarzi Ardakani V, Goordoyal H, Ordonez MV, Sophocleous F, Curtis S, Bedair R, Caputo M, Gambaruto A and Biglino G (2022) Isolating the Effect of Arch Architecture on Aortic Hemodynamics Late After Coarctation Repair: A Computational Study. Front. Cardiovasc. Med. 9:855118. doi: 10.3389/fcvm.2022.855118

INTRODUCTION

Aortic coarctation (CoA) is a discrete congenital heart defect with an incidence of 1/2,500 live births that can occur in isolation or in association with other left sided congenital lesions, such as bicuspid aortic valve (BAV) (1). The association between CoA and BAV is reported in up to 85% of CoA cases and has significant clinical implications on long-term outcomes, morbidity and mortality (1). Cardiovascular effects are mostly through new or persistent systemic hypertension; this may persist after surgery, which suggests that patients retain an abnormal vascular phenotype post-repair.

Aortic arch geometry patterns have been described as either "Gothic" (more angulated) or "Romanesque" (rounder) morphology. It has been suggested that arch geometry, together with increased arterial stiffness, contribute to the development of hypertension in CoA patients (2, 3). Abnormal aortic arch geometry has been associated with rest or exercise-induced hypertension in the long-term follow-up of patients after successful repair of CoA without residual obstruction of the arch (3–5). Hypertension has been linked to lower distensibility and elevated stiffness of the ascending aorta and greater loss of systolic wave amplitude across the aortic arch. This could partially explain the presence of late hypertension in the long-term follow-up of these patients, even in the absence of residual arch stenosis (6, 7). Furthermore, gothic arch geometry can unfavorably impact on left ventricular mass index (LVMI), independent of age and resting systolic blood pressure, suggesting a chronic increase in left ventricular afterload in the presence of gothic arch geometry (4).

The concept of "optimal surgical shape," based on a three-dimensional (3D) analysis of aortic morphology in BAV patients with and without CoA, has been recently introduced into the literature. This showed that patients with repaired CoA were more likely to have a gothic aortic arch morphology and this has been previously associated with new or persistent systemic hypertension in the long term (8). Furthermore, the "selfish brain" hypothesis was recently described, showing that vertebral artery hypoplasia with an incomplete posterior circle of Willis in repaired CoA subjects may be important in the development of hypertension or its persistence, following CoA repair (9). This is suggestive of a more global vascular developmental phenomenon, rather than simple hemodynamics.

Undoubtedly, CoA leads to long-term ventricular and arterial implications and cardiovascular outcomes, with these patients presenting significantly lower survival than the normal population (10), even in the modern era. Therefore, a thorough understanding of CoA hemodynamics and their ramifications is important. The motivation of the study is indeed to make use of computational modeling and the insight they offer in terms of isolating a variable of interest (in this case, aortic arch shape) to contribute to the understanding of aortic pressure changes in CoA patients. The broad clinical relevance of this approach is not only related to the observation that hypertension may be an inevitable consequence of CoA, even following early effective anatomical repair, but that maladaptive processes may be at play in these patients (11). Also in the context of interventional rather than surgical repair, the importance of the aortic arch anatomy in CoA patients is increasingly recognized as a parameter to define cases at higher risk of residual hypertension, even despite optimized isthmic stent implantation (12).

This work focuses purely on fluidodynamic aspects, aiming to analyze the relationship between aortic shape and hemodynamic parameters by means of computational fluid dynamics, purposely isolating the morphological variable and comparing patients with successfully repaired CoA, with unrepaired CoA and without CoA.

METHODS

Aortic Arch Models

The study is based on three aortic models derived from a previously described population of patients with BAV and CoA (8). Starting from $n = 108$ patients, the mean aortic arch

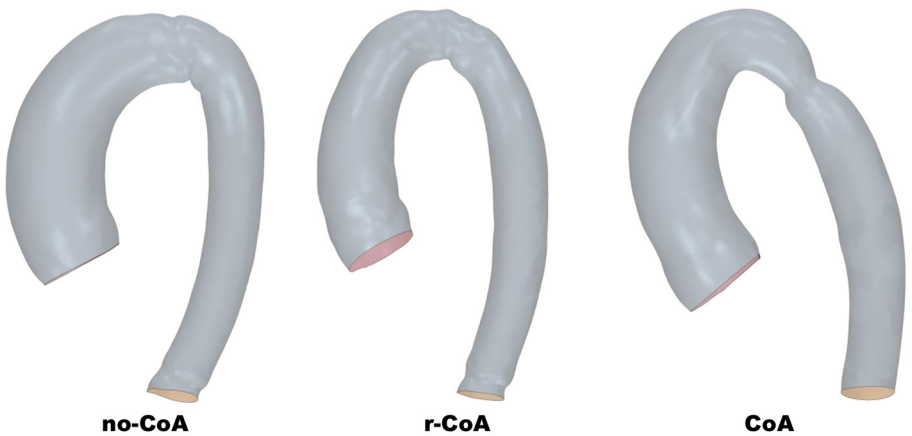

FIGURE 1 | Aortic geometries derived from statistical shape modeling.

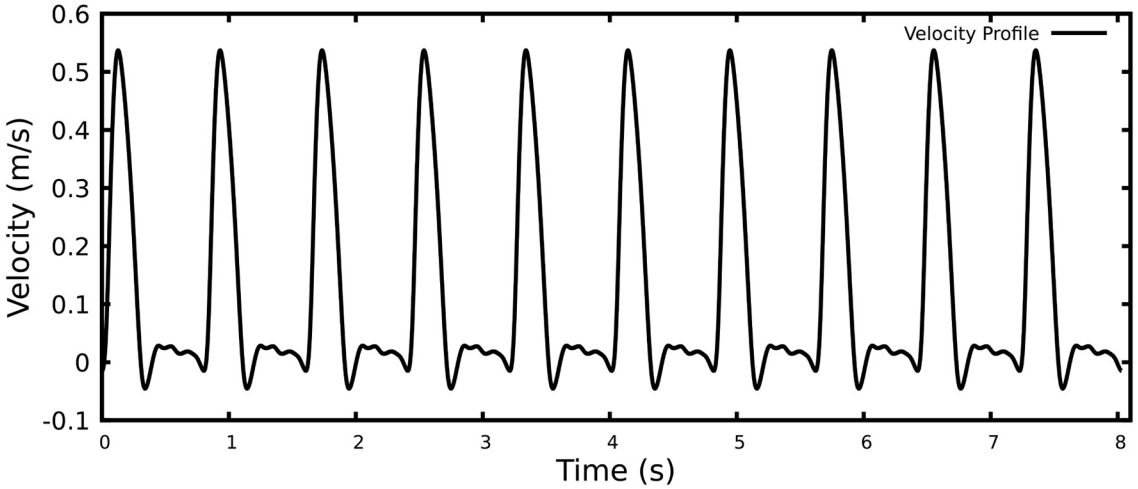

FIGURE 2 | Realistic pulsatile velocity profile for 10 heartbeats.

configuration was derived in patients without CoA ($n = 37$, "No-CoA"), with surgically repaired CoA ($n = 58$, "r-CoA") and with unrepaired CoA ($n = 13$, "CoA"). The aortic shapes were reconstructed from magnetic resonance imaging (MRI) data and the final three configurations were obtained by means of statistical shape modeling, thus producing three average models summarizing the geometrical features of the patients in each group. This resulted in three representative models for the three scenarios of interest (**Figure 1**). More details on the process of image reconstruction are available in (8) and details on the statistical shape modeling framework are available in (13). All datasets were anonymized and, in view of the retrospective study design, formal ethical approval was waived by the local Institutional Research and Innovation Department, and the rest of the study focused on computational simulations.

Computational Fluid Dynamics

Computational simulations were run in the three aortic models, purposely isolating the geo-metrical variable. The mesh generation and the numerical simulation were both carried out in STAR-CCM+ 13.04.010-r8 (Siemens). The flow was simulated using an unsteady implicit scheme, with the SIMPLE algorithm to solve the pressure and velocity in a segregated manner. Second order accuracy was chosen for both temporal and spatial discretization. The time step size and the convergence criteria were set to be $t = 0.001$ s and $\varepsilon = 10^{-8}$, respectively. The fluid was assumed to be incompressible and Newtonian, and the density and dynamic viscosity were set to $\rho = 1,060$ kg/m^3 and $\mu = 0.004$ Pa.s, respectively.

A polyhedral computational grid together with 10 prism layers was generated with an average total number of 6 M elements for the finite volume solver. In order to capture complex flow features as much as possible, the flow was modeled using Large Eddy Simulation (LES), more specifically Dynamic Smagorinsky Subgrid Scale. Literature has suggested that this model is reasonably capable of simulating aortic flows (14–16). A

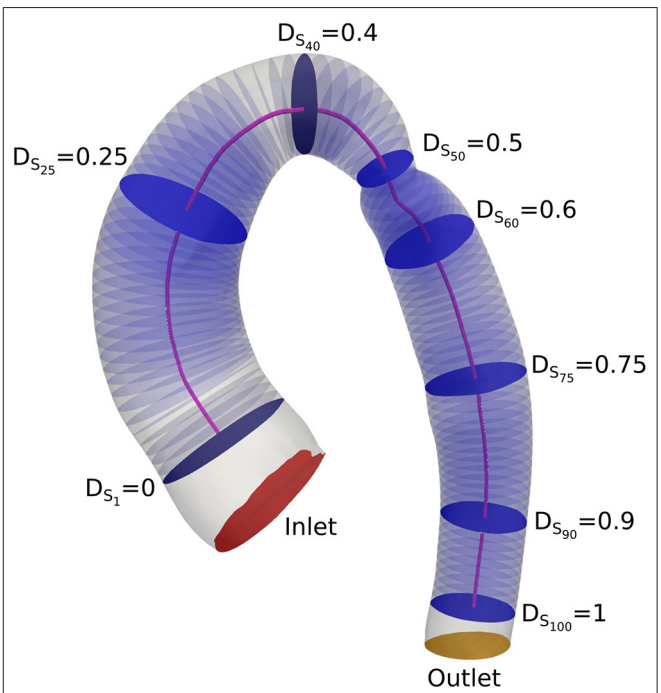

FIGURE 3 | Location of the cross-sections and the centerline.

realistic aortic flow waveform derived from MRI (**Figure 2**) was prescribed as the inlet velocity profile, with average flow rate of 6 L/min, peak velocity of 53.7 cm/s and average velocity of 11.7 cm/s. The outlet boundary condition was considered to be zero pressure. Ten cardiac cycles were simulated and only the last one was used for subsequent analyzes.

In order to compare the computed hemodynamic results with respect to geometric characteristics of the aortic arch, the medial axis of each geometry was computed using Vascular Modeling

Toolkit (VMTK) (17). One-hundred cross-sections along the aorta were further generated such that their normal vectors were locally tangent to the centerline. The average of flow parameters of interest (i.e., pressure, velocity, wall shear stress, vorticity) were measured on each cross-section along the aorta. The slices at positions 40, 50, and 60 were located before, across, and after the coarctation, respectively, and were selected for direct comparison between the different geometries. The slice at position 90 was also included to capture the effect of coarctation on the blood flow properties downstream of the narrowing, in the descending aorta. The location of the slices was normalized from 0 to 1, and is displayed in **Figure 3**.

Comparisons across the three aortic configurations were carried out at three time points, i.e., peak systole (0.13 s, 16% of the cardiac cycle), end systole (0.34 s, 43% of the cardiac cycle) and end diastole (0.80 s, 100% of the cardiac cycle). Key measurements included velocity (m/s, derived directly from the simulations), pressure drop (mmHg, measured as $P(S_{0.9})$–$P(S_{0.4})$, accounting for pressure recovery) and vorticity (defined as the curl of the velocity, which is a measure of the rotation of the flow, /s). Wall shear stress (WSS, dyn/cm^2) was also derived from the simulations. In order to identify areas of elevated WSS and draw comparisons between the three geometries, the average of the obtained WSS was calculated and areas with values higher than this were considered as elevated WSS. The length and number of strong separations in the descending aorta were also investigated by comparing velocity streamlines along the aortic arches.

Data Analysis

Results were compared for the three aortic configurations at the above mentioned three time instances along the length of the aorta. Whilst the aortic models summarize the geometrical features of dozens of patients, the

TABLE 1 | Average values of velocity (V), pressure (P), and vorticity (ω) on slices of 40, 50, 60, and 90.

		No-CoA			r-CoA			CoA		
		PS	ES	ED	PS	ES	ED	PS	ES	ED
S_{40}	V (m/s)	1.12 ± 0.3	0.13 ± 0.09	0.04 ± 0.01	1.57 ± 0.33	0.16 ± 0.07	0.05 ± 0.02	1.58 ± 0.05	0.17 ± 0.09	0.06 ± 0.03
	P (mmHg)	7.94 ± 1.94	−0.66 ± 0.1	−0.62 ± 0.002	8.08 ± 2.57	−1 ± 0.12	−0.66 ± 0.005	38.02 ± 7.19	−0.52 ± 0.1	−0.75 ± 0.007
	ω (/s)	252.5 ± 68	101.1 ± 120	17.11 ± 22	460.1 ± 1,211	129.8 ± 120	27.5 ± 31	458.8 ± 1,473	99.5 ± 137	32.9 ± 39
S_{50}	V (m/s)	1.14 ± 0.44	0.28 ± 0.13	0.04 ± 0.02	1.47 ± 0.62	0.29 ± 0.11	0.05 ± 0.02	3.61 ± 0.65	0.36 ± 0.21	0.11 ± 0.04
	P (mmHg)	4.55 ± 2.91	−0.97 ± 0.16	−0.52 ± 0.003	0.6 ± 3.51	−0.96 ± 0.26	−0.5 ± 0.006	−9.38 ± 4.52	−0.73 ± 0.23	−0.6 ± 0.03
	ω (/s)	386.9 ± 647	204.2 ± 157	24.04 ± 20	710.6 ± 991	289.2 ± 190	27.76 ± 24	1,495.14 ± 4,573	284 ± 376	75 ± 98
S_{60}	V (m/s)	1.13 ± 0.26	0.23 ± 0.13	0.06 ± 0.03	0.97 ± 0.31	0.32 ± 0.13	0.07 ± 0.03	1.78 ± 1.43	0.29 ± 0.13	0.07 ± 0.03
	P (mmHg)	5.51 ± 0.83	−0.74 ± 0.19	−0.44 ± 0.01	7.93 ± 0.65	−1.1 ± 0.28	−0.41 ± 0.01	−16.09 ± 2.44	−0.47 ± 0.24	−0.44 ± 0.01
	ω (/s)	250.7 ± 502	172.7 ± 173	39.63 ± 27	220.3 ± 320	285.3 ± 227	41.58 ± 26	1,077.7 ± 1,507	326.4 ± 232	45.94 ± 33
S_{90}	V (m/s)	1.33 ± 0.28	0.19 ± 0.09	0.05 ± 0.02	1.14 ± 0.25	0.2 ± 0.09	0.06 ± 0.02	1.43 ± 0.3	0.27 ± 0.1	0.05 ± 0.02
	P (mmHg)	2.74 ± 0.6	−0.29 ± 0.08	−0.16 ± 0.005	6.01 ± 0.37	−0.36 ± 0.09	−0.15 ± 0.007	1.52 ± 0.51	−0.38 ± 0.24	−0.17 ± 0.007
	ω (/s)	272.8 ± 552	158.5 ± 100	30.87 ± 24	238.4 ± 469	210.5 ± 136	27.24 ± 21	320.7 ± 686	320.9 ± 237	34.27 ± 24

PS, ES, ED stand for Peak Systole, End Systole, and End Diastole, respectively. Standard deviation is reported as the confidence interval. The location of slices is illustrated in ***Figure 3****.*

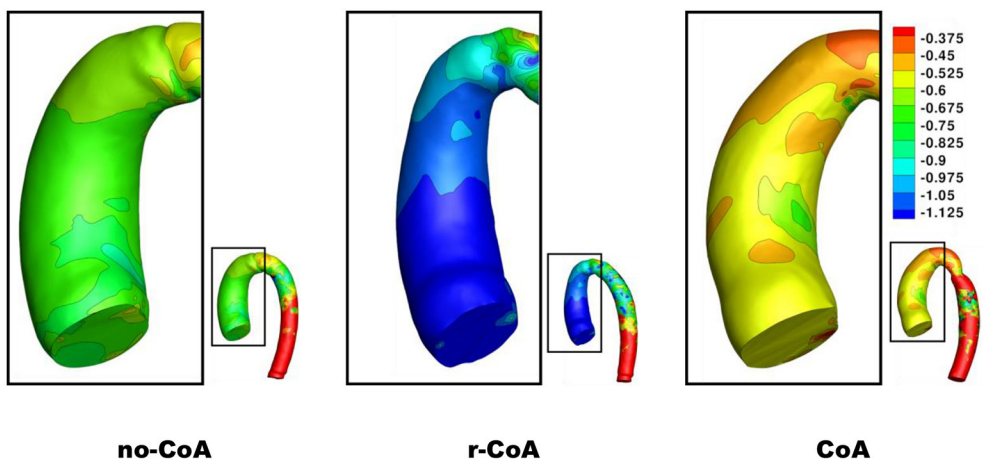

FIGURE 4 | Contour of pressure (mmHg) on the ascending aorta at end systole.

comparison was ultimately carried out on the three statistically derived shapes. This precluded a full statistical analysis, which was beyond the scope of this study, rather taking advantage of the fact that the representative aortic geometries in themselves summarize features from multiple patients.

RESULTS

Velocity, pressure and vorticity values for all geometries and time points are reported in **Table 1**.

Unsurprisingly, comparison between the no-CoA and the CoA models revealed much higher aortic pressure in the

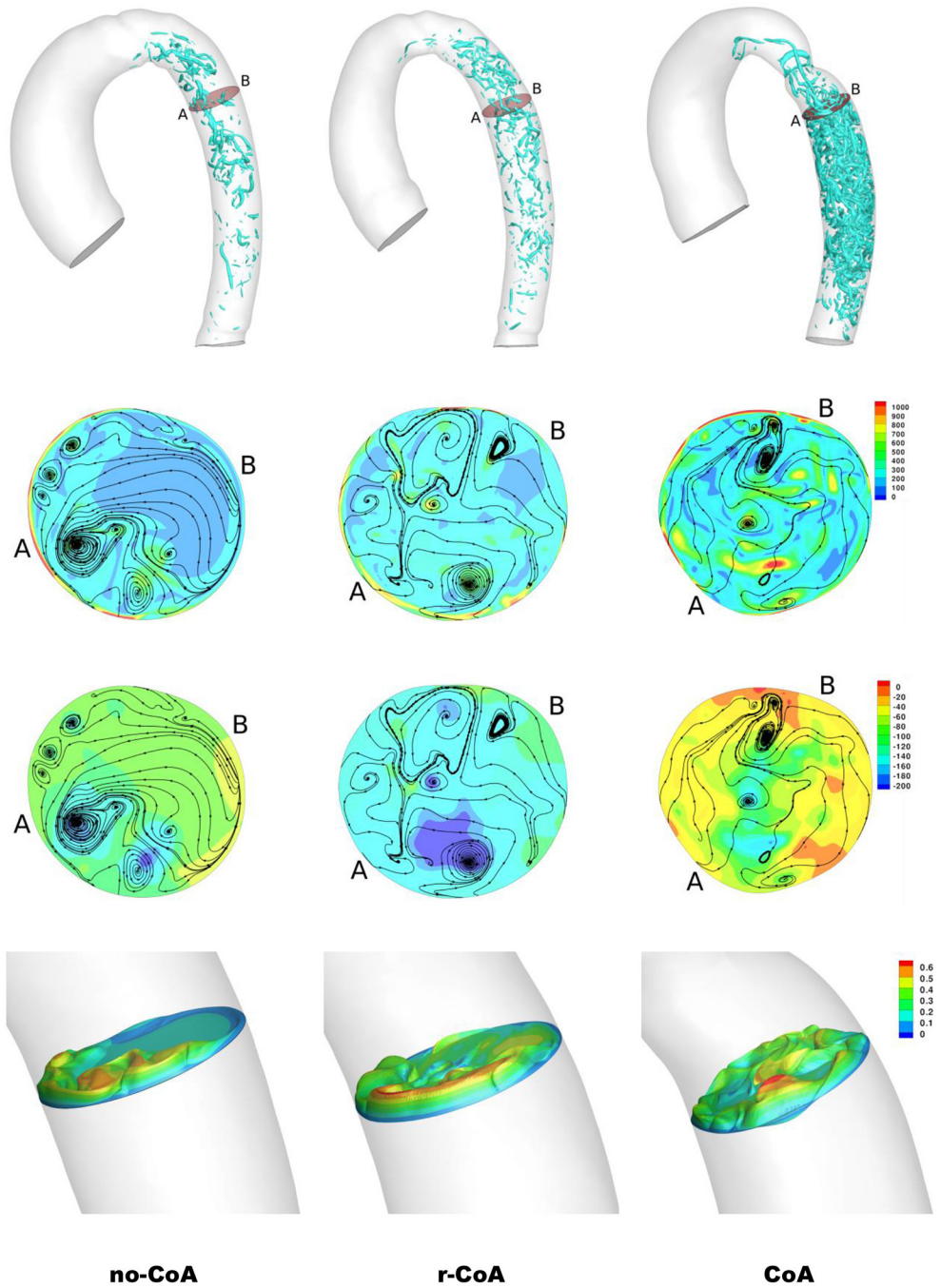

FIGURE 5 | Result of the simulations at end systole. First row: vortical structure by iso-surface of $\lambda_2 = -30,000$ in the descending aorta. Second row: contour of vorticity (/s) along with velocity streamlines. Third row: contour of pressure along with velocity streamlines. Fourth row: velocity cross-section (m/s). The cross-sections are identified in the first row.

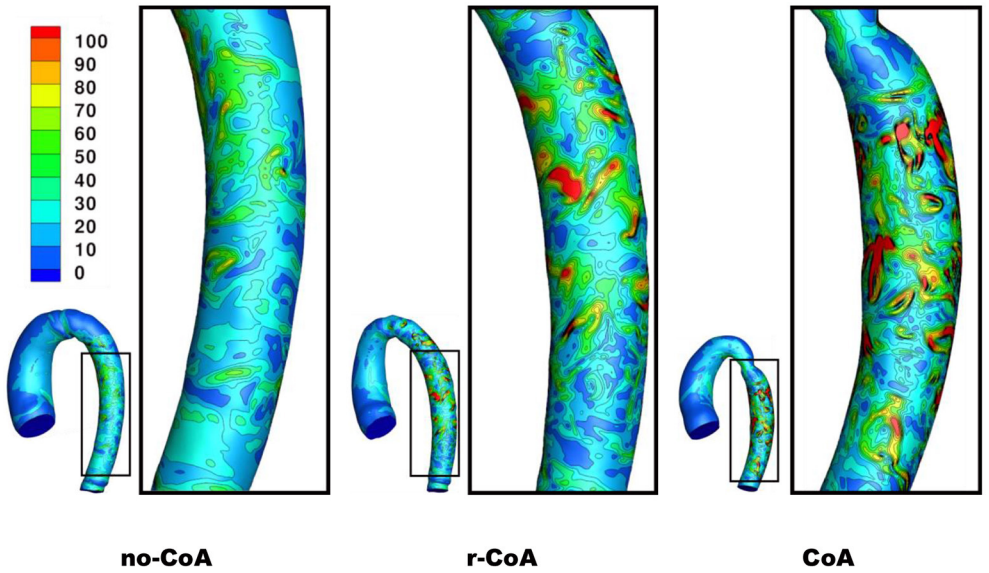

FIGURE 6 | Contour of wall shear stress (WSS) on the descending aorta at end systole.

ascending aorta (four-fold increase at peak systole) and a substantial pressure drop across the coarctation site (5.20 vs. 36.50 mmHg; **Figure 4**) in the CoA group, as well as much higher aortic velocity past the CoA (1.14 vs. 3.61 m/s). Vorticity showed approximately a four-fold increase between the two configurations in the descending aorta (387 vs. 1,495 1/s at location 0.5 and 251 vs. 1,078 1/s at location 0.6). Vortex cores and vorticity across the aortic cross-section in the descending aorta are shown in **Figure 5**. Given the obtained WSS maps (**Figure 6**), areas of elevated WSS were identified (WSS >50 dyn/cm^2) and noted in the descending aorta and no-CoA and CoA configurations were compared. There was an average 378% increase in the CoA group. Finally, a three-fold increase in power loss was observed at peak systole in the ascending aorta in the CoA group compared to the no-CoA group (0.9 vs. 3.2 W, No-CoA vs. CoA; **Figure 7**).

More interestingly, differences were also observed when comparing the no-CoA and r-CoA configurations, despite the latter representing qualitatively a successful CoA repair with a coarctation index >0.8 (i.e., no significant narrowing from a clinical standpoint). The hemodynamic observations in the r-CoA were mainly:

1) increased vorticity at the site of CoA repair (no-CoA: 387 1/s vs. r-CoA: 711 1/s at location 0.5), **Figure 5**;
2) regions of elevated WSS in the descending aorta of the r-CoA model more comparable to the CoA configuration (**Figure 6**), with an increase in areas of WSS (>50 dyn/cm^2) in 153% of the r-CoA model;
3) increased power loss (+22%) in the ascending aorta (no-CoA: 0.9 W vs. r-CoA: 1.1 W; **Figure 7**).

The velocity streamlines along the three aortic models are plotted in **Figure 8**. Two internal and external separations in the CoA aorta can be appreciated, leading to adverse pressure gradient in the descending aorta to such an extent that the average pressure in cross-sections $S_{0.5}$ and $S_{0.6}$ becomes negative at peak systole, as reported in **Table 1**. Internal separation was only observed in no-CoA and r-CoA aorta. The length of separations was measured and is reported in **Table 2**.

DISCUSSION

Computational simulations have been providing an accessible and versatile tool for gathering insight into the fluid dynamics of aortic coarctation for over a decade. Computational modeling analysis suggests that the concomitant presence of BAV with CoA results in increased maximal velocity, secondary flow, pressure loss, time-averaged wall shear stress and oscillatory shear index in the descending aorta, past the CoA, compared to a tricuspid valve scenario (18). Computational fluid dynamics can highlight regions of the thoracic aorta with unfavorable hemodynamics (19) and, in the presence of CoA, reveal differences in local WSS (20). Such insight can yield clinically relevant messages. For instance, WSS changes can be related to areas of plaque formation in locations influenced by surgical CoA repair, such as resection with end-to-end anastomosis (19). The modeling literature suggests that simulations can be used to assess changes in aortic wall biomechanics after a percutaneous procedure (e.g., stenting) (21), to detect unfavorable flow patterns in patients with re-CoA (22), and to plan interventions in complex scenarios (23). In the present study, a computational approach was chosen to isolate the effect of aortic arch geometry (based on representative anatomical configurations of the aortic arch derived from a statistical shape modeling framework, rather than individual patients' anatomies) and offer new insights into the hemodynamic effect of aortic arch architecture, particularly

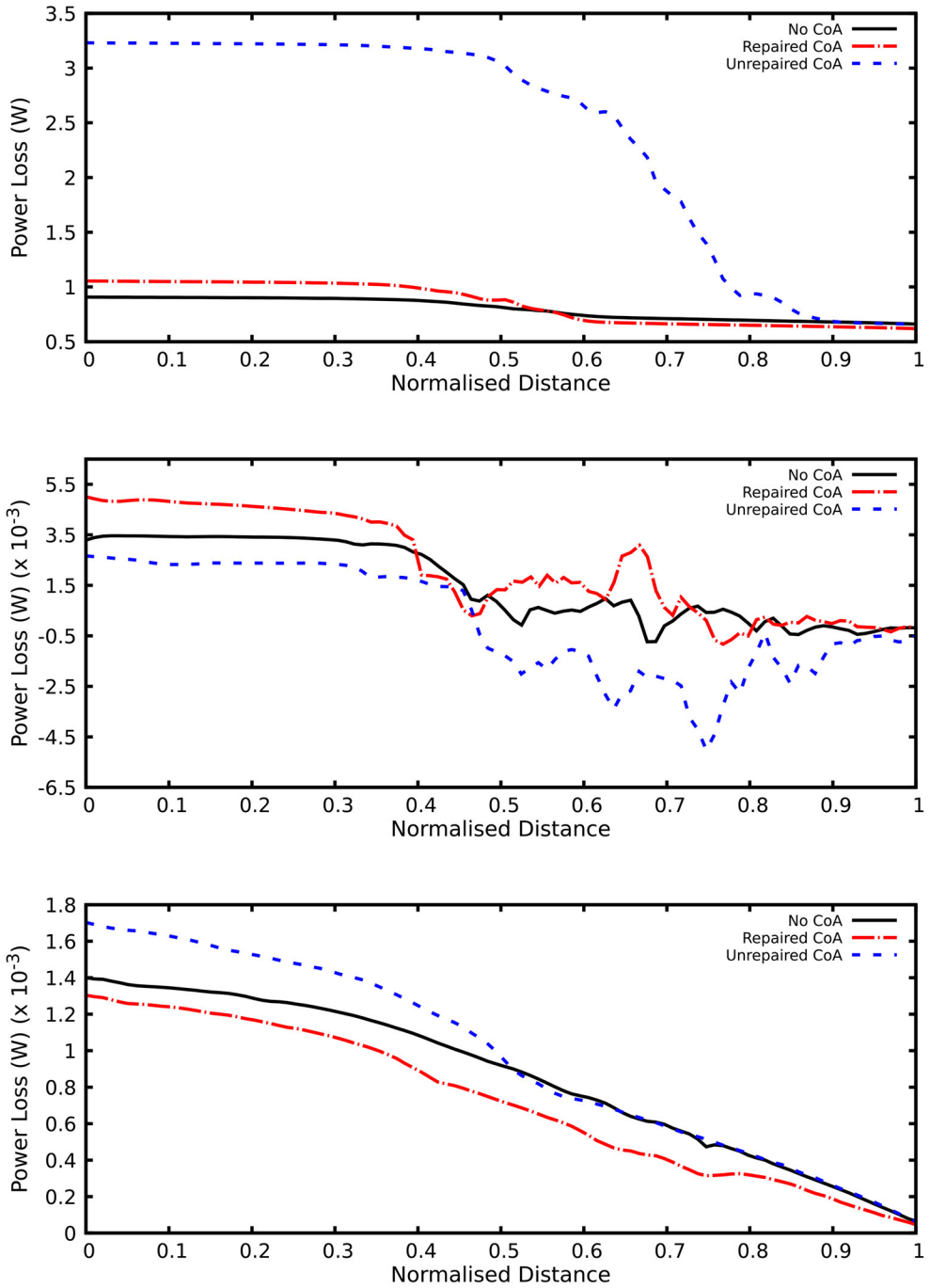

FIGURE 7 | Plot of power loss along the aorta. Order of plots from top to bottom: end systole, peak systole, and end diastole.

in the presence of a repaired CoA. Simulations revealed interesting differences in the repaired CoA setting. The idealized and purposely simplified scenario adopted here in the CFD simulations (i.e., same inflow, no aortic wall deformation) allowed us to isolate the effect of the geometry of CoA repair and determine the impact of that variable. Hemodynamic differences mainly included a nearly doubled value of vorticity in the descending aorta past the repaired CoA region, increased WSS in the descending aorta, a mild increase in pressure drop compared to the isolated BAV scenario, and an increase in power loss.

These findings suggest that even in a successfully repaired CoA (i.e., no residual narrowing with a clinically negligible CoA index and a qualitatively optimal aortic arch geometry), there are important changes in the architecture of the arch.

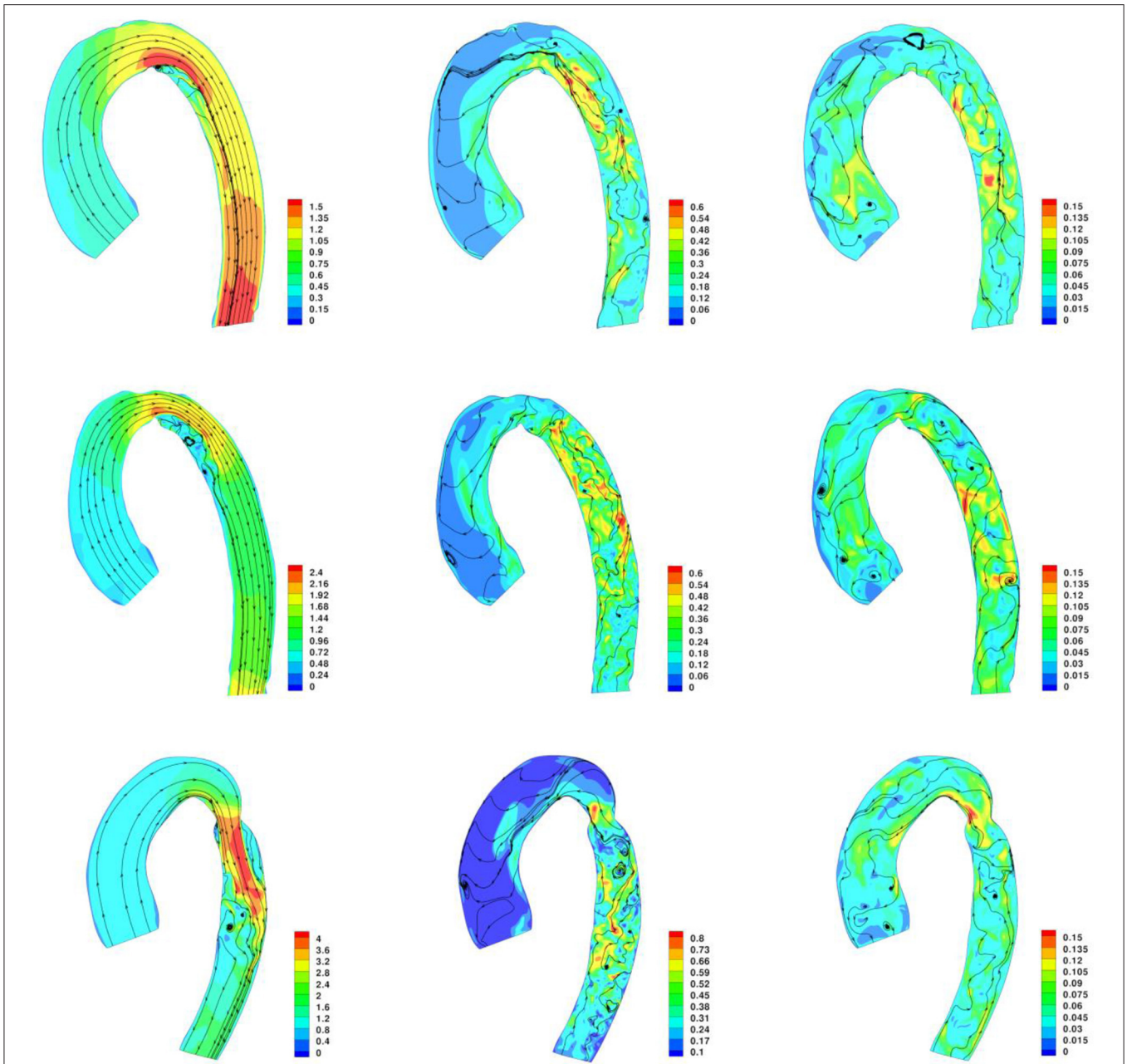

FIGURE 8 | Contour of velocity and velocity streamlines along the aorta at peak systole, end systole, and end diastole. Top row: No-CoA aorta; Middle row: r-CoA; Bottom Row: CoA.

The elevated WSS in the descending aorta may relate to some degree of dilation in this area that has been previously observed in a study focusing on aortic arch morphology in BAV with/without CoA (8). In addition, power loss (which is a function of the pressure drop and the aortic flow rate) was also found to be different in BAV patients with r-CoA compared to patients with isolated BAV. Power loss was higher in the presence of CoA (both repaired and unrepaired). This concurs with existing literature reporting an association between increasing stenosis level and increasing energy dissipation (24). Furthermore, previous work in other CHD, such as the geometry of the total cavopulmonary connection in Fontan patients, has shown that power loss increases dramatically in a non-linear fashion with increasing cardiac output and is dependent on geometrical variables, suggesting the importance of studying exercise conditions as well as rest conditions (25). While our simplified model focused on isolating differences related to aortic arch morphology, the observed differences in power loss, especially in the r-CoA scenario, warrant further study and extension to the investigation of the effect of exercise physiology,

TABLE 2 | Approximate length of separations in the three aortic configurations at peak systole.

	Separation length (cm)	
	Internal	**External**
No-CoA	1	–
r-CoA	1.5	–
CoA	1	2.6

as this is likely to exacerbate any differences. Another scenario that would be very relevant to include in such an analysis would be the case of transverse arch hypoplasia, particularly in light of recent work, based on principal component analysis (PCA), suggesting that arch morphology is not the major determinant of vascular load following coarctation repair and that caliber is more important than curvature (7). These observations are purely geometric and did not consider effects on the flow field, so they can be viewed as complementary alongside those presented in this article, contributing to refining our knowledge of CoA. Additionally, if a growth model of the aorta with CoA was developed following a recent methodology (26), it would be interesting to include factors such as recurrent arch obstruction, which is more prevalent in patients with a CoA index <0.7, extending the observations from this study.

The flow separation results suggest that small variations in the morphology of the aortic arch (native or resulting from surgical repair) lead to changes in flow velocity acceleration and also to changes in WSS in the descending aorta. Our observations agree with previous literature suggesting a relation between geometric irregularities and flow separation at the corners and that this increases from romanesque to crenel to gothic arches (27). It was particularly interesting to observe flow separation in the scenario of successful CoA repair with no residual significant narrowing, which reinforces previous observations that even when recreating a favorable anatomy after CoA repair, aortic hemodynamics are still not fully restored (28).

This study indeed reinforces observations that CoA repair does not restore normal hemodynamics, even if there is no residual narrowing. These patients could be assumed to have an abnormal vasculature from birth, regardless of repair with on-going cardiovascular risk, even in the absence of residual narrowing or systemic hypertension. It is crucially important to pay attention to the control of cardiovascular risk factors throughout life, such as refraining from smoking, actively managing elevated blood pressure and cholesterol and the encouragement of a healthy weight and exercise habits from an early age. Certain arch phenotypes may be most at risk and warrant intensive preventative therapy.

There are limitations to this study. The aortic models were set as rigid and the same realistic aortic inflow was used as a boundary condition for all three geometrical configurations. Whilst this was purposely done in order to isolate the geometrical variable, aortic distensibility and patient-specific flow features contribute to the hemodynamic changes in these patients. We suggest that we can further augment our knowledge of CoA hemodynamics by studying these variables in a parametric fashion in future studies. Furthermore, differences in relevant parameters such as WSS are likely to be affected by changes in the patients' physiological state, i.e., rest vs. exercise (28), which was not modeled in this study. Previous MRI-based analysis suggesting that transverse arch and isthmus hypoplasia rather than acute aortic arch angulation are involved in the pathophysiology of blood pressure response to peak exercise after CoA repair (29) and it has been observed that CoA patients without significant obstruction had higher exercise-induced systolic blood pressure changes than matched controls (30). Finally, whilst this study focused on aortic hemodynamics, it is important to note that CFD simulations in this context can also allow the comparison of relevant indices between the aorta and the brachiocephalic vessels, which is an important consideration in CoA patients, given the incidence of cerebrovascular events (28, 31). Whilst events may be related to hypertension, the role of arch geometry and anatomy of the head and neck vessels may well be a contributory factor.

CONCLUSION

This study adds to our appreciation of aortic hemodynamics in patients with repaired aortic coarctation, suggesting that even small alterations in the aortic morphology (such as those resulting following surgical repair) impact on key hemodynamic indices. This can in part contribute to explaining phenomena such as persistent hypertension even in the absence of any clinically significant narrowing.

DATA AVAILABILITY STATEMENT

The raw data supporting the conclusions of this article will be made available by the authors, without undue reservation.

ETHICS STATEMENT

Ethical review and approval was not required for the study on human participants in accordance with the local legislation and institutional requirements. The patients/participants provided their written informed consent to participate in this study.

AUTHOR CONTRIBUTIONS

VGA, MO, AG, and GB conceived the study. VGA and HG ran the computational simulations. FS provided the anatomical models. VGA and GB drafted the manuscript. All authors contributed to data interpretation and critically revising.

ACKNOWLEDGMENTS

VGA acknowledges support from the University of Bristol to carry out his Ph.D. Also, the authors gratefully acknowledge the support of the British Heart Foundation (Prof. Caputo's Chair and the Bristol BHF Accelerator Award) and the Bristol NIHR Biomedical Research Center (BRC).

REFERENCES

1. Kaemmerer H. Aortic coarctation and interrupted aortic arch. In: Gatzoulis MA, Webb GD, Daubeney PEF, editors. *Diagnosis and Management of Adult Congenital Heart Disease*. 2nd ed. Churchill Livingstone (2011). p. 261–70. doi: 10.1016/B978-0-7020-3426-8.00036-8
2. Ou P, Celermajer DS, Raisky O, Jolivet O, Buyens F, Herment A, et al. Angular (gothic) aortic arch leads to enhanced systolic wave reflection, central aortic stiffness, and increased left ventricular mass late after aortic coarctation repair: evaluation with magnetic resonance flow mapping. *J Thorac Cardiovasc Surg.* (2008) 135:62–8. doi: 10.1016/j.jtcvs.2007.03.059
3. Ou P, Celermajer DS, Mousseaux E, Giron A, Aggoun Y, Szezepanski I, et al. Vascular remodeling after "successful" repair of coarctation: impact of aortic arch geometry. *J Am Coll Cardiol.* (2007) 49:883–90. doi: 10.1016/j.jacc.2006.10.057
4. Ou P, Bonnet D, Auriacombe L, Pedroni E, Balleux F, Sidi D, et al. Late systemic hypertension and aortic arch geometry after successful repair of coarctation of the aorta. *Eur Heart J.* (2004) 25:1853–59. doi: 10.1016/j.ehj.2004.07.021
5. de Divitiis M, Rubba P, Calabrò R. Arterial hypertension and cardiovascular prognosis after successful repair of aortic coarctation: a clinical model for the study of vascular function. *Nutr Metab Cardiovasc Dis*. (2005) 15:382–94. doi: 10.1016/j.numecd.2005.08.002
6. Donazzan L, Crepaz R, Stuefer J, Stellin G. Abnormalities of aortic arch shape, central aortic flow dynamics, and distensibility pre-dispose to hypertension after successful repair of aortic coarctation. *World J Pediatr Congenit Heart Surg.* (2014) 5:546–53. doi: 10.1177/2150135114551028
7. Quail MA, Segers P, Steeden JA, Muthurangu V. The aorta after coarctation repair–effects of calibre and curvature on arterial haemodynamics. *J Cardiovasc Magn Res.* (2019) 21:1–9. doi: 10.1186/s12968-019-0534-7
8. Sophocleous F, Biffi B, Milano EG, Bruse J, Caputo M, Rajakaruna C, et al. Aortic morphological variability in patients with bicuspid aortic valve and aortic coarctation. *Eur J Cardiothorac Surg.* (2019) 55:704–13. doi: 10.1093/ejcts/ezy339
9. Rodrigues JC, Jaring MF, Werndle MC, Mitrousi K, Lyen SM, Nightingale AK, et al. Repaired coarctation of the aorta, persistent arterial hypertension and the selfish brain. *J Cardiovasc Magn Reson.* (2019) 21:1–10. doi: 10.1186/s12968-019-0578-8
10. Lee MG, Babu-Narayan SV, Kempny A, Uebing A, Montanaro C, Shore DF, et al. Long-term mortality and cardiovascular burden for adult survivors of coarctation of the aorta. *Heart.* (2019) 105:1190–96. doi: 10.1136/heartjnl-2018-314257
11. Kenny D, Polson JW, Martin RP, Paton JFR, Wolf AR. Hypertension and coarctation of the aorta: an inevitable consequence of developmental pathophysiology. *Hypertens Res.* (2011) 34:543–7. doi: 10.1038/hr.2011.22
12. Iriart X, Laik J, Cremer A, Martin C, Pillois X, Jalal Z, et al. Predictive factors for residual hypertension following aortic coarctation stenting. *J Clin Hypertens.* (2019) 21:291–8. doi: 10.1111/jch.13452
13. Bruse JL, McLeod K, Biglino G, Ntsinjana HN, Capelli C, Hsia T-Y, et al. A statistical shape modelling framework to extract 3d shape biomarkers from medical imaging data: assessing arch morphology of repaired coarctation of the aorta. *BMC Med Imaging.* (2016) 16:1–19. doi: 10.1186/s12880-016-0142-z
14. Tan F, Wood N, Tabor G, Xu X. Comparison of LES of steady transitional flow in an idealized stenosed axisymmetric artery model with a RANS transitional model. *J Biomech Eng.* (2011) 133:051001. doi: 10.1115/1.4003782
15. Varghese SS, Frankel SH, Fischer PF. Modeling transition to turbulence in eccentric stenotic flows. *J Biomech Eng.* (2008) 130:014503. doi: 10.1115/1.2800832
16. Mittal R, Simmons S, Udaykumar H. Application of large-eddy simulation to the study of pulsatile flow in a modeled arterial stenosis. *J Biomech Eng.* (2001) 123:325–32. doi: 10.1115/1.1385840
17. Antiga L, Piccinelli M, Botti L, Ene-Iordache B, Remuzzi A, Steinman DA. An image-based modeling framework for patient-specific computational hemodynamics. *Med Biol Eng Comput.* (2008) 46:1097–112. doi: 10.1007/s11517-008-0420-1
18. Keshavarz-Motamed Z, Garcia J, Kadem L. Fluid dynamics of coarctation of the aorta and effect of bicuspid aortic valve. *PLoS ONE.* (2013) 8:e72394. doi: 10.1371/journal.pone.0072394
19. Wendell DC, Samyn MM, Cava JR, Ellwein LM, Krolikowski MM, Gandy KL, et al. Including aortic valve morphology in computational fluid dynamics simulations: initial findings and application to aortic coarctation. *Med Eng Phys.* (2013) 35:723–35. doi: 10.1016/j.medengphy.2012.07.015
20. LaDisa JF Jr, Dholakia RJ, Figueroa CA, Vignon-Clementel IE, Chan FP, Samyn MM, et al. Computational simulations demonstrate altered wall shear stress in aortic coarctation patients treated by resection with end-to-end anastomosis. *Congenit Heart Dis*. (2011) 6:432–43. doi: 10.1111/j.1747-0803.2011.00553.x
21. Caimi A, Pasquali M, Sturla F, Pluchinotta FR, Giugno L, Carminati M, et al. Prediction of post-stenting biomechanics in coarcted aortas: a pilot finite element study. *J Biomech.* (2020) 105:109796. doi: 10.1016/j.jbiomech.2020.109796
22. Guillot M, Ascuitto R, Ross-Ascuitto N, Mallula K, Siwik E. Computational fluid dynamics simulations as a complementary study for transcatheter endovascular stent implantation for re-coarctation of the aorta associated with minimal pressure drop: an aneurysmal ductal ampulla with aortic isthmus narrowing. *Cardiol Young.* (2019) 29:768–76. doi: 10.1017/S1047951119000751
23. Tossas-Betancourt C, van Bakel TM, Arthurs CJ, Coleman DM, Eliason JL, Figueroa CA, et al. Computational analysis of renal artery flow characteristics by modeling aortoplasty and aortic bypass interventions for abdominal aortic coarctation. *J Vasc Surg.* (2020) 71:505–16. e4. doi: 10.1016/j.jvs.2019.02.063
24. Yap C-H, Dasi LP, Yoganathan AP. Dynamic hemodynamic energy loss in normal and stenosed aortic valves. *J Biomech Eng.* (2010) 132:021005. doi: 10.1115/1.4000874
25. Whitehead KK, Pekkan K, Kitajima HD, Paridon SM, Yoganathan AP, Fogel MA. Non-linear power loss during exercise in single-ventricle patients after the fontan: insights from computational fluid dynamics. *Circulation*. (2007) 116:I165–71. doi: 10.1161/CIRCULATIONAHA.106.680827
26. Sophocleous F, Bone A, Shearn AIU, Velasco Forte MN, Bruse JL, Caputo M, et al. Feasibility of a longitudinal statistical atlas model to study aortic growth in congenital heart disease. *Comput Biol Med.* (2022) 144:105326. doi: 10.1016/j.compbiomed.2022.105326
27. Olivieri LJ, de Zélicourt DA, Haggerty CM, Ratnayaka K, Cross RR, Yoganathan AP. Hemodynamic modeling of surgically repaired coarctation of the aorta. *Cardiovasc Eng Technol.* (2011) 2:288–95. doi: 10.1007/s13239-011-0059-1
28. LaDisa JF, Alberto Figueroa C, Vignon-Clementel IE, Jin Kim H, Xiao N, Ellwein LM, et al. Computational simulations for aortic coarctation: representative results from a sampling of patients. *J Biomech Eng.* (2011) 133:091008. doi: 10.1115/1.4004996
29. Ntsinjana HN, Biglino G, Capelli C, Tann O, Giardini A, Derrick G, et al. Aortic arch shape is not associated with hypertensive response to exercise in patients with repaired congenital heart diseases. *J Cardiovasc Magn Res.* (2013) 15:1–7. doi: 10.1186/1532-429X-15-101
30. Egbe AC, Allison TG, Ammash NM. Mild coarctation of aorta is an independent risk factor for exercise-induced hypertension. *Hypertension.* (2019) 74:1484–9. doi: 10.1161/HYPERTENSIONAHA.119.13726
31. Curtis SL, Bradley M, Wilde P, Aw J, Chakrabarti S, Hamilton M, et al. Results of screening for intracranial aneurysms in patients with coarctation of the aorta. *Am J Neuroradiol.* (2012) 33:1182–86. doi: 10.3174/ajnr.A2915

Conflict of Interest: The authors declare that the research was conducted in the absence of any commercial or financial relationships that could be construed as a potential conflict of interest.

frontiers | Frontiers in Pediatrics

TYPE Systematic Review
PUBLISHED 04 October 2022
DOI 10.3389/fped.2022.915045

OPEN ACCESS

EDITED BY
Christian Apitz,
Ulm University Medical Center, Germany

REVIEWED BY
Rachael Cordina,
Sydney Local Health District, Australia
Carl Backer,
Cincinnati Children's Hospital Medical Center, United States

*CORRESPONDENCE
Antonio F. Corno
antonio.f.corno@uth.tmc.edu

SPECIALTY SECTION
This article was submitted to Pediatric Cardiology, a section of the journal Frontiers in Pediatrics

RECEIVED 07 April 2022
ACCEPTED 26 August 2022
PUBLISHED 04 October 2022

CITATION
Greenleaf CE, Lim ZN, Li W, LaPar DJ, Salazar JD and Corno AF (2022) Impact on clinical outcomes from transcatheter closure of the Fontan fenestration: A systematic review and meta-analysis.
Front. Pediatr. 10:915045.
doi: 10.3389/fped.2022.915045

Impact on clinical outcomes from transcatheter closure of the Fontan fenestration: A systematic review and meta-analysis

Christopher E. Greenleaf[1], Zhia Ning Lim[2], Wen Li[3], Damien J. LaPar[1], Jorge D. Salazar[1] and Antonio F. Corno[1*]

[1]Pediatric and Congenital Cardiac Surgery, Children's Heart Institute, Memorial Hermann Children's Hospital, UTHealth, McGovern Medical School, Houston, TX, United States, [2]University College of London (UCL) Great Ormond Street Institute of Child Health, University College London, London, United Kingdom, [3]Division of Clinical and Translational Sciences, Department of Internal Medicine, UTHealth, McGovern Medical School, Houston, TX, United States

Background: Meta-analysis of the impact on clinical outcome from transcatheter closure of Fontan fenestration.

Methods: Cochrane, Embase, MEDLINE, and Open-Gray were searched. Parameters such as changes in oxygen saturation, cavo-pulmonary pressure, maximum heart rate during exercise, exercise duration, and oxygen saturation after fenestration closure were pooled and statistical analysis performed.

Results: Among 922 publications, 12 retrospective observational studies were included. The included studies involved 610 patients, of which 552 patients (90.5%) had a fenestration. Of those patients, 505 patients (91.5%) underwent attempt at trans-catheter closure. When it could be estimated, the pooled overall mean age at trans-catheter fenestration closure was 6.6 ± 7.4 years, and the mean follow-up time was 34.4 ± 10.7 months. There were 32 minor (6.3%) and 20 major (4.0%) complications during or after trans-catheter Fontan fenestration closure. The forest plots demonstrate that following fenestration closure, there was a significant increase in the mean arterial oxygen saturation of 7.9% (95% CI 6.4–9.4%, $p < 0.01$). There was also a significant increase in the mean cavo-pulmonary pressure of 1.4 mmHg (95% CI 1.0–1.8 mmHg, $p < 0.01$) following fenestration closure. The exercise parameters reported in 3 studies also favored closing the fenestration as well, yet the exercise duration increase of 1.7 min (95% CI 0.7–2.8 min, $p < 0.01$) after fenestration closure is probably clinically insignificant.

Conclusion: Late closure of a Fontan fenestration has the impact of improving resting oxygen saturation, exercise oxygen saturation, and a modest improvement of exercise duration. These clinical benefits, however, may be at the expense of tolerating slightly higher cavo-pulmonary mean pressures.

KEYWORDS

congenital heart defects, congenital heart surgery, fenestration, Fontan circulation, meta-analysis, systematic literature review, univentricular hearts

Introduction

In the 50 years following the introduction of the procedure named after Francis Fontan (1), the indications as well as the surgical techniques have substantially evolved. The Fontan operation, which may be performed with various surgical techniques, is the final stage of surgical palliation for functionally univentricular hearts (1–20). A surgically created fenestration (or connection) between the Fontan circuit and the atrial cavity to reduce excessively elevated systemic venous pressures and to improve cardiac output by increasing the filling of the single ventricle may be beneficial in the immediate post-operative period (21–24). To date, the only available prospective randomized study examining the impact of Fontan fenestration demonstrated a reduction in hospital and intensive care unit length of stays with a fenestration (25), even if other studies reported data on this issue (26–28). These potential benefits, however, may be realized at the expense of lower systemic oxygenation, an increased risk of systemic embolism, and the possible need for catheter-based fenestration closure later in life (29, 30).

The long-term management of Fontan fenestrations remains controversial. First, catheter-based Fontan fenestration closure is not without risk, and the concerns related to a closed or absent fenestration are still present long after the postoperative period. Second, long-term systemic thromboembolic risk with an open fenestration has to be balanced against the Fontan paradox of relative systemic venous hypertension and pulmonary arterial hypotension. Third, after Fontan failure develops, the gold standard of treatment is heart transplant. As donor hearts for transplantation remain a scarce resource, other palliative strategies including trans-catheter Fontan fenestration enlargement or creation have been attempted. These attempts were made to improve quality of life, reduce failure symptoms, and possibly improve waitlist safety.

Unfortunately, the overwhelming majority of published literature examining outcomes after transcatheter closure of Fontan fenestrations are observational in nature and underpowered to detect important differences. Heterogenous indications between centers and unclear indications within centers, prevent concrete conclusions of management of the Fontan fenestration in the catheterization lab. To address these limitations, the present systematic review and meta-analysis was conducted to assess the consequences of trans-catheter Fontan fenestration closure on clinical outcomes.

Materials and methods

This analysis was registered on Prospero (CRD42019139395) on August 21st, 2019. The study was conducted in accordance with the Meta-Analysis of Observational Studies in Epidemiology Guidelines (31). The manuscript was structured in accordance with Systematic Reviews and Meta-Analyses (PRISMA) guidelines and recommendations (32). All reviewed literature was assessed using the Cochrane tools, which cover six domains of bias: selection bias, performance bias, detection bias, attrition bias, reporting bias, and other bias (33). The PICO question for this systematic review and meta-analysis is in fenestrated Fontan patients, what is the change in clinical outcomes from baseline or fenestrations that are left open associated with transcatheter fenestration closure?

Search strategy

A systematic search was conducted on Cochrane, Embase and MEDLINE. Search terms are provided in **Figure 1**. Moreover, to avoid losing any related publications, an Open-Gray search was conducted. Related journals and reference lists of identified articles were cross-checked for other relevant studies of interest. Retrospective and prospective observational or randomized controlled trials from the year 200, written in English, reporting the pre-determined outcomes including children or adults undergoing catheter-based intervention on a Fontan fenestration in human subjects were included. Exclusion criteria were case reports, non-original articles, systematic reviews, meta-analyses, non-published works, studies not describing any of the pre-determined outcome measures,

Cochrane strategy

#1	Fontan:ti,ab,kw
#2	[mh "Fontan procedure"]
#3	("lateral tunnel"):ti,ab,kw
#4	((cavo-pulmonary or "cavo pulmonary" or cavopulmonary) NEXT (anastomosis or anastomoses or shunt or shunts)):ti,ab,kw
#5	"total right heart bypass":ti,ab,kw
#6	(("stage 3" or "stage III") NEAR/1 norwood):ti,ab,kw
#7	fenestrat*:ti,ab,kw
#8	(non-fenestrat* or nonfenestrat*):ti,ab,kw
#9	defenestrat*:ti,ab,kw
#10	{OR #1-#6}
#11	{OR #7-#9}
#12	#10 AND #11

Embase strategy

1	Fontan.mp. (8592)
2	Fontan procedure/ (6122)
3	lateral tunnel.mp. (463)
4	(total adj (cavo-pulmonary or cavo pulmonary or cavopulmonary) adj (anastomosis or anastomoses or shunt or shunts)).mp. (163)
5	cavopulmonary connection/ (1756)
6	total right heart bypass.mp. (14)
7	((stage 3 or stage III) adj1 norwood).mp. (0)
8	fenestrat*.mp. (12870)
9	(non-fenestrat* or nonfenestrat*).mp. (285)
10	defenestrat*.mp. (142)
11	fenestration/ (4962)
12	1 or 2 or 3 or 4 or 5 or 6 or 7 (9432)
13	8 or 9 or 10 or 11 (13011)
14	12 and 13 (990)
15	case report/ or case study/ (2382941)
16	14 not 15 (771)
17	limit 16 to (english language and yr="2000 -Current") (647)

Medline strategy

1.	Fontan.mp.
2.	Fontan procedure/
3.	lateral tunnel.mp.
4.	(total adj (cavo-pulmonary or cavo pulmonary or cavopulmonary) adj (anastomosis or anastomoses or shunt or shunts)).mp.
5.	total right heart bypass.mp.
6.	((stage 3 or stage III) adj1 Norwood).mp.
7.	fenestrat*.mp.
8.	(non-fenestrat* or nonfenestrat*).mp.
9.	defenestrat*.mp.
10.	1 or 2 or 3 or 4 or 5 or 6
11.	7 or 8 or 9
12.	10 and 11
13.	limit 12 to case reports
14.	12 not 13
15.	limit 14 to (english language and yr="2000 -Current")

Open-Grey strategy

Fontan OR "lateral tunnel" OR "total cavo-pulmonary anastomosis" OR "total cavo-pulmonary anastomoses" OR "total cavo-pulmonary shunt" OR "total cavo-pulmonary shunts" OR "total cavo pulmonary anastomosis" OR "total cavo pulmonary anastomoses" OR "total cavo pulmonary shunt" OR "total cavo pulmonary shunts" OR "total cavopulmonary anastomosis" OR "total cavopulmonary anastomoses" OR "total cavopulmonary shunt" OR "total cavopulmonary shunts" OR "cavo-pulmonary connection" OR "cavo pulmonary connection" OR "cavopulmonary connection" OR "total right heart bypass" OR "stage 3 norwood" OR "stage III Norwood") AND (fenestrat* OR "non-fenestrat*" OR nonfenestrat* OR defenestrate*

FIGURE 1
Literature search strategy.

or studies that included > 20% of spontaneous fenestration closures. The search was conducted with the assistance of two experienced librarians.

Two independent reviewers (Z.N.L. and A.F.C.) screened all identified studies. In case of multiple publications with sample overlap, the most recent report was included. In each article, the criteria for inclusion and exclusion were independently evaluated by the two reviewers to verify the correctness of selection. In the case of disagreement between reviewers, a consensus was agreed upon. In multiple studies with overlapping study populations, the study with the greatest overall follow-up was included. The first author and/or the corresponding author of three of the included studies were contacted to clarify reported data, particularly regarding the size of the fenestration at the time of surgery.

Data extraction

Study design, year of Fontan surgery, surgical type of Fontan, fenestration use, and clinical follow-up were documented. The baseline demographics were extracted from the individual studies. The outcomes extracted included early or late mortality, Fontan takedown, heart transplantation, stroke, thromboembolism, or peri-interventional complications. Per-interventional changes in vital signs and changes in hemodynamic parameters including cardiac index, exercise duration, minute ventilation, maximal oxygen consumption, peak exercise oxygen pulse, and ventilatory anaerobic threshold were extracted. Additional clinical outcomes of interest, including protein-losing enteropathy, plastic bronchitis, and arrhythmias were similarly recorded. Complications were deemed major if the grade was > 2 or minor if the grade was ≤ 2 on the Clavien-Dindo classification system (34).

Statistical analysis

A meta-analysis was performed to compare the outcomes before and after catheter-based Fontan fenestration closure. Outcomes were compared before and after fenestration enlargement or creation for Fontan failure. The mean differences and the corresponding 95% confidence intervals (CI) were estimated using a random effects meta-analysis model, which accounts for variability induced by between-study heterogeneity. Cochran's Q statistic and I^2 index was used to quantify and test heterogeneity between studies (35). All statistical analyses were performed using R software version 3.6.3 (36) and the meta-package (37). Probabilities with P-value < 0.05 were considered statistically significant, and all statistical tests were two-sided.

Results

A complete literature search resulted in 922 candidate publications, of which 263 were removed as duplicates. Of the remaining 659 articles, 389 were excluded due to irrelevance. Of the remaining 151 studies, 12 articles met final inclusion

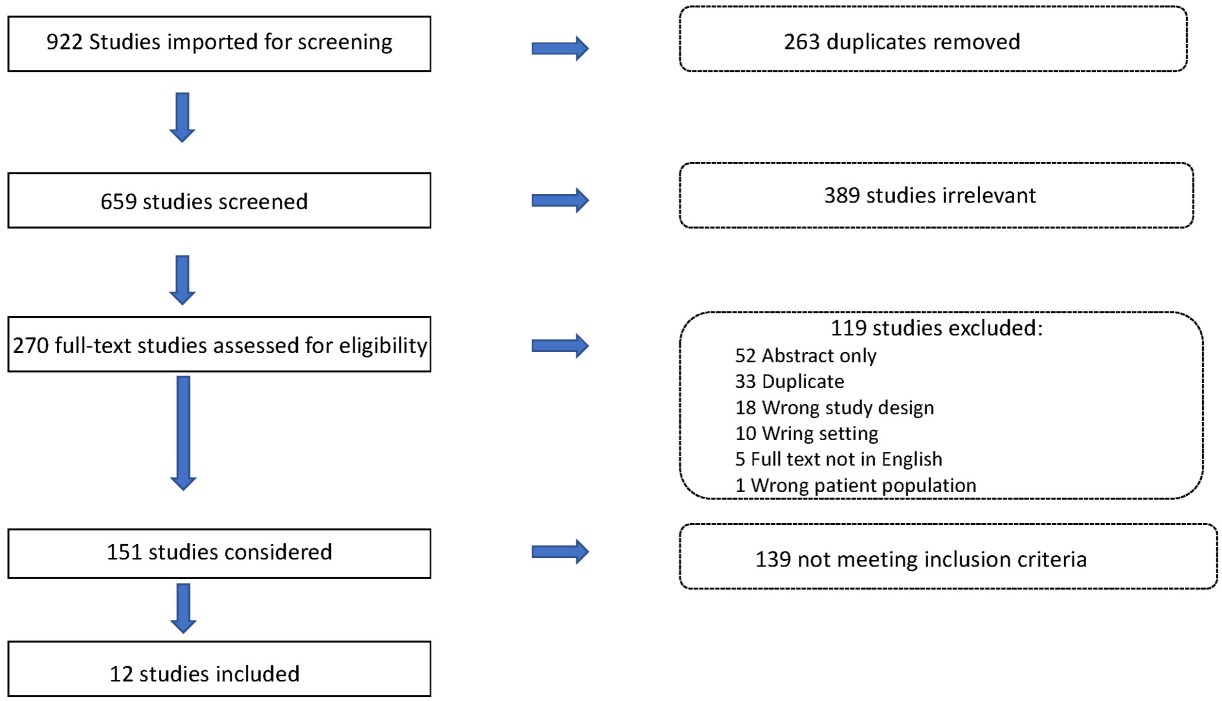

FIGURE 2
Flowchart of articles screening.

criteria (Figure 2). References are represented together with the baseline characteristics of all individual studies. Of the included studies, only 1 study (8%) included all of their Fontan patients done at their center. The rest of the studies used a selected cohort of their overall Fontan population to describe in their study. The included studies involved 610 patients, of which 552 patients (90.5%) had a fenestration. Of those patients, 505 patients (91.5%) underwent attempt at trans-catheter closure.

When it could be estimated, the pooled overall mean age at trans-catheter fenestration closure was 6.6 ± 7.4 years, and the mean follow-up time was 34.4 ± 10.7 months (Table 1). There were 32 minor (6.3%) and 20 major (4.0%) complications during or after trans-catheter Fontan fenestration closure. The 3 most common minor complications were 10 patients (2.0%) who needed new medications for a diagnosis of heart failure, 8 patients (1.6%) with an arrhythmia, and 4 patients (0.8%) with a vascular access site bleed. The 3 most common major complications were 6 patients (1.2%) who needed device retrieval for failure or malposition, 2 long-term mortalities (0.4%), and 1 early death (0.2%). Forest plots were constructed containing the individual and pooled mean differences for the oxygen saturation, cavo-pulmonary pressure, maximum heart rate during exercise, and exercise duration and oxygen saturation after fenestration closure are presented in Figures 3A–E. The forest plots demonstrate that following fenestration closure, there was a significant increase in the mean arterial oxygen saturation of 7.9% (95% CI 6.4–9.4%, $p < 0.01$) (Figure 3A). There was also a significant increase in the mean cavo-pulmonary pressure of 1.4 mmHg (95% CI 1.0–1.8 mmHg, $p < 0.01$) (Figure 3B) following fenestration closure. The exercise parameters reported in 3 studies also favored closing the fenestration as well (Figures 3C–E), yet the exercise duration increase of 1.7 min (95% CI 0.7–2.8 min, $p < 0.01$) (Figure 3D) after fenestration closure is probably clinically insignificant.

Discussion

The present systematic review and meta-analysis suggests that trans-catheter closure of a Fontan fenestration is associated with improved resting and exercise oxygenation, lower maximal heart rate during exercise, and longer exercise duration (Figures 3A,C–E), even if this is at the expense of slightly higher pulmonary artery mean pressures (Figure 3B). This analysis demonstrates that the immediate results of Fontan fenestration closure are fairly consistent. There is a systemic oxygen saturation mean increase of 7.9% (range 4.1–12.8%, Figure 3A). The pulmonary pressure slightly increases by 1.4 mm Hg (range 0.8–5.8 mm Hg, Figure 3B). Exercise tolerance does increase, but this length is short and was only tested in 2 studies (Figure 3C).

A fenestration eases the transition to the Fontan circulation for patients by providing a consistent source of systemic ventricular preload. Secondary benefits include decreased

TABLE 1 Patients who underwent late closure of the fenestration (> 30 days after Fontan procedure).

Study	Year of publication	Inclusion period	Type of study	Fontan patients, N	Patients with a fenestration, N	Fenestration size, mm	Mean age in years at transcatheter closure ± SD, or median (range)	Transcatheter fenestrations closure, N	% Fenestrations closed in the cath lab, %	Minor complication (Clavien-Dindo grade =2)	Manor complication (Clavien-Dindo grade >2)	Early mortality	Late mortality	Total follow-up after closure
Bordacovae t al. (44)	2007	2002–2006	Retrospective case series	26	26	Mean 3.5 (3–4)	10.4 ± 0.8	26	100	0	1	0		NA
Boshoff et al. (45)	2010	2001–2009	Retrospective cohort study	68	65	Median 5 (4–6)	6.4 ± 2.9	63	96.9	5	7	0		NA
Cowley et al. (48)	2000	1998–1999	Retrospective case series	13	13	4	4.6 ± 4.8	13	100	2	2	0		10.4 ± 4.6 months
Goff et al. (52)	2000	1989–1999	Cross sectional study	154	154	4	4.2 ± 11.8	154	100	7	5	0	2	Median3.4 years(0.4–10.3 years)
Goreczny et al. (53)	2017	2000–2014	Case control study	102	47	5.1 ± 1.2	Median 6.1 (3.9–10.6)	47	100	7	3	0	0	Median19.6(8–33.5)months
Hansen et al. (56)	2012	1996–2010	Retrospective cohort study	90	90	>4	Median 4.4 (1–14.2)	48	53.3	NA	NA	NA	NA	66 ±36.3months
Malekzadeh et al. (29)	2015	2005–2012	Retrospective case series	50	50	5, 6, 7	7.8 ± 3.8	50	100	6	2	1	0	49 months
Masura et al. (60)	2008	1997–2007	Retrospective case series	41	41	NA	Median 8 (2.5–26)	38	92.7	3	0		0	Median12(0.1–10 years
Mays et al. (61)	2008	NA	Retrospective observational study	20	20	NA	11.4± 5.5	20	100	2	0			NA
Meadows et al. (63)	2008	2005–2007	Prospective observational study	20	20	4	13.8 ± 10.4	20	100	NA	NA	0	0	12 months
Momenahet al. (65)	2007	NA	Retrospective case series	16	16	4, 5, 6	Median 10.3 (6–13)	16	100	NA	NA	0	0	NA
Moore et al. (66)	2000	1998–1999	Retrospective case series	10	10	4, 5, 6	7.0 ± 4.1	10	100	0	0	0	0	6 months

10.3389/fped.2022.915045

postoperative pleural effusions and hospital length of stay (25, 38). Fenestrating most Fontans has become commonplace in the modern era of Fontan management.

Different institutional practices toward the management of the Fontan fenestration

There is no concrete guidance on what should be done for the fenestration over the medium or the long-term. Because of this, there is dramatic heterogeneity fenestration management amongst centers. Because of the theoretic risk of thromboembolism and detrimental effects of prolonged cyanosis, some centers routinely close all fenestrations in the catheterization lab at about 12 months postoperatively (39). Patients who had spontaneous closure of their fenestration probably did so because of low trans-pulmonary pressures and resultant minimal relative flow across their fenestrations. This patient population, who can make up to about 40% of fenestrated Fontan patients, represent a low risk for Fontan failure (40). The long-term answer surrounding the question of what to do for the other 60% of patients was not clear. A persistent fenestration may be a surrogate for physiologic intolerance of the Fontan circulation, and this difference may not be readily apparent by pre-Fontan hemodynamic parameters (41–75). This has led some centers to either shift from routine closure to not closing any fenestrations (76) or to be very selective in which patients are referred for transcatheter closure (54, 62). For instance, McCrossan and Walsh (62). Will refer patients for trans-catheter Fontan fenestration closure if there is persistent hypoxia, satisfactory ventricular function, and absence of significant Fontan circuit obstruction.

Contraindications for fenestration closure

After the patient is referred to the catheterization lab, the interventional cardiologist may find that the patient is not appropriate for closure. Many centers use the parameters set forth by the group at Boston Children's Hospital in 1995 (77). At the time of catheterization and after measuring baseline features, the fenestration is then test occluded for 10 min. If the right atrial pressure exceeded 18 mmHg, or the arteriovenous difference in oxygen saturation increased by > 33%, or the right atrial saturation was < 40%, then the patient was considered to have an unfavorable response to test occlusion ad the fenestration was left open. Similarly, Goreczny et al. will do the 10-min test occlusion and will avoid permanent fenestration closure if the systemic venous pressure is above 18 mmHg or if there is an increase of 5 mmHg after balloon occlusion (53). At the Children's Hospital of Michigan closure is deferred after balloon occlusion if the Fontan pressure is ≥ 20 mmHg, the Fontan pressure increases by 4 mmHg or more, if there is a decrease in cardiac output by ≥ 50%, or a decrease in systemic oxygen transport of ≥ 46% (78).

These strict criteria during test occlusion may identify patients that would not tolerate fenestration closure, but it may be that this provocative measure is sensitive but not specific for those patients that may not have the proper hemodynamics but would tolerate closure anyway. Ozawa et al. studied the long-term outcomes after fenestration closure in patients at risk for Fontan failure. They compared high-risk Fontan patients, as defined by pre-Fontan mean pulmonary arterial pressure ≥ 15 mmHg or systemic atrio-ventricular valve regurgitation ≥ moderate, compared to a standard risk group and a group whose fenestration had closed spontaneously. Protein-losing enteropathy-free survival rates did not differ between groups ($p = 0.72$). This was at the expense, in the high-risk group, of persistent cyanosis from veno-venous collaterals and lower peak oxygen consumption ($p = 0.019$) and lower anaerobic threshold ($p = 0.023$) compared to the standard risk group (79).

Exercise capacity

Exercise capacity as described by maximal oxygen consumption (VO_2 max) has found diametrically opposite conclusions in certain reports. Mays et al. investigated 20 patients before and after Fontan fenestration closure. In their analysis, the VO_2 max increased to 1.24 ± 0.35 L/min from 1.18 ± 0.46 L/min, $p < 0.005$ (61). Conversely, Meadows and colleagues also investigated 20 patients before and after fenestration closure. In this series, the percent predicted VO_2 max increased to 74 ± 18.6% from 70.9 ± 18.6%, P = NS. In both studies, there was a wide variation in patient age and size (63). To take into account growth-related changes between pre- and post-fenestration closure exercise tests, different measurement endpoints were considered. Such differences may explain why exercise capacity was statistically significant in one study but not the other. Another potential explanation may be a combination of competing interests. One would surmise that increasing systemic arterial saturation would improve VO_2 max and exercise duration, but this increase in systemic arterial saturation was at the expense of cardiac index and mixed venous oxygen saturation. Furthermore, neither study was able to define the amount of right to left shunting under exercise conditions. In his series Meadows stated that, at rest in the catheterization lab, all patients had no more than trivial shunting at the end of the catheterization, but that does not exclude the possibility that more significant shunting could have occurred with effort (63). The cardiopulmonary response to exercise in the Fontan circulation is complicated by an inability to regulate heart rate or stroke volume in response to

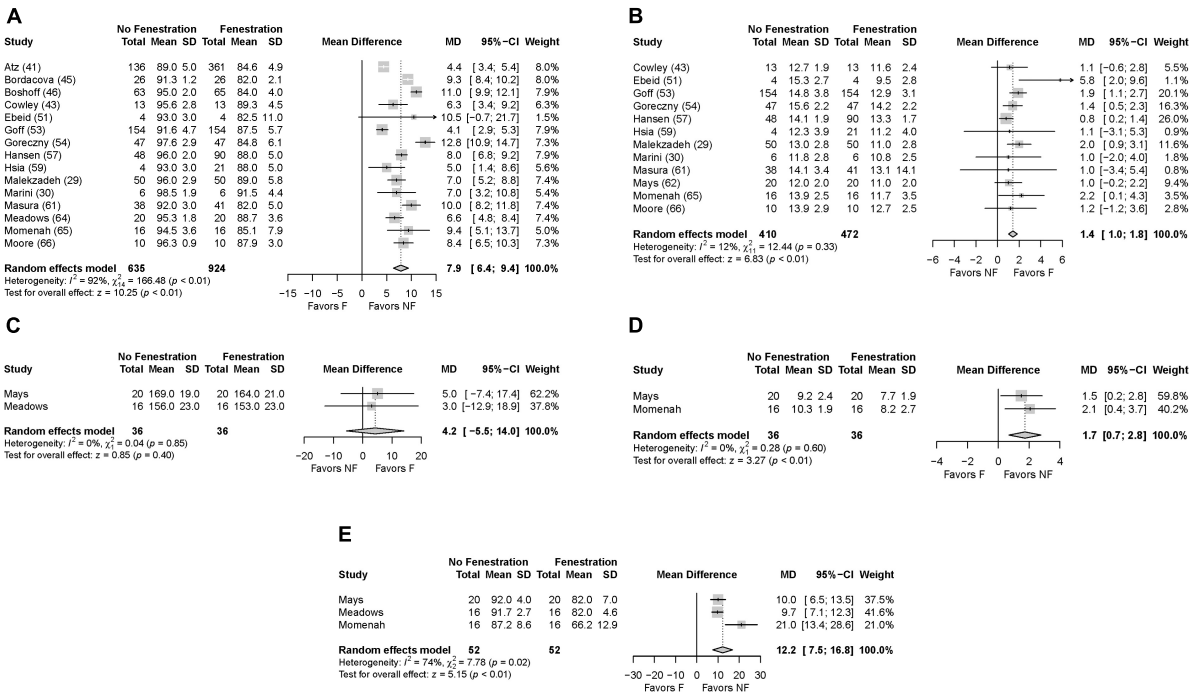

FIGURE 3
Forest plots after closure of the fenestration. **(A)** Oxygen saturation, **(B)** pulmonary artery pressure, **(C)** exercise heart rate, **(D)** exercise duration, **(E)** exercise oxygen saturation.

exercise, systemic venous flow dynamics, and the compound contribution of ventilation on the Fontan circuit.

Long-term consequences of an open or closed fenestration

As stated earlier, the Fontan fenestration is associated with well documented early postoperative benefits. Studies identifying long-term benefits are sparse. Atz et al. showed a significant increase in the rate of fenestration across multiple centers between 1987 and 2002. After adjusting for era, patient age, and year of Fontan, this large, multi-center cross-sectional study found few associations between a persistent fenestration and negative long-term outcomes (40). There was a greater number of non-fenestrations associated catheter re-interventions, most commonly for coiling of systemic venous and aorticopulmonary collaterals. Unsurprisingly, the resting oxygen saturation was lower with a fenestration in the long-term, but they found no difference in the number of long-term re-interventions, incidence of protein-losing enteropathy or arrhythmias. The Australian and New Zealand Fontan registry has been a wealth of knowledge in understanding the Fontan outcomes in the modern era (80). In a propensity score-matched analysis they demonstrated that there was no difference in long-term survival (87% vs. 90% at 20 years; p = 0.16) or freedom from failure (73% vs. 80% at 20 years; p = 0.10) between patients with and without fenestration, respectively. There was more freedom from thromboembolism in the non-fenestrated vs. the fenestrated group (89% vs. 84%; p = 0.03) (80). On the other hand, in the study from Children's Hospital of Michigan, the incidence of a composite outcome of death, transplant, deteriorated heart failure, plastic bronchitis, or protein-losing enteropathy was significantly higher when there was an open fenestration (60% vs. 6%; p < 0.01) (78). As mentioned earlier the patients with the open fenestration in this study were a select group of patients who failed to meet proper hemodynamics with test occlusion which may be the difference in the findings between these studies (78).

Limits of the study

The present review and meta-analysis have select limitations. First, a large number of published articles reported incomplete data. For instance, no suitable data were reported to analyze the impact of complications after closure of the fenestration, such as stroke and/or systemic thrombo-embolism, as well as the occurrence of liver failure due to the increased systemic venous pressure. We therefore limited our presentation of the results to the most relevant information in regard to the long-term outcome of fenestration. Second, data extracted

from observational study designs should be interpreted with caution due to the inherent limitations of confounding and a high degree of selection bias. Most importantly, select studies on the management of Fontan fenestration in patients with failed Fontan circulation had inadequate statistical analyses, which limited the ability to rigorously assess this fundamental question in the present analysis. Third, the first two limits are the consequence of the considerable controversy and widely varying institutional practices concerning Fontan fenestrations in respect to indication for establishment as well as management during long-term follow-up.

Conclusion

Late closure of a Fontan fenestration has the impact of improving resting oxygen saturation, exercise oxygen saturation, and a modest improvement of exercise duration. These clinical benefits, however, may be at the expense of tolerating slightly higher cavo-pulmonary mean pressures. There is a substantial lack of high-quality evidence supporting any therapeutic decision regarding Fontan fenestration, and this is reflected in the difficulties encountered in our literature review and meta-analysis.

Data availability statement

The original contributions presented in this study are included in the article/**Supplementary material**, further inquiries can be directed to the corresponding author.

Author contributions

All authors contributed to the idea and design of the study, preparation, review and approval of the manuscript.

Acknowledgments

We would like to acknowledge Coral Pepper, librarian at the University Hospitals of Leicester, and Keith Nockels, librarian at the University of Leicester, for their highly professional help in the preparation of the protocols, and their help in running the search on Cochrane, Embase and Medline.

Conflict of interest

The authors declare that the research was conducted in the absence of any commercial or financial relationships that could be construed as a potential conflict of interest.

Publisher's note

All claims expressed in this article are solely those of the authors and do not necessarily represent those of their affiliated organizations, or those of the publisher, the editors and the reviewers. Any product that may be evaluated in this article, or claim that may be made by its manufacturer, is not guaranteed or endorsed by the publisher.

Supplementary material

The Supplementary Material for this article can be found online at: https://www.frontiersin.org/articles/10.3389/fped.2022.915045/full#supplementary-material

References

1. Fontan F, Baudet E. Surgical repair of tricuspid atresia. *Thorax.* (1971) 26:240–8. doi: 10.1136/thx.26.3.240

2. Choussat A, Fontan F, Besse P, Vallot F, Chauve A, Bricaud H. Selection criteria for Fontan's procedure. In: Anderson RH, Shinebourne EA editors. *Paediatric Cardiology*. Edinburgh: Churchill Livingstone (1977). p. 559–66.

3. Corno AF, Becker AE, Bulterijs AHK, Lam J, Nijveld A, Schuller JL, et al. Univentricular heart: can we alter the natural history? *Ann Thorac Surg.* (1982) 34:716–26. doi: 10.1016/S0003-4975(10)60917-4

4. Fontan F, Kirklin JW, Fernandez G, Costa F, Naftel DC, Tritto F, et al. Outcome after a "perfect" Fontan operation. *Circulation.* (1990) 81:1520–36. doi: 10.1161/01.CIR.81.5.1520

5. Gewillig M, Brown SC. The Fontan circulation after 45 years: update in physiology. *Heart.* (2016) 102:1081–6. doi: 10.1136/heartjnl-2015-307467

6. Kreutzer GO, Galindez E, Bono H, de Palma C, Laura JP. An operation for the correction of tricuspid atresia. *J Thorac Cardiovasc Surg.* (1973) 66:613–21. doi: 10.1016/S0022-5223(19)40598-9

7. Yacoub MH, Radle-Smith R. Use of a valved conduit from right atrium to pulmonary artery for "correction" of a single ventricle. *Circulation.* (1976) 54:III63–70.

8. Lee CN, Schaff HV, Danielson GK, Puga FJ, Driscoll DJ. Comparison of atriopulmonary versus atrioventricular connections for modified Fontan/Kreutzer repair of tricuspid valve atresia. *J Thorac Cardiovasc Surg.* (1986) 92:1038–43. doi: 10.1016/S0022-5223(19)35820-9

9. Bjork VO, Olin CL, Bjarke BB, Thoren CA. Right atrial-right ventricular anastomosis for correction of tricuspid atresia. *J Thorac Cardiovasc Surg.* (1979) 77:452–8. doi: 10.1016/S0022-5223(19)40916-1

10. Coles JG, Leung M, Kielmanowicz S, Freedom RM, Benson LN, Rabinovitch M, et al. Repair of tricuspid atresia: utility of right ventricular incorporation. *Ann Thorac Surg.* (1988) 45:384–9. doi: 10.1016/S0003-4975(98)90010-8

11. Ilbawi MN, Idriss FS, DeLeon SY, Kucich VA, Muster AJ, Paul MH, et al. When should the hypoplastic right ventricle be used in a Fontan operation? An experimental and clinical correlation. *Ann Thorac Surg.* (1989) 47:533–8. doi: 10.1016/0003-4975(89)90428-1

12. de Leval MR, Kilner P, Gewillig M, Bull C. Total cavopulmonary connection: a logical alternative to atriopulmonary connection for complex Fontan operations. *J Thorac Cardiovasc Surg.* (1988) 96:682–95. doi: 10.1016/S0022-5223(19)35174-8

13. Jonas RA, Castaneda AR. Total cavo-pulmonary connection. *J Thorac Cardiovasc Surg.* (1988) 96:830. doi: 10.1016/S0022-5223(19)35196-7

14. Marcelletti C, Corno AF, Giannico S, Marino B. Inferior vena cava to pulmonary artery extracardiac conduit: a new form of right heart bypass. *J Thorac Cardiovasc Surg.* (1990) 100:228–32. doi: 10.1016/S0022-5223(19)35562-X

15. Giannico S, Corno AF, Marino B, Cicini MP, Gagliardi MG, Amodeo A, et al. Total extracardiac right heart bypass. *Circulation.* (1992) 86(Suppl.):II110–7.

16. Corno AF, Horisberger J, Jegger D, von Segesser LK. Right atrial surgery with unsnared inferior vena cava. *Eur J Cardiothorac Surg.* (2004) 26:219–20. doi: 10.1016/j.ejcts.2004.03.023

17. Nakano T, Kado H, Ishikawa S, Shiokawa Y, Ushinohama H, Sagawa K, et al. Midterm surgical results of total cavopulmonary connection: clinical advantages of the extracardiac conduit method. *J Thorac Cardiovasc Surg.* (2004) 127:730–7. doi: 10.1016/S0022-5223(03)01184-X

18. Yetman AT, Drummond-Webb J, Fiser WP, Schmitz ML, Imamura M, Ullah S, et al. The extracardiac Fontan procedure without cardiopulmonary bypass technique and intermediate-term results. *Ann Thorac Surg.* (2002) 74:S1416–21. doi: 10.1016/S0003-4975(02)03922-X

19. Klima U, Peters T, Peuster M, Hausdorf G, Haverich A. A novel technique for establishing total cavopulmonary connection: from surgical preconditioning to interventional completion. *J Thorac Cardiovasc Surg.* (2000) 120:1007–9. doi: 10.1067/mtc.2000.107824

20. Prabhu S, Maiya S, Shetty R, Murthy K, Ramachandra P, Karl TR. Improved technique for interventional extracardiac Fontan. *World J Pediatr Congenit Heart Surg.* (2020) 11:488–92. doi: 10.1177/2150135120918541

21. Laks H, Pearl JM, Haas GS, Drinkwater DC, Milgalter E, Jarmakani JM, et al. Partial Fontan: advantages of an adjustable interatrial communication. *Ann Thorac Surg.* (1991) 52:1084–94. doi: 10.1016/0003-4975(91)91286-5

22. Bridges ND, Lock JE, Castaneda AR. Baffle fenestration with subsequent catheter closure: modification of the Fontan operation for patients with increased risk. *Circulation.* (1990) 82:1681–9. doi: 10.1161/01.CIR.82.5.1681

23. Do-Nguyen CC, Kilcoyne MF, Gray P, Jonas RA. The evolution of surgical technique of the fenestrated Fontan procedure. *J Card Surg.* (2020) 35:1407–9. doi: 10.1111/jocs.14617

24. Guariento A, Pradegan N, Castaldi B, Cattapan C, Weixler V, Blitzer D, et al. Modified extracardiac Fontan with a fenestrated pericardial patch. *J Card Surg.* (2020) 35:1618–20. doi: 10.1111/jocs.14595

25. Lemler MS, Scott WA, Leonard SR, Stromberg D, Ramaciotti C. Fenestration improves clinical outcome of the Fontan procedure: a prospective randomized study. *Circulation.* (2002) 105:207-12. doi: 10.1161/hc0202.102237

26. Salazar JD, Zafar F, Siddiqui K, Coleman RD, Morales DLS, Heinle JS, et al. Fenestration during Fontan palliation: now the exception instead of the rule. *J Thorac Cardiovasc Surg.* (2010) 140:129–36. doi: 10.1016/j.jtcvs.2010.03.013

27. Li D, Li M, Zhou X, An Q. Comparison of the fenestrated and non-fenestrated Fontan procedures. A meta-analysis. *Medicine.* (2019) 98:29–39. doi: 10.1097/MD.0000000000016554

28. Bouhout I, Ben-Ali W, Khalaf D, Raboisson MJ, Poirier N. Effect of fenestration on Fontan procedure outcomes: a meta-analysis and review. *Ann Thorac Surg.* (2020) 109:1467–74. doi: 10.1016/j.athoracsur.2019.12.020

29. Malekzadeh-Milani S, Ladouceur M, Bajolle F, Bonnet D, Boudjemline Y. Closure of Fontan fenestration with the use of covered stents: short- and mid-term results in a cohort of 50 patients. *Cardiol Young.* (2015) 25:868–73. doi: 10.1017/S1047951114000894

30. Marini D, Boudjemline Y, Agnoletti G. Closure of extracardiac Fontan fenestration by using the covered Cheatham platinum stent. *Cath Cardiovasc Int.* (2007) 69:1003–6. doi: 10.1002/ccd.20664

31. Stroup DF, Berlin JA, Morton SC, Olkin I, Williamson GD, Rennie D, et al. Meta-analysis of observational studies in epidemiology: a proposal for reporting. Meta-analysis of observational studies in epidemiology (MOOSE) group. *JAMA.* (2000) 283:2008–12. doi: 10.1001/jama.283.15.2008

32. Shamseer L, Moher D, Clarke M, Ghersi D, Liberati A, Petticrew M, et al. Preferred reporting items for systematic review and meta-analysis protocols (PRISMA-P) 2015: elaboration and explanation. *Br Med J.* (2015) 350:g7647. doi: 10.1136/bmj.g7647

33. Higgins JP, Altman DG, Gotzsche PC, Juni P, Moher D, Oxman AD, et al. The Cochrane Collaboration's tool for assessing risk of bias in randomized trials. *Br Med J.* (2011) 343:d5928. doi: 10.1136/bmj.d5928

34. Clavien PA, Barkun J, de Oliveira ML, Vauthey JN, Dindo D, Schulick RD, et al. The Clavien-Dindo classification of surgical complications: five-year experience. *Ann Surg.* (2009) 250:187–96. doi: 10.1097/SLA.0b013e3181b13ca2

35. Higgins JP, Thompson SG, Deeks JJ, Altman DG. Measuring inconsistency in meta-analyses. *Br Med J.* (2003) 327:557–60. doi: 10.1136/bmj.327.7414.557

36. R Core Team. *R: A Language and Environment for Statistical Computing. R Foundation for Statistical Computing, Vienna, Austria*. Vienna: R Core Team (2021).

37. Balduzzi S, Rücker G, Schwarzer G. How to perform a meta-analysis with R: a practical tutorial. *Evid Based Ment Health.* (2019) 22:153–60. doi: 10.1136/ebmental-2019-300117

38. Anderson PAW, Sleeper LA, Mahony L, Colan SD, Atz AM, Breitbart RE, et al. Contemporary outcomes after the Fontan procedure: a Pediatric Heart Network multicenter study. *J Am Coll Cardiol.* (2008) 52:85–98. doi: 10.1016/j.jacc.2008.01.074

39. Webb MK, Hunter LE, Kremer TR, Huddleston CB, Fiore AC, Danon S, et al. Extracardiac Fontan fenestration device closure with Amplatzer vascular plug II and septal occlude: procedure results and medium-term follow-up. *Pediatr Cardiol.* (2020) 41:703–8. doi: 10.1007/s00246-019-02283-0

40. Atz AM, Travison TG, McCrindle BW, Mahony L, Quartermain M, Williams RV, et al. Late status of Fontan patients with persistent surgical fenestration. *J Am Coll Cardiol.* (2011) 57:2437–43. doi: 10.1016/j.jacc.2011.01.031

41. Al-Hay AAA, Shaban LA, Al-Qbandi M, Al-Anbaei M. Occlusion of Fontan fenestration using Amplatzer septal occluder. *Int J Cardiovasc Imaging.* (2011) 27:483–90. doi: 10.1007/s10554-010-9694-0

42. Apostolopoulou SC, Laskari CV, Kiaffas M, Papagiannis J, Rammos S. Diverse experience with CardioSEAL and STARFlex septal occluders. *Cardiol Young.* (2004) 14:367–72. doi: 10.1017/S1047951104004032

43. Azakie A, McCrindle BW, Benson LN, Van Arsdell GS, Russell J, Coles JG, et al. Total cavopulmonary connection in children with a previous Norwood procedure. *Ann Thorac Surg.* (2001) 71:1541–6. doi: 10.1016/S0003-4975(01)02465-1

44. Bordacova L, Kaldararova M, Masura TP. Experiences with fenestration closure in patients after the Fontan operation. *Bratisl Lek Listy.* (2007) 108:344–7.

45. Boshoff DE, Brown SC, DeGiovanni J, Stumper O, Wright J, Mertens L, et al. Percutaneous management of a Fontan fenestration: in search of the ideal restriction/occlusion device. *Cath Cardiovasc Interv.* (2010) 75:60–5. doi: 10.1002/ccd.22275

46. Bradley TJ, Human DG, Culham JAG, Duncan WJ, Patterson MWH, LeBlanc JG, et al. Clipped tube fenestration after extracardiac Fontan allow for simple transcatheter coil occlusion. *Ann Thorac Surg.* (2003) 76:1923–8. doi: 10.1016/S0003-4975(03)01192-5

47. Brown JW, Ruzmetov M, Dsechner BW, Rodefeld MD, Turrentine MW. Lateral tunnel Fontan in the current era: is it still a good option? *Ann Thorac Surg.* (2010) 89:556–63. doi: 10.1016/j.athoracsur.2009.10.050

48. Cowley CG, Badran S, Gaffney D, Rocchini AP, Lloyd TR. Transcatheter closure of Fontan fenestrations using the Amplatzer septal occlude: initial experience and follow-up. *Cath Cardiovasc Int.* (2000) 51:301–4. doi: 10.1002/1522-726X(200011)51:3<301::AID-CCD12>3.0.CO;2-G

49. Day RW, Denton DM, Jackson WD. Growth of children with a functionally sungke ventricle following palliation at moderately increased altitude. *Cardiol Young.* (2000) 10:193–200. doi: 10.1017/S1047951100009100

50. Ebeid MR, Mehta I, Gaymes CH. Closure of external tunnel Fontan fenestration: a novel use of the Amplatzer vascular plug. *Pediatr Cardiol.* (2009) 30:15–9. doi: 10.1007/s00246-008-9268-2

51. Franco E, Balbacid Domingo EJ, Arreo del Val V, Guereta da Silva LG, del Cerro Marin MJ, Fernandez Ruiz A, et al. Percutaneous interventions in Fontan circulation. *IJC Heart Vasculature.* (2015) 8:138–46. doi: 10.1016/j.ijcha.2015.06.008

52. Goff DA, Blume ED, Gauvreau K, Mayer JE, Lock JE, Jenkins KJ. Clinical outcome of fenestrated Fontan patients after closure. The first 10 years. *Circulation.* (2000) 102:2094–9. doi: 10.1161/01.CIR.102.17.2094

53. Goreczny S, Dryzek P, Morgan GJ, Mazurek-Kula A, Moll JJ, Moll JA, et al. Fenestration closure with Amplatzer duct occlude II in patients after total cavo-pulmonary connection. *Arch Med Sci.* (2017) 13:337–45. doi: 10.5114/aoms.2016.61836

54. Gorla SR, Jhingoeri NK, Chakraborty A, Raja KR, Garg A, Sandhu S, et al. Incidence and factors influencing the spontaneous closure of Fontan fenestration. *Congenit Heart Dis.* (2018) 13:776–81. doi: 10.1111/chd.12652

55. Hannah RL, Zabinsky JA, Salvaggio JL, Rossi AF, Khan DM, Alonso FA, et al. The Fontan operation: the pursuit of associated lesions and cumulative trauma. *Pediatr Cardiol.* (2011) 32:778–84. doi: 10.1007/s00246-011-9973-0

56. Hansen JH, Runge U, Uebing A, Scheewe J, Kramer HH, Fischer G. Cardiac catheterization and interventional procedures as part of staged surgical palliation for hypoplastic left heart syndrome. *Congenit Heart Dis.* (2012) 7:565–74. doi: 10.1111/j.1747-0803.2012.00709.x

57. Hosein RBM, Clarke AJB, McGuirk SP, Griselli M, Stumper O, DeGiovanni J, et al. Factors influencing early and late outcome following the Fontan procedure in the current era. The "Two commandments"? *Eur J Cardiothorac Surg.* (2007) 31:344–52. doi: 10.1016/j.ejcts.2006.11.043

58. Hsia TY, Khambadkone S, Redington AN, de Leval MR. Effect of fenestration on the sub-diaphragmatic venous hemodynamics in the total cavo-pulmonary connection. *Eur J Cardiothorac Surg.* (2001) 19:785–92. doi: 10.1016/S1010-7940(01)00705-9

59. Kim SH, Kang IS, Huh J, Lee HJ, Yang JH, Jun TG. Transcatheter closure of fenestration with detachable coils after the Fontan operation. *J Korean Med Sci.* (2006) 21:859–64. doi: 10.3346/jkms.2006.21.5.859

60. Masura J, Borodacova L, Tittel P, Berden P, Podnar T. percutaneous management of cyanosis in Fontan patients using Amplatzer occluders. *Cath Cardiovasc Interv.* (2008) 71:843–9. doi: 10.1002/ccd.21540

61. Mays WA, Border WL, Knecht SK, Gerdes YM, Pfriem H, Claytor RP, et al. Exercise capacity improves after transcatheter closure of the Fontan fenestration in children. *Congenit Heart Dis.* (2008) 3:254–61. doi: 10.1111/j.1747-0803.2008.00199.x

62. McCrossan BA, Walsh KP. Fontan fenestration closure with Amplatzer duct occlude II device. *Cath Cardiovasc Interv.* (2015) 85:837–41. doi: 10.1002/ccd.25770

63. Meadows J, Lang P, Marx G, Rhodes J. Fontan fenestration closure has no acute effect on exercise capacity but improves ventilatory response to exercise. *J Am Coll Cardiol.* (2008) 52:108–13. doi: 10.1016/j.jacc.2007.12.063

64. Momenah TS, Eltayb H, El Oakley R, Al Qethamy H, Al Faraidi Y. Effects of transcatheter closure of Fontan fenestration on exercise tolerance. *Pediatr Cardiol.* (2008) 29:585–8. doi: 10.1007/s00246-007-9154-3

65. Moore JW, Murdison KA, Baffa GM, Kashow K, Murphy JD. Transcatheter closure of fenestration and excluded hepatic veins after Fontan: versatility of the Amplatzer device. *Am Heart J.* (2000) 140:534–40. doi: 10.1067/mhj.2000.108517

66. Reinhardt Z, de Giovanni J, Stickley J, Bhole V, Anderson B, Murtuza B, et al. Catheter interventions in the staged management of hypoplastic left heart syndrome. *Cardiol Young.* (2014) 24:212–9. doi: 10.1017/S1047951113000024

67. Sfyridis PG, Lytrivi ID, Avramidis DP, Zavaropoulos PN, Kirvassilis GV, Papagiannis JK, et al. The Fontan procedure in Greece: early surgical results and excellent mid-term outcome. *Hellenic J Cardiol.* (2010) 51:323–9.

68. Stamm C, Friehs I, Duebener LF, Zurakowski D, Mayer JE, Jonas RA, et al. Improving results of the modified Fontan operation in patients with heterotaxy syndrome. *Ann Thorac Surg.* (2002) 74:1967–78. doi: 10.1016/S0003-4975(02)04124-3

69. Aldoss O, Divekar A. Modified technique to create Diabolo stent configuration. *Pediatr Cardiol.* (2016) 37:728–33. doi: 10.1007/s00246-015-1339-6

70. Bar-Cohen Y, Perry SB, Keane JF, Lock JE. Use of stent to maintain atrial defects and Fontan fenestrations in congenital heartv disease. *J Interven Cardiol.* (2005) 18:11–8. doi: 10.1111/j.1540-8183.2005.04049.x

71. Hirsch JC, Goldberg C, Bove EL, Salehian S, Lee T, Ohye RG, et al. Fontan operation in the current era. A 15-year single institution experience. *Ann Surg.* (2008) 248:52–60. doi: 10.1097/SLA.0b013e3181858286

72. Petko M, Myung RJ, Wernovsky G, Cohen MI, Rychik J, Nicolson SC, et al. Surgical reinterventions following the Fontan procedure. *Eur J Cardiothorac Surg.* (2003) 24:255–9. doi: 10.1016/S1010-7940(03)00257-4

73. Quandt D, Ramchandani B, Bhole V, Penford G, Mehta C, Dhillon R, et al. Initial experience with the Cook Formula balloon expandable stent in congenital heart disease. *Cath Cardiovasc Interv.* (2015) 85:259–66. doi: 10.1002/ccd.25543

74. Rupp S, Schieke C, Kerst G, Mazhari N, Moysich H, Latus H, et al. Creation of a transcatheter fenestration in children with failure of Fontan circulation: focus on extra cardiac conduit connection. *Cath Cardiovasc Interv.* (2015) 86:1189–94. doi: 10.1002/ccd.26042

75. Vyas H, Driscoll DJ, Cabalka AK, Cetta F, Hagler DJ. Results of transcatheter Fontan fenestration to treat protein-losing enteropathy. *Cath Cardiovasc Interv.* (2007) 69:584–9. doi: 10.1002/ccd.21045

76. Imielski BR, Woods RK, Mussatto KA, Cao Y, Simpson PM, Tweddell JS, et al. Fontan fenestration closure and event-free survival. *J Thorac Cardiovasc Surg.* (2013) 145:183–7. doi: 10.1016/j.jtcvs.2012.09.006

77. Bridges ND, Lock JE, Mayer JE, Burnett J, Castaneda AR. Cardiac catheterization and test occlusion of the interatrial communication after the fenestrated Fontan operation. *J Am Coll Cardiol.* (1995) 25:1712–7. doi: 10.1016/0735-1097(95)00055-9

78. Kawasaki Y, Sasaki T, Forbes TJ, Ross RD, Kobayashi D. Optimal criteria for transcatheter closure of Fontan fenestration: a single-center experience with a review of literature. *Heart Vessels.* (2021) 36:1246–55. doi: 10.1007/s00380-021-01798-y

79. Ozawa H, Hoashi T, Ohuchi H, Kurosaki K, Ichikawa H. Long-term outcomes after fenestration closure in high-risk Fontan candidates. *Pediatr Cardiol.* (2021) 42:1356–64. doi: 10.1007/s00246-021-02619-9

80. Daley M, Buratto E, King G, Grigg L, Iyengar A, Alphonso N, et al. Impact of Fontan fenestration on long-term outcomes: a propensity score-matched analysis. *J Am Heart Assoc.* (2022) 11:e026087. doi: 10.1161/JAHA.122.026087

frontiers | Frontiers in Pediatrics

TYPE Original Research
PUBLISHED 10 October 2022
DOI 10.3389/fped.2022.866994

OPEN ACCESS

EDITED BY
Martin Koestenberger,
Medical University of Graz, Austria

REVIEWED BY
Omar R.J Tamimi,
King Fahd Medical City, Saudi Arabia
Hannah Bellsham-Revell,
Evelina London Children's Hospital, United Kingdom
Donald Hagler,
Mayo Clinic, United States

*CORRESPONDENCE
Giulia Tuo
giuliatuo@gaslini.org

SPECIALTY SECTION
This article was submitted to Pediatric Cardiology, a section of the journal Frontiers in Pediatrics

RECEIVED 31 January 2022
ACCEPTED 08 August 2022
PUBLISHED 10 October 2022

CITATION
Tuo G, Paladini D, Marasini L, Buratti S, De Tonetti G, Calevo MG and Marasini M (2022) Fetal aortic coarctation: A combination of third-trimester echocardiographic parameters to improve the prediction of postnatal outcome. *Front. Pediatr.* 10:866994. doi: 10.3389/fped.2022.866994

Fetal aortic coarctation: A combination of third-trimester echocardiographic parameters to improve the prediction of postnatal outcome

Giulia Tuo[1]*, Dario Paladini[2], Lucia Marasini[3], Silvia Buratti[4], Gabriele De Tonetti[5], Maria G. Calevo[6] and Maurizio Marasini[1]

[1]Department of Surgery, Pediatric Cardiology and Cardiac Surgery, Istituto di Ricovero e Cura a Carattere Scientifico (IRCCS) Istituto Giannina Gaslini, Genova, Italy, [2]Department of Critical Care and Perinatal Medicine Fetal Medicine and Surgery Unit, IRCCS Istituto Giannina Gaslini, Genova, Italy, [3]Department of Neuroscience, Rehabilitation, Ophthalmology, Genetics, Maternal and Child Health (DINOGMI), IRCCS Istituto Giannina Gaslini, University of Genoa, Genova, Italy, [4]Critical Care and Emergency Department, Neonatal and Pediatric Intensive Care Unit, IRCCS Istituto Giannina Gaslini, Genova, Italy, [5]Department of Critical Care and Perinatal Medicine, Obstetric Anesthesia, IRCCS Istituto Giannina Gaslini, Genova, Italy, [6]Epidemiology and Biostatistics Unit, Scientific Direction, IRCCS Istituto Giannina Gaslini, Genova, Italy

Objectives: This study aims to determine a combination of third-trimester echocardiographic parameters for improving the prenatal prediction of coarctation of the aorta (CoA) after birth.

Methods: We included all cases of suspected CoA during fetal echocardiography performed in the second and/or third trimester of pregnancy at Gaslini Children's Hospital between January 2010 and December 2020. The last prenatal ultrasound evaluation was reviewed considering most of the echocardiographic criteria were already published for prenatal CoA diagnosis. Associated minor cardiac anomalies, such as a ventricular septal defect, persistent left superior vena cava (PLSCV), and redundant foramen ovale (FO) membrane, as well as postnatal outcomes, were reported. Initial perinatal management was defined based on the risk stratification of CoA during prenatal echocardiography. Neonates were divided into two groups depending on the presence or absence of CoA after birth.

Results: A total of 91 fetuses with CoA suspicion were selected, of which 27 (30%) were confirmed with CoA after birth and underwent surgical repair. All cardiac parameters except redundant FO membrane and PLSCV showed a significant correlation with CoA. Statistical analysis confirmed that cardiovascular disproportion with right predominance carries an increased risk for occurrence of CoA, especially if already evident during the ultrasound evaluation in the second trimester. Aortic valve (AV) z-score and distal transverse aortic arch (TAA) z-score resulted as the best predictors of CoA after birth. The best cutoff point for CoA discrimination with ROC analysis was an AV z-score of −1.25 and a distal TAA z-score of −0.37. A total of 46% of those without CoA were diagnosed with a cardiac defect, which was not diagnosed in utero, pulmonary hypertension, or a genetic syndrome.

10.3389/fped.2022.866994

Conclusion: The current criteria for diagnosing CoA *in utero* allow accurate diagnosis of most severe cases but the rate of false positives remains relatively high for milder cases. A combination of anatomic and functional echocardiographic parameters might be used in stratifying the risk of CoA. We proposed the AV and the TAA diameter z-scores as the best predictors of CoA after birth. In addition, neonates without CoA deserve proper monitoring at birth because prenatal evidence of a significant cardiovascular discrepancy between the right and left cardiac structures has an inherent risk for additional morbidity postnatally.

KEYWORDS

coarctation of the aorta, prenatal diagnosis, cardiovascular disproportion, fetal echocardiography, risk stratification

Introduction

The coarctation of the aorta (CoA) is the narrowing of the thoracic aorta in the region of the insertion of the arterial duct, with or without additional abnormalities of the aortic arch (1). CoA occurs in 7–8% of newborn children with congenitally malformed hearts and is a cause of remarkable morbidity and mortality if not diagnosed early (1, 2). Upon birth and after ductal closure, a critical CoA will cause an increase in left ventricular afterload with severe cardiac failure and poor perfusion of the lower body (3).

It has already been demonstrated that the diagnosis of prenatal CoA improves perioperative condition and survival of affected neonates by allowing planned delivery in a tertiary care center and early institution of prostaglandin treatment to prevent the closure of the duct (4, 5). However, *in utero* diagnosis of CoA still remains challenging and is affected by a high rate of false positives, especially during the third trimester, because it relies on indirect and non-specific signs, such as cardiac asymmetry with right dominance that may also be seen in normal fetuses in late pregnancy (6).

Several echocardiographic measurements have already been proposed to improve the detection rate of prenatal diagnosis of CoA, including two-dimensional measurements of the ventricular inflow and outflow tracts and the derived z-scores, the comparison of left and right side structure diameters, Doppler signs, and other features like the presence of a persistent left superior vena cava (LSVC), the visualization of a juxtaductal shelf, and the carotid subclavian index (7–18).

This study aimed to review the institutional experience in the prenatal diagnosis and the perinatal and postnatal management of fetuses with the suspicion of CoA. We also sought to confirm the usefulness of several previously published echocardiographic predictors of postnatal CoA, especially in those fetuses referred to a tertiary care center from an extra-regional care facility during late pregnancy.

Methods

All cases of suspected CoA detected at fetal echocardiography in the second and/or third trimester of pregnancy at Gaslini Children's Hospital between January 2010 and December 2020 were retrieved from our Cardiology Department database. The suspicion of CoA was based on prenatal features consistent with this condition, including the evidence of cardiovascular disproportion, which is defined as the discrepancy in the size of either cardiac chambers or great vessels detected during the ultrasound evaluation (7).

All transabdominal fetal echocardiograms including pulsed, continuous, and color Doppler examination (iE33, Philips, Amsterdam, The Netherlands) were reviewed offline. The retrospective analysis was carried out by two authors (G.T. and M.M.) on stored videos imported into the Xcelera Philips R3.3L1 software platform for offline analysis. Gestational age (GA) was determined by the last menstruation. Fetal heart examination routinely included the transverse view of the upper abdomen, the four-chamber view, the three-vessel view, the left and right ventricular outflow tract view, and the aortic arch view.

The last prenatal echocardiography, which was performed during the third trimester of pregnancy, was reviewed taking into consideration most of the echocardiographic criteria already published for the prenatal CoA diagnosis (7–18). The following retrospective measurements were carried out: mitral valve (MV) z-score; mitral/tricuspid valve (MV/TV) ratio; left/right ventricular (LV/RV) diameter ratio; aortic valve (AV) z-score; aortic/pulmonary valve (AV/PV) ratio; main pulmonary artery/ascending aorta ratio (MPA/AA); distal transverse aortic arch (TAA) and aortic isthmus diameter (AI) z-score; aortic isthmus/arterial duct (AI/AD) ratio. Cardiac dimensions were measured at their maximum size and measurements were taken from the inner edge to the inner edge. The diameter of the atrioventricular valves was measured in an apical four-chamber view. The internal diameter of the aortic isthmus was measured

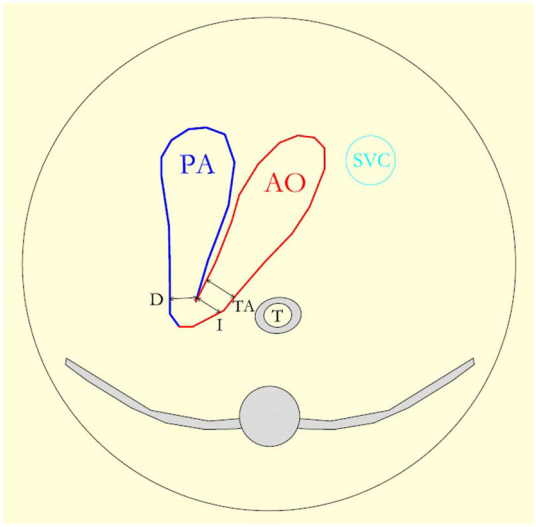

FIGURE 1
The diagram reproduces the three vessel and the tracheal view and shows the pulmonary artery (PA) leading into the arterial duct (D), the aortic arch (AO), and the superior vena cava (SVC). The lines show the measurement of, respectively, the isthmus (I), the duct, and the distal transverse aortic arch (TA) diameter.

immediately proximal to the insertion of the arterial duct in the three vessels and in tracheal view. The ductal diameter and the distal transverse aortic arch diameter were also acquired in the three vessels and in tracheal view (Figure 1) (15). The subjective appearance of both the aortic arch (either diffuse hypoplasia of the whole aortic arch or not) and the left ventricle ("borderline" left ventricle or adequate size) was reported. The appearance of the foramen ovale was studied, and the foramen ovale membrane was defined as redundant when it herniated into the left atrium for more than 50% of the left atrial diameter (19). GA was used to calculate the z-score (20). Color Doppler assessment of flow, respectively, at the aortic arch (antegrade flow alone or antegrade and reversed ductal-dependent flow) and at the foramen ovale (right to left or bidirectional) were recorded. Fetuses with associated minor cardiac anomalies, such as ventricular septal defect (VSD), bicuspid aortic valve suspicion, persistent left superior caval vein (PLSCV), and redundant foramen ovale (FO) membrane, were included in the study. Fetuses with hypoplastic left heart syndrome class IV, isolated aortic valve stenosis, aortic arch interruption type B or C, or other complex heart defects were not included in the study. We also excluded fetuses with unknown postnatal echocardiogram and/or outcomes.

Medical records were also reviewed for the following: indication for referral to a specialized tertiary care center, mean gestational age at the last fetal echocardiographic evaluation, associated extra-cardiac anomalies (ECA) or syndromes, karyotyping result, if performed, and postnatal diagnosis and outcomes.

Echocardiographic parameters acquired during the last fetal echocardiogram were compared between patients with confirmed surgical CoA and those without CoA detected at the postnatal ultrasound examination.

The risk of developing CoA after birth was stratified into low, moderate, or high based on obstetrical history (i.e., family history of CoA, early suspicion of cardiac asymmetry during the ultrasound scan in the second trimester) and major echocardiographic parameters detected at the last fetal echocardiographic examination. Low CoA risk fetuses received the first diagnosis of CoA suspicion during the third trimester of pregnancy (> 28 weeks of GA, late diagnosis), had an aortic isthmus narrowing (-3 < isthmus z-score $\leq$-2; 0.5 < AI/AD ratio <0.7) but a good size transverse aortic arch at the subjective analysis, and a mild discrepancy between the right and left side structures (LV/RV ratio $\geq$0.6). Moderate CoA risk fetuses received an early diagnosis (<28 weeks of GA), had an aortic isthmus narrowing (isthmus z-score $\leq$-3; AI/AD ratio $\leq$0.5), and a more evident discrepancy between left and right side dimensions both at the level of the ventricles (mitral z-score <-3, LV/RV ratio <0.6) and of the great arteries (MPA/AA ratio 2) compared to the low CoA risk fetuses. High-risk fetuses presented moderate-risk anatomic features with marked hypoplasia of the aortic arch (distal TAA z-score <-1), a borderline LV with MV hypoplasia (z-score <-5), and an aortic arch flow reversal and bidirectional flow at the level of the foramen ovale.

Delivery of all neonates with prenatal CoA suspicion, regardless of the CoA risk degree, was planned at our institute, which is a major pediatric tertiary care center where high-risk pregnancies are centralized and also includes cardiac and cardiothoracic surgery services. Initial perinatal management was defined based on the prenatal risk stratification performed by the fetal cardiologist.

All neonates with a low risk of CoA at birth received a daily physical examination by pediatricians with palpation of femoral pulses, measurement of oxygen saturation, and systolic right brachial–right ankle pressure difference in a nursery setting. Echocardiography was performed by a pediatric cardiologist always between 48 and 72 h after birth. Those with a moderate or high risk of CoA were transferred at birth to the cardiac unit and received clinical monitoring and a echocardiogram respectively within first 12 hours or 4 hours after birth according to the estimated prenatal risk. Then, serial echocardiograms were performed until the diagnosis of CoA resulted in positive or negative confirmation. We did not place any umbelical venous arterial catheter and did not commence prostaglandin E1 (PGE1) until we had the confirmation of neonatal CoA.

Coarctation of the aorta was confirmed by postnatal echocardiography or CT. The diagnosis of CoA usually relies on the presence of a localized narrowing of the thoracic aorta

just beyond the origin of the left subclavian artery, owing to a posterior shelf protruding from the posterior aspect of the aorta, together with the high-velocity flow (> 2 m/s) across the stenosis. Associated findings, such as isthmus and aortic arch hypoplasia, were diagnosed if the z-score was <-2, according to normal reference ranges (21).

Assessment of postnatal outcomes included the following: postnatal evidence of associated cardiac and extracardiac anomalies, chromosome or genetic disorders, presence of persistent neonatal pulmonary hypertension (PNPH), drug administration, need for one or more interventions, and/or age and cause of death, at least within the first 6 months of life. Neonates who were not diagnosed with CoA at birth underwent a cardiologic follow-up, including echocardiography at 1 and 6 months of life to rule out a late CoA.

Persistent neonatal pulmonary hypertension was defined as a failure of the normal circulatory transition that occurs after birth with the progressive reduction of pulmonary vascular resistance. The severity of PNPH was based on its duration and the need for respiratory support and medications. PNPH was defined as self-limiting (lasting less than 6 weeks) or persistent (lasting more than 6 weeks) (22, 23).

This study was approved by our institutional ethics committee, and informed consent to view files and echocardiographic reports was obtained from the parents.

Statistical analysis

Descriptive statistics were generated for the whole cohort and data were expressed as mean and SD for continuous variables. Median value and range as well as absolute or relative frequencies for categorical variables were calculated and reported. Demographic and clinical characteristics were compared using the χ^2 or Fisher's exact test and the Mann-Whitney U test for categorical and continuous variables, respectively. A univariate analysis was carried out to determine characteristics that were significantly more frequent among the patients with CoA. Logistic regression analyses were used for each variable, and the results were reported as odds ratio (OR) with their 95% confidence intervals (CIs). A multivariate analysis was then performed, and only variables that proved to be statistically or borderline significant in the univariate analysis ($P < 0.08$) were included in the model. The model showing the best fit was based on backward stepwise selection procedures, and each variable was removed if it did not contribute significantly. In the final model, a p-value of < 0.05 was considered statistically significant, and all p-values were based on two-tailed tests. Receiver operating characteristic (ROC) curves and area under the curve (AUC) were calculated for echocardiographic parameters significantly associated with the postnatal development of CoA. Cutoff points with corresponding sensitivity and specificity are provided.

TABLE 1 Prenatal details of the study population (fetuses with suspected coarctation of the aorta, CoA).

Variable	Value
Fetal study population	91
Type of pregnancy	
Single	89
Twin	2
Referral reason	
Suspected cardiac asymmetry	71
Suspected cardiac anomaly (VSD, PLSCV, Redundant FO Membrane)	8
Family medical history	7
Extracardiac anomaly	4
Chromosomal anomaly	1
Associated minor cardiac anomalies	49
Persistent left superior vena cava	10
CoA Risk assignment at last fetal echocardiography	
Low	39
Moderate	29
High	23
Extracardiac anomalies	8
Labiopalatoschisis	1
Congenital cystic adenomatoid malformation	1
Micropenis	1
Single umbilical artery	1
Renal dysplasia and anhydramnios	1
Polimalformative complex	1
Spinal Dysraphism	1
Esophageal atresia and Polyhydramnios	1
Karyotype analysis	23
Chromosomal abnormalities	3
Turner syndrome or monosomy 45 X	1
Partial deletion of short arm of chromosome 5	1
Partial Deletion of short arm of chromosome 4	1

Statistical analysis was performed using Statistical Package for the Social Sciences (SPSS) for Windows (SPSS Inc., Chicago, IL).

Results

Between January 2010 and December 2020, 102 consecutive fetuses with a suspicion of CoA in the second or third trimester of pregnancy were identified. Six pregnancies were terminated: three for the development of Shone's syndrome, two for CoA suspicion in Turner's syndrome, and one for CoA associated with hydrops fetalis. Five fetuses were lost at prenatal cardiac follow-up. The study population included 91 newborn fetuses (Table 1). Of which, 27 (30%) were confirmed with CoA after birth and underwent surgical procedures within the first month of life. CoA risk was prenatally estimated to be high in 22 out

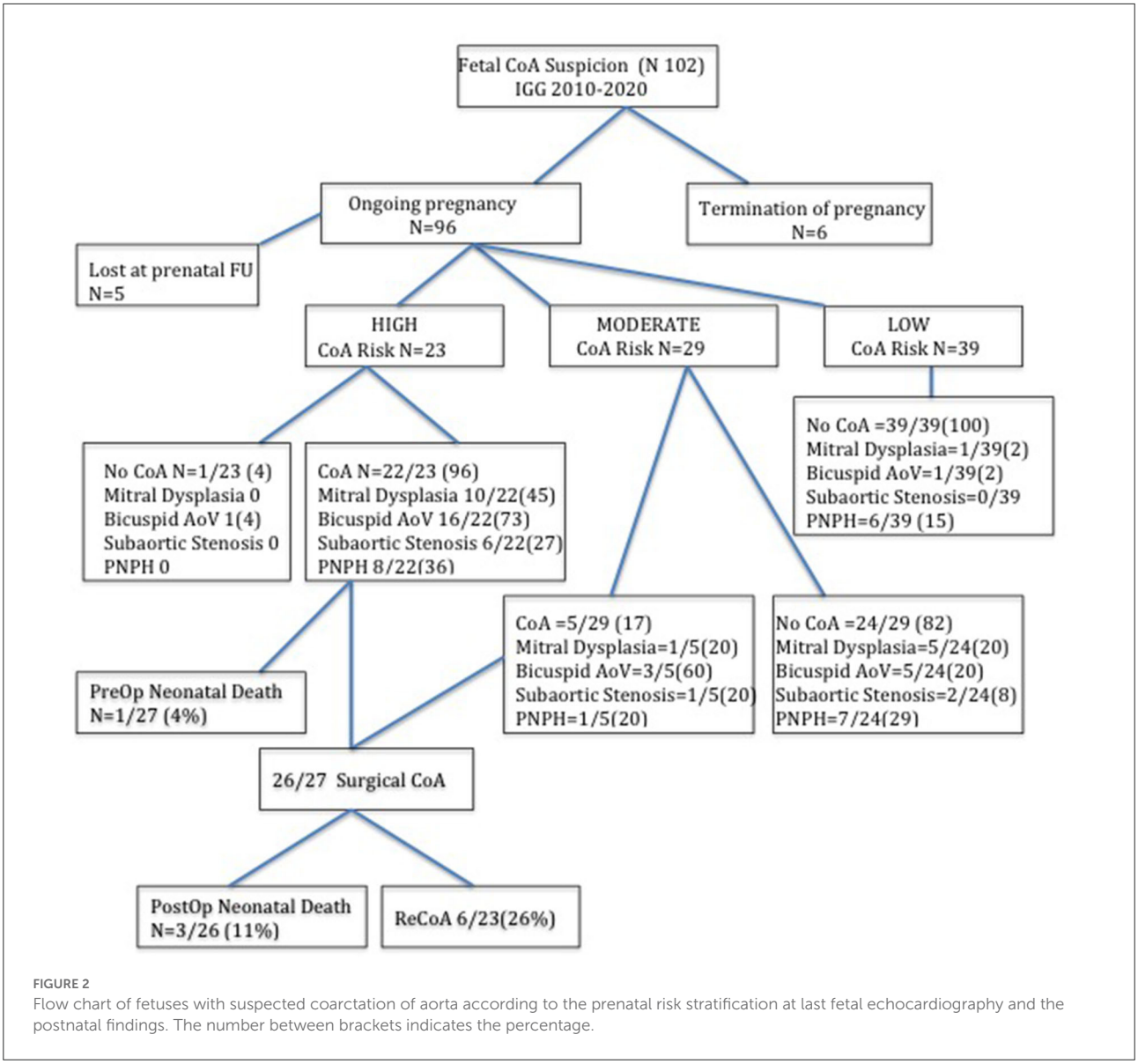

FIGURE 2
Flow chart of fetuses with suspected coarctation of aorta according to the prenatal risk stratification at last fetal echocardiography and the postnatal findings. The number between brackets indicates the percentage.

of 27 of them and moderate in 5 out of 27. Among the other 64/91 fetuses that did not develop CoA after birth, 24/64 were prenatally considered to have a moderate CoA risk and 40/64 a low CoA risk.

All neonates with a prenatal diagnosis of high-risk CoA suspicion required aortic arch repair except in one case that deserved further clinical and echocardiographic evaluation because of a bicuspid aortic valve and a VSD at the ultrasound examination of the neonate. Accordingly, surgical CoA was much more common in high (22/23, 96%) than moderate-risk CoA fetuses (5/29, 20%) and was never demonstrated in mild-risk CoA fetuses (0/39). There was no significant difference in the gestational age between different CoA risk categories (Figure 2).

Among the high and moderate CoA risk fetuses that developed surgical CoA (27/91), we also found mitral dysplasia in 11 cases (11/27, 40%) and a bicuspid valve in 19 cases (19/27, 70%) cases. Nine out of 27 (33%) neonates showed PNPH that was self-limiting but required temporary respiratory support. Following echocardiographic evaluation, we detected mild subaortic stenosis in 7 out of 27 neonates (26%). Three neonates died after the surgical procedure (3/27, 11%), of whom two had a complex form of CoA associated with Shone's syndrome. One more neonate with CoA was diagnosed with the CHARGE Syndrome postnatally and died before surgical correction.

TABLE 2 Prenatal ultrasound findings of the study population (fetuses with suspected CoA), according to postnatal outcomes (neonates normal and with CoA).

Variable all patients $N = 91$	No CoA $N = 64$	CoA $N = 27$	*p*-value
GA at last fetal ECHO	35.29 (2.18)	35.48 (2.24)	0.72
Early CoA diagnosis (≤ 28 weeks)	16 (25%)	23 (85.2%)	0.0001
Borderline LV	0	10 (37%)	0.0001
Inflow tracts			
z-score MV	−2.67 (1, 02)	−3.93 (1, 30)	0.0001
MV/TV ratio	0.65 (0.09)	0.51 (0.08)	0.0001
LV/RV ratio	0.64 (0.08)	0.53 (0.11)	0.0001
Outflow tract			
z-score AV	−0,74(0.94)	−2.22 (1.27)	0.0001
AV/PV ratio	0,75 (0.30)	0,56 (0.09)	0.0001
MPA/AA ratio	1,52 (0.33)	1,88 (0.26)	0.0001
Aortic Arch (on three vessel view)			
AI z-score	−2.26 (1.14)	−3.59 (1.12)	0.0001
Hypoplastic TAA	9 (14%)	26 (96%)	0.0001
TAA z-score	0.71 (1.35)	−1.76 (0.94)	0.0001
AI/AD ratio	0.51 (0.13)	0.43 (0.1)	0.009
Functional features			
Reversed or mixed flow at the aortic arch	17 (26.6%)	13 (48.1%)	0.05
Bidirectional flow at the foramen ovale	8 (12.5%)	17 (63%)	0.0001
Associated cardiac anomalies			
VSD	9 (14.1%)	9 (33.3%)	0.05
Redundant FO membrane	26 (40.6%)	5 (18.8%)	0.05
LSCV	7 (17.9%)	3 (15%)	1
Bicuspid aortic valve suspicion	5 (8%)	10 (37%)	0.0001
Quantitative results are expressed as mean (standard deviation)			

Univariate analysis.

During the subsequent clinical and echocardiographic follow-up, 6 out of 23 (26%) neonates showed re-CoA and underwent percutaneous dilatation by balloon angioplasty.

Among the moderate and low-risk CoA patients that did not develop CoA (63/91), one was postnatally diagnosed with superior sinus venosus atrial septal defect and partial anomalous pulmonary venous drainage of the right upper pulmonary veins into the superior vena cava and underwent surgical correction. One patient was diagnosed with Cardiospondylocarpofacial syndrome after birth. Moreover, out of 63, 6 (9.5%) of them were found to have mitral dysplasia, 6 (9.5%) had a bicuspid aortic valve, and 5 (8%) had a diffuse hypoplastic aortic arch. One patient with a bicuspid aortic valve subsequently developed a moderate degree of aortic valve stenosis and ascending aorta dilatation that did not require any interventional procedure until now. Two out of 63 patients developed subaortic stenosis during the follow-up. In total, 13 out of 63 (21%) neonates without CoA needed temporary respiratory support for self-limiting neonatal PNPH.

Therefore, only 34 out of 91 (37%) patients with prenatal CoA suspicion did not show any cardiac or extracardiac anomaly after birth, and they belonged to the prenatal low and moderate-risk CoA groups.

The comparative analysis between newborns with confirmed or without confirmed surgical CoA is detailed in Table 2. There was no significant difference in gestational age between the two groups. In the univariate analysis, all parameters were statistically significant except for the LSCV. The mean MV diameter z-score and the LV/RV ratio were significantly lower in fetuses with CoA than in those without CoA. Furthermore, the mean aortic valve diameter z-score was significantly lower in fetuses with CoA. In contrast, MPA/AA ratio was significantly higher in fetuses with CoA. Mean aortic isthmus diameter z-score and mean distal transverse aortic arch z-score were significantly lower in fetuses with CoA than in those without CoA, and the subjective impression of a diffuse hypoplastic aortic arch was associated with the occurrence of CoA (Figures 3, 4). Whereas, the presence of a redundant foramen ovale resulted

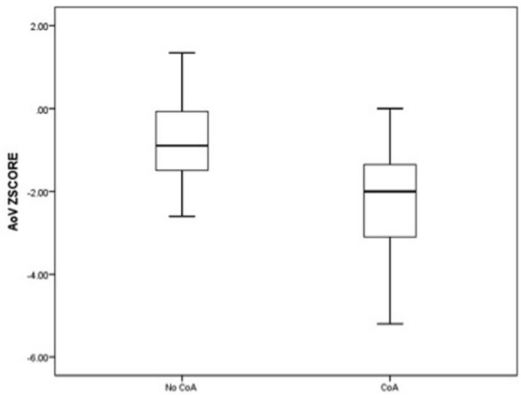

FIGURE 3
Box and whisker plots of the z-score, respectively, for aortic valve annulus and the distal transverse aortic arch at the third-trimester echocardiography.

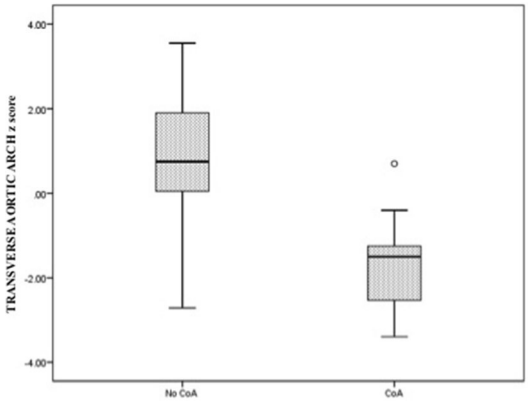

FIGURE 4
Box and whisker plots of the z-score, respectively, for aortic valve annulus and the distal transverse aortic arch at the third-trimester echocardiography.

in a protective feature against the development of surgical CoA after birth.

Considering the significant variables in a multiple logistic regression analysis revealed that only AV z-score, LV/RV diameter ratio, and TAA z-score were statistically significant. Therefore, a higher measure of AV z-score, LV/RV diameter ratio, and TAA z-score resulted in protection against surgical CoA diagnosis after birth (Table 3).

We selected the two echocardiographic parameters that showed the strongest association with postnatal CoA, respectively, AV and distal TAA z-scores, and we presented data related to specificity and sensitivity, as well as cutoff points related to the ROC curves. The best cutoff point for CoA discrimination with ROC analysis was an AV z-score of −1.25 and a distal TAA z-score of −0.37. The value of the area under

TABLE 3 Multivariate logistic regression analysis of potential risk factors for CoA.

	No CoA	CoA	*OR (95%CI)*	*p-value*
	N = 64	*N* = 27		
AV z-score	−0,74 (0.94)	−2.22 (1.27)	0.27 (0.09–0.80)	**0.02**
LV/RV diameter	0.64 (0.08)	0.53 (0.11)	0 (0–0.06)	**0.01**
TAA z-score	0.71 (1.35)	−1.76 (0.94)	0.22 (0.10–0.48)	**0.0001**

OR, odds ratio; *CI*, confidence interval.

the curve relative to the AV z-score was 0.82 while for the variable distal TAA z-score was 0.93. The parameter with the greatest sensitivity and specificity was the distal TAA z-score ≤-0.37 with 96.3 and 81.2%, respectively (Table 4, Figure 5).

The left carotid to left subclavian artery (LCSA) distance was not retrievable for all fetuses at the retrospective analysis but it was measured at postnatal ultrasound examination in all patients, and it resulted significantly ($p < 0.0001$) higher in those who developed CoA (median 7; minimum 0.9 mm; maximum 11 mm) than in those without CoA (median 4 mm ±1.16; minimum 1.4, maximum 7.5 mm).

Discussion

Coarctation of the aorta is one of the most common congenital heart defects and is life-threatening if undiagnosed (24). As already demonstrated, prenatal diagnosis of CoA may improve survival and the preoperative condition of neonates presenting for surgery (4). However, CoA is still challenging to diagnose *in utero* despite advances in prenatal screening for congenital heart defects and the application of detailed techniques that combine measurements of cardiac structures and Doppler analysis at the time of fetal echocardiographic evaluation (7–18). Moreover, pulse oximetry screening is misdiagnosed in up to 80% of cases of CoA before discharging home (25–27), and the delayed diagnosis increases morbidity and mortality of affected neonates.

Due to the pre- and post-natal screening system limits, many institutions adopted a cautious postnatal management plan once antenatal suspicion is raised, although contributing to the increase in false positive cases. This is warranted considering the severity of the disease if left undiagnosed, but the unnecessary admission of the neonate with the suspicion of CoA to the cardiac or neonatal intensive care unit may contribute to family distress due to the increased medicalization of an otherwise normal infant (27, 28).

Reviewing our experience relative to the last 11 years of diagnosis and management of fetuses with CoA suspicion, we confirmed that the specificity of prenatal CoA diagnosis is still poor with a high false positive rate. The accuracy of our impression in predicting the need for postnatal arch repair was

TABLE 4 Cutoff points, sensitivity, specificity, and 95% confidence interval (CI) for CoA.

	Cut-off value	Sensitivity (%) (95% CI)	Specificity (%) (95% CI)
AV z-score	≤-1.25	77.8 (62.1; 93.5)	70.3 (59.1; 81.5)
TAA z-score	≤-0.37	96.3 (89.2; 100)	81.2 (71.7; 90.8)
AV z-score + TAA z-score	≤-1.25 or ≤-0.37	100 (100; 100)	56.2 (44.1; 68.4)

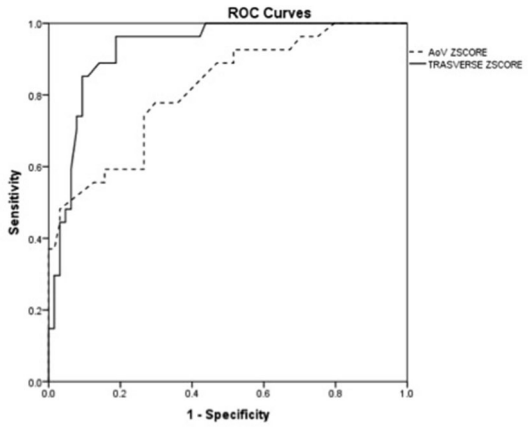

FIGURE 5
The receiver operating characteristic curve of the z-score aortic valve annulus and the z-score distal transverse aortic arch z-score at the third-trimester echocardiography.

high for cases that were highly likely to develop CoA (96% of true positive cases) but poor in fetuses with moderate (20% of true positive cases) and low risk of CoA (0/39 cases).

Our results were in concordance with Sharland et al.'s study in 1994 when they reported their experience at Guy's Hospital in London (6). The most severe forms of CoA were associated with relative hypoplasia of the left heart structures compared with the right, detected already in early pregnancy. On the contrary, the milder forms of CoA were consistent with a normal early fetal echocardiogram and with the evidence of a ventricular size discrepancy only during the ultrasound screening in the third trimester. Whereas in late pregnancy, the right heart structure may appear larger than the left in the normal fetus, and the examination of all the available echocardiographic parameters may not always be sufficient to distinguish between the real and the false positive cases. This has to be considered an inherent limitation of prenatal diagnosis.

Our study thus confirms the need for a risk-stratified approach to the neonate with prenatally diagnosed CoA suspicion, aiming to maximize the sensibility of true positives cases while minimizing morbidity of false positives.

Many echocardiographic parameters have been suggested until now to potentially improve the detection rate of CoA and the risk stratification process of CoA. A recent review published in circulation in 2017 demonstrated that fetuses with CoA have significant differences in several parameters, particularly in the left inflow and outflow tracts. Evidence of the hypoplastic aortic arch led to the best prenatal predictor of postnatal CoA (7).

In our experience, the cardiovascular disproportion between the left and right cardiac structures and the predominance of the right carries an increased risk for the occurrence of CoA, especially if already evident during the ultrasound evaluation in the second trimester. The statistical analysis defined AV z-score and distal TAA z-score as the best predictors of CoA after birth. These parameters were shown to have the best balance between sensitivity and specificity for the diagnosis of CoA in fetuses with isolated cardiac asymmetry. When combined, these parameters contribute to increasing the sensibility of the prenatal ultrasound examination but with the concomitant expected reduction of the specificity.

We determined the best cutoff value for the AV valve z-score was −1.25 (based on gestational age). In our opinion, during the third trimester, measuring the diameter of the aortic valve appeared easy, reproducible, and more predictive than the measurement of aortic isthmus diameter, which is in contrast to the other findings (9, 10, 13, 15). Gomez-Montes et al. (12) already demonstrated that measuring aortic isthmus diameter is not helpful to identify true false positive cases in late pregnancy (>28 weeks of gestation) because it is normal to observe a gradual tapering of the normal aortic arch whose narrowest site is the distal isthmus (12). Professor A. Rudolph previously explained that, in late gestation, the volume flowing across the aortic isthmus is quite low and probably represents only about 8% of combined ventricular output (29).

In our experience, the diffuse hypoplastic aortic arch was strongly associated with the occurrence of CoA as reported by several authors before (11, 12). However, the definition of the arch as hypoplastic has always been based on subjective impressions and not on a specific cutoff value. We, therefore, focused on the measurement of the distal TAA diameter, and we derived the relative z-score, which resulted in the parameter with the greatest sensitivity and specificity. To the best of our knowledge, we reported for the first time the best cutoff value for the distal TAA diameter z-score (based on gestational age).

Previous studies used sagittal or coronal views of the aortic arch for the definition of arch morphology and dimension (8).

We considered the three vessel and tracheal view as the ideal plane for the direct comparison of arches size of the aorta and duct and the aortic isthmus measurement. Moreover, the sagittal view of the aortic arch was often technically difficult to acquire during the last echocardiogram because of the unfavorable fetal position or the abdomen's bad acoustic window. For these reasons, we could not include in the statistical analysis the presence of a posterior shelf or the distal displacement of the left subclavian artery. However, the LCSA distance was measured at the postnatal echocardiogram in all neonates with prenatal CoA suspicion and resulted significantly higher in those who developed CoA, confirming to be a helpful tool to predict CoA both postnatally and prenatally, if the sagittal view of the arch is achievable.

As already demonstrated, also in our experience, both bidirectional flow across the foramen ovale and reverse flow in the aorta were significantly more frequent among patients with confirmed CoA after birth. However, none of the two characteristics were identified as strong prenatal CoA predictors in the multivariate logistic analysis. In fact, these functional parameters may also be detected in the presence of an isolated redundant foramen ovale membrane that may mimic fetal aortic coarctation, especially during the third trimester of pregnancy, increasing the rate of false positive CoA diagnosis (6, 30–32).

It has been hypothesized that PLSVC may increase the likelihood of CoA (33). In this study, the incidence of PLSVC was quite similar in fetuses that proved to have CoA and in normal fetuses. Our results confirm that this venous abnormality may induce cardiac asymmetry because coronary sinus dilatation decreases left ventricular filling, leading to a false-positive diagnosis of CoA (13).

The incidence of the bicuspid aortic valve was diagnosed frequently in patients with CoA after birth. However, the difficulty in reliable prenatal diagnosis of bicuspid aortic valve makes this well-recognized association less helpful prenatally. It is also noteworthy that neonates that did not develop CoA showed a higher incidence of the bicuspid aortic valve than in the general population.

We developed protocols for both low risk and moderate-to-high risk CoA at Gaslini Children's Hospital based on our growing experience in the management of neonates with prenatal CoA suspicion. The mothers of suspected neonates were indicated to deliver in our center and transfer the neonate to the cardiac unit or the nursery setting based on prenatal risk stratification. Our policy seeks to reduce the necessity of transferring a sick neonate from another hospital after the symptoms of coarctation have developed in case of false negative cases, improve the rates of nursery admission, allow earlier initiation of breastfeeding, and decrease medicalization for those neonates with prenatal low-risk CoA suspicion and unconfirmed CoA upon birth (34).

However, our retrospective analysis has also highlighted the importance of proper monitoring of false positive cases of CoA because their postnatal course may still be complicated due to prenatally undetected congenital malformations or transition problems as already described by Van Nisselrooij et al. (23). In our study population, 46% of neonates that had not developed CoA after birth were diagnosed with a cardiac defect or a genetic syndrome that had not been diagnosed *in utero* or with PNPH.

Overall, 20% of all non-CoA cases coped with temporary self-limiting neonatal PNPH that needed respiratory support during the neonatal observation. The prevalence of PNPH in this group of neonates was higher than that reported in unselected cohorts (1.9 per 1000 live births) (22). As previously hypothesized, the altered hemodynamics in fetal life, with right ventricular dominance and increased flow entering the pulmonary circulation, might have an effect on pulmonary vascular development, causing an abnormal transition phase from fetus to newborn and the evidence of PNPH (22, 23).

Therefore, we suggest that parents should be alerted at the time of prenatal counseling of the possible occurrence of other minor or major defects or potential transition problems, whenever there is evidence of significant cardiovascular disproportion, even if CoA suspicion is not confirmed after birth.

There are some limitations to our study. The first is the retrospective design and the small number of included cases. The second limitation is that this study was not planned to evaluate the efficacy of a fetal cardiac screening program but to assess the feasibility of fetal echocardiography for diagnosing CoA, especially during the third trimester of pregnancy. Therefore, we did not report the cases of CoA undiagnosed at prenatal screening and detected only postnatally. We are well aware that it will be necessary to validate our results in future studies. A large multicenter prospective study including all fetuses with CoA suspicion is needed to evaluate the actual diagnostic performance of fetal echocardiography in the diagnosis of CoA.

Conclusion

The current criteria for diagnosing CoA *in utero* allow accurate diagnosis of most severe CoA cases, but the milder ones are still difficult to be detected and the rate of false positives remains relatively high. A combination of anatomic and functional echocardiographic parameters might help in stratifying the risk of CoA, and the prenatal detection rate of CoA may improve when a multiple criteria prediction model is adopted. We proposed the aortic valve and the transverse aortic arch diameter z-score as predictors of CoA after birth. In addition, neonates without CoA deserve proper monitoring at birth because prenatal evidence of a cardiovascular discrepancy between the right and left cardiac structures has an inherent risk for additional morbidity postnatally.

Data availability statement

The raw data supporting the conclusions of this article will be made available by the authors, without undue reservation.

Ethics statement

The studies involving human participants were reviewed and approved by Regione Liguria Ethical Board. Written informed consent to participate in this study was provided by the participants' legal guardian/next of kin.

Author contributions

GT and MM conceptualised and designed the study, drafted the initial manuscript, and reviewed and revised the manuscript. GT, MM, and LM collected data. MC carried out the statistical analysis and critically reviewed and revised the manuscript. DP, SB, and GD critically reviewed the manuscript for important intellectual content. All authors approved the final manuscript as submitted and agree to be accountable for all aspects of the work.

Conflict of interest

The authors declare that the research was conducted in the absence of any commercial or financial relationships that could be construed as a potential conflict of interest.

Publisher's note

All claims expressed in this article are solely those of the authors and do not necessarily represent those of their affiliated organizations, or those of the publisher, the editors and the reviewers. Any product that may be evaluated in this article, or claim that may be made by its manufacturer, is not guaranteed or endorsed by the publisher.

References

1. Anderson RH, Baker EJ, Penny D, Redington AN, Rigby ML, Wernovsky G. *Aortic Coarctation and interrupted Aortic Arch in the Paediatric Cardiology*, Third Edition. Churchill Livingstone: Elsevier. (2010).

2. Hoffman JI, Kaplan S. The incidence of congenital heart disease. *J Am Coll Cardiol.* (2002) 39:1890–900. doi: 10.1016/S0735-1097(02)01886-7

3. Wren C, Reinhardt Z, Khawaja K. Twenty-year trends in diagnosis of life-threatening neonatal cardiovascular malformations. *Arch Dis Child.* (2008) 93:F33–5. doi: 10.1136/adc.2007.119032

4. Franklin O, Burch M, Manning N, Sleeman K, Gould S, Archer N. Prenatal diagnosis of coarctation of the aorta improves survival and reduces morbidity. *Heart.* (2002) 87:67–9. doi: 10.1136/heart.87.1.67

5. Houshmandi MM, Eckersley L, Fruitman D, Mills L, Power A, Hornberger LK. Fetal Diagnosis is Associated with Improved Perioperative Condition of Neonates Requiring Surgical Intervention for Coarctation. *Pediatr Cardiol.* (2021) 42:1504–11. doi: 10.1007/s00246-021-02634-w

6. Sharland GK, Chan KY, Allan LD. Coarctation of the aorta: Difficulties in prenatal diagnosis. *Br Heart J.* (1994) 71:70–5. doi: 10.1136/hrt.71.1.70

7. Familiari A, Morlando M, Khalil A, Sonesson SE, Scala C, Rizzo G, et al. Risk factors for coarctation of the aorta on prental ultrasound. a systematic review and meta-analysis. *Circulation.* (2017) 135772–85. doi: 10.1161/CIRCULATIONAHA.116.024068

8. Arya B, Bhat A, Vernon M, Conwell J, Lewin M. Utility of novel fetal echocardiographic morphometric measures of the aortic arch in the diagnosis of neonatal coarctation of the aorta. *Prenat Diagn.* (2016) 36:127–34. doi: 10.1002/pd.4753

9. Toole BJ, Schlosser B, McCracken CE, Stauffer N, Border WL, Sachdeva R. Importance of relationship between ductus and isthmus in fetal diagnosis of coarctation of aorta. *Echocardiography.* (2016) 33:771–7. doi: 10.1111/echo.13140

10. Marginean C, Marginean CO, Muntean I, Toganel R, Voidazan S, Gozar L. The role of ventricular disproportion, aortic, and ductal isthmus ultrasound measurements for the diagnosis of fetal aortic coarctation, in the third trimester of pregnancy. *Med Ultrason.* (2015) 17:475–81. doi: 10.11152/mu.2013.2066.174.rvd

11. Durand I, Deverriere G, Thill C, Lety AS, Parrod C, David N, et al. Prenatal detection of coarctation of the aorta in a non-selected population: a prospective analysis of 10 years of experience. *Pediatr Cardiol.* (2015) 36:1248–54. doi: 10.1007/s00246-015-1153-1

12. Gómez-Montes E, Herraiz I, Gómez-Arriaga PI, Escribano D, Mendoza A, Galindo A. Gestational age-specific scoring systems for the prediction of coarctation of the aorta. *Prenat Diagn.* (2014) 34:1198–206. doi: 10.1002/pd.4452

13. Jowett V, Aparicio P, Santhakumaran S, Seale A, Jicinska H, Gardiner HM. Sonographic predictors of surgery in fetal coarctation of the aorta. *Ultrasound Obstet Gynecol.* (2012) 40:47–54. doi: 10.1002/uog.11161

14. Gomez-Montes E, Herraiz I, Mendoza A, Escribano D, Galindo A. Prediction of coarctation of the aorta in the second half of pregnancy. *Ultrasound Obstet Gynecol.* (2013) 41:298–305. doi: 10.1002/uog.11228

15. Matsui H, Mellander M, Roughton M, Jicinska H, Gardiner HM. Morphological and physiological predictors of fetal aortic coarctation. *Circulation.* (2008) 118:1793–801. doi: 10.1161/CIRCULATIONAHA.108.787598

16. Pasquini L, Mellander M, Seale A, Matsui H, Roughton M, Ho SY, et al. Z-scores of the fetal aortic isthmus and duct: an aid to assessing arch hypoplasia. *Ultrasound Obstet Gynecol.* (2007) 29:628–33. doi: 10.1002/uog.4021

17. Quartermain MD, Cohen MS, Dominguez TE, Tian Z, Donaghue DD, Rychik J. Left ventricle to right ventricle size discrepancy in the fetus: the presence of critical congenital heart disease can be reliably predicted. *J Am Soc Echocardiogr.* (2009) 22:1296–301. doi: 10.1016/j.echo.2009.08.008

18. Berg C, Knüppel M, Geipel A, Kohl T, Krapp M, Knöpfle G, et al. Prenatal diagnosis of persistent left superior vena cava and its associated congenital anomalies. *Ultrasound Obstet Gynecol.* (2006) 27:274–80. doi: 10.1002/uog.2704

19. Wilson AD, Syamasundar R, Aeschlimann S. Normal fetal foramen flap and transatrial Doppler velocity pattern. *J Am Soc Echo.* (1990) 3:491–4. doi: 10.1016/S0894-7317(14)80366-0

20. Schneider C, McCrindle BW, Carvalho JS, Hornberger LK, McCarthy KP, Daubeney PE. Development of Z-scores for fetal cardiac dimensions from echocardiography. *Ultrasound Obstet Gynecol.* (2005) 26:599–605. doi: 10.1002/uog.2597

21. Pettersen MD, Du W, Skeens ME, Humes RA. Regression equations for calculation of z scores of cardiac structures in a large cohort of healthy infants, children, and adolescents: an echocardiographic study. *J Am Soc Echocardiogr.* (2008) 21:922–34. doi: 10.1016/j.echo.2008.02.006

22. Steurer MA, Jelliffe-Pawlowski LL, Baer RJ, Partridge JC, Rogers EE, Keller RL. Persistent pulmonary hypertension of the newborn

in late preterm and term infants in California. *Pediatrics.* (2017) 139:e20161165. doi: 10.1542/peds.2016-1165

23. Van Nisselrooij AEL, Rozendaal L, Linskens IH, Clur SA, Hruda J, Pajkrt E, et al. Postnatal outcome of fetal isolated ventricular size disproportion in the absence of aortic coarctation. *Ultrasound Obstet Gynecol.* (2018) 52:593–8. doi: 10.1002/uog.17543

24. Rosenthal E. Coarctation of the aorta from fetus to adult: curable condition of life long disease process? *Heart.* (2005) 91:1495–502. doi: 10.1136/hrt.2004.057182

25. Chang RK, Gurvitz M, Rodriguez S. Missed diagnosis of critical congenital heart disease. *Arch Pediatr Adolesc Med.* (2008) 162:969–74. doi: 10.1001/archpedi.162.10.969

26. de-Wahl Granelli A, Wennergren M, Sandberg K, Mellander M, Bejlum C, Inganas L, et al. Impact of pulse oximetry screening on the detection of duct dependent congenital heart disease: a Swedish prospective screening study in 39,821 newborns. *BMJ.* (2009) 338:a3037. doi: 10.1136/bmj.a3037

27. Diller CL, Kelleman MS, Kupke KG, Quary SC, Kochilas LK, Oster ME. A modified algorithm for critical congenital heart disease screening using pulse oximetry. *Pediatrics.* (2018) 141:4065. doi: 10.1542/peds.2017-4065

28. Hede SVH, DeVore G, Satou G, Sklansky M. Neonatal management of prenatally suspected coarctation of the aorta. *Prenat Diagn.* (2020) 40:942–8. doi: 10.1002/pd.5696

29. Rudolph A. *Aortic Arch Obstruction in Congenital Diseases of the Heart. Clinical-Physiological Considerations*. Third Edition. Wiley-Blackwell. (2009).

30. Channing A, Szwast A, Natarajan S, Degenhardt K, Tian Z, Rychik J. Maternal Hyperoxygenation improves left heart filling in fetuses with atrial septal aneurysm causing impediment to left ventricular inflow. *Ultrasound Obstet Gynecol.* (2015) 45:664–9. doi: 10.1002/uog.14688

31. Vena F, Donarini G, Scala C, Tuo G, Paladini D. Redundancy of foramen ovale flap may mimic aortic coarctation. *Ultrasound Obstet Gynecol.* (2020) 56:857–63. doi: 10.1002/uog.22008

32. Feit LR, Copel JA, Kleinman CS. Foramen ovale size in the normal and abnormal human fetal heart: an indicator of transatrial flow physiology. *Ultrasound Obstet Gynecol.* (1991) 1:313–9. doi: 10.1046/j.1469-0705.1991.01050313.x

33. Gustapane S, Leombroni M, Khalil A, Giacci F, Marrone L, Bascietto F, et al. Systematic review and meta-analysis of persistent left superior vena cava on prenatal ultrasound: associated anomalies, diagnostic accuracy and postnatal outcome. *Ultrasound Obstet Gynecol.* (2016) 48:701–8. doi: 10.1002/uog.15914

34. Busse M, Stromgren K, Thorngate L, Thomas KA. Parents' responses to stress in the neonatal intensive care unit. *Crit Care Nurse.* (2013) 33:52–9. doi: 10.4037/ccn2013715

Frontiers in Pediatrics

Addresses ongoing challenges in child health and patient care

Explores research that meets ongoing challenges in pediatric patient care and child health, from neonatal screening to adolescent development.

Discover the latest Research Topics

See more →

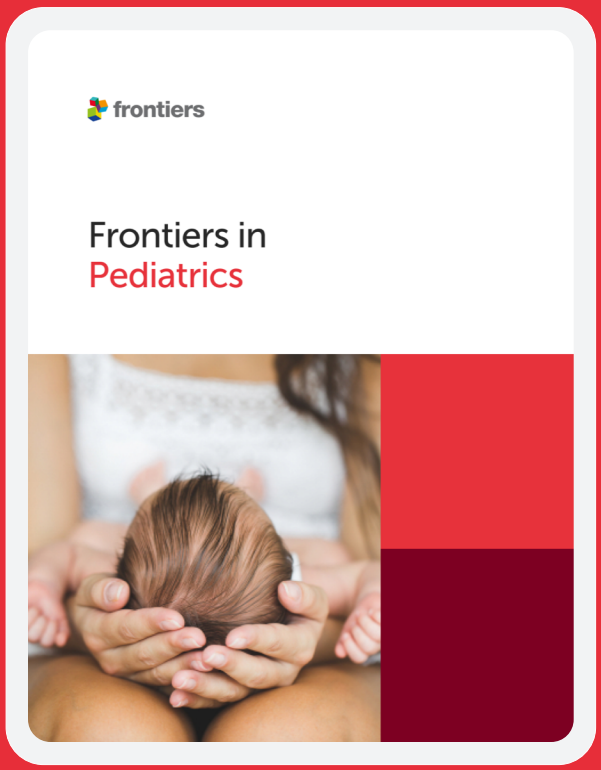

Frontiers

Avenue du Tribunal-Fédéral 34
1005 Lausanne, Switzerland
frontiersin.org

Contact us

+41 (0)21 510 17 00
frontiersin.org/about/contact